Dissertation zur Erlangung des Doktorgrades der Fakultät für Chemie und Pharmazie der Ludwig-Maximilians-Universität München

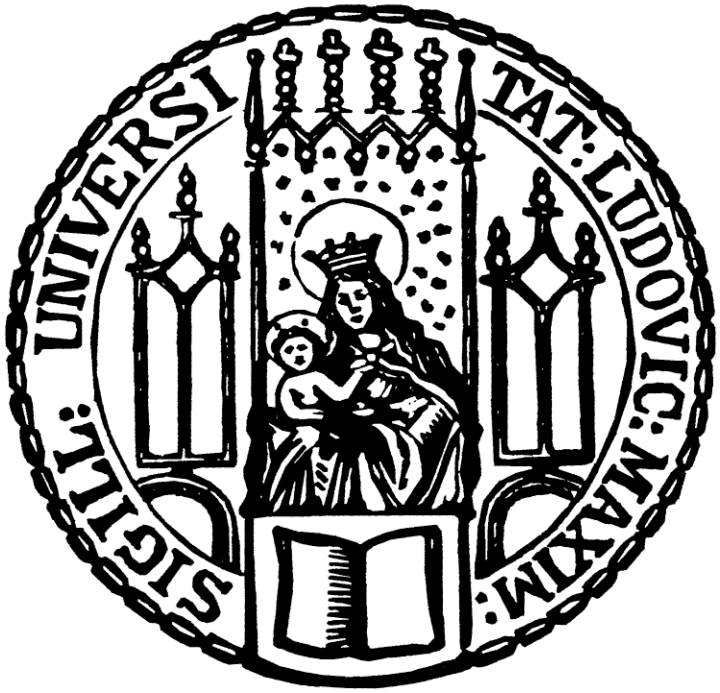

Lead structure-based optimization of SirReal-type Sirtuin 2 inhibitors

Matthias Frei

aus

Marktoberdorf

2024

Erklärung

Diese Dissertation wurde im Sinne von §7 der Promotionsordnung vom 28. November 2011 von Herrn Prof. Dr. Franz Bracher betreut.

Eidesstattliche Versicherung

Diese Dissertation wurde eigenständig und ohne unerlaubte Hilfe erarbeitet.

München, den 21.10.2024

_____

Matthias Frei

Dissertation eingereicht am 22.10.2024
1. Gutachter: Prof. Dr. Franz Bracher
2. Gutachter: Prof. Dr. Franz Paintner
Mündliche Prüfung am 13.12.2024

Danksagung

An allererster Stelle möchte ich mich bei meinem Doktorvater Prof. Dr. Franz Bracher für die engagierte und hilfsbereite Betreuung, Unterstützung und Förderung sowie für die ausgezeichneten Rahmenbedingungen während der Erstellung der Dissertation bedanken.

Des Weiteren möchte ich mich herzlich bei allen bedanken die zu der Entstehung dieser Arbeit beigetragen haben, insbesondere gilt mein Dank folgender Personen:
Herrn Prof. Dr. Franz Paintner für die Übernahme des Koreferats und allen weiteren Mitgliedern der Prüfungskommission; Dr. Lars Allmendinger und Claudia Glas für die Aufnahme der NMR-Spektren sowie Dr. Werner Spahl und Sonja Kosak für die Durchführung der Massenspektrometrie; Martina Stadler für die Durchführung der MTT- und Agardiffusionstests und Anna Niedrig für die HPLC-Analytik; Dr. Thomas Wein für Durchführung der Dockingstudien sowie Dr. Eva Huber und Prof. Dr. Michael Groll für die Kooperation bezüglich der kristallographischen Untersuchungen; Dr. Desirée Heerdegen und Dr. Ramona Schütz für die professionelle Einarbeitung und Unterstützung in den Anfängen der Promotionszeit.

Besonderer Dank gilt Dr. Jürgen Kraus für das entgegengebrachte Vertrauen hinsichtlich der Betreuung des Arzneistoffanalytikpraktikums sowie allen anderen Assistenten, allen voran Philipp, dessen hilfsbereite und freundschaftliche Zusammenarbeit ich in der Lehre besonders vermissen werde.

Bei allen ehemaligen und aktuellen Mitgliedern des AK Brachers sowie weiteren Kollegen möchte ich mich bedanken, allen voran bei Thomas, Ricky, Ferdinand, Mika, Melis, Christian, Arunthadi, Christoph, Sonja, Alexandra, Bernhard, Karl, Irene, Katharina, Ilya und Milka.

Vom ersten bis zum letzten Tag haben wir miteinander im Labor die Kolben geschwungen, und ich werde die gemeinsame Zeit, Erlebnisse und Diskussionen immer in Erinnerung behalten - danke Pavlos! Dein unbeschwerter Charakter und deine stets hilfsbereite Weise, Can, waren für mich jederzeit eine echte Bereicherung. Ina, immer konnte ich mich auf bedingungslose Unterstützung und deine selbstlose und warmherzige Art verlassen. Mit euch zusammen diese Promotionszeit erleben zu dürfen, war für mich das größte Geschenk.

Danke auch an Krisztián, durch den ich Jörg, Heinrich, Patrick, Vanessa, Tobias und Corina kennengelernt habe. Unsere gemeinsamen Abende vor allem während der Coronapandemie waren für mich von unersetzlichem Wert.

Christian und Julian - Berlin 2017.

Größter Dank jedoch gilt meiner **Familie**. Ohne die immerwährende Unterstützung und den grenzenlosen Rückhalt meiner Eltern und Geschwister wäre diese Arbeit nicht möglich gewesen.

Für meine Eltern

Georg und Brigitte

Table of contents

1 Introduction

Sirtuins are enzymes that essentially contribute to epigenetic regulation, influencing gene expression and cellular function. Modulating their activity with small molecules holds significant potential and substantial pharmaceutical value, making medicinal chemistry research crucial for developing corresponding compounds and discovering new therapeutic innovations.[1]

1.1 Fundamentals of epigenetics

Epigenetic processes play a fundamental role in the determination of cell functions, allowing different differentiation and specialization based on identical DNA sequences. Even in monozygotic twins, who share identical genetic characteristics, differences in lifestyle and environmental influences over the course of their lives can lead to epigenetic-related twin pair discrepancies, which may manifest as disease discordance.[2] This shows that the respective development is not only influenced by the individual genetic make-up (genotype), but also by the dynamic process of gene expression and gene silencing, which shapes the unique phenotype of an organism[3].

In eukaryotic cells the DNA is organized as chromosomes and wrapped around histone proteins to be further packaged with additional proteins to form chromatin (see **Figure 1**)[4]. Histones are octameric protein complexes that are formally positively charged at physiological pH due to the dominating basic properties of the amino acids lysine and arginine that they contain. Positive charge allows histones to bind to the negatively charged phosphate backbones of DNA through ionic interactions. This binding facilitates the compaction of DNA by winding it around histones, forming nucleosomes, which represent the fundamental organizational structure of chromatin.[5-6]

The condensation of chromatin structure is highly influenced by epigenetic modifications, with loosely packed, transcriptionally active euchromatin standing in contrast to silenced heterochromatin[7].The translational accessibility of the chromatin structure is regulated by various reversible chemical modifications of DNA and chromatin-associated proteins. Thereby, this dynamic epigenetic network is controlled by three main groups: writers (enzymes that add modifications), readers (proteins that bind to epigenetic modifications), and erasers (enzymes that remove these modifications).[8]

In principle, the specific reversible chemical modifications of DNA and histones are diverse, however, enzymatically catalyzed (de)methylations and (de)acetylations are the most prominent and pharmaceutically addressed to date[9]. The primary targets of these modifications are the DNA base cytosine as well as the amino acids lysine and arginine, which are located on the N-terminal histone tails that protrude from the nucleosomes. The chromatin structure, the recruitment of chromatin-modifying proteins and the binding of transcription

factors are regulated and influenced by corresponding epigenetic modifications. These as a result, have a direct and indirect effect on the level of gene expression and therefore leading to fundamental consequences for biological processes such as cell function and differentiation.[10]

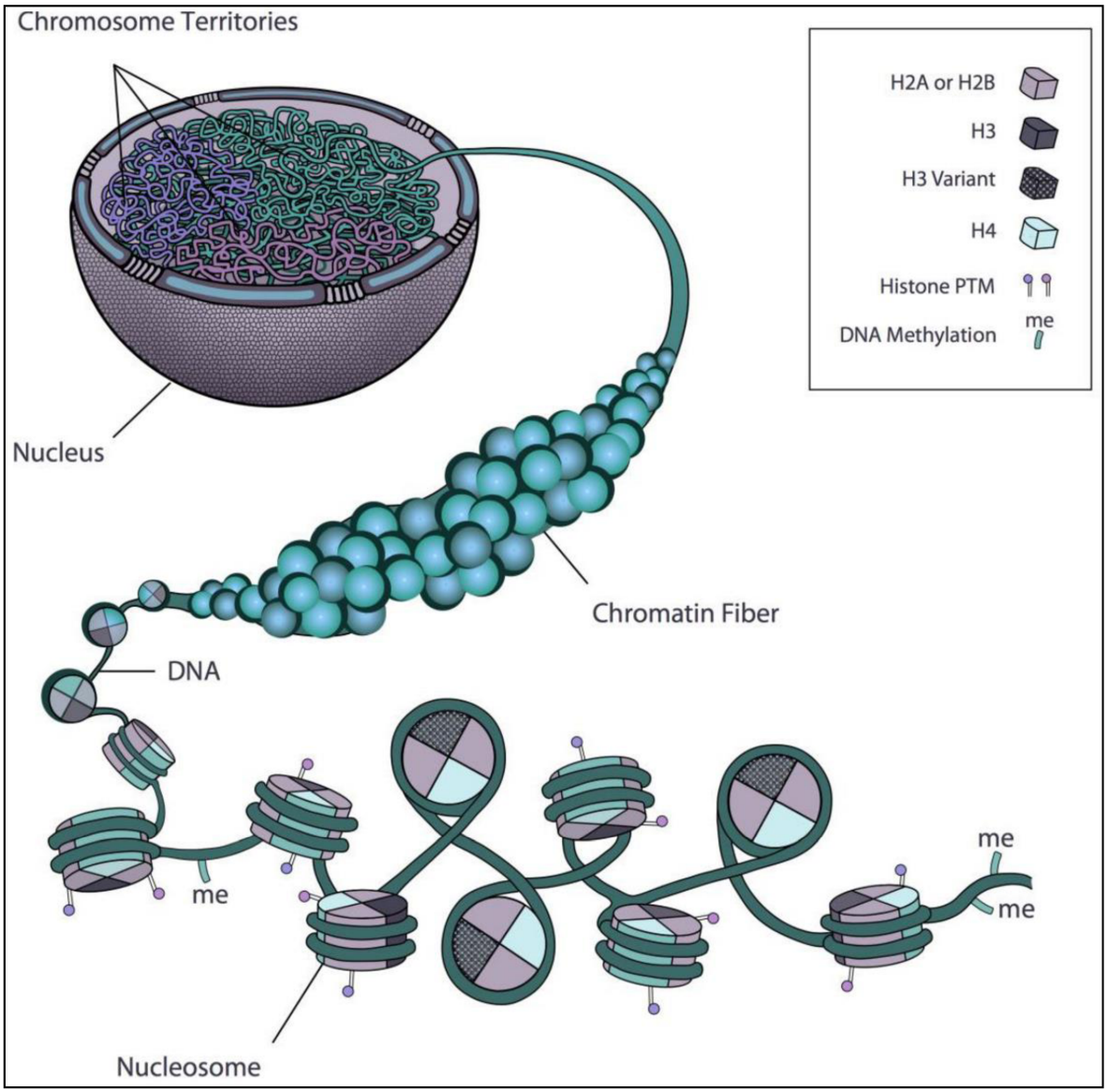

Figure 1: Histones form an octameric unit, composed of core histones (H2A, H2B, H3, and H4) and linker histones (H1; in few organisms H5). The H3-H4 dimers combine to form an H3-H4 tetramer, which, together with two H2A-H2B dimers, constitutes the histone octamer. By winding 147 base pairs of DNA around this histone core, a nucleosome is formed, which is further linked by the H1 linker histone. Nucleosomes are then compacted into chromatin with the help of additional non-histone proteins, such as various DNA-binding proteins. This chromatin is further organized into chromatin fibers, which can be maximally condensed into chromosomes during cell division processes.[6] Figure adapted from Rosa et. al.[11].

An organism, based on its unchanging genotype, is thus able to respond to varying demands through epigenetic regulation in the form of flexible gene expression. Moreover, the potential

inheritance of these acquired epigenetic characteristics to subsequent generations contributes relevantly to evolutionary processes.[12]

Imbalances in epigenetic processes and aberrant gene expression are associated with cancer, immune and nervous system disorders and metabolic diseases. Drugs that target these epigenetic mechanisms represent a valuable therapeutic approach, which has already been successfully established in the treatment of certain cancers. Due to a broad range of potential applications and the progress achieved so far in oncology, epigenome targeting drugs hold immense potential for the treatment of complex and challenging diseases.[9, 13-14]

1.2 Epigenetic mechanisms as targets for the development of drugs

The wide variety of epigenetic modifications represents promising targets for the development of drugs for the treatment of various diseases, therefore new drug candidates with different mechanisms of action are constantly being investigated in preclinical and clinical studies (see **Figure 2**).

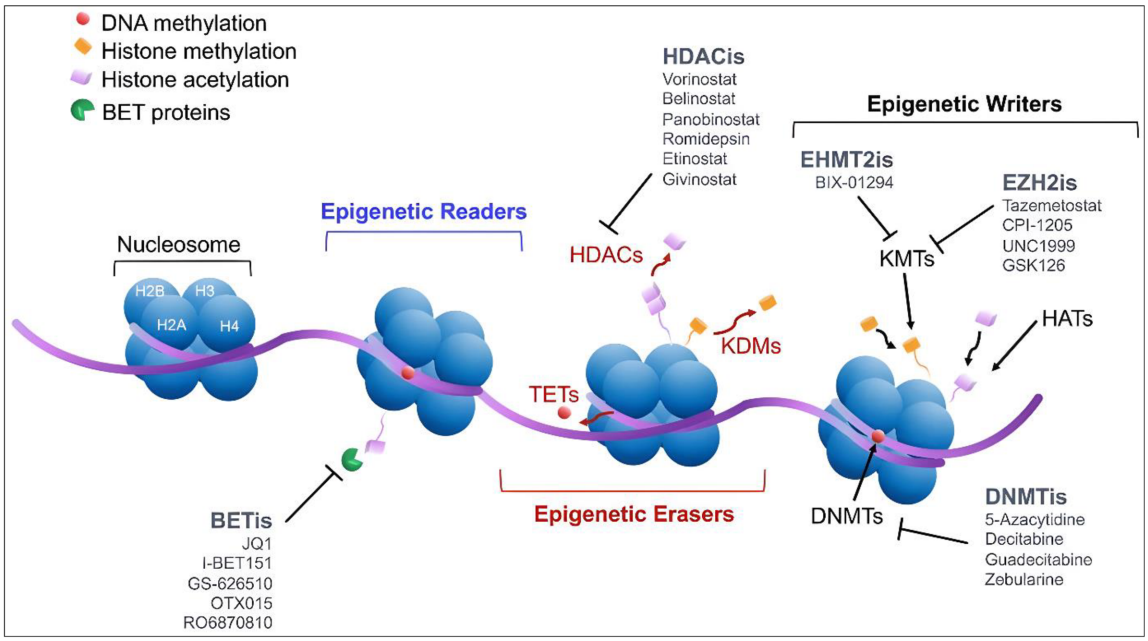

Figure 2: Key epigenetic mechanisms and selections of approved and experimental inhibitors. The figure was adapted from Citron et al.[15]. TETs (ten-eleven translocation enzymes, DNA-demethylases). HATs (histone acetyltransferases), KMTs (general term for lysine methyltransferases) and KDMs (general term for lysine demethylases). EHMTis 2: euchromatic histone-lysine N-methyltransferase 2 inhibitors). BETis: bromo-and extra-terminal domain inhibitors. Bromodomains are protein domains that bind to acetylated lysine residues on histones, recruiting chromatin-modifying proteins that promote transcription factors and euchromatin formation, indirectly influencing the activity of histone-modifying enzymes.[16]

By addressing directly related epigenetic mechanisms such as DNA methylation, histone methylation and histone deacetylation, several drugs have already been successfully approved as anticancer agents (see **Figure 3**).[16-17] A key epigenetic regulation is the DNA methylation

of the cytosine base, catalyzed by DNA methyltransferases (DNMTs), which hinders the binding of transcription factors and creates a more condensed chromatin structure, reducing accessibility for gene transcription. FDA approved DNA methyltransferase inhibitors (DNMTis), such as Azacitidine and Decitabine, block these processes, leading to the reactivation of silenced tumor suppressor genes.[18]

In addition to direct chemical modifications of DNA, histone modifications are also playing a crucial role in epigenetic regulation[19]. The complex interplay between methylation and demethylation, as well as acetylation and deacetylation of N-terminal amino acids of histones, catalyzed by specific enzymes, is fundamental for major epigenetic processes and serves as a relevant target for established therapeutic agents[20].

Histone methyltransferases (HMTs) catalyze the N-methylation of specific lysine or arginine residues on histones, which depending on the position and number of methyl groups, can lead to either gene activation or repression by altering the chromatin structure. For example, Tazemetostat, an FDA-approved EZH2 methyltransferase inhibitor (HMTi), reduces excessive cancer-related enzyme activity, promoting the reactivation of corresponding tumor suppressor genes.[21] Histone deacetylase inhibitors (HDACis), such as the FDA-approved Vorinostat, Romidepsin, Belinostat and Panobinostat, prevent the removal of acetyl groups from N-acetylated lysine on histones, therefore reducing the ionic interactions between the DNA strand and histones. The resulting relaxed chromatin structure enables increased gene expression, leading to antiproliferative effects such as the activation of tumor suppressor genes and the induction of apoptotic processes in corresponding cancer cells.[22-23]

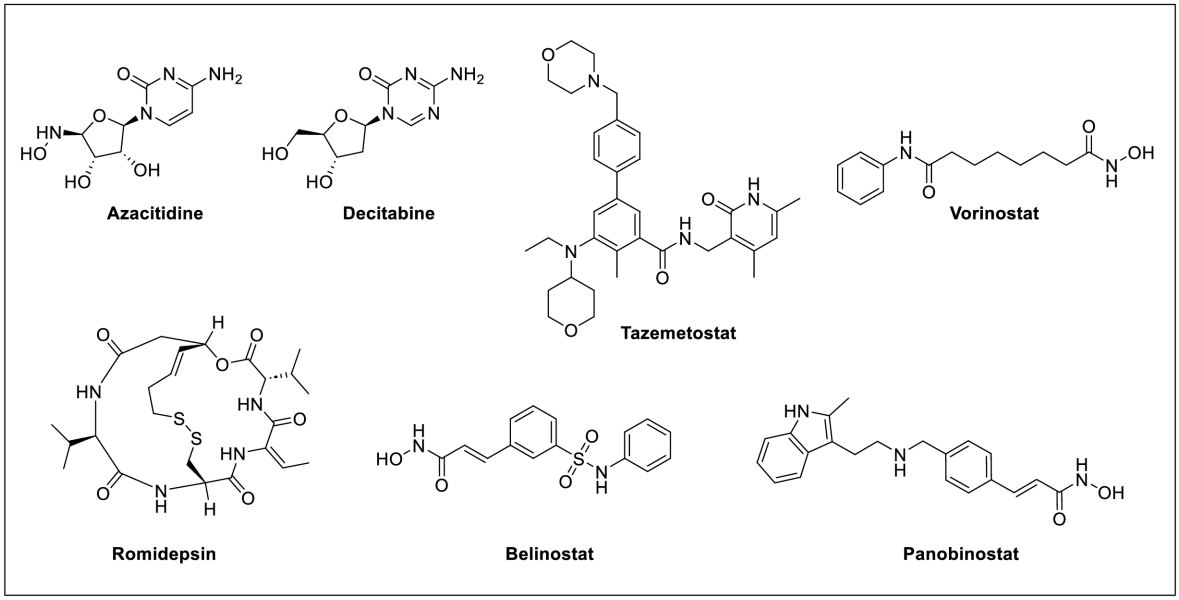

Figure 3: FDA-approved (as of 2023) drugs that directly affect epigenetic mechanisms (cf. lit. [17, 24]).

1.3 Unique feature of sirtuins within histone deacetylases

Histone deacetylase inhibitors display an important therapeutic option in oncology, representing a significant advance in the treatment of certain types of cancer. As of 2023, of the seven FDA-approved drugs that directly affect epigenetic mechanisms, four of them (Vorinostat, Romidepsin, Belinostat and Panobinostat) are histone deacetylase inhibitors.[16-17, 25] Based on their homology to yeast proteins, histone deacetylases (HDACs) are classified into four main classes (I-IV), with corresponding subtypes showing different cellular localizations and functions. They are furthermore categorized according to their catalytic mechanism into zinc-dependent (classes I, II and IV) and nicotinic adenine dinucleotide (NAD^+)-dependent (class III, also known as sirtuins). Moreover, the sirtuins are subdivided into seven subtypes (Sirt1-Sirt7) due to the successive discovery of their individual functions and cellular localizations (see **Figure 4**).[26-27]

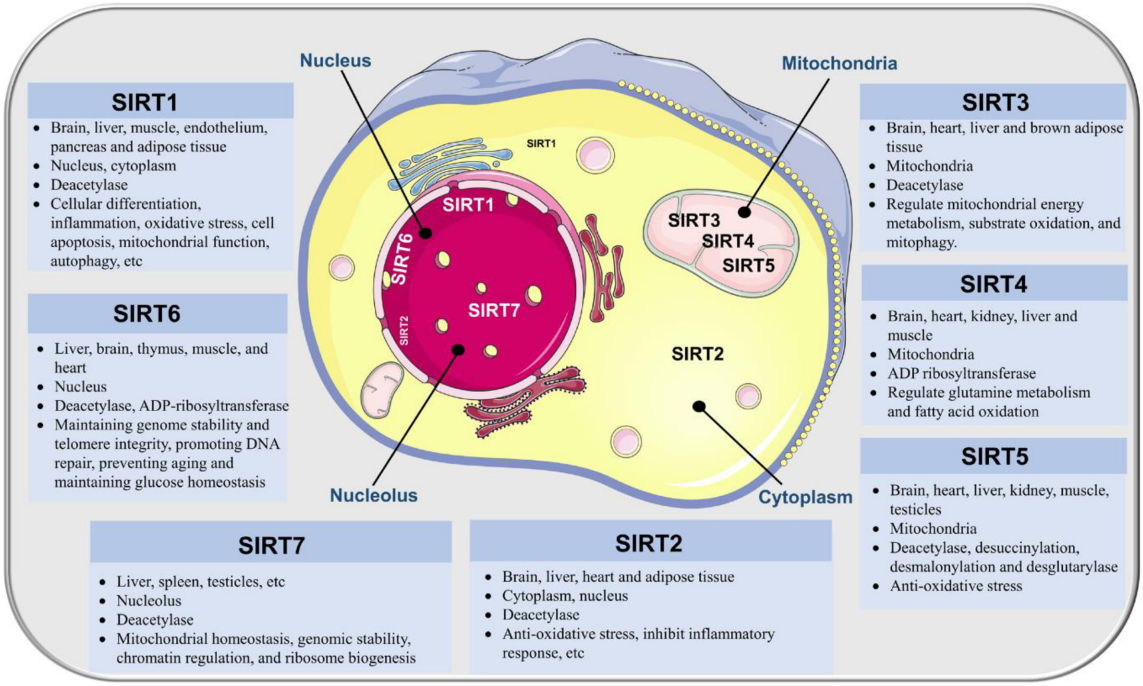

Figure 4: Overview of the seven sirtuin subtypes focusing cell localization, predominant tissue expression and related physiological effects. Although sirtuins are primarily known as deacetylases, some also carry out additional or alternative key catalytic functions. The figure was adapted from Liu et al.[28].

All currently (as of 2023) approved histone deacetylase inhibitors target the zinc-dependent classes and are used to treat various cancer related diseases[25]. Despite their fundamental involvement in various cellular processes and the resulting therapeutic potential in the treatment of cancer and immunological, neurodegenerative and metabolic diseases, the sirtuin regulators unfortunately have not been convincing in clinical trials yet[13, 29-31]. Further extensive research is therefore necessary to understand the effects of sirtuins and to unlock their

therapeutic potential for the treatment of related diseases through the development of new drugs[32].

1.4 Sirtuin 2 and current state of research on corresponding inhibitors

Recent findings highlight the importance of Sirtuin 2 (Sirt2) in the treatment, understanding and pathogenesis of complex diseases such as cancer, Alzheimer's disease, Parkinson's disease, and Huntington's disease. The development and application of highly potent and selective Sirtuin 2 inhibitors thereby showed several promising treatment effects and is therefore a crucial contribution to the investigation of the pathophysiological roles of Sirt2 and its fundamental part in epigenetic processes.[33-35] Unlike inhibitors of zinc-dependent histone deacetylases, equipped with zinc-binding structural motifs, sirtuin inhibitors require a different and more general medicinal chemistry design due to their NAD^+ dependency (catalytic mechanism described in Chapter 3.2.1, **Figure 15**) and the distinct structural environment within their active sites[36]. Over the past several years, substantial progress has been made in the discovery and development of highly potent and selective Sirt2 inhibitors (see **Figure 5**).

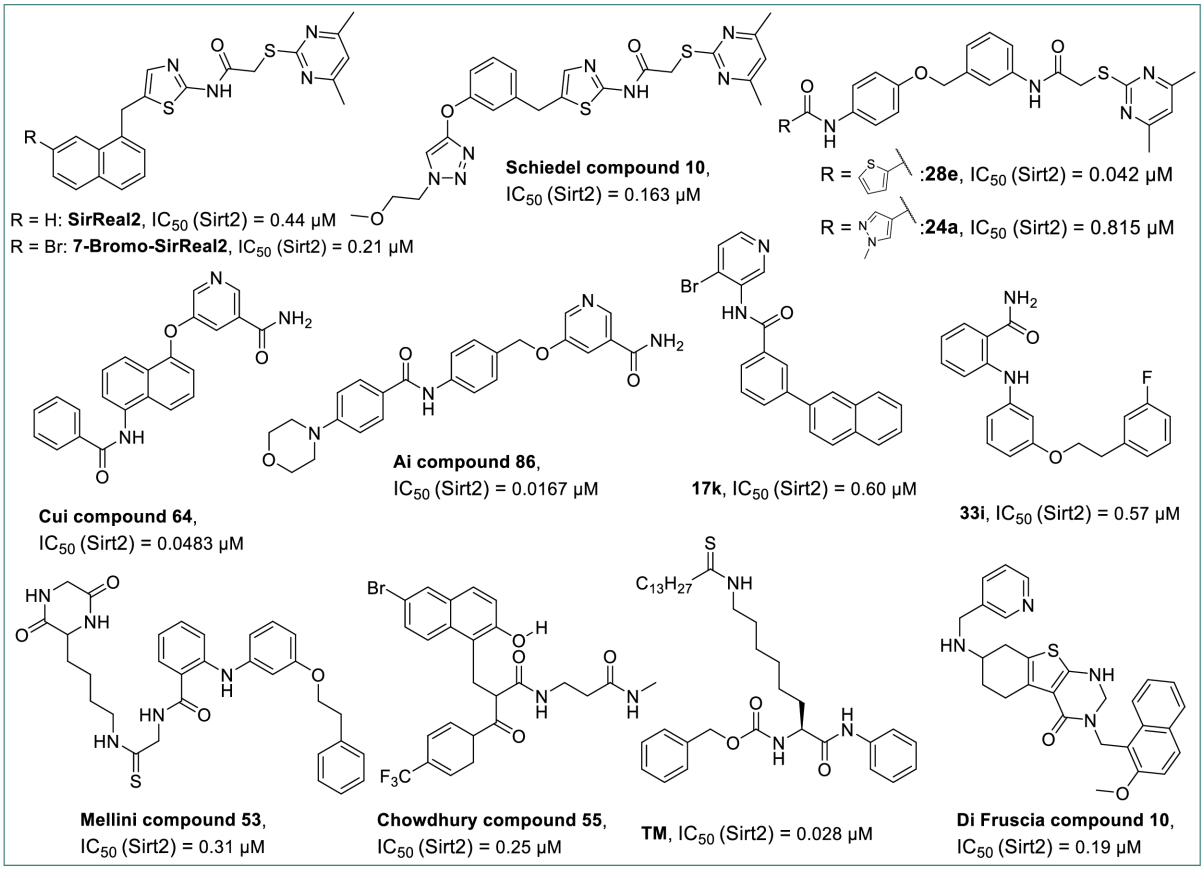

Figure 5: Selection of current (as of 2024) highly potent submicromolar Sirt2 inhibitors displaying respective chemical structures and inhibitory activities (cf. lit. [37-40]). The IC_{50} values (inhibitory concentration 50%, substance concentration to achieve half maximal target inhibition) shown are to be treated with caution regarding direct comparability, as the individual test conditions differ.

The revolutionary discovery of SirReal-type inhibitors (sirtuin-rearranging ligands) and selectivity pocket binder principle by Prof. Manfred Jung (Freiburg, Germany) marks a milestone in the systematic structural design of inhibitors and especially extensive investigations on **SirReal2** contributed significantly to deeper understanding of the structure-activity relationships and requirements of the catalytic center of Sirt2[38, 41].

Through ligand-induced structural rearrangement within the catalytic center of Sirt2, an *in situ* formation of a so-called "selectivity pocket" occurs, allowing the occupation of a structural element with appropriate chemical properties (in the case of SirReal-inhibitors, the 2-((4,6-dimethylpyrimidin-2-yl)thio)acetamide moiety)[40, 42-43].

Based on the selectivity pocket binder motif of the original SirReal-inhibitors, further structural variations and analogues were developed that exhibit extended binding modes and show increased potency (for example **Schiedel compound 10**, **28e** and **24a**, see **Figure 5**). Furthermore, additional inhibitors were discovered that induce the selectivity pocket of Sirt2 and occupy it with various novel selectivity pocket binding motifs of different chemical structures (see **Figure 6**).

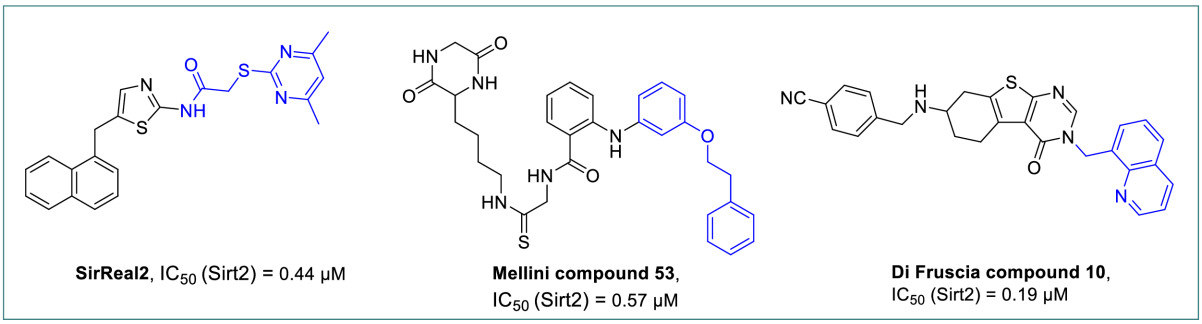

Figure 6: Selection of highly potent and selective Sirt2 inhibitors taking advantage of the induced selectivity pocket ensuring favorable ligand alignment and subtype selectivity, confirmed by crystal structure analysis (cf. lit. [42, 44-45]). Blue coloring marks the structural part referred to as the selectivity pocket binder motif, interacting with the Sirt2 selectivity pocket formed in the respective ligand binding process.

In consequence, a selective binding principle results for Sirt2 over other sirtuin subtypes and corresponding inhibitors provide the foundation for a high inhibitory potential for Sirt2[39, 41, 46].

The catalytic domain (see **Figure 7**) of Sirt2 contains binding sites for the substrate, specifically the N-terminal acetylated lysine of histones (lysine channel), and the cofactor NAD^+. In this process, the nicotinamide from NAD^+ is accommodated in the C-pocket, while the corresponding ADP-ribose is taken up by the A- and B-pockets.[47] Although established Sirt2 inhibitors generally target the same binding site, they can influence the function of the enzyme and its conformation in different ways, making interactions between the substrate and cofactor more difficult, thereby weakening the catalytic processes[48-50].

Due to the flexibility of the enzyme and the tendency for certain rearrangements, such as the formation of the selectivity pocket or other structural configurations, additional inhibitory

opportunities are possible. The specific orientation and interactions within the binding site are diverse, leading to various binding modes that target the C-pocket, the extended C-site (ECS) including the selectivity pocket and the lysine channel (substrate channel). Notably, in terms of medicinal chemistry strategy development the combination of different binding modes has led to the discovery of the most potent and selective Sirt2 inhibitors known to date.[47, 51-52]

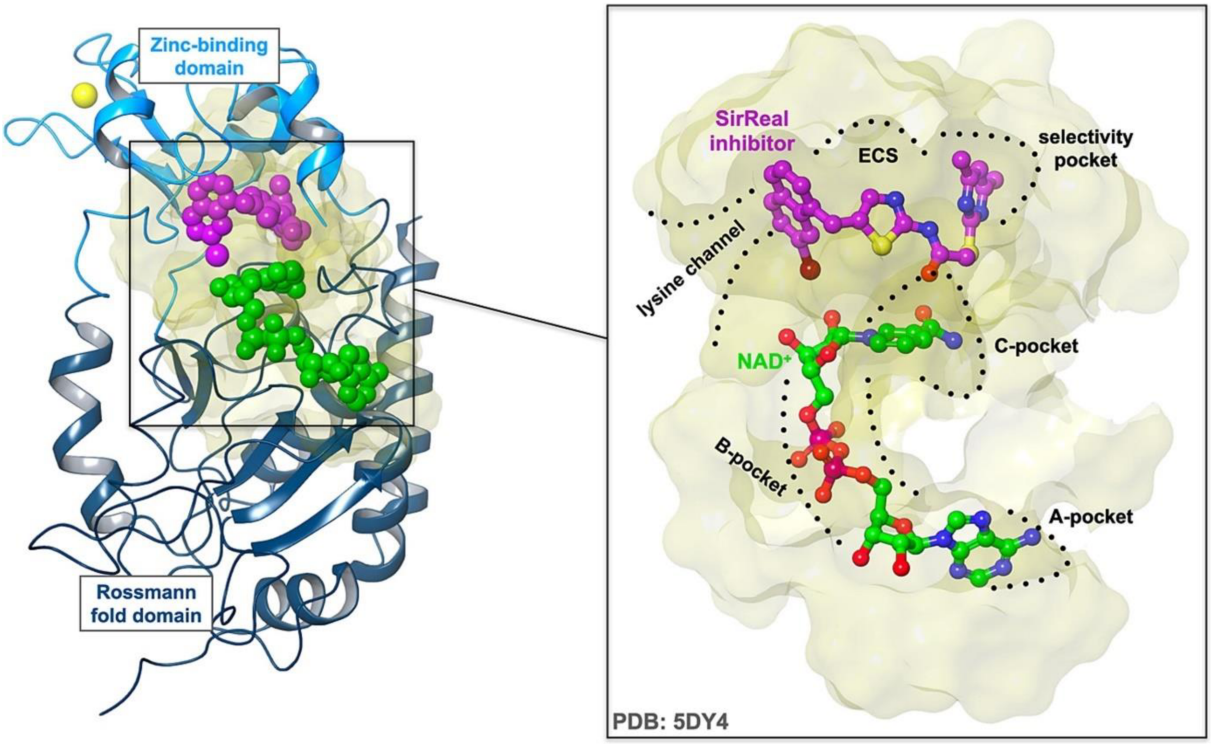

Figure 7: Insights into the active site of Sirt2 and detailed display of the respective binding pocket. The common binding mode of SirReal-type inhibitors is vizualizied by the spartial orientation of the crystal structure of **7-bromo-SirReal2** and NAD^+ within the catalytic center of Sirt2. The figure was adapted from Kaya et al.[52].

Knowledge of the selectivity-pocket binding principle and its potential for the development of highly potent and selective Sirt2 inhibitors provides a promising opportunity for further medicinal chemistry approaches to extend structure-activity relationships and thus represents a valuable pharmaceutical contribution to sirtuin research through the design and synthesis of novel inhibitors.

2 Objectives

The discovery of the selectivity pocket binder principle opens a multitude of variations and possible applications for improving existing structures and designing new compounds. The fundamental idea of this thesis is to build a library of new generation high potent and selective Sirt2 inhibitors by synthesizing novel compounds in order to make a decisive contribution to the understanding of the structure-activity relationship of Sirt2 inhibitors. Due to its extensive cellular function, Sirt2 is involved in a wide variety of physiological and pathophysiological development processes. For this reason, the synthesized compounds can act as chemical tools to deeper investigate the corresponding cellular processes. The therapeutic relevance of developing novel inhibitors is underlined by the fact, that selective inhibition is associated with numerous positive effects in the treatment of neurodegenerative and tumor related diseases. Guided by docking experiments, the aim of this dissertation is to optimize selected lead compounds by approved medical chemical approaches such as rigidization, introduction of electrophilic warheads to target cofactor NAD^+ by covalent binding mechanism and lead structure-based hybridization drug design.

One of the most important representatives of Sirt2 inhibitors based on the selectivity pocket binder principle is **SirReal2** published by Rumpf *et al.*[42] and the corresponding modifications (e.g., compound **28e**) by Yang *et.al.*[53] (see **Figure 8**).

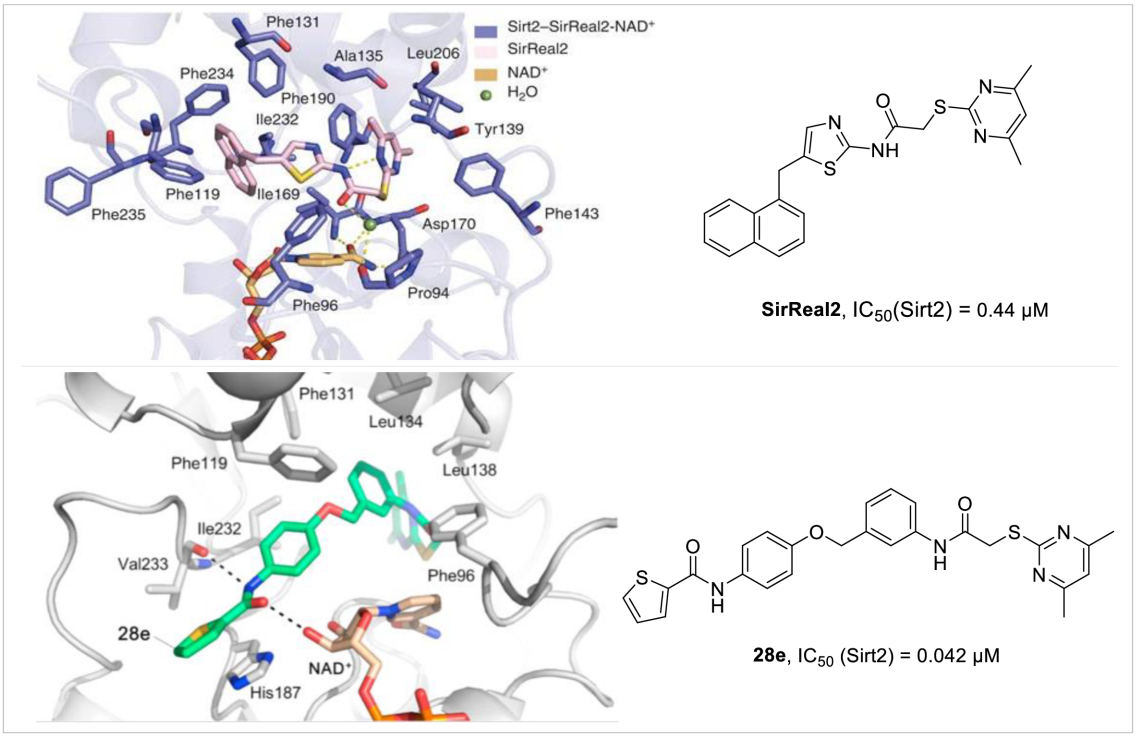

Figure 8: (a) Crystal structure of **SirReal2** (adapted from Rumpf *et al.*[42]) and docking pose of **28e** (adapted from Yang *et al.*[53]) with Sirt2, as well as chemical structures and published biological activities.

Crystal structure analysis of **SirReal2** (published IC_{50} value: 0.44 µM on Sirt2) reveals that the substrate channel residue binding processes can be significantly characterized by the hydrophobic interactions of the naphthyl group with various phenylalanine residues of the protein[40, 42]. In contrast, **28e** (published IC_{50} value: 0.041 µM on Sirt2) is equipped with a thiophene-2-carboxamide residue instead, which enables additional polar interactions with Ile232 and the cofactor NAD^+ according to prediction[53]. Inspired by **SirReal2** and **28e**, this thesis focuses on the development of new selective SirReal-type Sirtuin 2 inhibitors using different medicinal chemistry approaches to optimize the inhibitory potential of the corresponding lead compounds. Systematic rigidization using suitable spacers aims for an ideal geometrical arrangement of the polar amide residue of **28e**, whereby the angular orientation caused by the ether partial structure should be frozen and mimicked. Various functional groups such as boronic acids, nitriles and aldehydes are suitable warheads for the development of inhibitors offering a reversible covalent binding mechanism. Introduced in a proper position in lead compound **SirReal2**, the spatial proximity to NAD^+ should enable the interaction with this cofactor and thus provide a further inhibitory mode. Using lead structure-based drug design, hybrid compounds of **28e** and **SirReal2** represent promising inhibitor candidates that combine the structural advantages of both lead compounds. The different approaches to the envisaged lead compound optimization are illustrated in **Scheme 1**.

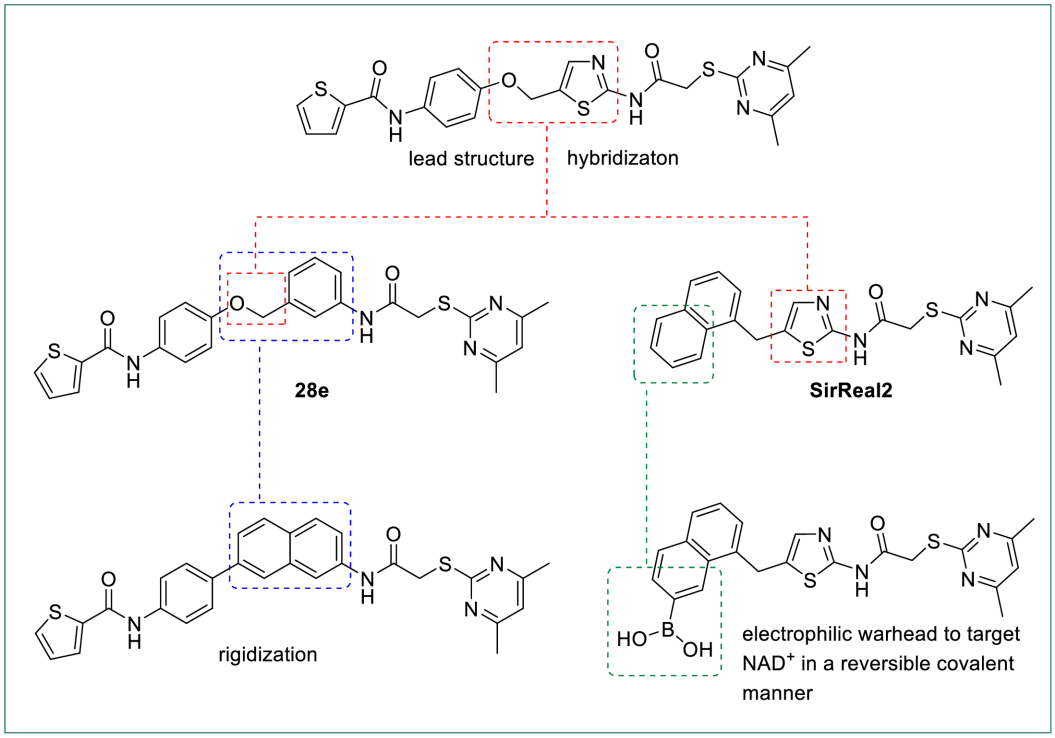

Scheme 1: Overview of different approaches and the associated structural variations with regard to lead structure optimization. The concrete derivations from the lead compounds presented are also to be extended by further structural variations for a comprehensive structure-activity relationship study.

3 Results and discussion

3.1 Rigidization approach of lead compound 28e to increase the inhibitory activity towards Sirt2

3.1.1 Rigidization as a fundamental principle of structural optimization in medicinal chemistry

Rigidization is an established method in medicinal chemistry for optimizing the lead structure in order to increase the binding affinity and thereby the corresponding biological activity of a ligand. By introducing rigid structural elements, the flexibility of the molecule is restricted and the number of possible conformations is reduced so that the therefore preorganized structure can selectively bind to the appropriate target with a decisive entropic advantage.[54-56]

The strength of a protein-ligand interaction is described by the free Gibbs energy of binding (G), which is influenced by enthalpy (H), entropy (S) and temperature (T). The individual variables are related *via* the Gibbs equation $\Delta G = \Delta H - T\Delta S$. A negative ΔG indicates a thermodynamically favorable binding process. Enthalpy represents the strength and type of interactions (mainly hydrophobic, electrostatic, complexometric and H-bonds) between the protein and the ligand, while entropy describes the degree of disorder of the corresponding system. A conformational constraint through rigidization reduces the flexibility and degrees of freedom of the ligand, resulting in a lower entropy, which may advantageously impact the binding free energy in total, increasing the protein-ligand binding affinity.[57]

However, it is important to consider with rigidization efforts that enthalpy and entropy can be interdependent. Although the introduction of a rigid element can increase entropy, it may reduce protein-ligand interactions and thus ΔH, too. Ideally, enthalpy and entropy contribute synergistically to a significant increase in affinity, through rigidization improving ligand interactions on the one hand and reduced degrees of freedom leading to a particularly favorable decrease in ΔG on the other. However, strong conformational constraints may still carry risks, as in addition to altered interactions, steric effects of the corresponding rigidizing structural elements may hinder protein-ligand binding.[58] Nevertheless, a rigidization approach provides valuable insights into structure-activity relationships and is therefore an important tool within drug development processes[54].

Figure 9 illustrates the principle of structural optimization by means of rigidization by comparing a rigidized molecule with its more flexible predecessor. Usually, conformations are restricted by aliphatic linkers in terms of cyclization, however aromatic ring structures that exhibit significant changes in chemical structure can contribute to enhancing the desired biological effect, as seen in the case of Adapalene.

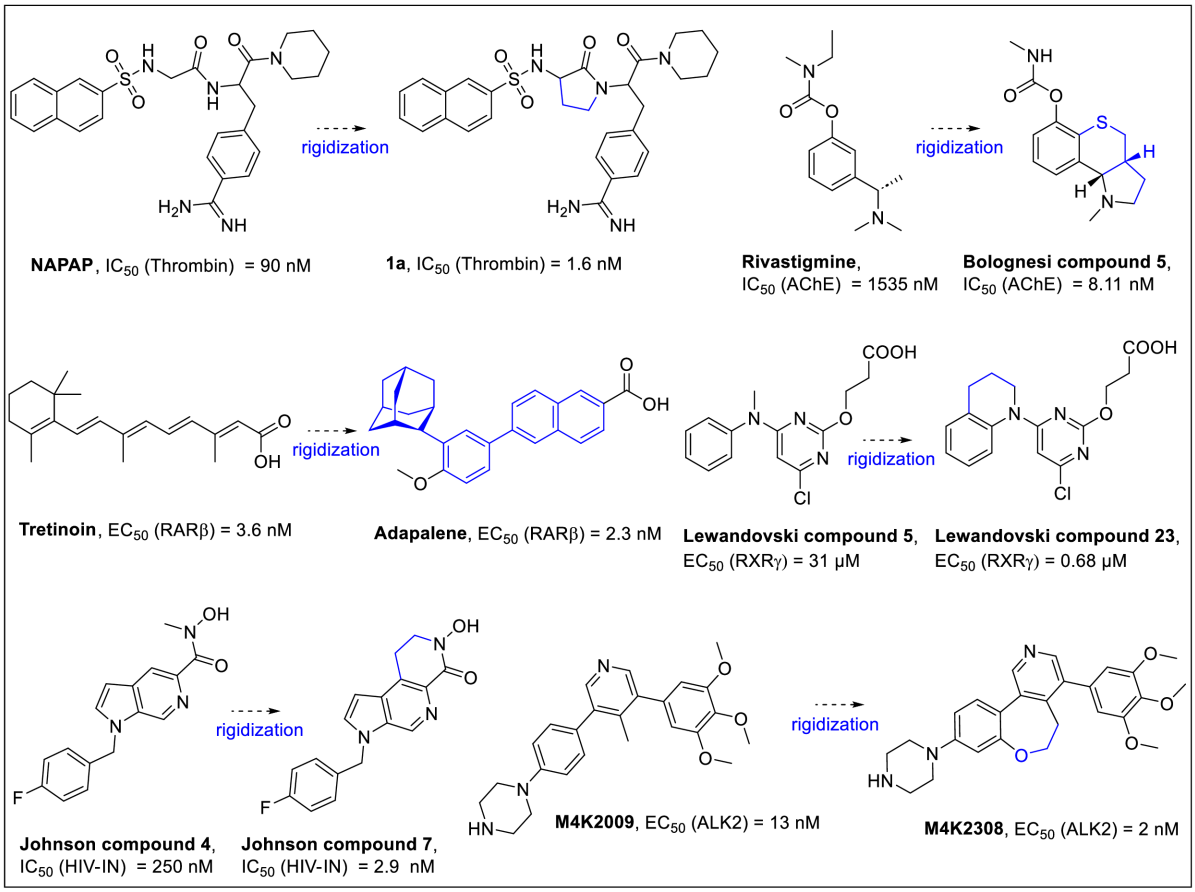

Figure 9: Selection of successfully rigidized molecules and the corresponding predecessors with related biological activities (cf. lit.[54, 56, 59-63]). Illustration of the implemented conformal restrictions in blue coloring. Abbreviations: EC_{50} (effective concentration 50%): substance concentration to achieve 50% of the maximum biological effect. AChE: acetylcholinesterase, RAR: retinoic acid receptors, RXR: retinoid X receptor, HIV-IN: retroviral integrase of human immunodeficiency viruses, ALK2: activin receptor-like kinase-2.

These examples visualize that rigidization of certain structure elements may represent a powerful strategy to enhance biological activity of compounds, therefore corresponding possibilities of conformational restriction with regard to the development of novel Sirt2 inhibitors are to be investigated subsequently. Based on lead compound **28e**, the rigidization potential was evaluated in advance in docking experiments in order to identify promising candidates.

3.1.2 Docking studies guided strategy to identify high potential rigid analogues of lead compound 28e

The docking pose analysis of **28e** indicated the potential for the application of a rigidization approach (see **Figure 10**). The respective docking experiments were carried out by our cooperation partner Dr. Thomas Wein, for further experimental details see Chapter 5.4.1. The presence of the ether group enables a high degree of spatial freedom, which can be restricted using a corresponding naphthalene element, resulting in candidate **FM50** (see **Figure 10**). Here, the molecular angulation occurring in the binding pocket is represented by the rigidization. Benzothiazole **FM129** was selected to provide an additional rigid variation due to its 6-plus5-ring characteristics and the associated change in geometric orientation of attached residues. In addition, this element was preferred, along with various other conceivable options, firstly because of its synthetic accessibility and secondly because of the structural similarity of the aminothiazole partial structure of **SirReal2**.

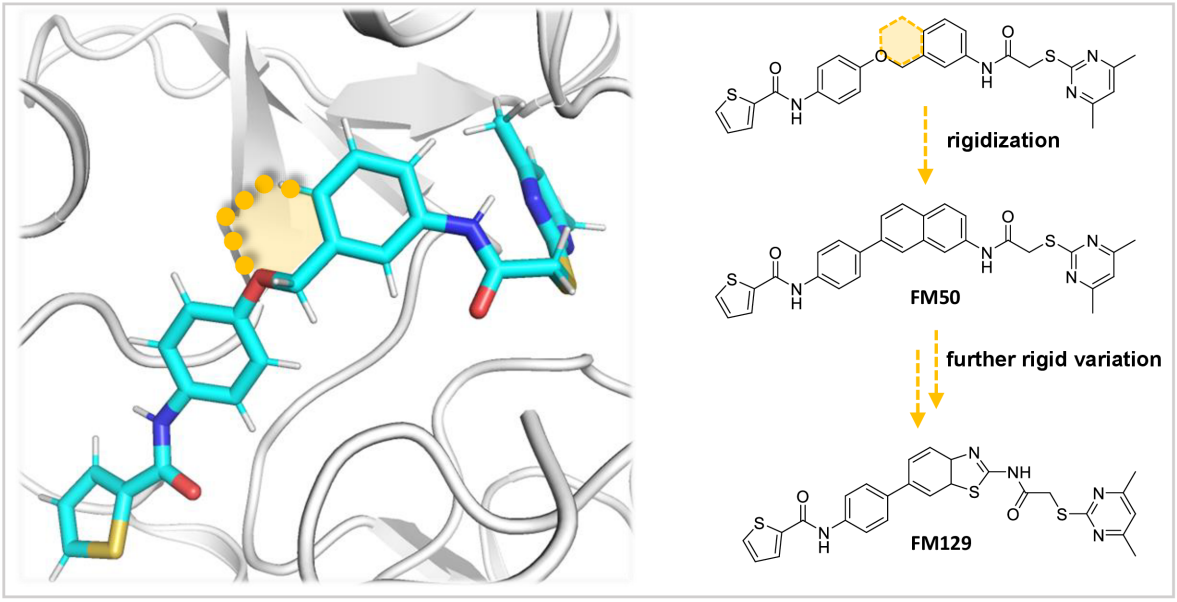

Figure 10: Sirt2 docking pose (based on PDB ID: 5YQO) of **28e** and vizualisation of the fundamental rigidization condsiderations **FM50** and **FM129**.

These initial ideas should then be validated in a further docking experiment (see **Figure 11**), which involves the specific structural variation of **28e** with a naphthyl element (**FM50**) and an alternative benzothiazole structure (**FM129**). The docking experiment of the two main rigid candidates (**FM50** and **FM129**) showed very promising results. **FM50** (red) displays a similar binding mode as the reference compound **28e** (blue), especially the selectivity pocket binder structure motif (2-((4,6-dimethylpyrimidin-2-yl)thio)acetamide moiety) in the right-hand part of the molecule is perfectly aligned and thus should guarantee high selectivity. According to calculations, **FM50** rigidized by the naphthalene element occupies the position of the replaced

benzyl ether structure and the geometry framed by the naphthalene motif in this case enables the substrate channel residue to be directed into the desired orientation.

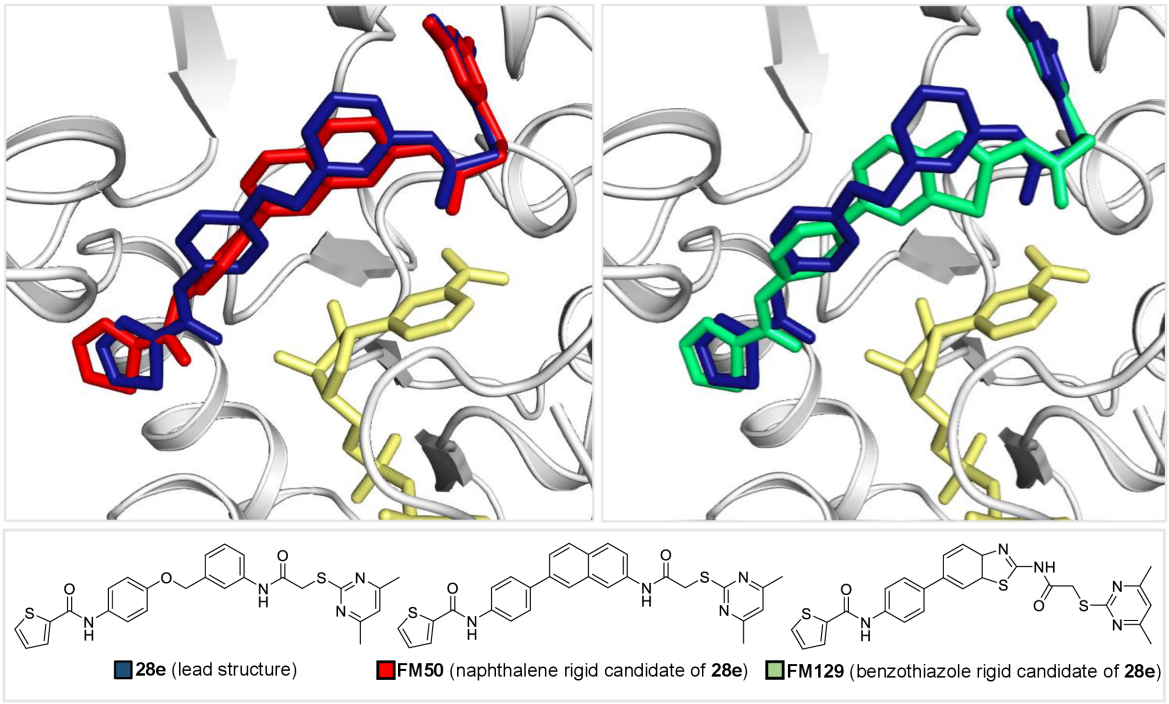

Figure 11: Sirt2 docking poses of rigid variations (PDB ID: 5YQO prediction), lead compound **28e** (blue) acts as reference. NAD^+ (in yellow) is displayed as PDB ID: 4RMG extraction. Left) Naphthalene-based rigid candidate **FM50** (red). Right) and benzothiazole-based rigid candidate **FM129** (green).

The docking calculation for benzothiazole **FM129** (green) likewise predicted a spatial orientation within the Sirt2 binding pocket that is comparable to the reference substance **28e**, showing a notable overlap with the substrate channel and the selectivity pocket residue. The benzothiazole partial structure in this case is located in the same binding region as the benzyl ether to be replaced, although the benzothiazole structure has an even stronger orientation towards NAD^+.

Based on these encouraging docking study results, an effective synthesis route for the presented rigidized target compounds should be established. The rigid naphthalene and benzothiazole elements constrain the bonding geometry and align the substrate channel residue accordingly. Replacing the thiophen-2-carboxamide residue in the intended rigid target compounds **FM50** and **FM129** with various amide-containing substrate channel residues offers further interaction potential and introduces additional structural diversity, facilitating the development of a comprehensive compound library of rigidized molecules for structure-activity relationship studies (see subsequent Chapter 3.1.3).

3.1.3 Synthesis of selected rigid analogues of lead compound 28e

To characterize the effect of rigidization more precisely, the further benzyl ether structures based on **28e** previously published by Yang *et al.* were predominantly used as reference and the most promising variations were equipped with the corresponding rigid elements[53]. Following this article, the selected candidates with high inhibitory potential are characterized by different amide-based substrate channel residues and their corresponding substitution in *meta* and *para* position. Based on these specifications, the envisaged target compounds were identified resulting in a total of 20 molecules as rigid analogues of **28e** (see **Scheme 2**).

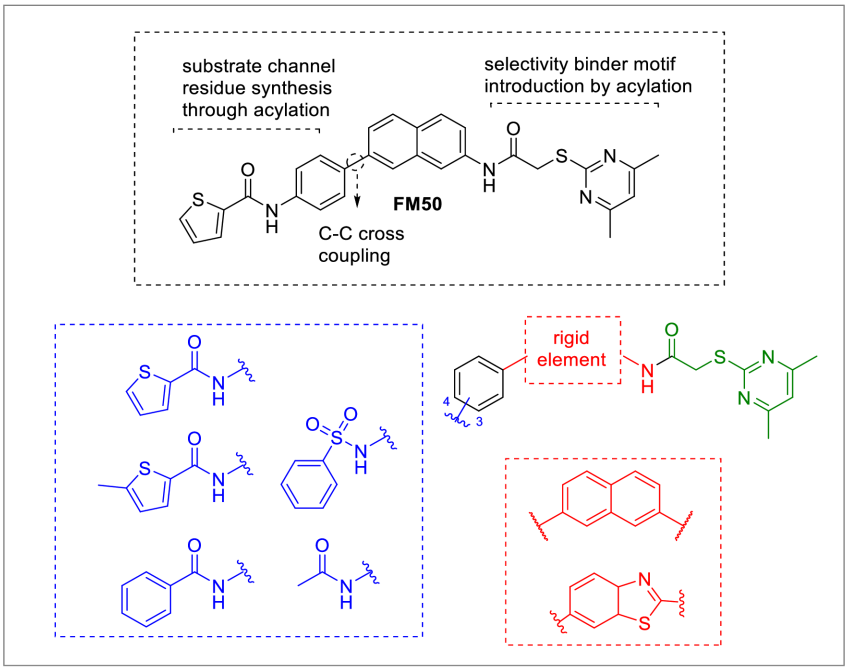

Scheme 2: Intended rigidized target compound library and fundamental approach of the synthesis strategy, exemplified by **FM50**; the naphthalene element rigidized version of **28e**.

A synthesis strategy was subsequently developed to provide general access to the desired target compounds. Briefly, the fundamental intention was to link naphthalene and benzothiazole to the selectivity pocket binding motif and, through C-C coupling, establish the foundation for the subsequent introduction of amide-based substrate channel residues.

3.1.3.1 Naphthalene-based rigid analogues of lead compound 28e

The initial approach involved connecting the naphthalene element to the selectivity pocket binder motif to subsequently prepare the desired compounds by cross-coupling and amidation reactions (see **Scheme 3**). A decisive advantage of this efficient 5-step synthesis design is the early introduction of the selectivity pocket binder motif (2-((4,6-dimethylpyrimidin-2-yl)thio)acetamide moiety), which protects the molecule from subsequent selectivity difficulties in the amide synthesis of the substrate channel residue. The preparation of the 7-phenylnaphthyl-2-amine substructure is the crucial part of the synthesis design, which is based on the central building block 7-bromonaphthalen-2-amine, obtained by a literature-known protocol[64] *via* Bucherer reaction[65]. Following the addition of sodium bisulfite to the C-4 position of alcohol **1**, the predominantly tautomeric keto group at C-2 undergoes nucleophilic attack by ammonia, leading to the formation of the 2-naphthylamine **2** after dehydration[66].

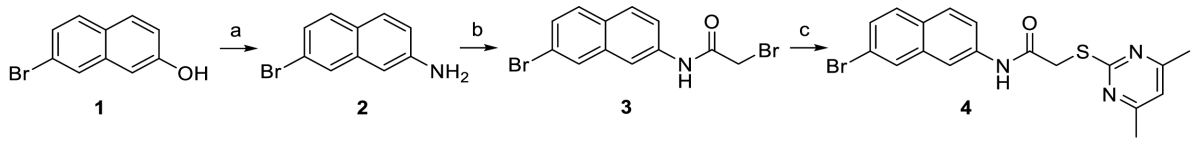

Scheme 3: Primary synthesis strategy with early introduction of the selectivity pocket binder motif. Conditions: a) $NaHSO_3$, NH_3 (aq., 25% w/w), 180 °C, 72 h, 88%; b) 2-bromoacetyl bromide, DCM, rt, 2 h, 82%; c) 4,6-dimethylpyrimidine-2-thiol, DMF, *t*-BuOK, rt, 4 h, 89%.

The next step included the introduction of the selectivity pocket binder motif, which is inspired by the literature-known two-step procedure[40] consisting of N-acylation of the amine **2** using 2-bromoacetyl bromide with subsequent formation of the thioether **4** *via* base catalyzed (*t*-BuOK) S_N2-reaction of compound **3** with 4,6-dimethylpyrimidine-2-thiol. The bromine substitution of **4** enabled the synthesis of the required 2-phenylnaphthalene unit by Suzuki reaction. Unfortunately, neither the originally desired amine **5** nor the nitro-substituted alternative **6** could be obtained using various reaction conditions (see **Table 1**).

Standard Suzuki conditions include the use of potassium carbonate, catalyst $Pd(PPh_3)_4$, and the appropriate boronic acid in DMF. Initially, commercially available 4-(aminophenyl)boronic acid pinacol ester, was used. However, after a failed synthesis, the reaction was attempted with a different catalyst, palladium acetate, but this also remained unsuccessful. Due to the stronger electron-withdrawing properties and the lack of nucleophilic reactivity, additional attempts were made using 4-(nitrophenyl)boronic acid, although this required an extra step for the reduction of the nitro group to an amine. Unfortunately, this did not have a beneficial effect on the reaction outcome. A plausible explanation for this unsuccessful conversion might be the presence of the sulfur atom in the reactant, potentially reducing the catalytic activity of the palladium species, therefore further attempts to optimize the Suzuki reaction were not pursued

and the synthesis strategy was adapted so that no additional synthesis steps were required. For this purpose, the Suzuki reaction with 7-bromonaphthalene-2-amine (**2**) as reactant was carried out first followed by the introduction of the selectivity pocket-binding motif.

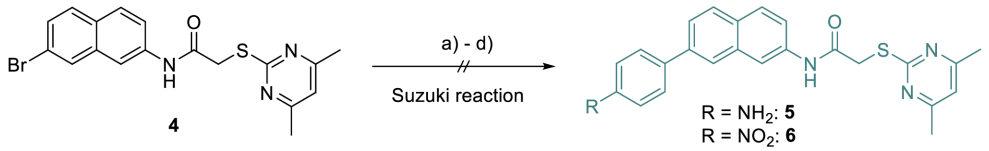

entry	residue	boronic acid	catalyst	conditions	yield [%]
a	$-NH_2$	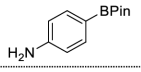	$Pd(PPh_3)_4$	K_2CO_3, DMF, 105 °C, 23 h	0
b	$-NH_2$	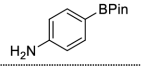	$Pd(OAc)_2$	K_2CO_3, DMF, 105 °C, 23 h	0
c	$-NO_2$	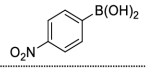	$Pd(PPh_3)_4$	K_2CO_3, DMF, 105 °C, 23 h	0
d	$-NO_2$	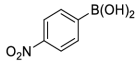	$Pd(OAc)_2$	K_2CO_3, DMF, 105 °C, 23 h	0

Table 1: Suzuki cross coupling reactions attempts using compound **4** as precursor.

Remarkably, this reaction was successful at the first attempt using previously the presented conditions and 7-(4-nitrophenyl)naphthalen-2-amine (**7**) was isolated with a yield of 42% (see **Scheme 4**). Therefore, the nitro substituted boronic acid was used, as otherwise the obtained ring would contain two aromatic amines. Leading to selectivity problems in subsequent reactions, the nitro group acts as a protecting group in this case so the naphtalene-2-amine structure is acylated exclusively.

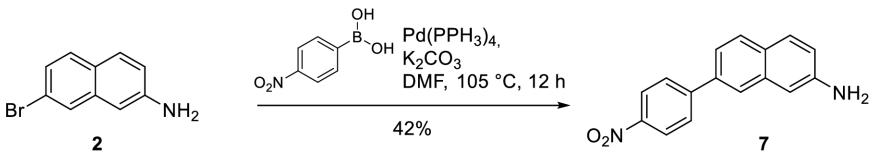

Scheme 4: Successful preparation of 7-(4-nitrophenyl)naphthalene-2-amine (**7**) as first step of the rearranged synthesis route *via* Suzuki reaction with 7-bromonaphthalen-2-amine (**2**).

Based on the established Suzuki reaction for the synthesis of compound **7**, a new synthetic approach was designed (see **Scheme 5**). In the adjusted synthetic route, 7-bromo-naphthalene-2-amine (**2**), previously synthesized *via* the Bucherer reaction, was subjected to a Suzuki reaction with the appropriate nitrophenylboronic acid, yielding compounds **7** and **8**. These compounds were then acylated *via* 2-bromoacetyl bromide. Using 4,6-dimethylpyrimidine -2-thiol and *t*-BuOK, thioethers **6** and **11** were synthesized from compounds **9** and **10**. The nitro group of compounds **6** and **11** were subsequently reduced with iron and acetic acid to afford amines **5** and **12**, used as starting materials for the preparation of various final compounds.

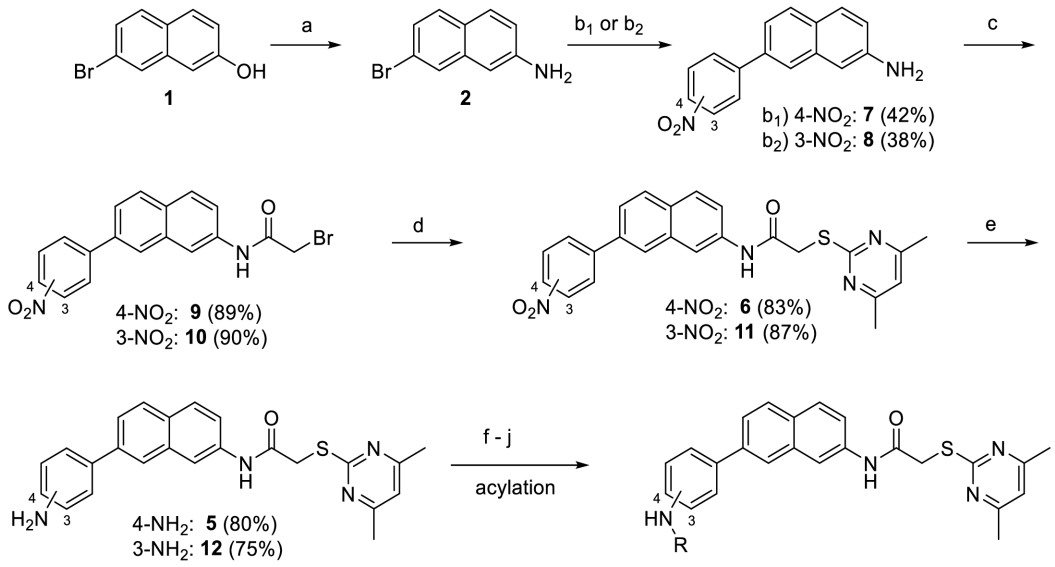

Scheme 5: Synthesis route of naphthalene-based rigid analogues of **28e**. Conditions: a) $NaHSO_3$, NH_4OH, 180 °C, 72 h, 88%; b_1) (4-nitrophenyl)boronic acid, K_2CO_3, $Pd(PPh_3)_4$, DMF, 105 °C, 23 h; b_2) (3-nitrophenyl)boronic acid, K_2CO_3, $Pd(PPh_3)_4$, DMF, 105 °C, 23 h; c) 2-bromoacetyl bromide, DCM, 0 °C, 2 h; d) 4,6-dimethylpyrimidine-2-thiol, DMF, *t*-BuOK, rt, 4 h; e) Fe, AcOH, 50 °C, 3 h; f)-j) shown in **Table 2**.

The desired target compounds, which were previously defined in Chapter 3.1.3, were finalized using appropriate carboxylic acid and sulfonyl chlorides, as well as acetic anhydride (see **Table 2**). This established synthetic route successfully yielded all 10 desired naphthalene-based rigid analogues of **28e**, whose biological activity against Sirt2 and related subtypes is presented in Chapter 3.1.4.

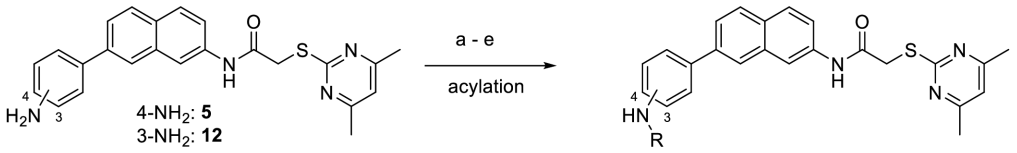

entry	reaction conditions		position	residue R	compound ID	yield [%]
f)	2-thiophenecarbonyl chloride, NEt_3, DCM	rt, 2 h	3		**FM48**	31
			4		**FM50**	53
g)	5-methylthiophene-2-carbonyl chloride, NEt_3, DCM	rt, 5 h	3	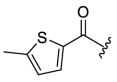	**FM66**	83
		40 °C, 3 h	4		**FM69**	74
h)	benzoyl chloride, NEt_3, DCM	rt, 2 h	3		**FM54**	87
			4		**FM53**	78
i)	benzenesulfonyl chloride, NEt_3, DCM	rt, 4 h	3		**FM47**	47
		40 °C, 7 h	4		**FM56**	40
j)	acetic anhydride, NEt_3, DCM	rt, 2 h	3		**FM46**	91
			4		**FM26**	72

Table 2: Last synthesis step and final preparation of naphthalene-based rigid analogues of **28e**.

3.1.3.2 Benzothiazole-based rigid analogues of lead compound 28e

The synthesis of the benzothiazole-derived molecules (see **Scheme 6**) was initially based on the synthesis route previously established for the naphthalene compounds.

Starting from 4-bromoaniline (**13**), 2-amino-6-bromobenzothiazole (**14**) was prepared through intramolecular cyclization using potassium thiocyanate and bromine in acetic acid, following a literature-known method[67].Unfortunately, cross coupled compound **15** using 3-(nitrophenyl)boronic acid could not be synthesized using the previously established Suzuki reaction protocol (see previous Chapter 3.1.3.1, **Scheme 4**).

However, after carrying out several test experiments, suitable reaction conditions were successfully discovered (see **Table 3**).

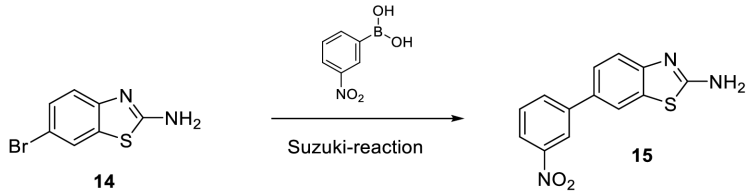

entry	base	catalyst	conditions	yield [%]
a	K_2CO_3	$Pd(PPh)_3$	DMF, 105 °C, 48 h	0
b	K_2CO_3	$Pd(OAc)_2$	DMF, 105 °C, 48 h	0
c	K_3PO_4	$Pd(OAc)_2$	dioxane/water, 95 °C, 72 h	0
d	K_3PO_4	$Pd(PPh)_3$	dioxane/water, 95 °C, 42 h	19
e	Cs_2CO_3	$Pd(PPh)_3$	dioxane/water, 80 °C, 21 h	61

Table 3: Suzuki reaction optimization to synthesize 6-(3-nitrophenyl)benzo[d]thiazol-2-amine (**15**).

By applying a method presented by Gull *et al.* using potassium phosphate in combination with catalytic amounts of $Pd(PPh_3)$ in dioxane/water, the very first preparation of the previously unknown 6-(3-nitrophenyl)benzo[d]thiazol-2-amine (**15**) was achieved with a yield of 19%[68]. A further optimization inspired by Dr. Alexandra Kamlah (research group of Prof. Franz Bracher) gave a satisfactory yield of 61% by using cesium carbonate as the base[69].

The improved Suzuki reaction conditions were subsequently used to prepare the *para*-substituted compound **16**. However, this resulted in a very low yield of 8% and unfortunately the compound **16** proved to be particularly poorly soluble in common solvents. The fact that these difficulties already occurred in the second synthesis step suggested an adjustment of the previous strategy, as a practicable and efficient method for the preparation of the target compounds should be developed. The use of 4-(*N*-Boc-amino)phenylboronic acid instead of the 4-(nitro)phenylboronic acid increased the yield of the cross-coupling reaction by 3.5-fold and provided compound **17** with significantly improved solubility properties without changing the initial synthesis route in fundamental terms. The acylation of amines **15** and **17** with 2-bromoacetyl bromide and triethylamine yielded compounds **18** and **19**.

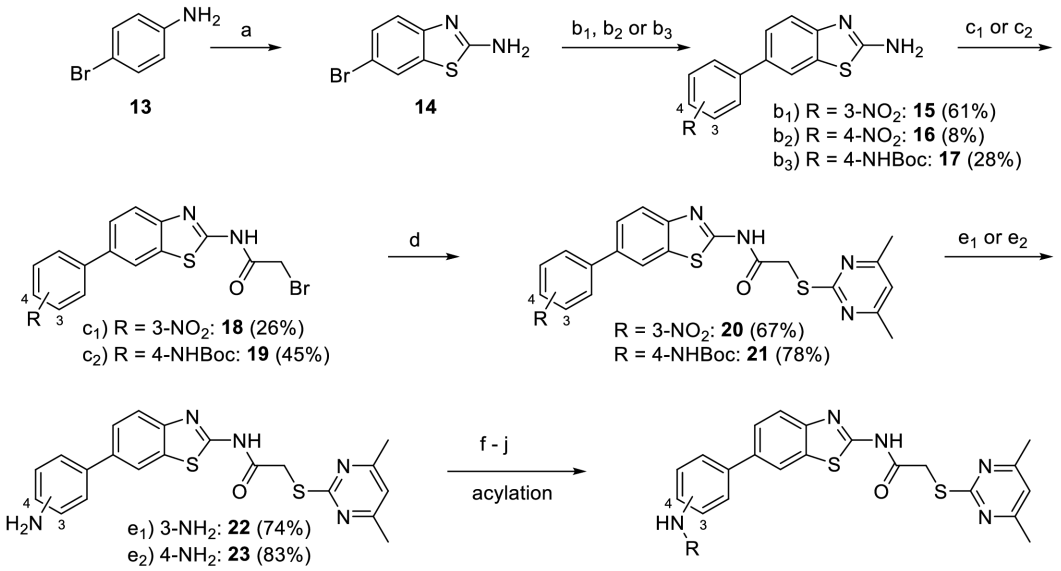

Scheme 6: Synthesis route of benzothiazole-based rigid target compounds. Conditions: a) KSCN, Br_2, AcOH, 0 °C, 23 h, 35%; b_1) 3-nitrophenyl)boronic acid, Cs_2CO_3, $Pd(PPh_3)_4$, dioxane/water, 80 °C, 21 h; b_2) (4-nitrophenyl)boronic acid, Cs_2CO_3, $Pd(PPh_3)_4$, dioxane/water, 80 °C, 21 h; b_3) 4-(*N*-Boc-amino)phenylboronic acid pinacol ester, Cs_2CO_3, $Pd(PPh_3)_4$, dioxane/water, 80 °C, 20 h; c_1) 2-bromoacetyl bromide, NEt_3, DCM/DMF (6:1), 40 °C, 3 h; c_2) 2-bromoacetyl bromide, NEt_3, EtOAc, 77 °C, 3 h; d) 4,6-dimethylpyrimidine-2-thiol, DMF, *t*-BuOK, rt, 3 h; e_1) Fe, MeOH/water, NH_4Cl, 65 °C, 3 h; e_2) TFA, chloroform, rt, 24 h; f) - j) shown in **Table 4**.

Due to solubility issues it was necessary to add DMF or switch to EtOAc as solvent. Thioethers **20** and **21** were then synthesized by default from respective compounds **18** and **19** using 4,6-dimethylpyrimidine-2-thiol and *t*-BuOK. The Boc protecting group of compound **21** was cleaved off using trifluoroacetic acid to obtain amine **23**, which is subsequently acylated to prepare the desired target compounds in the next step.

To reduce the nitro group of compound **20** in order to obtain amine **22**, the previously used standard iron/acetic acid system was changed favoring iron/MeOH/water to avoid expected acetic acid related extraction difficulties. Based on previous acylations (see Chapter 3.1.3.1, **Table 2**), *meta*-substituted amine **22** and *para*-substituted amines **23**, were subsequently converted to the desired target molecules, defined in Chapter 3.1.3 (see **Scheme 2**), using appropriate acid- and sulfonyl chlorides, as well as acetic anhydride (see **Table 4**).

In conclusion, all 10 desired benzothiazole-based rigid analogues of **28e** were successfully synthesized. Their biological activity against Sirt2 and related subtypes, along with the naphthalene-based target compounds, is presented in the following Chapter 3.1.4.

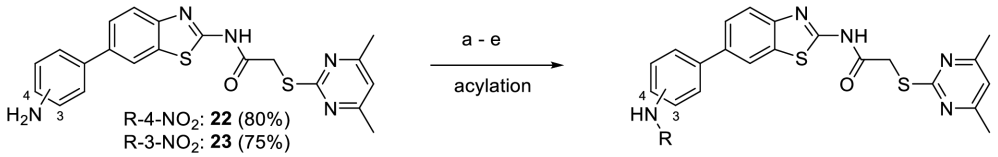

entry	reaction conditions		position	residue R	compound ID	yield [%]
a)	2-thiophenecarbonyl chloride, NEt_3, DCM	rt, 1 h	3	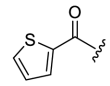	**FM96**	81
			4		**FM129**	77
b)	5-methylthiophene-2-carbonyl chloride, NEt_3, DCM	rt, 2 h	3	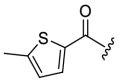	**FM108**	46
			4		**FM131**	45
c)	benzoyl chloride, DCM NEt_3,	rt, 3 h	3	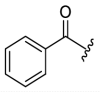	**FM95**	66
			4		**FM127**	46
d)	benzenesulfonyl chloride, NEt_3, DCM	rt, 1 h	3		**FM104**	15
		40 °C, 8 h	4		**FM130**	59
e)	acetic anhydride, NEt_3, DCM	rt, 3 h	3		**FM94**	96
			4		**FM128**	60

Table 4: Last synthesis step and final preparation of benzothiazole-based rigid analogues of **28e**

3.1.4 Biological evaluation of synthesized conformal-restricted target inhibitors

3.1.4.1 Inhibitory activity on Sirt2 and corresponding subtype selectivity

Using fluorescence-based sirtuin assays the IC_{50} values for Sirt2 and the selectivity on subtype Sirt1, Sirt3 and Sirt5 of the synthesized compounds were determined by Reaction Biology Corporation (Malvern, USA) to subsequently evaluate the biological impact of the accomplished structural rigidization (see **Figure 12**).

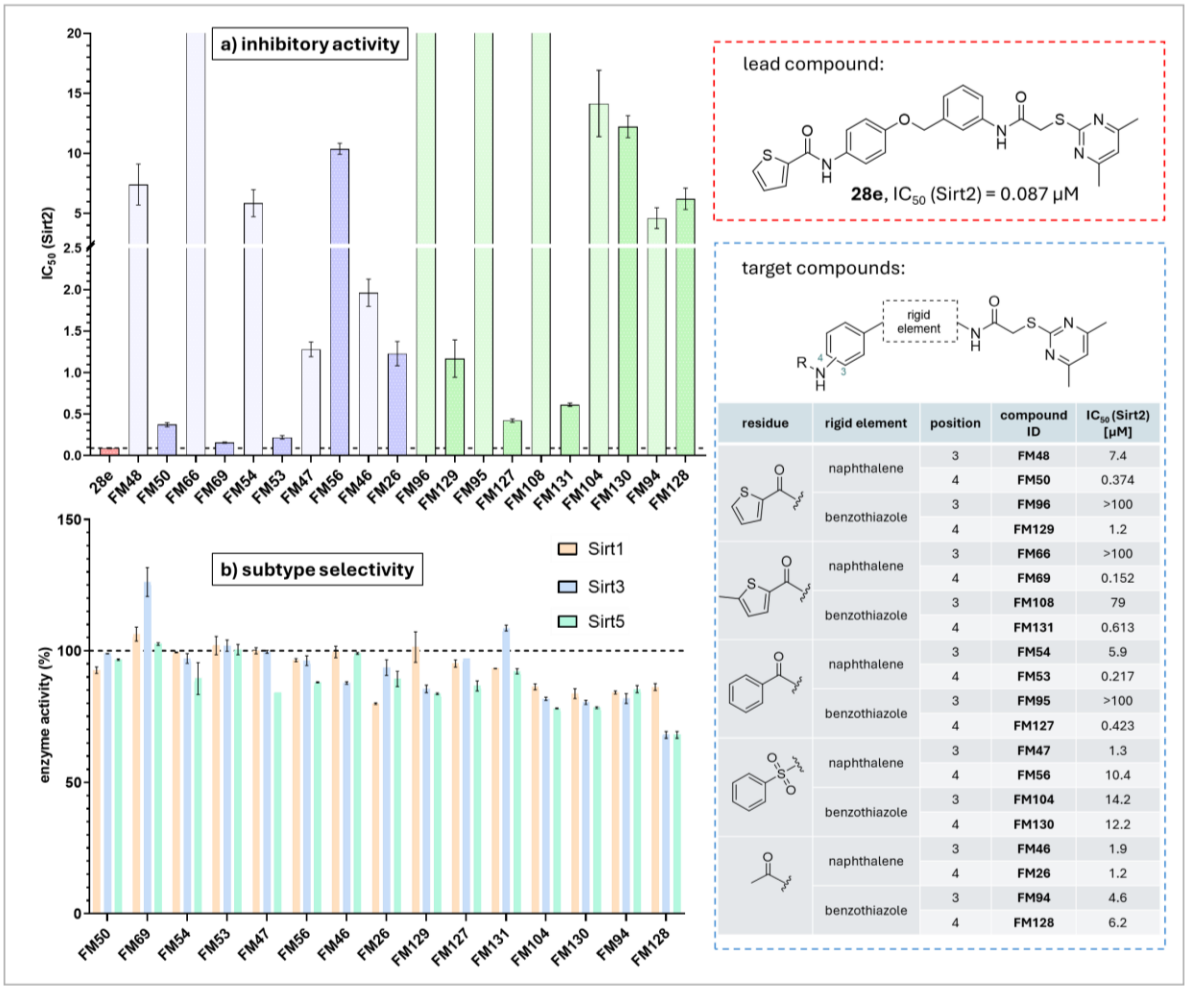

residue	rigid element	position	compound ID	IC_{50} (Sirt2) [µM]
	naphthalene	3	FM48	7.4
		4	FM50	0.374
	benzothiazole	3	FM96	>100
		4	FM129	1.2
	naphthalene	3	FM66	>100
		4	FM69	0.152
	benzothiazole	3	FM108	79
		4	FM131	0.613
	naphthalene	3	FM54	5.9
		4	FM53	0.217
	benzothiazole	3	FM95	>100
		4	FM127	0.423
	naphthalene	3	FM47	1.3
		4	FM56	10.4
	benzothiazole	3	FM104	14.2
		4	FM130	12.2
	naphthalene	3	FM46	1.9
		4	FM26	1.2
	benzothiazole	3	FM94	4.6
		4	FM128	6.2

Figure 12: Determination of the inhibitory activity of the test substances on the corresponding sirtuin enzymes, based on a fluorescence-based assay (for details see 5.3.3) by Reaction Biology Corporation (Malvern, USA). a) Inhibitory activity (IC_{50}) on Sirt2 of lead compound **28e** (red) and the synthesized rigid molecules based on naphthalene (blue) and benzothiazole (green). Differences in the brightness of the respective colors represent the corresponding substitution pattern of the synthesized compounds. The lighter color therefore describes the 3-position (*meta* substitution) and the darker color the 4-position (*para* substitution) of the respective pairs of substances. **FM66**, **FM96**, **FM95** and **FM108** are determined at least with IC_{50} > 50 µM. For each serially diluted replicate of the triplet, an IC_{50} value was determined by sigmoidal curve fitting and the presented mean and standard deviation (displayed as error bars) were then calculated from the three resulting IC_{50} values. b) Subtype selectivity screening of synthesized rigid target compounds: the percentage enzyme activity of Sirt1, Sirt3 and Sirt5 in the presence of the corresponding test substances was determined at 50 µM in duplicate, giving the presented mean and corresponding standard deviation (displayed as error bars). **FM66, FM96, FM95 and FM108** determined at least with IC_{50} > 50 µM on Sirt2 were not included in the respective subtype selectivity analysis.

According to the literature, the lead compound **28e**, which was reported to have an IC_{50} of 0.042 µM (42 nM) against Sirt2, was also synthesized as a reference and included in the corresponding assays, where it was determined with an IC_{50} of 0.087 µM (87 nM) towards Sirt2[53]. Considering the determined value of purchased **SirReal2** of 0.235 µM (235 nM) on Sirt2 (published IC_{50} = 0.44 µM, Sirt2, the announced superiority of **28e** over **SirReal2** in terms of inhibitory potency with respect to Sirt2 can be confirmed and the experimentally determined results are of a comparable magnitude to the published values[40].

Variations in IC_{50} values due to different testing conditions and assay formats are common and often complicate direct comparison. Thus, including the lead compound in the same testing system as the target compounds ensures a direct and reliable assessment due to consistent conditions and data evaluation. The evaluated and processed biological results are assigned and presented in **Figure 12**. Additional information regarding particular Sirt2 assay and subtype selectivity screening conditions as well as detailed information on determined IC_{50} values and enzyme activity are provided in Chapter 5.3.3.

Although unfortunately none of the tested compounds exceed the inhibitory activity of lead compound **28e** (IC_{50} = 0.087 µM, Sirt2), **FM69** shows a respectable inhibitory potential with an IC_{50} value of 0.152 µM on Sirt2.

Since further effective substances were identified in the Sirt2 screening, an overview of relevant inhibitors with submicromolar IC_{50} values is shown in **Figure 13**.

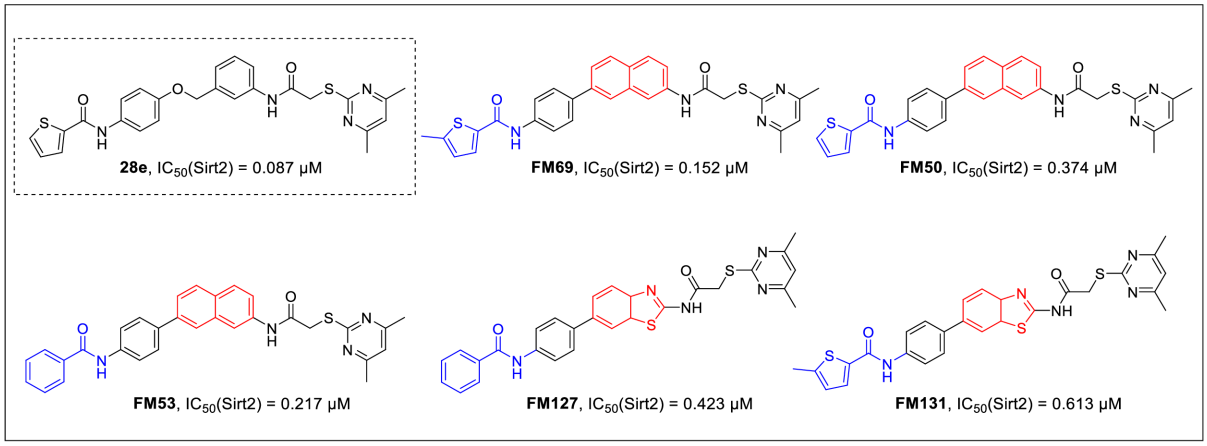

Figure 13: Sirt2 screening results of synthesized compounds: Overview of the most effective inhibitors derived of the rigidization approach displaying submicromolar IC_{50} values on Sirt2, as well as the corresponding lead compound **28e**.

As expected, the analysis of the subtype selectivity of synthesized compounds (see **Figure 12**) showed that none of the key active compounds display significant activity on other closely related isoforms of Sirt2: Sirt1, Sirt3 and Sirt5. Therefore, the respective enzyme activity at 50 µM was determined, excluding any relevant inhibitory potential on determined sirtuin subtypes especially in direct comparison with the submicromolar IC_{50} values of the tested compounds

on Sirt2. The determined residual enzyme activity therefore indicates at least an IC_{50} value greater than 50 µM for the respective subtypes.

3.1.4.2 SAR-analysis of rigidized target compounds

Analyzing the structure-activity relationship of the rigidized compounds, a clear conclusion becomes apparent: the 4-position (*para*) at the phenyl ring is clearly preferred in terms of inhibitory potential compared to the *meta*-substituted substances. The strong effect of the different substitution patterns on the inhibitory potency can be vividly illustrated by comparing IC_{50} values of **FM66** (IC_{50} >100 µM, Sirt2) and **FM69** (IC_{50} = 0.152 µM, Sirt2), which indicates a high steric and spatial requirement of the Sirt2 binding pocket. The four weakest inhibitors (**FM66**, **FM96**, **FM95** and **FM108**) with IC_{50} values above 50 µM on Sirt2 all show a *meta*-substituted substrate channel residue. The corresponding thiophenyl-, 2-methylthiophenyl- and phenyl residues proved to be fundamentally advantageous in the amide-based substrate channel residues variations, whereas sulfonyl- and acetyl substituted compounds were not convincing in terms of biological activity. Interestingly, naphthalene-based **FM50** and benzothiazole-based **FM129**, which represent the directly rigidized versions of lead compound **28e**, have noticeable potency, which is less strong than **FM69** and **FM131**, carrying an additional methyl group at C-5 of the thiophene ring, possibly due to additional hydrophobic interactions. In addition, the compounds rigidized with a naphthalene structure are generally superior to those with benzothiazole.

Based on the aforementioned biological study of inhibitory activity against Sirtuin 2, including corresponding selectivity assessments, five selective inhibitors with submicromolar IC_{50} values were identified out of the 20 tested target substances. Among these, **FM69** exhibited the strongest inhibitory potential within the compound library, with an IC_{50} value of 0.152 µM on Sirt2. The SAR-analysis demonstrates that the optimization of inhibitors by rigidization is a major challenge and therefore requires strong efforts to achieve favorable conformational constraints. Although potency of lead compound **28e** was not surpassed, the impact of various amide-based substrate channel residues variations on biological activity revealed significant potential for further structural variation of the synthesized rigid compounds.

3.2 Warhead-based Sirt2 inhibitor modification approach targeting the NAD^+ cofactor *via* reversible covalent binding principle

3.2.1 Overview of cofactor-based enzyme inhibition, reversible covalent binding principle in medicinal chemistry and application to Sirt inhibitors

Incorporating the corresponding cofactor of a targeted enzyme into the molecular mechanism of action of an inhibitor displays an established and promising drug design approach with several approved pharmaceuticals taking advantage of this principle (see **Figure 14**)[70].

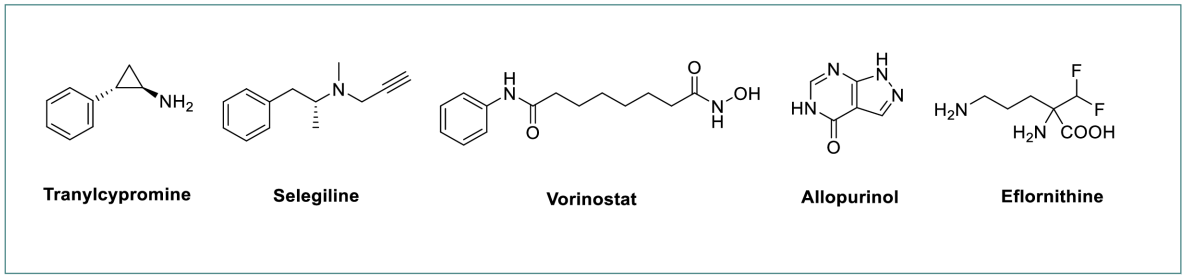

Figure 14: Selection of FDA-approved drugs with cofactor involvement in the corresponding inhibitory mechanism.

Tranylcypromine, an antidepressant, causes irreversible enzyme inhibition by covalently binding to flavin adenine dinucleotide (FAD), the cofactor of the targeted monoamine oxidases[71-72].

The same applies to Selegiline, a selective irreversible monoamine oxidase B inhibitor used in the treatment of depression and Morbus Parkinson[73].

Vorinostat, as a representative of FDA-approved HDAC inhibitors (also see Chapter 1.2), utilizes a hydroxamic acid-based warhead to bind zinc, which serves as a cofactor in the zinc-dependent histone deacetylases[22].

The xanthine oxidase inhibitor Allopurinol is a uricostatic agent used in the treatment of gout. By binding to the molybdenum cofactor of xanthine oxidase, the active metabolite of Allopurinol, Alloxanthin, blocks the physiological production of uric acid from purine precursors.[73]

Eflornithine causes irreversible enzyme inhibition by interaction with the pyridoxal phosphate cofactor of ornithine decarboxylase, leading to reduced cellular development, which enables its therapeutic use in the treatment of hirsutism and human African trypanosomiasis[74-75].

Regarding Sirtuin 2, the use of mechanism-based warheads has led to the creation of a novel class of inhibitors that irreversibly bind to NAD^+ by forming covalent conjugates with the cofactor[48].

The physiological function of sirtuins involves the NAD^+-dependent deacetylation of acetylated lysine residues on histones and other target proteins. An inhibitor equipped with a mechanism-

based warhead additionally interacts with NAD^+ in the sirtuin binding pocket, mimicking the usual acetylated lysine substrate, resulting in the formation of a cofactor-inhibitor conjugate (see **Figure 15**).[37]

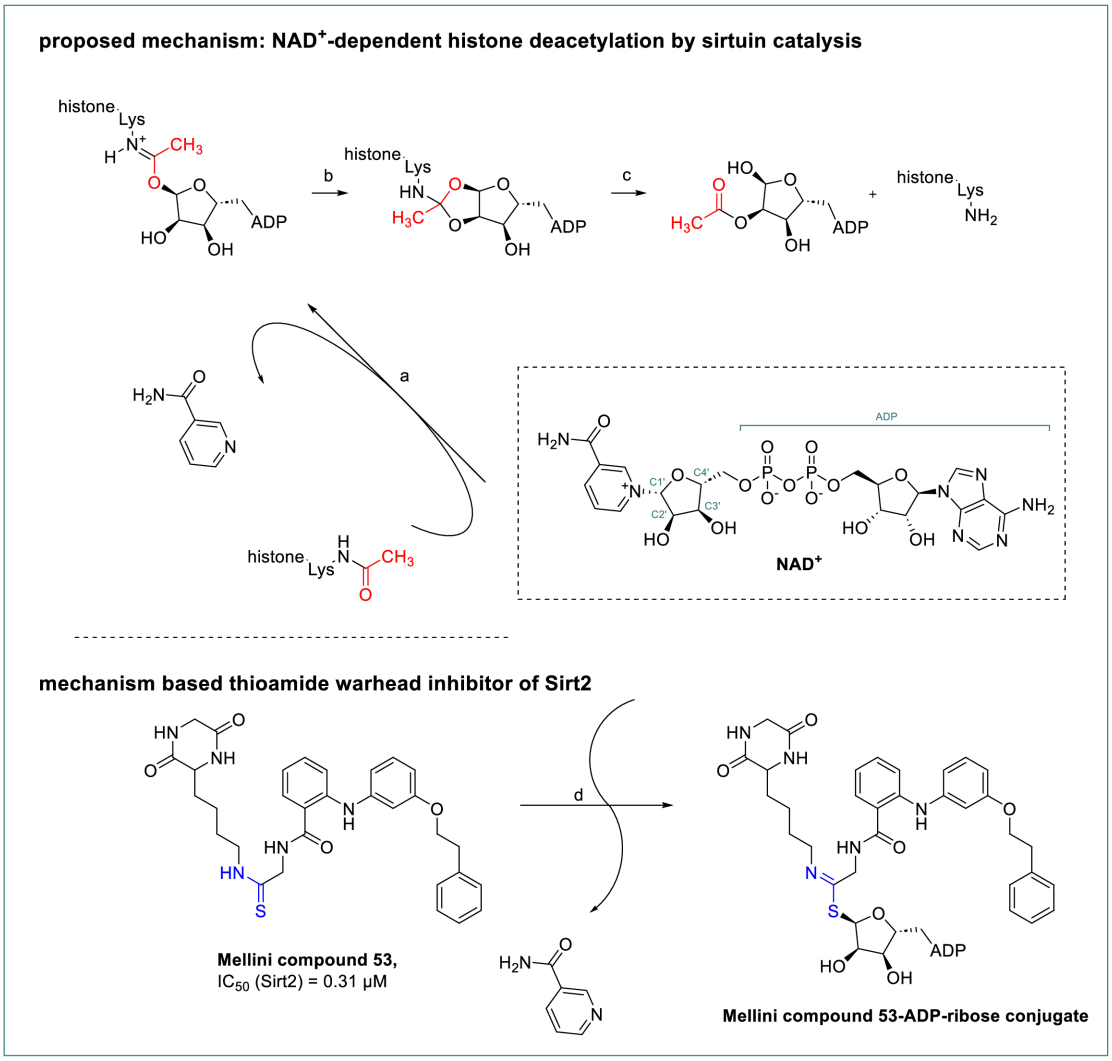

Figure 15: Simplified overview of the proposed sirtuin catalysis mechanism of NAD^+-dependent histone deacetylation (cf. lit.[76-77]) and corresponding intervention of a mechanism-based warhead Sirt2 inhibitor: **Mellini compound 53** (cf. lit. [45]). a) N-acetylated lysine initially transfers the acetyl group to NAD^+ *via* S_N2-based reaction on C1' of the ribose with temporary formation of an *O*-alkylamidate and cleavage of nicotinamide. b) Intramolecular electrophilic attack at C2'-OH with the formation of a corresponding cyclic acetal. c) Hydrolysis to C2'-O-acetylated ADP-ribose and deacetylated lysin. d) Processed by NAD^+, thioamide-based warhead Sirt2 inhibitor **Mellini compound 53** forms imidothiodate ADP-ribose conjugate.

To imitate the chemical structure of the sirtuin substrate, primarily structural elements based on thioureas, thioamides and occasionally carboxamides are utilized as respective warheads[48]. For instance, **Mellini compound 53** represents an innovative thioamide-type mechanism-based warhead that irreversibly binds cofactor NAD^+, forming an ADP-ribose inhibitor conjugate. In direct comparison with its corresponding unreactive carboxamide analog

(IC_{50} = 0.60 µM, Sirt2), which does not interact with NAD^+, the inhibitory activity of the **Mellini compound 53** (IC_{50} = 0.31 µM, Sirt2) nearly doubled.[45]

However, in principle a beneficial effect is not necessarily guaranteed, as respective mechanism-based warhead modifications may negatively impact inhibitory activity[78-79]. In the structure-activity relationship study on the development of inhibitor **28e**, a corresponding thiourea variant was found to be disadvantageous[80].

The current mechanism-based warheads result in irreversible NAD^+ binding, not necessarily enhancing potency and require comprehensive chemical modification. This thesis investigates the innovative approach of reversible covalent binding of NAD^+ to seamlessly integrate the cofactor into the binding mechanism. The reversible covalent binding mode offers an advantage over purely irreversible inhibitors, as off-target side reactions are less pronounced due to non-permanent interaction, leading to a successful approval of reversible covalent inhibitors for various targets and indications (see **Figure 16**).[81]

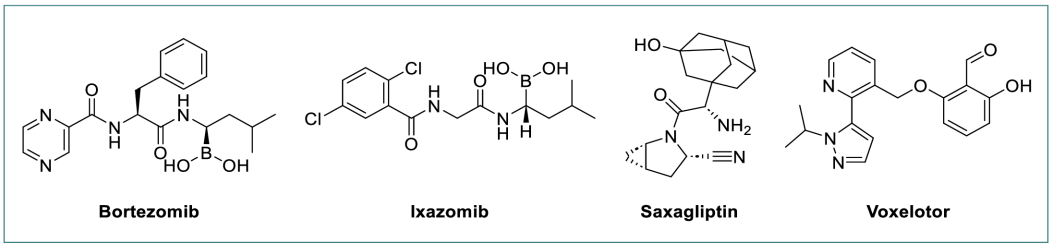

Figure 16: Chemical structures of selected FDA-approved drugs with reversible covalent binding mechanism.

Drugs containing a boronic acid functionality are known to form reversible covalent bonds with alcohols. Bortezomib marked a milestone in drug research for the treatment of multiple myeloma as its reversible covalent binding to a threonine residue in the 20S subunit of proteasomes was confirmed crystallographically.[81-82] Following the success of Bortezomib, Ixazomib was developed as a second-generation proteasome inhibitor and approved as an oral treatment option[83].

The antidiabetic agent Saxagliptin is a dipeptidyl peptidase 4 inhibitor based on the interaction between its nitrile structure element and Ser630 of the enzyme, creating a corresponding imidate[84].

Voxlelotor was approved as an aldehyde-based active substance that forms a reversible covalent bond to hemoglobin *via* imine formation for the treatment of sickle cell disease[85-86].

Hemiacetal formation by aldehyde warhead-equipped inhibitors in the presence of hydroxyl groups was demonstrated using the example of serine proteases such as trypsin or prolyl oligopeptidase[87-88].

Instead of using substrate-mimicking structural elements (like thioureas, thioamides and carboxamides), the novel approach involves boronic acid, nitrile and aldehyde-based warheads that should specifically bind the hydroxyl groups of ribose of NAD^+ in a reversible covalent manner.

Due to the reliable and extensive data available for the reversible covalent binding property of boronic acids in particular and the confirmed formation of a corresponding cyclic boronic acid ester between arylboronic acids and NAD^+ (see **Scheme 7**), especially boronic acids offer an extremely promising modification with a reversible covalent binding mode[89-90].

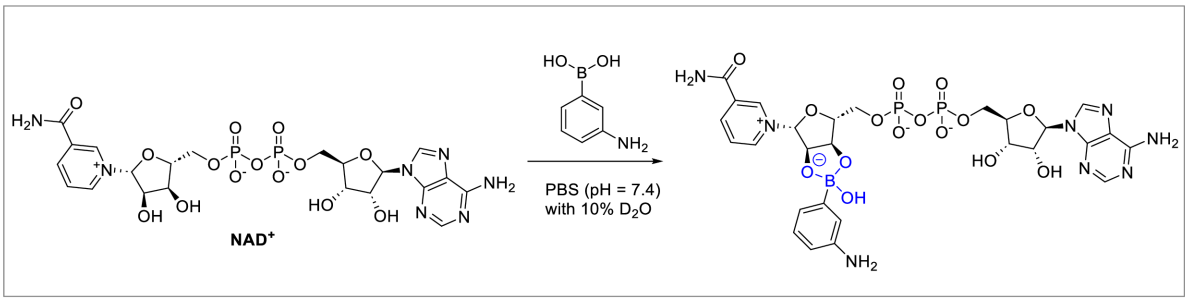

Scheme 7: NAD^+ forms anionic tetrahedral boronic esters with arylboronic acids under physiological pH conditions[91].

Based on systematic analyses of published crystal structures of known SirReal-inhibitors, the possibility of corresponding reversible covalent binding warheads and suitable substitution positions were to be investigated subsequently.

3.2.2 Crystal structure-based evaluation of the envisaged reversible covalent binding approach to target the cofactor NAD^+

Extensive preliminary studies by Schiedel *et al.* in the research group of Prof. Dr. Manfred Jung (Albert-Ludwigs-University Freiburg, Germany) formed the fundament and inspiration for further structural modifications of **SirReal2**[40]. It was demonstrated that halogenation with chlorine or bromine at position 7 of the naphthalene ring of **SirReal2** is associated with increased inhibitory activity, without affecting the original binding mode (see **Figure 17**, left). While the previously predicted halogen bridge with His187 and Val233 could not be confirmed in further crystallographic studies, it was possible to attribute the observed increase in potency to the reorientation of the naphthyl ring caused by halogen substitution and the therefore improved hydrophobic interactions. Thus, the mentioned variations of **SirReal2** resulted in an increase in potency without involving the corresponding halogens directly in the binding mode through specific interactions. To unlock the potential of appropriate naphthalene substitutions of **SirReal2** for further interactions, NAD^+, which is located in close spatial proximity, presents itself as a promising target. In this thesis, **SirReal2** was equipped with polar electrophilic functional groups, such as boronic acids, nitriles and aldehydes, with the aim of selectively targeting the alcohols of the ribose structure through a reversible covalent binding mechanism. (see **Figure 17**, right).

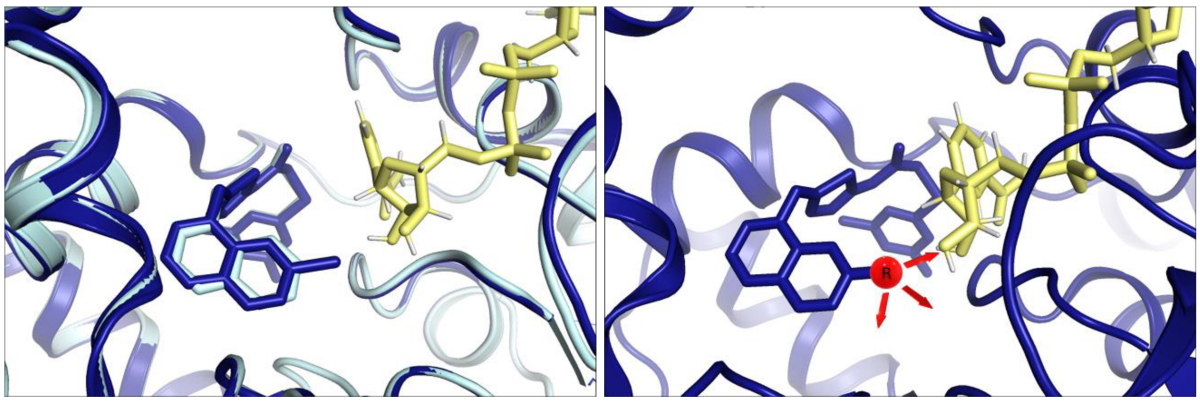

Figure 17: Left: Sirt2 crystal structure superimposition of **SirReal2** (grey, PDB ID: 4RMG) and **7-bromo-SirReal2** (blue, PDB ID: 5DY4) together with NAD^+ (yellow). Right: Envisaged reversible covalent binding warhead modification based on **7-bromo-SirReal2** (blue, PDB ID: 5DY4) and NAD^+ (yellow).

3.2.3 Early proof of concept study using boronic acid modification of simplified SirReal2-analogue 28a

3.2.3.1 Molecular docking-based verification of envisaged boronic acid substitution patterns

Due to the promising achievements of approved Bortezomib and its analogs and the confirmed reversible covalent binding mechanism of arylboronic acids and NAD^+ (see **Scheme 7**, Chapter 3.2.1), the boronic acid warhead was chosen as an early prototype modification. For an initial proof of concept study, instead of synthesizing the chemically challenging boronic acid-substituted derivative of **SirReal2** (SirReal2-boronic acid **FM206**) first, the simplified variation **28a** published by Yang *et al.* was selected (see **Scheme 8**)[53].

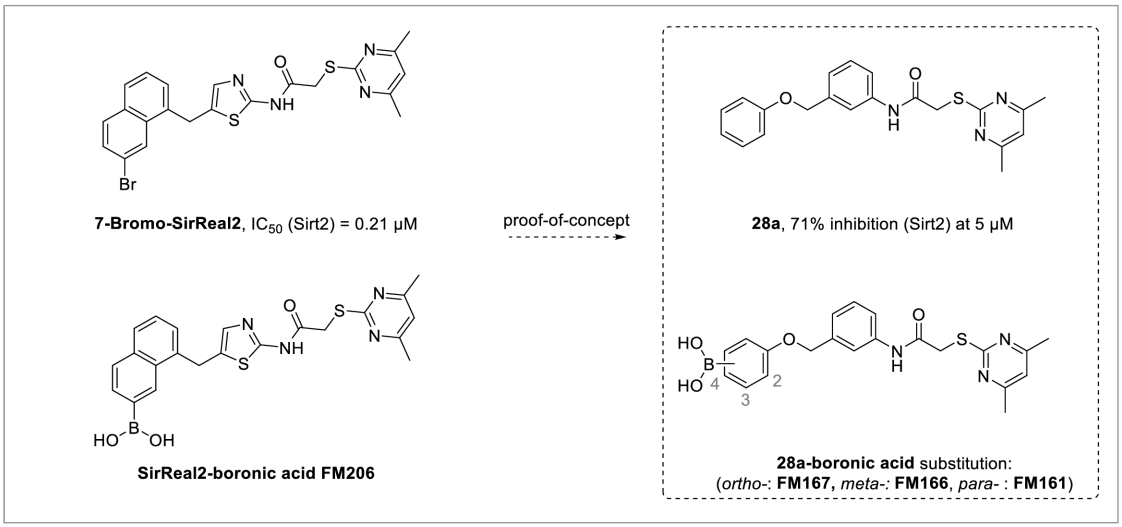

Scheme 8: Lead compounds **7-bromo-SirReal2** and simplified variant **28a** as well as envisaged boronic acid warhead modifications **FM206**, **FM167**, **FM166** and **FM161** to target NAD^+ in reversible covalent manner.

To gain insights into the potential orientation of the boronic acid relative to the cofactor NAD^+, docking experiments were conducted to evaluate the different substitution patterns of the boronic acid (see **Figure 18**). The respective docking calculations were carried out by our cooperation partner Dr. Thomas Wein, for further experimental information see Chapter 5.4.1. Particular attention will be paid to comparing the binding mode of the lead compounds and the proposed docking poses of corresponding boronic acid modifications, as well as the initially hypothesized orientation of the boronic acid in relation to NAD^+ proximity.

Analysis of the predicted spatial orientations of the proposed boronic acid-equipped molecules revealed an initial fundamental correlation with the lead structure of **7-bromo-SirReal2**. The alignment of the selectivity pocket binder motifs (2-((4,6-dimethylpyrimidin-2-yl)thio)acetamide moieties) is similarly favorable across all three substitution patterns, and the benzene ring replacing the thiazole occupies a comparable position in the binding pocket, suggesting a

generally analogous binding mode. Expected differences are observed in the orientation of the boronic acid-substituted substrate channel residue compared to the naphthyl ring of the corresponding lead structure **7-bromo-SirReal2**.

Due to the presence of the ether linkage, the phenylboronic acids exhibit increased spatial freedom, which can result in varied orientations. In the docking experiment, the *ortho*-substituted variant **FM167** shows the smallest change in orientation, remaining in the same plane as the planar naphthalene ring of the lead compound. In contrast, the *meta*-substituted modification **FM166** deviates significantly from the naphthalene position and protrudes into the substrate channel of Sirt2. The predicted *para*-substituted boronic acid **FM161**, however, aligns itself more closely with NAD^+. These docking studies provide encouraging results, as the fundamental agreement between the reference crystal structure and the predicted candidates suggests promising selectivity and predictable inhibitory activity.

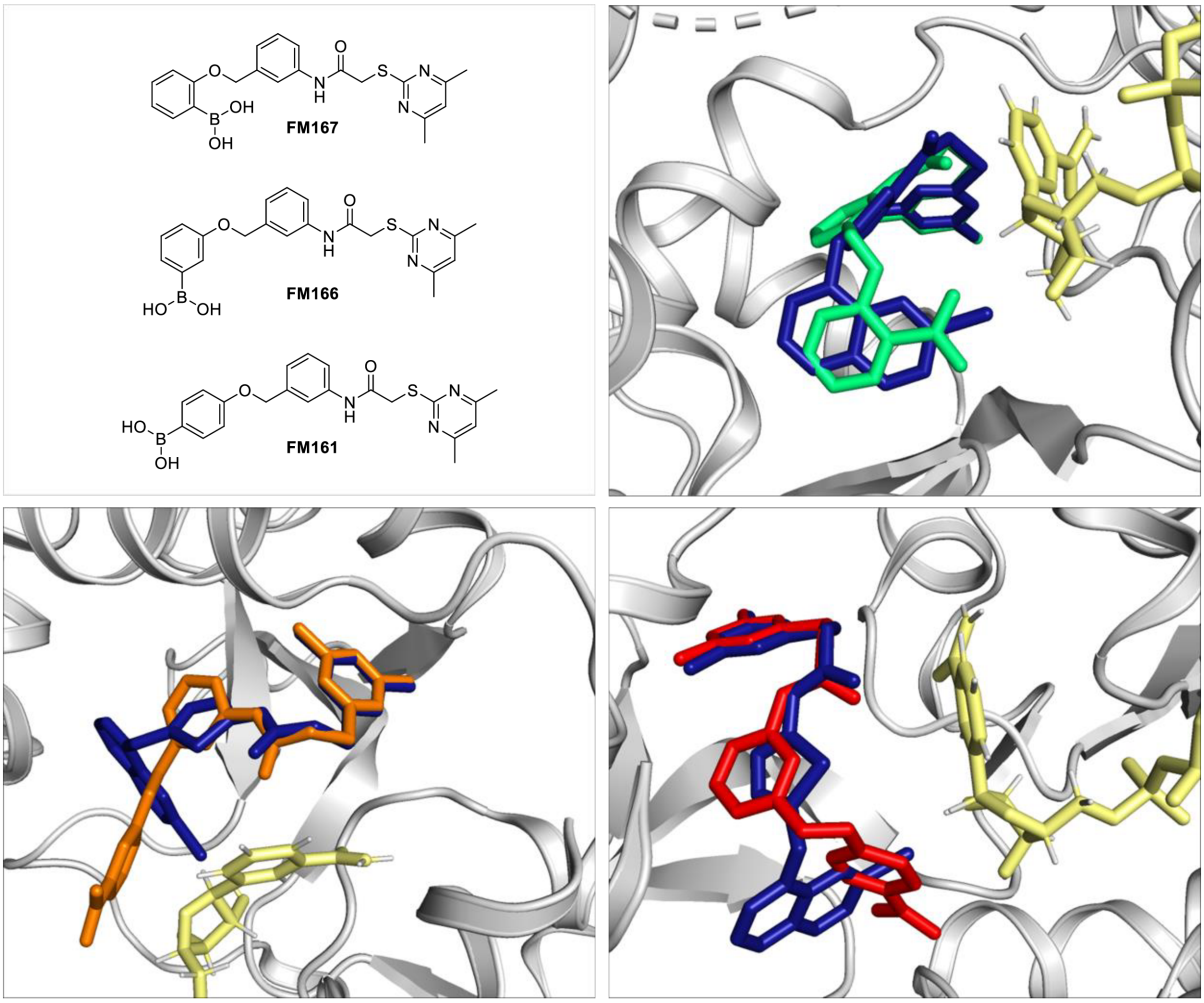

Figure 18: Substitution strategy and docking poses of envisaged boronic acid modifications of lead compound **28a**: *ortho* (**FM167**): green, *meta* (**FM166**): orange, *para* (**FM161**): red with Sirt2 inclusive NAD^+ (yellow) based on PDB ID: 4RMG. Visualization of **7-bromo-SirReal2** (blue, PDB ID: 5DY4) as crystal structure extraction.

The varying orientations of the boronic acid isomers in the substrate channel of Sirt2, due to different substitutions, offer significant potential for a wide range of additional interactions and

the targeting of cofactor NAD^+. Consequently, efforts are being made to develop the most efficient synthesis of the boronic acid-modified candidates (**FM167**, **FM166**, **FM161**) of lead compound **28a** to quickly confirm their anticipated positive effects on inhibitory potential.

3.2.3.2 Synthesis of boronic acid modifications of first lead compound 28a

3.2.3.2.1 Strategy development based on retrosynthetic approach

For initial considerations regarding the synthesis strategies of the target inhibitors, key building blocks were identified through retrosynthetic analysis (see **Scheme 9**).

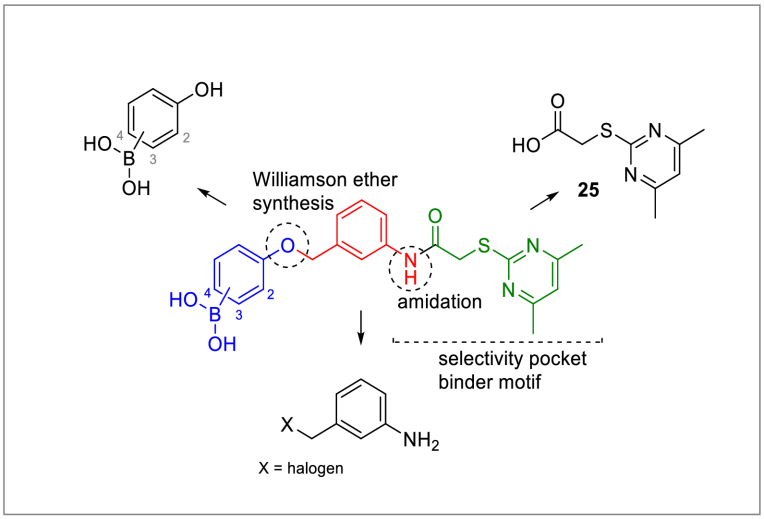

Scheme 9: Retrosynthetic approach of envisaged boronic acid warhead prototype inhibitors revealing key building blocks and fundamental synthesis options.

In this context, both the amidation to the known (2-((4,6-dimethylpyrimidin-2-yl)thio)acetamide moiety-based selectivity pocket binder motif and the ether synthesis of an appropriate hydroxyphenylboronic acid with the corresponding benzyl halide structure should ensure an efficient and convenient synthesis approach.

However, the synthesis of the lead compound **28a** served as a template and inspiration, the published synthetic approach[53] is not suitable for the feasible synthesis of the intended target compounds, as the essential ether synthesis is conducted unfavorably in the initial step. By incorporating the ether synthesis in the final step of the synthetic route, the different substitution patterns of boronic acid-based target compounds as well as the lead compound **28a** can be derived from the same precursor.

3.2.3.2.2 Early chemical difficulties regarding initial step of the envisaged synthesis plan

Based on the commercially available 3-nitrobenzyl bromide (**26**), a patent method[92] suggested the conversion to 3-(bromomethyl)aniline (**27**) *via* reduction with iron/hydrochloric acid in EtOH.

However, this outcome proved to be unreproducible, as undesired polymerization side products and dehalogenation were observed. Further attempts[80, 93-95] (see **Scheme 10**) including different reduction conditions inspired by related substructures failed as well, leading to the rejection of this synthesis strategy due to generally limited published data on this specific reaction.

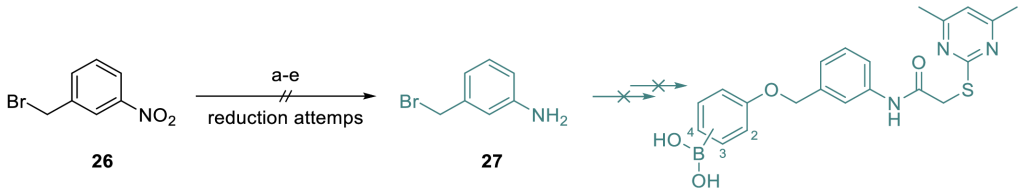

26 **27**

Scheme 10: Failed reduction attempts to prepare 3-(bromomethyl)aniline (**27**). Conditions: a) Fe/$HCl_{aq.}$, EtOH, rt → 85 °C, 2 h; b) Fe/NH_4Cl, $MeOH/H_2O$, 95 °C, 6 h; c) Fe/AcOH, 8 h; d) $SnCl_2$ x 2 $H_2O/HCl_{aq.}$, acetone, 50 °C, 12 h; e) H_2, Pd/C, MeOH, rt, 3 h.

3.2.3.2.3 Successful modification of synthesis strategy enables preparation of target inhibitors

To avoid unintended side reactions caused by the concurrent presence of both the primary aromatic amine and the reactive alkyl halide, as seen in the attempted preparation of 3-(bromomethyl)aniline (**27**), a new synthesis design was preferred, involving the initial amidation of an aniline-based building block and subsequent preparation of the benzyl halide structure to perform the required ether synthesis as a final step (see **Scheme 11**).

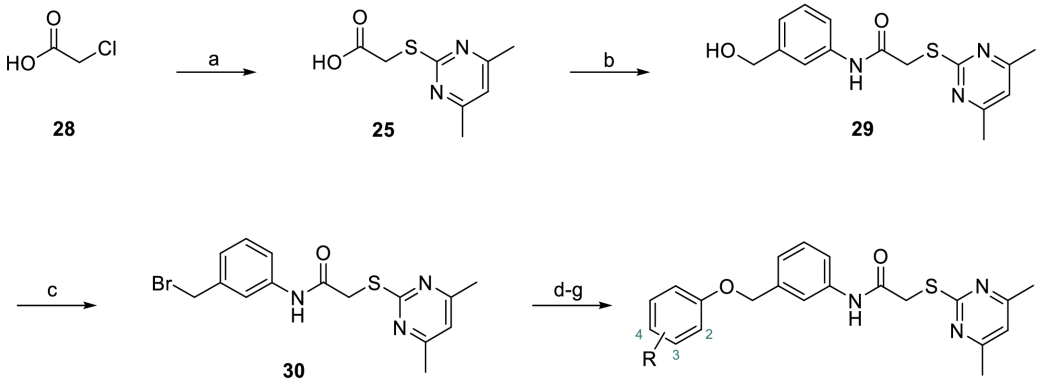

28 **25** **29** **30**

d) R = H: **28a** (**FM159**) f) R = 4-$B(OH)_2$: **FM161**
e) R = 3-$B(OH)_2$: **FM166** g) R = 2-$B(OH)_2$: **FM167**

Scheme 11: Synthesis of boronic acid substituted analogues of **28a**. Conditions: a) 4,6-dimethylpyrimidine-2-thiol, NEt_3, acetonitrile, rt, 24 h, 81%; b) 3-(hydroxymethyl)aniline, HATU, DIPEA, DMF, rt, 3 h, 30%; c) PBr_3, DCM, rt, 0.5 h, 85%; d) phenol, *t*-BuOK, DMF, rt, 2 h, 43%, e) 3-hydroxyphenylboronic acid, K_2CO_3, acetonitrile, rt, 6 h, 41%; f) 4-hydroxyphenylboronic acid, *t*-BuOK, DMF, rt, 0.5 h, 15%; g) 2-hydroxyphenylboronic acid, *t*-BuOK, DMF, rt, 4 h, 6%.

The previously used two-step preparation of the selectivity pocket binder motif (for example see **Scheme 3**, Chapter 3.1.3.1), as described in corresponding reference literature was replaced with a one-step amidation process using 2-((4,6-dimethylpyrimidin-2-yl)thio)acetic

acid (**25**). Firstly, formerly used 2-bromoacetyl bromide is unpromising in the context of a primary alcohol due to its reactivity. Secondly, this adaption offers advantages, as the previously synthesized carboxylic acid **25** can be directly used for the preparation of further target compounds.

The coupling of 2-chloroacetyl chloride (**28**) with 4,6-dimethylpyrimidine-2-thiol to 2-((4,6-dimethylpyrimidin-2-yl)thio)acetic acid (**25**) was initially carried out according to a published protocol[96] in a NaOH/H_2O system, which however, resulted in scale-related isolation complications, due to heat sensitivity and universal solubility properties of **25**. Therefore, the reaction was adjusted to anhydrous conditions with triethylamine as base and acetonitrile as solvent, allowing flash column chromatographic purification by gentle evaporation *in vacuo* without prior work-up or recrystallisation. HATU-mediated amidation of carboxylic acid **25** with the commercially available 3-(hydroxymethyl)aniline, inspired by Dr. Carina Glas[79] (research group Prof. Bracher) yields alcohol **29**, which is subsequently converted into the corresponding benzyl bromide **30** *via* PBr_3. Using the benzyl bromide **29** and the appropriate phenols, the desired target inhibitors were synthesized using Williamson ether synthesis. In principle, the Willamson ether synthesis was based on the reaction conditions published by Yang *et al.*[53], but adapted accordingly due to differing polarities and chemical properties. With the combination of *t*-BuOK/DMF, enough product formation could be achieved, as for lead compound **28a** (**FM159**), **FM161**, **FM167** the milder standard system of K_2CO_3 and acetonitrile, used for the preparation of **FM166** was not sufficient. Although DMF shows excellent solvent properties, it negatively affects work-up and extraction compared to acetonitrile, especially regarding the highly polar products obtained.

The successfully synthesized target compounds were subsequently examined for their biological activity on Sirt2 and selectivity over other subtypes to determine the impact of the potentially reversible covalent binding of boronic acid groups in order to incorporate the obtained knowledge into future strategies on more complex inhibitors.

3.2.3.2.4 Biological evaluation and SAR-analysis of synthesized target inhibitors **FM161**, **FM166** and **FM167**

The Sirt2 inhibitory activity and subtype selectivity regarding Sir1, Sirt3 and Sirt5 (see **Figure 19**) was determined by Reaction Biology Corporation (Malvern, USA) using a fluorescence-based assay (detailed conditions, values and procedures see Chapter 5.3.3).

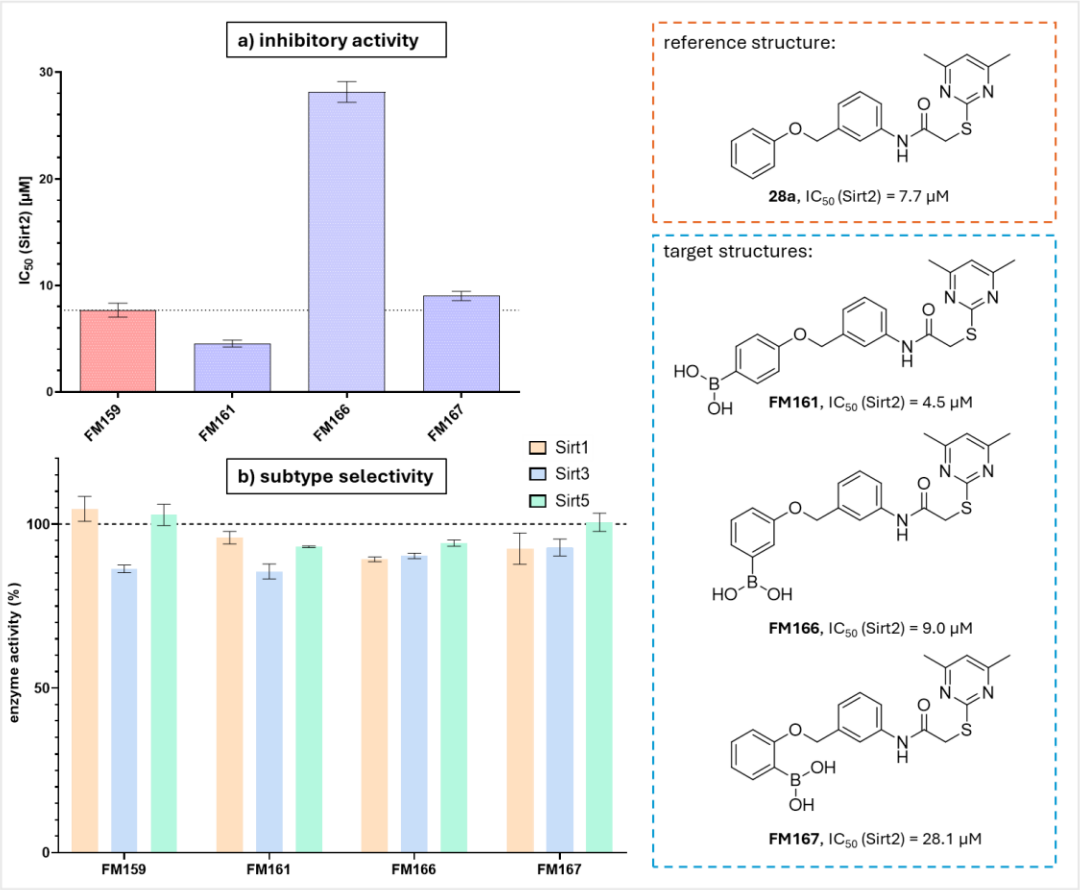

Figure 19: Determination of the inhibitory activity of the test substances on the corresponding sirtuin enzymes, based on a fluorescence-based assay (for details see Chapter 5.3.3) by Reaction Biology Corporation (Malvern, USA). a) Inhibitory activity (IC_{50}) on Sirt2 of reference substance **28a** and the corresponding boronic acid substituted analogues. For each serially diluted replicate of the triplet, an IC_{50} value was determined by sigmoidal curve fitting and the presented mean and standard deviation (displayed as error bars) were then calculated from the three resulting IC_{50} values. b) Subtype selectivity screening of synthesized compounds. The percentage residual enzyme activity of Sirt1, Sirt3 and Sirt5 in the presence of the corresponding test substances was determined at 50 µM in duplicate, giving the presented mean and corresponding standard deviation (displayed as error bars).

Lead compound **28a**, acting as a reference substance, previously reported with 71% inhibition on Sirt2 at 5 µM[53] was determined with an IC_{50} value of 7.7 µM. **FM161**, **the** *para*-substituted boronic acid analogue of **28a,** shows a 1.7-fold increase in potency with an IC_{50} value of 4.5 µM on Sirt2, which can clearly be interpreted as a positive result. The *ortho*-substituted variant **FM166**, with an IC_{50} value of 28.1 µM towards Sirt2, falls clearly short of expectations and represents a 3.6-fold reduction in inhibitory activity in relation to **28a**. The *meta*-substituted

boronic acid **FM167** (IC_{50} = 9.0, Sirt2) was 1.2 times less potent than the reference substance. The considerably lower inhibitory activity of the **FM166** cannot be directly reconciled with the findings of the docking studies. Docking experiments only provide a theoretical statement due to the complex binding processes, which are associated with certain limitations and can therefore deviate from the actual conditions, as in the case for the *ortho*-substituted boronic acid.

The screening of subtype selectivity on the related subtypes Sirt1, Sirt3 and Sirt5 is based on the determination of the residual enzyme activity in % at an inhibitor concentration of 50 µM. Since all tested inhibitors still show a pronounced enzyme activity of at least greater than 85% (average percentage) at 50 µM inhibitor concentration on all subtypes (residual enzyme activity indicates at least IC_{50} > 50 µM on respective subtypes), the determined IC_{50} values of Sirt2 confirm a pronounced subtype selectivity.

The synthesized boronic acids exhibit a selective inhibitory activity with respect to Sirt2, which is however, strongly dependent on the corresponding substitution pattern in the novel arylboronic acid subunit. Compared to the unsubstituted lead compound **28a**, only the *para*-substituted variant **FM161** shows improved inhibitory activity, whereas the *meta*-substituted variant **FM167** is determined with slightly poorer potency and the *ortho*-substituted **FM166** is clearly inferior (*para*>*meta*>>*ortho*). The results indicate that the alignment of the boronic acid group and its specific position are crucial for inhibitory potential. A proper substitution pattern of the boronic acids has been shown to enhance the potency compared to the reference lead compound. Evidence for a hoped-for reversible covalent bond with NAD^+ is not pursued further here, as **FM161** only achieved a moderate increase in potency. Nevertheless, the findings provide valuable insights for further project planning. This proof of concept demonstrates that a favorable alignment through targeted modification of the lead compound can enhance its potency. It is expected that an appropriate boronic acid modification will further increase the inhibitory activity of the already more effective lead compound of **SirReal2**, possibly due to a reversible covalent binding mode.

3.2.4 Transfer and application of the reversible covalent binding warhead approach on lead compound SirReal2

3.2.4.1 Docking experiment guided pre-verification of envisaged SirReal2-boronic acid modification FM206

The previously described proof of concept study indicates that achieving a beneficial effect on inhibitory activity requires careful consideration of different substitutions. Based on this conclusion, the three-dimensional alignment of the boronic acid modification of **SirReal2** is predicted (docking calculations carried out by cooperation partner Dr. Thomas Wein, for further information see Chapter 5.4.1) and analyzed using the **7-bromo-SirReal2** analogue crystal structure in a subsequent docking experiment (see **Figure 20**).

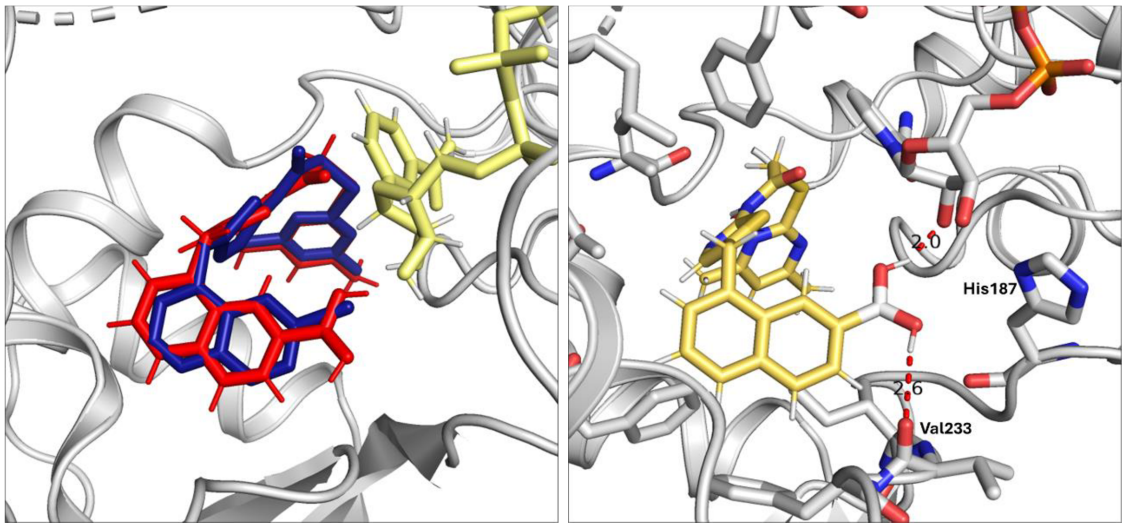

Figure 20: Left: Docking studies of SirReal2-boronic acid **FM206** warhead modification (red) and NAD^+ (yellow) based on PDB ID: 4RMG prediction with visualization of crystal structure of **7-bromo-SirReal2** (PDB ID: 5DY4, blue, extraction). Right: Detailed view of SirReal2-boronic acid **FM206** warhead modification prediction based on PDB ID: 4RMG and neighboring amino acids in the Sirt2 binding pocket. Predicted polar contact distances of boronic acid warhead with the ribose subunit of NAD^+ (oxygen atoms in red) and Val233 are given in Ångström.

Occupying a position analogous to the bromine atom in **7-bromo-SirReal2**, the boronic acid not only adopts a favorable docking pose similar to the lead compound but also reduces the risk of unwanted spatial clashes, thus providing a suitable environment for the intended substitution. While polar interactions between the bromine atom of **7-bromo-SirReal2** and Val233 and His187 were suggested by Schiedel *et al.* based on initial docking experiments, subsequent crystallographic studies did not confirm these predicted contacts[40]. Introducing various polar electrophilic functional groups such as boronic acids, aldehydes, or nitriles aims to provoke corresponding polar interactions and, in best case, enable reversible covalent inhibition by bonding to the hydroxy group(s) of the ribose subunit of the cofactor NAD^+.

Notably, the docking prediction for SirReal2-boronic acid **FM206** indeed indicates polar interactions between the boronic acid subunit and Val233 in the enzyme, as well as a secondary alcohol in the ribose structure of NAD^+. This interaction not only has the potential to enhance inhibitory potency but also could allow for the formation of a reversible covalent bond *via* an electrophilic attack of the boron atom on the ribose hydroxy group, resulting in the formation of a boronic acid ester.

Considering the promising predicted spatial orientation of **FM206** and the advantageous positioning of the boronic acid group, which suggests additional interactions with the binding pocket and the cofactor NAD^+, a synthesis strategy was subsequently developed. This synthetic approach (see next Chapter 3.2.4.2) involves the substitution with a boronic acid group as well as the subsequent incorporation of other intended polar electrophilic functional groups, such as aldehydes and nitriles as warheads for reversible covalent binding to the cofactor NAD^+.

3.2.4.2 Synthesis of SirReal2-based reversible covalent binding warhead modifications

3.2.4.2.1 Synthesis design and strategy considerations

Although the envisaged structural modifications differ only slightly from the corresponding **SirReal2** and **7-bromo-SirReal2** lead compounds, an adapted approach was required (see **Scheme 12**). Since the reactivity of the polar electrophilic functional groups to be introduced (boronic acid, nitrile and aldehyde) must be taken into account with regard to undesired side reactions and instability, the use of appropriate protecting groups and synthesis within the final synthesis step is recommended. The synthesis of the respective 5-(arylmethyl)thiazol-2-amines follows a literature-known protocol[40] using a modified version of the Meerwein arylation[97-98].

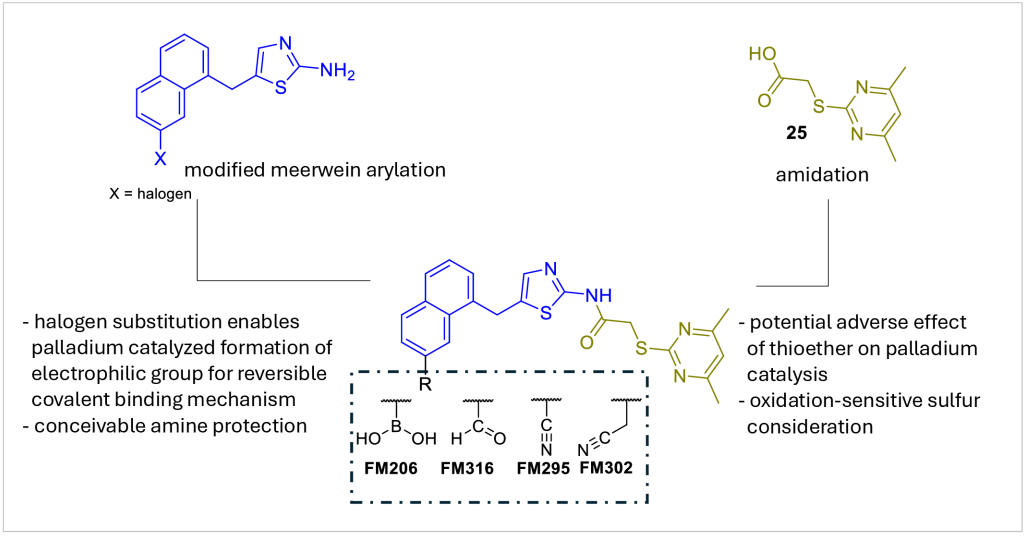

Scheme 12: Strategy development to synthesize the envisaged reversible covalent binding warhead modifications (boronic acid **FM206**, nitrile **FM295**, acetonitrile **FM302** and aldehyde **FM316**) based on **7-bromo-SirReal2**.

Introducing the boronic acid group presents certain challenges that need to be considered within the synthesis strategy. Common methods include halogen-metal exchange, Grignard reagent-based boronic acid formation, or Miyaura borylation. Due to the harsh reaction conditions associated with lithiation reagents and aryl magnesium bromides, a palladium-catalyzed cross-coupling was favored for the synthesis of the boronic acid.[99]

This method yields a corresponding boronic acid pinacol ester, which has subsequently to be deprotected to yield the free boronic acid. The oxidative cleavage of the respective pinacol ester to the free boronic acid is a reliable and established deprotection method, which, due to the potential oxidation sensitivity of the thioether-containing selectivity pocket binder motif (2-((4,6-dimethylpyrimidin-2-yl)thio)acetamide moiety), is preferably carried out prior to amidation.[100] Direct formylation of **SirReal2** is avoided due to expected selectivity issues,

favoring an aldehyde synthesis starting from the corresponding halogen precursor, which is also used for the proposed nitrile substitution to selectively introduce the nitrile group.

3.2.4.2.2 Synthesis of SirReal2-boronic acid **FM206**

The method utilized by Schiedel *et al.* for the preparation of aminothiazole **35** involves a modified Meerwein arylation protocol starting from 7-bromonaphthalene-2-amine (**33**), which was synthesized by an unselective 5-step nitration-based synthesis with an overall yield of 8%[40]. By applying an alternative literature-known method for the preparation of 7-bromonaphthalene-1-amine (**33**)[101], the compound was synthesized in a convenient two-step synthesis in a threefold higher yield of 25% in total (see **Scheme 13**).
After 7-bromonaphthalene-1-amine (**33**) has been transferred to the corresponding diazonium salt with *in situ* generated nitrous acid from sodium nitrite and hydrochloric acid, it reacts with acrolein to form the α-chloropropanal **34**, which subsequently condenses with thiourea to form the desired aminothiazole **35**.

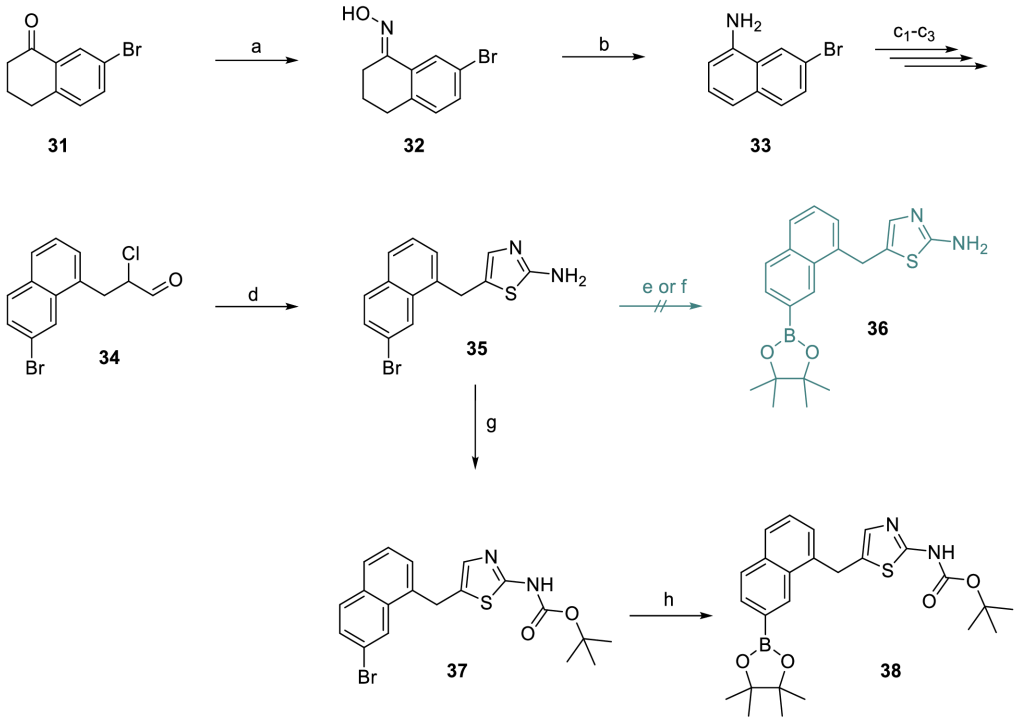

E

Scheme 13: Synthesis of 7-bromonaphtalene-2-amine (**33**), key aminothiazole (**35**) and subsequent Miyaura-borylation attempts. Conditions: a) NH_2-OH·HCl, NaOAc, EtOH, 2 h, 80 °C, quant.; b) Ac_2O, H_2SO_4, AcOH 60 °C, 24 h, 25%, c_1) $NaNO_2$, HCl then $FeCl_3 \cdot 6H_2O$, HCl, H_2O, 0 °C, c_2) $CuCl_2 \cdot 2H_2O$, HCl, acetone/EtOH, 0 °C, c_3) acrolein, acetone/H_2O, 4 h; d) thiourea, EtOH, 80 °C, 30 h; 41% over 4 steps (c_1-c_3 + d); e) pinacolborane, $PdCl_2(PPh_3)_2$, NEt_3, dioxane, 100 °C, 2 h, 0%; f) bis(pinacolato)diboron, Pd(dppf)Cl_2 · CH_2Cl_2, KOAc, dioxane, 80 °C, 19 h, traces; g) di-*tert*-butyl dicarbonate, toluene, 100 °C, 4.5 h, 85%; h) bis(pinacolato)diboron, Pd(dppf)Cl_2 · CH_2Cl_2, KOAc, dioxane, 80 °C, 1 h, then rt 2 h, 51%.

Starting from 7-bromo-1-tetralone (**31**), the first step consists of the conversion to the corresponding oxime **32**, which is then aromatized using Semmler-Wolff reaction[102] to the desired bromonaphthalene-1-amine (**33**) using sulfuric acid and acetic anhydride in acetic acid. Subsequently, aminothiazole **35** was further synthesized according to the published method of Schiedel et al.[40] As direct Miyarua-borylation of the previously synthesized aminothiazole **35** to compound **36** was not successful using general literature-inspired conditions[103-104], the corresponding *N*-Boc-protected variant **37** was prepared. The Boc protection finally allowed the successful introduction of the boronic acid pinacol ester resulting in compound **38** using previously applied patent procedure[104] within the synthesis attempt of compound **36.**

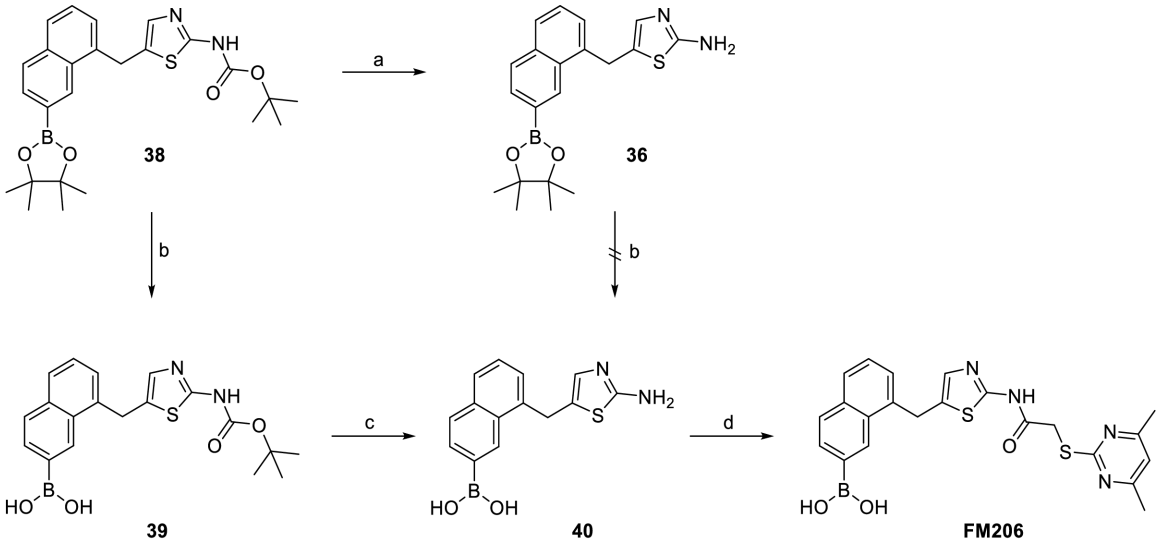

Scheme 14: Deprotection attempts und final amidation to SirReal2-boronic acid **FM206**. Conditions: a) TFA, chloroform, rt, 17 h quant.; b) sodium periodate, THF/water rt, 1 h then aq. HCl (1 M), rt, 3 h, 84%; c) TFA, chloroform, rt, 17 h, 79%; 2-((4,6-dimethylpyrimidin-2-yl)thio)acetic acid, DMAP, EDC·HCl, DMF, rt, 16 h, 17%.

The next step comprises the removal of the respective amine and boronic acid protecting groups from compound **38**, starting with the cleavage of the previously introduced Boc protecting group to compound **36** to enable the oxidative cleavage of the boronic acid pinacol ester to boronic acid **40** inspired by literature[105]. Unfortunately, the respective boronic acid **40** could not be released in the presence of the primary aromatic amine of **36**. After rearranging the reaction sequence by initial pinacol ester cleavage using sodium periodate and hydrochloric acid to boronic acid **39** and subsequent cleavage of the Boc protecting group with trifluoroacetic acid, compound **40** was realized. Referring back to the previously established method for the one-step introduction of the selectivity pocket binder motif (see Chapter 3.2.3.2.3, **Scheme 11**), the HATU-mediated amidation (yield 6%) initially carried out in this regard was replaced in favor of a more efficient EDC-supported alternative (17%) to give the target SirReal2-boronic acid **FM206**, generally inspired by other synthesis efforts of Dr. Thomas Klaßmüller[106] of research group Prof. Bracher.

3.2.4.2.3 Synthesis of nitrile-substituted SirReal2 analogue **FM295** and **FM302**

Due to previous negative experience with unprotected aminothiazoles **35** and **36** (see **Scheme 13** and **Scheme 14**, Chapter 3.2.4.2.2) and the associated disadvantageous impact of Miaura-borylation and pinacol ester deprotection, the synthesis of the corresponding nitrile-substituted target compound **FM295** was precautionary envisaged starting from the amine-protected bromoarene **37** (see **Scheme 15**).

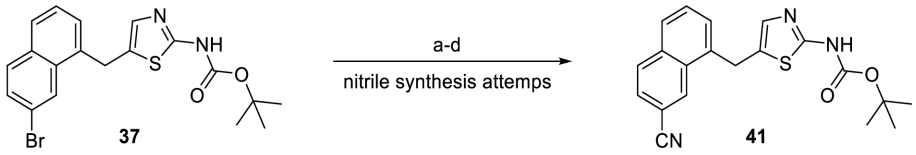

Scheme 15: Nitrile synthesis attempts based on Boc-protected aminothiazole **37**. Conditions: a) NaCN, CuI, KI, 1,2-diaminoethane, toluene, 110 °C, 24 h, traces; b) Na_2CO_3, $K_4[Fe(CN)_6]$, $Pd(OAc)_2$, NMP, 120 °C, 23 h, no conversion of reactant; c) KCN, $Pd_2(dba)_3 \cdot CHCl_3$, DPPF, NMP, 60 °C, 24 h, traces, d) zinc cyanide, $Pd(PPh_3)_4$, DMF, 80 °C, 18 h, 35%.

Various general strategies for introducing a nitrile group from a halogen-containing precursor are described in the literature (see **Scheme 15**). These methods typically involve a suitable catalyst and an appropriate cyanide donor reagent. In a common Rosemund-von Braun reaction protocol, CuI and sodium cyanide are used to synthesize aryl nitriles[107]. However, when applied to Boc-protected aminothiazole **37**, only trace amounts of the product were detected. Using $K_4[Fe(CN)_6]$ and $Pd(OAc)_2$ as described by Yang *et al.*[108] no conversion could be observed, while employing the method of Shi *et al.*[109] with KCN and $Pd_2(dba)_3$ in $CHCl_3$ resulted in only trace amounts of the product. Finally, a successful synthesis of nitrile **41** with a yield of 35% was achieved using zinc cyanide and $Pd(PPh_3)_4$ according to a patent method[110].

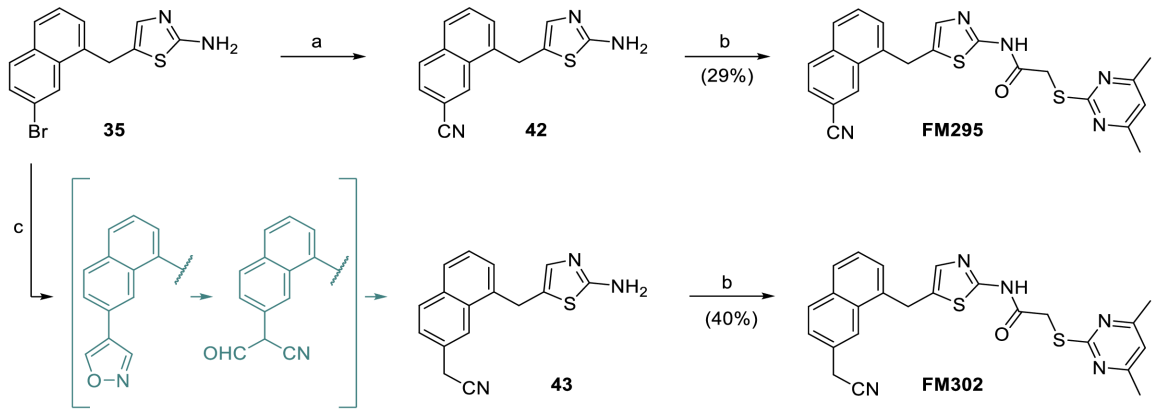

Scheme 16: Final synthesis of nitrile substituted analogues of **SirReal2** based on aminothiazole **35**. Conditions: a) zinc cyanide, $Pd(PPh_3)_4$, DMF, 80 °C, 18 h, 61%; b) ((4,6-dimethylpyrimidin-2-yl)thio)acetic acid, HATU, DIPEA, DMF, rt ,18 h, (yields given in parentheses); c) isoxazole-4-boronic acid pinacol ester, KF/H_2O, $Pd(dppf)Cl_2 \cdot CH_2Cl_2$, 90 °C, DMF, 20 h, 26%; proposed reaction intermediates of cyanomethylation displayed in brackets.

For the sake of interest, the reaction conditions determined for the Boc-protected aminothiazole **37** were transferred to the unprotected aminothiazole **35** in order to possibly achieve a detour-free nitrile synthesis (see **Scheme 16**).
Contrary to expectations, the introduction of the nitrile group with the unprotected aminothiazole **35** was successful with an even better yield of 61%. Encouraged by these positive results, the preparation of the arylacetonitrile **43** was achieved through the application of a general one-pot palladium-catalyzed cyanomethylation method[111], based on an initial Suzuki cross-coupling of aminothiazole **35** with isoxazole-4-boronic acid pinacol ester followed by subsequent base-induced fragmentation of the respective isoxazole to an α-formyl-nitrile intermediate, which finally undergoes deformylation to the desired arylacetonitrile **43** (proposed reaction intermediates visualized in **Scheme 16**).
Both nitrile intermediates **42** and **43** were then converted to the respective target compounds **FM295** and **FM302** using previously established HATU-mediated (see Chapter 3.2.3.2.3, **Scheme 11**) amidation procedure.

3.2.4.2.4 Synthesis of aldehyde-based SirReal2 variation **FM316**

The synthesis of the aldehyde-containing target molecule **FM316** poses further challenges due to the aldehyde's reactivity and ability to form imines with primary amines, particularly under acidic conditions. Accordingly, the simultaneous presence of aldehyde and primary amine should be avoided at best, which would not be possible when using the Boc-protected aminothiazole **37** due to the subsequent, standard acid-catalyzed deprotection.

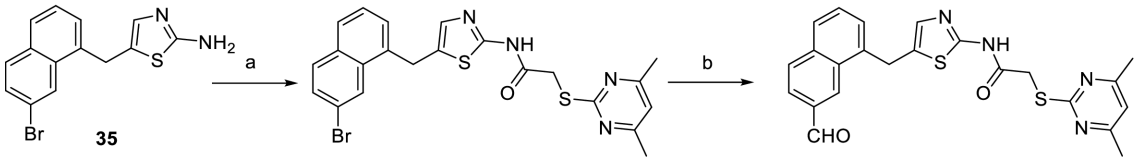

Scheme 17: Aldehyde synthesis and final amidation to SirReal2-aldehyde **FM316**. Conditions: a) ((4,6-dimethylpyrimidin-2-yl)thio)acetic acid, DMAP, EDC·HCl, DMF, rt, 16 h, 52%, b) N-formylsaccharin, Na_2CO_3, $Pd(OAc)_2$, DPPF, triethylsilane, DMF, 80 °C, 16 h, 11%;

Despite poor experience with previously attempted palladium-catalyzed reactions and the thioether containing selectivity pocket binder structural motif (see Chapter 3.1.3.1, **Table 1**), an attempt was made to introduce the aldehyde group directly from **7-Bromo-SirReal2** (**FM315**) previously prepared from aminothiazole **35** by EDC-mediated amidation (see **Scheme 17**). Fortunately, the synthesis of the SirReal2-aldehyde derivative **FM316** was successfully achieved (but as expected with a low yield) using an established general palladium-catalyzed reductive carbonylation procedure[112], with *N*-formylsaccharin serving as a carbon monoxide (CO) surrogate. *N*-formylsaccharin is a crystalline CO source that

generates CO *in situ* under safe reaction conditions, offering a more practical alternative to the use of toxic CO gas for introducing aldehyde moieties into aryl halides.[113]
The low yield of 11% is attributable on the one hand to the incomplete conversion of the starting material, but predominantly to observed decomposition during isolation and purification.

By following the synthesis strategy, the lead compound **SirReal2** was successfully modified with the intended polar and electrophilic residues (boronic acid, nitrile, aldehyde) capable of forming reversible covalent bonds under appropriate preconditions. Subsequently, the inhibitory activity against Sirt2 and the subtype selectivity of the synthesized target compounds were evaluated in the following Chapter 3.2.4.3.

3.2.4.3 Biological evaluation and SAR-analysis of synthesized envisaged reversible covalent binding SirReal2 derivatives

3.2.4.3.1 Sirt2 inhibitory activity (IC_{50} determination) and subtype selectivity screening (Sirt1, Sirt3 and Sirt5)

The determination of the inhibitory activity of the synthesized target molecules and the corresponding selectivity regarding Sirt2 (see **Figure 21**) was carried out by Reaction Biology Corporation (Malvern, USA).

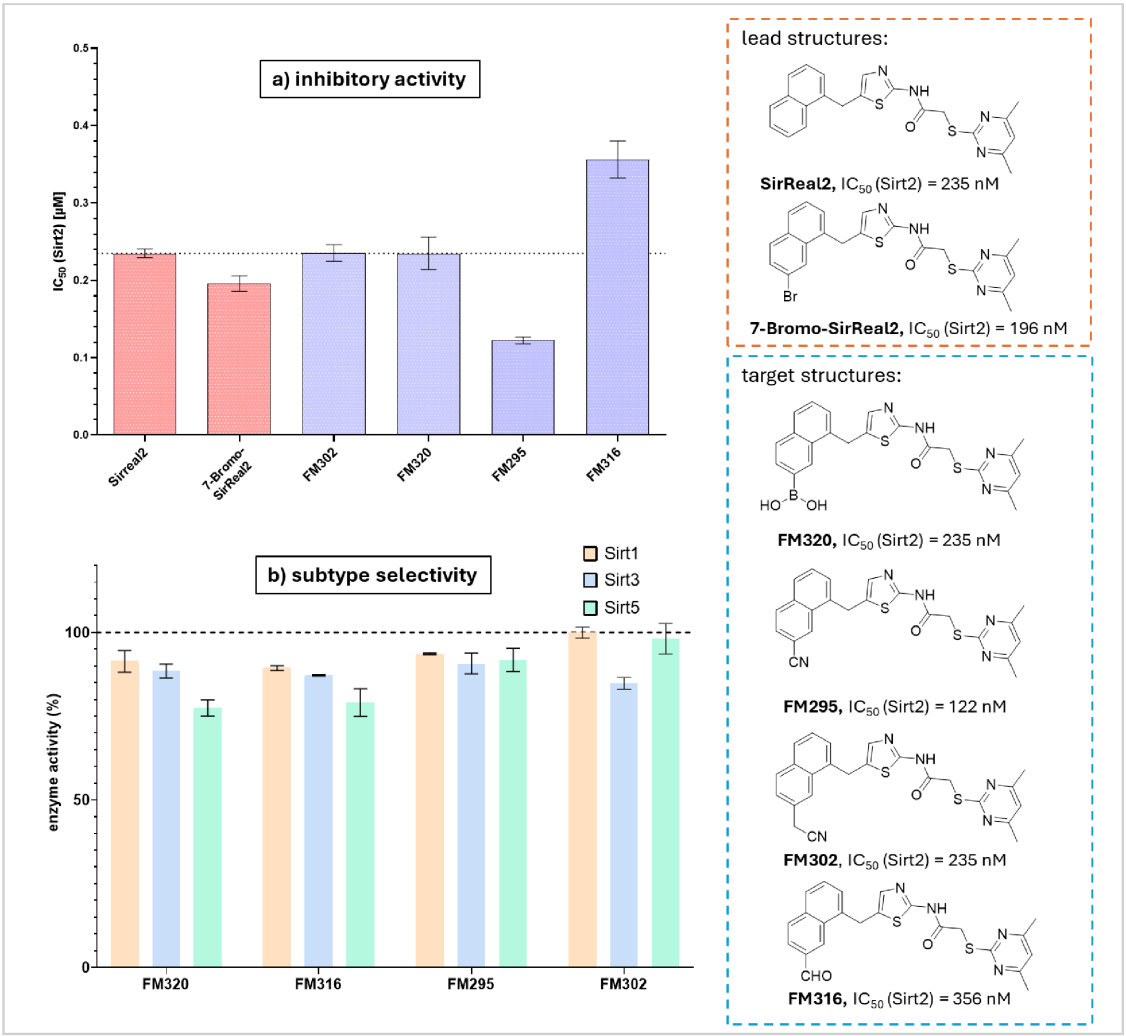

Figure 21: Determination of the inhibitory activity of the test substances on the corresponding sirtuin enzymes, based on a fluorescence-based assay (for details see Chapter 5.3.3) by Reaction Biology Corporation (Malvern, USA). a) Inhibitory activity (IC_{50}) on Sirt2 of reference substances **SirReal2** and **7-bromo-SirReal2** as well as the corresponding synthesized reversible covalent binding warhead modifications. For each serially diluted replicate of the triplet, an IC_{50} value was determined by sigmoidal curve fitting and the presented mean and standard deviation (displayed as error bars) were then calculated from the three resulting IC_{50} values. b) Subtype selectivity screening of target substances on Sirt1, Sirt3 and Sirt 5. The percentage residual enzyme activity of the respective sirtuin isoforms in the presence of the target inhibitors was determined at 50 µM in duplicate, giving the presented mean and corresponding standard deviation (displayed as error bars).

The detailed experimental conditions and results of the fluorescence-based assays performed are summarized in Chapter 5.3.3. The lead compound **SirReal2**, which was purchased by Sigma-Aldrich (Merck, Darmstadt, Germany) was determined with an IC_{50} value of 235 nM towards Sirt2 and the expectedly more potent **7-bromo-SirReal2** showed an IC_{50} value of 196 nM, both serving as a reference for the warhead-modifications prepared. According to literature **SirReal2** was reported with an IC_{50} value of 0.44 µM on Sirt2 and **7-bromo-SirReal2** (IC_{50} = 0.21, Sirt2) was published as an optimized derivative[40]. When comparing the literature values of the lead compounds with the values determined in this thesis, the IC_{50} values for **7-bromo-SirReal2** are consistent, indicating that it represents a more potent development of **SirReal2**. While **7-bromo-SirReal2** shows improved potency over **SirReal2**, it does not achieve the more than double increase in potency as published. Instead, **SirReal2** was found to have 1.9 times the inhibitory activity compared to the reported values. Due to variations in assay conditions, IC_{50} values may differ and are not directly comparable. However, the lead compounds were confirmed as potent inhibitors in the lower submicromolar range, and **7-bromo-SirReal2** was identified as a more potent derivative of **SirReal2**, demonstrating that the overall outcome of the commercial test system is consistent.

The SirReal2-boronic acid **FM206** and the SirReal2-acetonitrile derivative **FM302** similarly display an IC_{50} value of 235 nM on Sirt2 and are therefore equipotent to **SirReal2**, but slightly inferior to **7-bromo-SirReal2** (IC_{50} = 196 nM, Sirt2). The SirReal2 aldehyde derivative **FM316** (IC_{50} = 356 nM, Sirt2) demonstrated a 1.7-fold lower inhibitory activity than **SirReal2** and represents the least favorable structural modification compared to the competing inhibitors. Encouragingly, the SirReal2-nitrile derivative **FM295** with an IC_{50} value of 122 nM on Sirt2 showed a distinct 1.9-fold increase in potency in relation to **SirReal2** and a clear improvement by a factor of 1.8 compared to **7-bromo-SirReal2**. These values can also be transferred to the corresponding SirReal2-acetonitrile derivative **FM302** allowing a direct assessment of the effect of the corresponding methylene extension. Although the homologous variant increases the flexibility of the nitrile group, its larger spatial requirements and associated alignment constraints may negatively impact the binding strength of the inhibitor. The high demands on inhibitors of the Sirt2 binding pocket for structural modifications involving polar functional groups, as noted in Chapter 3.2.3.2.4, were successfully addressed through effective structure-activity relationship analysis. All synthesized compounds exhibited strong inhibitory activity, and the SirReal2-nitrile derivative **FM295** significantly advanced the **SirReal2** lead compound, resulting in a notable increase in potency.

Sirtuin 2 selectivity was confirmed in a subsequent subtype selectivity screening, in which all synthesized target compounds showed an average enzyme activity of over 77% on closely related sirtuin isoforms (Sirt1, Sirt3 and Sirt5) at 50 µM inhibitor concentration. Based on

demonstrated submicromolar IC_{50} values on Sirt2 of the examined target inhibitors, the remaining enzyme activity at the investigated subtypes indicates IC_{50} values at least greater than 50 µM.

All synthesized structural modifications exhibit potent and selective biological activity on sirtuin 2, with SirReal2-nitrile derivative **FM295** successfully developed as an inhibitor that outperforms the lead compound **SirReal2** by 1.9-fold in potency. Based on these positive results, an investigation of the specific binding mode of the respective inhibitors in the Sirt2 binding pocket through crystal structure analysis was considered.

3.2.4.3.2 Crystallography-based binding mode investigation of boronic acid modification of SirReal2: **FM206**

For the analysis and characterization of the respective binding modes, the synthesized compounds were investigated by PD. Dr. Eva Huber (research group of Prof. Dr. Michael Groll) at the Center for Functional Protein Assemblies of the Technical University of Munich the to create corresponding protein-ligand crystal structures. Further information on applied crystallographic background are outlined in Chapter 5.4.2.

The analysis of the binding properties and specific interactions of the corresponding inhibitors can provide valuable insights into the potential presence of reversible covalent bonds, similar to the approach used by Groll *et al.* who successfully demonstrated a reversible covalent mechanism by the crystallization of Bortezomib with its target proteasome[114]. Unfortunately, up to now only the cocrystal structure of SirReal2-boronic acid **FM206** in low resolution (4.2 Å) with Sirt2 could be recorded, while the other structural modifications eluded further crystallographic investigation (see **Figure 22**). As predicted in the previously performed docking experiment (see Chapter 3.2.4.1), SirReal2-boronic acid **FM206** occupies a similar position in the binding pocket as the lead compound **SirReal2** and is characterized by comparable interactions with the protein; a possible explanation for the similar potency of **SirReal2** and **FM206** (both IC_{50} = 235 nm, Sirt2). However, the resulting crystal structure of **FM206** with Sirt2 lacks the obligatory cofactor NAD^+, representing the actual target for the formation of the envisaged reversible covalent bond with the boronic acid. In principle, a displacement of NAD^+ by a Sirt2 is not unusual, since lead compound predecessor **SirReal1** (in contrast to **SirReal2**) acts as a competitive inhibitor towards NAD^+ (see **Figure 23**)[42]. However, there are more backgrounds to consider: possible steric hindrance and low resolution of the crystallographic experiment. By visualizing the usual NAD^+ orientation in the Sirt2 binding pocket on the basis of the crystallographic data of the **SirReal2** lead compound

(PDB ID: 4RMG), the high spatial proximity of the ribose part of NAD^+ and the boronic acid moiety of **FM206** is evident (see **Figure 22**, B).

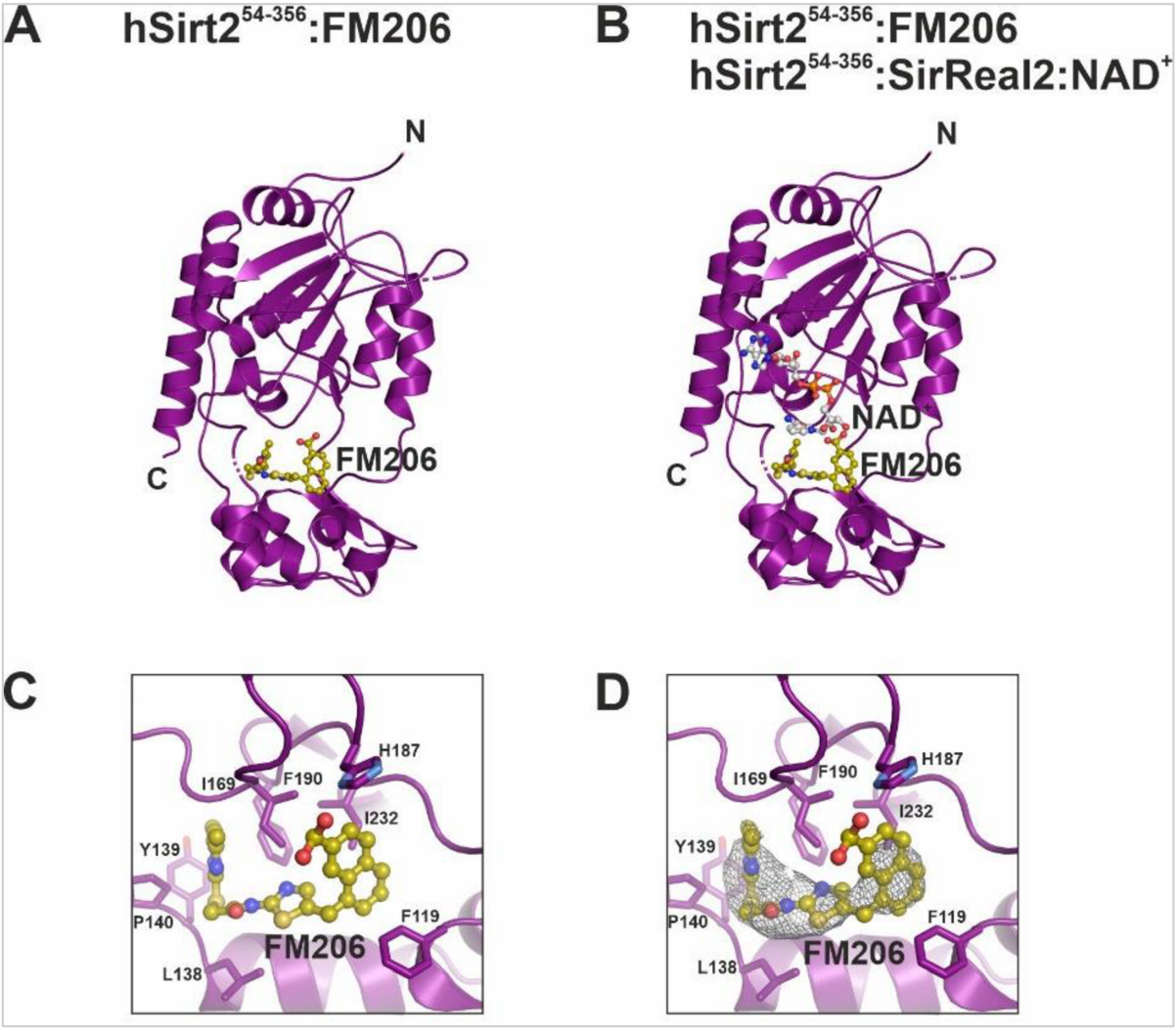

Figure 22: **FM206** cocrystal structure with Sirt2 shows similar spatial arrangement as predicted in previous docking experiments (see Chapter 3.2.4.1). A) General display of obtained crystal structure with **FM206** in the Sirt2 binding pocket. Contrary to expectations cofactor NAD^+ was not detected in the crystallographic experiment. B) Symbolized theoretical position of NAD^+ by subsequent insertion of the respective crystal structure based on existing data (PDB ID: 4RMG) indicates sterically demanding environment. C) Detailed view of **FM206** and surrounding amino acids in the Sirt2 binding pocket. D) Electron density illustration of **FM206** in the Sirt2 binding pocket.

Therefore, it is conceivable that the cofactor could be displaced, making a reversible covalent bond unavailable. The low resolution and the slow crystallization process of the cocrystal could also be a reason why the cofactor NAD^+ could not be observed, which is why efforts are currently being made to improve the resolution and the experimental conditions. Furthermore, the absence of the cofactor may also explain the laborious and complicated crystallographic process of the SirReal2-boronic acid **FM206** protein complex, and the difficulties observed during crystallization of the remaining structural modifications. Despite significant challenges, the cocrystallization of **FM206** succeeded, enabling the visualization of the underlying binding

mode and the validation of the orientation of the boronic acid group in close proximity to the binding site of the NAD^+ ribose structure, as predicted previously.

As a result, within the scope of this specific crystallographic investigation and the underlying resolution of the conducted experiment, the inhibitory potency of **FM206** cannot be attributed to a reversible covalent binding mode.

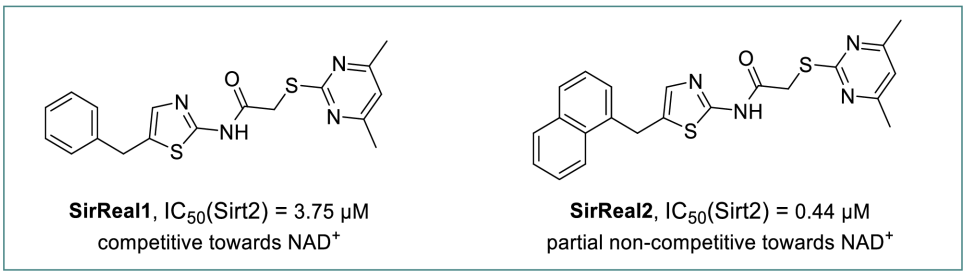

Figure 23: **SirReal1** represents a less potent relative of **SirReal2** and is an inhibitor that, unlike **SirReal2**, is competitive towards NAD^+. Consequently, **SirReal1** has the ability to displace NAD^+ from the active site of Sirt2.[42]

Consequently, the remaining nitrile and aldehyde modifications, particularly SirReal2-nitrile derivative **FM295** (IC_{50} = 122 nM, Sirt2), continue to be promising inhibitors with the potential to form a reversible covalent bond with the NAD^+ cofactor. Therefore, further crystallization efforts are being undertaken and corresponding crystallographic studies are being intensively pursued to identify the specific binding mode.

3.3 Lead structure-based hybridization drug design strategy for developing optimized Sirt2 inhibitors

3.3.1 Lead structure-based hybridization as a fundamental approach in medicinal chemistry

The availability of established lead compounds offers the opportunity for a lead structure-based hybridization approach, allowing the sophisticated combination of relevant pharmacophoric structural elements, predominantly based on initial crystallographic analysis, to achieve optimized hybrid compounds[115].This strategy offers valuable insights into the complex interaction processes within the binding pocket and serves as a targeted method for the systematic advancement and customization of further inhibitors (see **Figure 24**)[116].

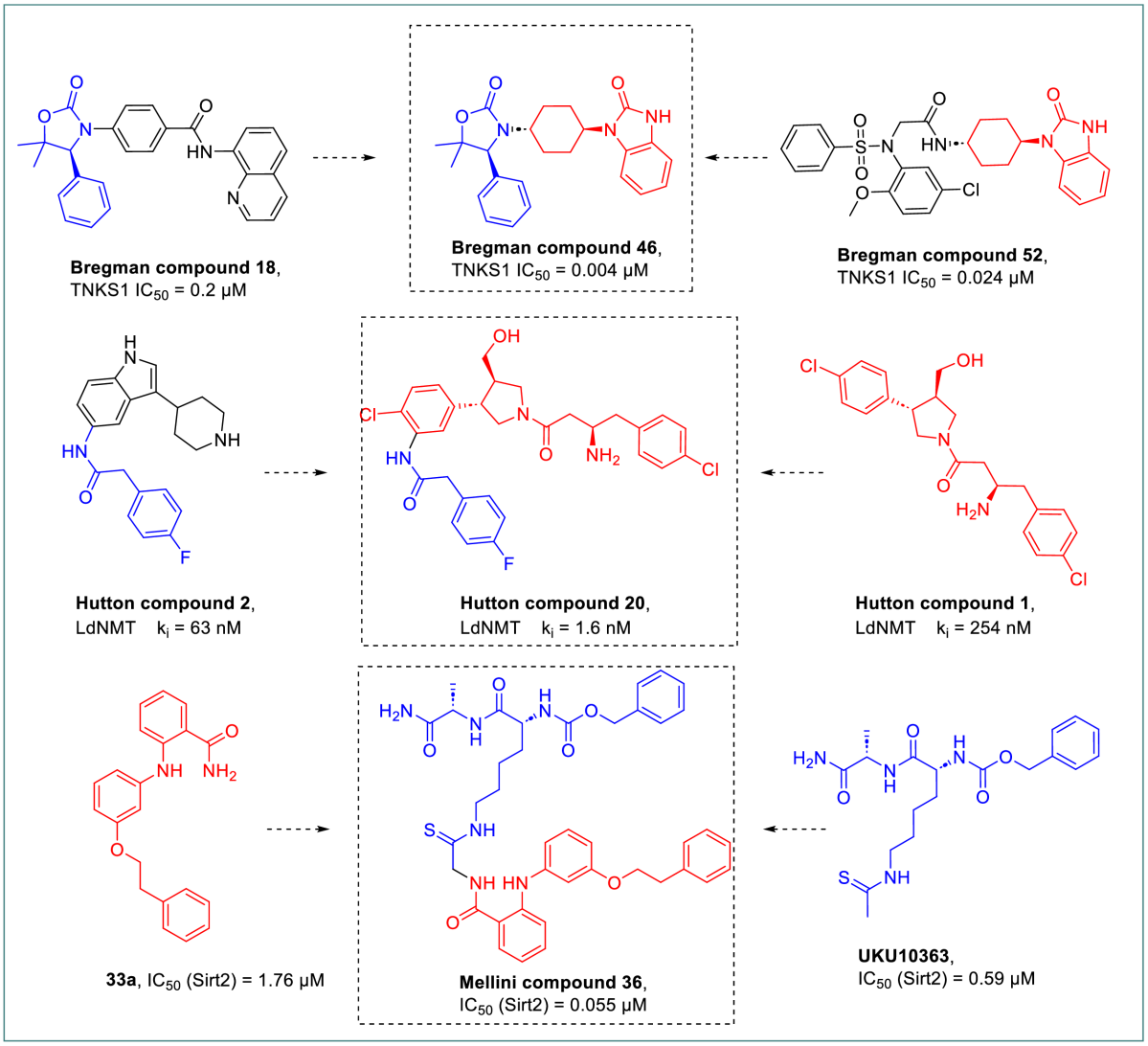

Figure 24: Successful application lead structure-guided hybridization approach to improve the binding affinity of selected inhibitors, based on fusion or merging key structural elements to visualize hybrid approach principle (cf. lit.[78, 116-120]) Abbreviations: TNSK1 (tankyrase 1), LdNMT (*Leishmania N*-myristoyltransferase), k_i (inhibition constant): describes the binding affinity of an inhibitor as the equilibrium concentration between dissociation and association with the enzyme.

Particularly regarding Sirtuin 2, lead structure-based hybridization based on available crystal structures offers excellent prospects. This approach has been successfully demonstrated with the hybrid **Mellini compound 36** through the fusion of compounds **33a** and **UKU10363** (see **Figure 24**). The application to **SirReal2** and further optimized derivatives offers promising potential, which will be evaluated in the following Chapter 3.2.2.

3.3.2 Selection and design of novel lead structure-based hybrid candidates

3.3.2.1 Crystal structure analysis of lead compounds as inspiration for envisaged hybridization approach

Existing cocrystal structures of potent inhibitors can be utilized to identify key structural elements designing improved analogue compounds. In the subsequent crystallographic investigation of the lead compounds **SirReal2** and **24a**, potential hybrid candidates will be identified and evaluated (see **Figure 25**).

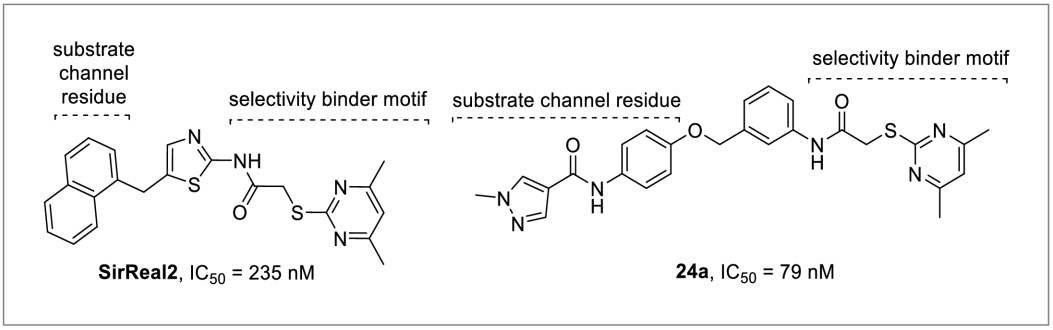

Figure 25: Selected lead compounds **SirReal2** and **24a** for a molecular hybridization approach. For direct comparability, the IC_{50} values on Sirt2 of the lead compounds determined using the assay system of this thesis (see Chapter 5.3.3) are provided, as published literature values cannot be directly compared due to varying test conditions.

Inhibitor **24a** as a direct related but more potent further development of **SirReal2** shares the same (2-((4,6-dimethylpyrimidin-2-yl)thio)acetamide moiety selectivity pocket binder motif, connected *via* an amide bond to the corresponding aromatic ring (thiazole for **SirReal2**, benzene for **24a**)[80]. The substrate channel residue, in case of **SirReal2** the naphthalene is methylene linked, for **24a** the amide-based substrate channel residue is connected *via* a methyl ether bridge. Due to the structural similarity, a comparable binding mode can be expected, which was subsequently confirmed by superimposing the respective cocrystal structures (see **Figure 26**). The methyl ether element of **24a** enables the necessary spatial alignment of the amide-based substrate channel residue, considering to be a crucial structural feature. The thiazole of **SirReal2** and corresponding benzene ring of **24a** occupy similar positions in the binding pocket, making their interchangeable replacement feasible, enabling further variations possibilities. Due to their structural similarities, **SirReal2** and **24a** possess the ideal

prerequisites for identifying and strategically applying pharmacophoric fragments. The common and crucial selectivity pocket binder motif (2-((4,6-dimethylpyrimidin-2-yl)thio)acetamide moiety) represents an essential and unchangeable structural element for the development of corresponding hybrid compounds.

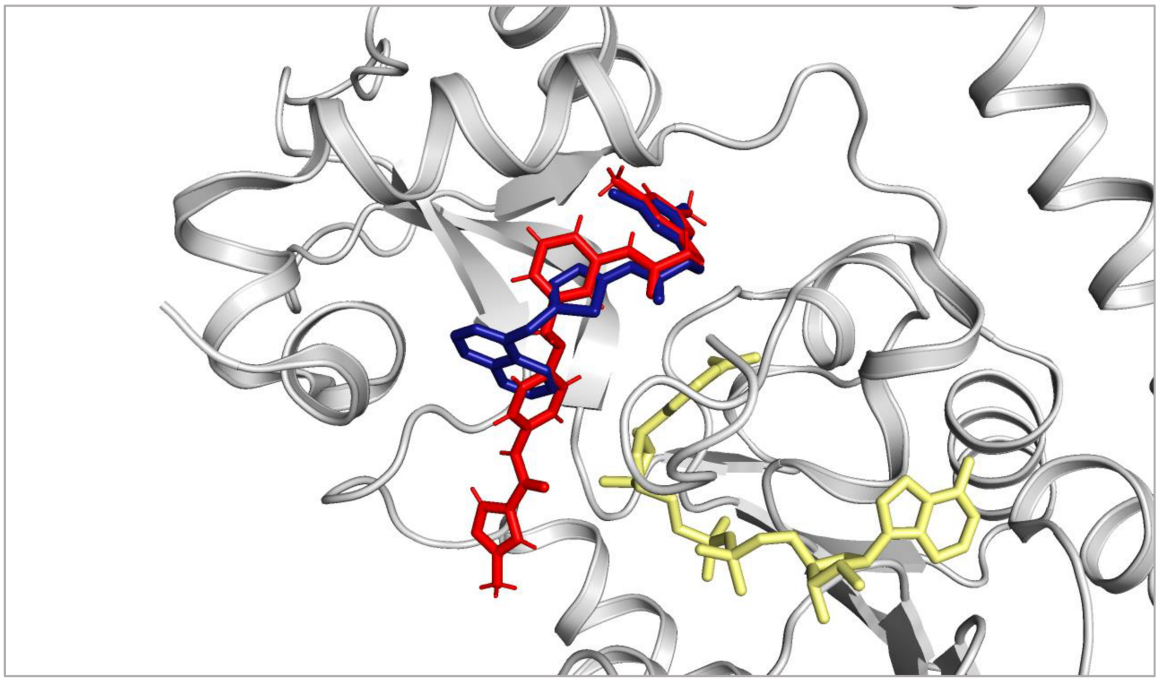

Figure 26: Stacked crystal structure visualization (prediction based on PDB ID: 4RMG) of lead compounds **SirReal2** (blue, PDB ID: 4RGM) and **24a** (red, PDB ID: 5YQO) together with cofactor NAD^+ (yellow: PDB ID: 4RMG) for molecular hybridization considerations.

Whereas **SirReal2** is mainly characterized by hydrophobic and π-π stacking interactions of the naphthalene within the substrate channel, **24a** shows additional polar interactions through the amide unit, contributing to a stronger inhibition of Sirt2[42, 80].

Based on the crystal structure analysis of the selected **SirReal2** and **24a**, several shared and alternate structural elements involved in the biological activity of the inhibitors were identified. Considering these aspects, novel hybrid candidates will subsequently be designed through lead structure-based hybridization approach (see next Chapter 3.3.2.2).

3.3.2.2 Assembly of selected structural elements to create a promising library of novel hybrid candidates

Regarding **SirReal2**, two relevant structural elements are identified: the thiazole ring and its adjoining methylene bridge (see **Scheme 18**). In contrast, the more effective inhibitor **24a** and **28e** features the corresponding amide-based substrate channel residue linked *via* a benzyl ether structure. Based on the assumption that a certain spatial flexibility of the inhibitor is advantageous and necessary, as concluded in previous rigidization approaches (see Chapter 3.1.4), the methyl ether group was considered the crucial fragment for the design of the desired hybrid inhibitor candidates.

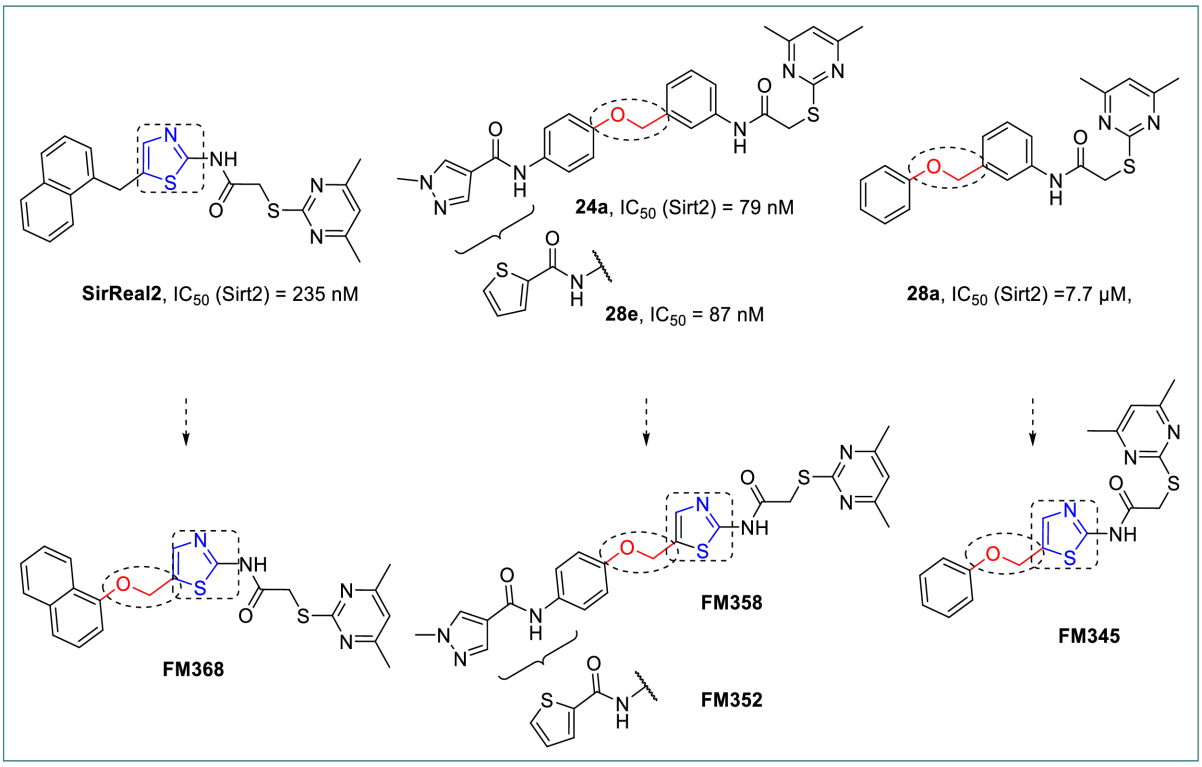

Scheme 18: Combination of key structural elements (methylether and thiazole) of selected lead compounds (**SirReal2**, **24a**, **28e**, and **28a**) to design promising hybrid candidates. For direct comparability, the IC_{50} values of the lead compounds determined using the assay system, of this thesis are provided (for details see Chapter 5.3.3), as published literature values cannot be directly compared in this case due to varying test conditions.

Therefore, a modification of **SirReal2** with the corresponding ether group to **FM368** is required to analyze the assumed beneficial effect on inhibitory activity. The incorporation of the thiazole ring represents a hybridization-based approach for the further development of **24a** and **28e** with hybrid candidates **FM358** and **FM352**, since polarity alterations and substrate channel residue realignment due to the change from benzene to thiazole will potentially enable favorable interactions within the active site of Sirt2. These fundamental considerations can be expanded to include additional lead compounds such as **28a** allowing further comparative and

relational analyses of the impact of lead structure-based hybridization drug design approach based on target compound **FM345**.

3.3.2.3 Docking experiment-guided validation of proposed hybrid candidates

Prior to initial synthesis efforts, the proposed hybrid candidates were to be evaluated by molecular docking experiments (carried out by our cooperation partner Dr. Thomas Wein, for further details see Chapter 5.4.1) focusing particularly on general binding properties and fitting accuracy. The determination of equivalent binding modes is particularly desirable regarding the alignment of the selectivity pocket binder motif (2-((4,6-dimethylpyrimidin-2-yl)thio)acetamide moiety) and substrate channel residues, as an excessive change in conformation due to moderate structural adjustments is not expected or considered favorable. The docking studies of **FM345** and **FM368** showed encouraging results, as both hybrid candidates assume a spatial orientation comparable to the reference lead compound **SirReal2** (see **Figure 27**).

FM368 is characterized by close similarity regarding the selectivity pocket binder motif and corresponding thiazole positioning. Expected deviations are observed around the ether group, as the less restricted spatial arrangements of hybrid candidate **FM368** enable alternative alignment positions of the naphthalene residue within the respective binding pocket of Sirt2.

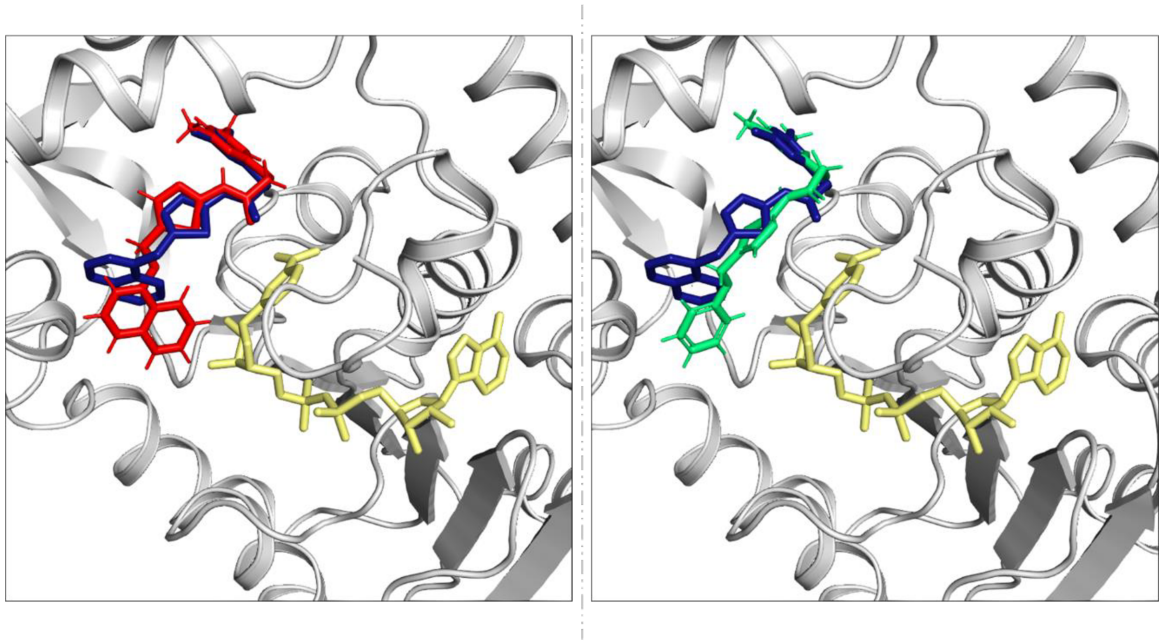

Figure 27: Sirt2 docking experiment results of **FM368** (red) and **FM345** (green) based on the crystal structure of the corresponding lead compound **SirReal2** (blue, PDB ID: 4RMG) and NAD^+ (yellow).

Similarly, **FM345** displays a positional reorientation of the corresponding benzene residue due to the presence of the ether group in the docking experiment. This reorientation is accompanied by a more extended occupation of the substrate channel of Sirt2. Despite the apparent overlap of the selectivity binder motif, **FM345** shows a partial deviation from the

reference **SirReal2**, including the thiazole ring positioned similarly but exhibiting a different orientation.

In related docking experiments (see **Figure 28**), the hybrid candidates **FM358** and **FM352** were found to match perfectly with the crystal structure of lead compound **24a** with regard to the predicted position within the binding pocket.

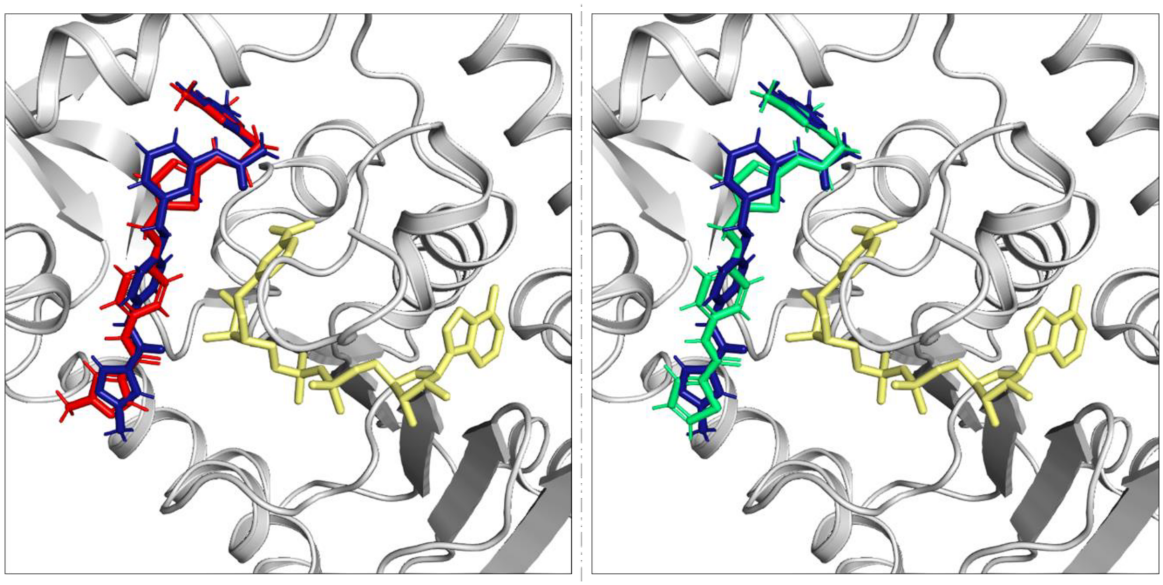

Figure 28: Sirt2 docking experiment results of **FM358** (red) and **FM352** (green) based on the crystal structure of the corresponding lead compound **24a** (blue, PDB ID: 5YQO) and NAD^+ (yellow, PDB ID: 4RMG extraction).

The selectivity pocket binder motif fits precisely in both cases, the thiazole ring has a suitable orientation, and the amide-based substrate channel residues demonstrate promising alignments. Fundamentally, the intended hybrid candidates (**FM345**, **FM368**, **FM352** and **FM358**) designed intuitively on paper first and confirmed by docking studies, expectedly display similar binding modes as their respective lead compounds. However, small changes to the structural elements can have significant impacts, creating (or destroying) additional binding opportunities and interactions within the binding pocket, which offer the potential to develop a stronger inhibitory effect. Based on the positive results in the molecular docking experiments a strategy for synthesizing the corresponding hybrid compounds was subsequently devised (see next Chapter 3.3.3).

3.3.3 Synthesis of hybridization-based target inhibitors

3.3.3.1 Retrosynthetic-analysis for envisaged hybrid candidates

In an exemplary retrosynthetic study of **FM345** three main building blocks were identified, consisting of phenol (**44**) (additionally substituted in the case of the other hybrid candidates), carboxylic acid **25** and a 5-(halomethyl)-2- aminothiazole unit (see **Scheme 19**). However, the synthesis design had to consider the commercial availability of the intended reactants and the potentially strong electrophilic property of the alkyl halogen species with respect to nucleophilic structures such as primary amines or thioethers to ensure an efficient and sophisticated approach.

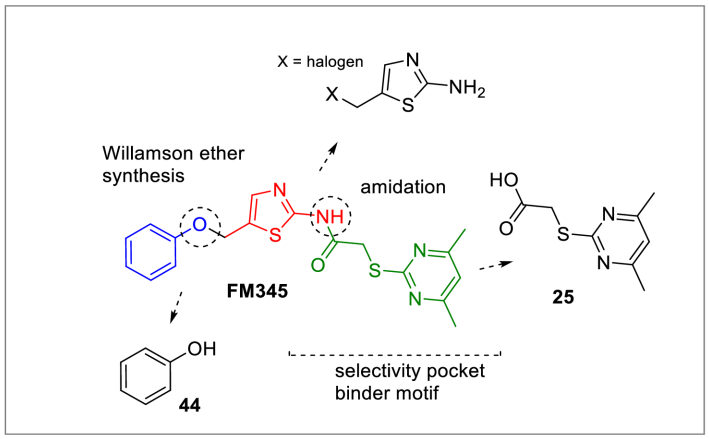

Scheme 19: Retrosynthetic analysis of ether hybrid candidates; exemplary visualization with phenoxy-substituted target inhibitor **FM345**.

Due to difficult synthetic access, lack of commercially available options and concerns regarding stability and reactivity of respective halomethyl aminothiazoles, the use of widely available and well established 2-amino-5-formylthiazole (**45**) as starting material was favored.

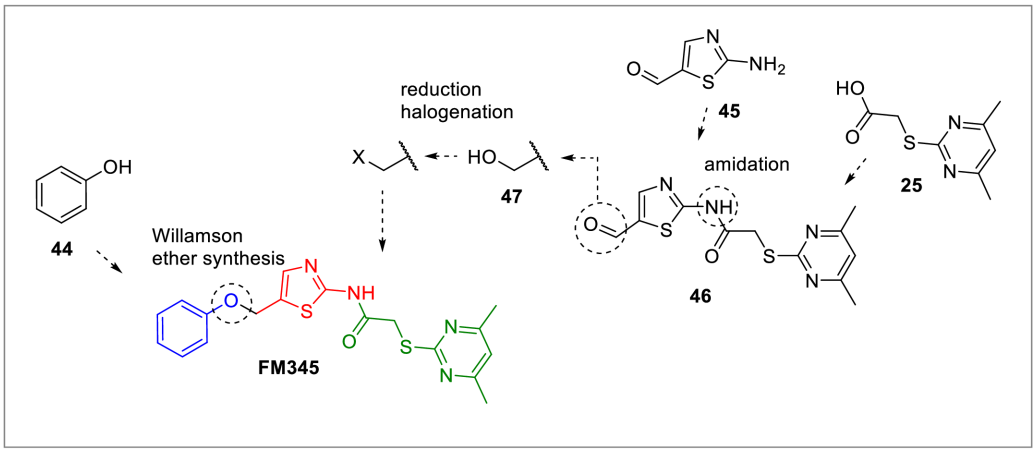

Scheme 20: Modified retrosynthetic approach after comprehensive analysis of various synthesis options.

Therefore, the synthesis design was adapted (see **Scheme 20**) and it was intended to link 2-amino-5-formylthiazole (**45**) with carboxylic acid **25** first, so that the respective aldehyde **46** can subsequently be reduced to the corresponding primary alcohol **47** to prepare an appropriate alkyl halide compound required for the final ether synthesis step. The synthesis plan takes into account the possible reactivity of the alkyl halogen species by preferably excluding the presence of primary amines as reaction partners in advance. Therefore, the amidation of amino-5-formylthiazole (**45**) has to take place at an early stage, followed by the subsequent ether synthesis. Due to positive experience using Williamson ether synthesis on similar compounds especially **28a** (**FM159**) (see **Scheme 11**, Chapter 3.2.3.2.3) and related literature, the synthesis of the so far poorly investigated class of 2-aminothiazole methyl ethers was carried out based on previous used reaction conditions (see next Chapter 3.3.3.2).

3.3.3.2 Synthesis of a (bromomethyl)thiazole intermediate as precursor for the intended Williamson ether synthesis to prepare aryloxymethylthiazolamides

The key element of the synthesis strategy is the preparation of the ether structure *via* Williamson ether synthesis, connecting the (bromomethyl)thiazole **48** with the corresponding phenolic substrate channel residue (see **Scheme 21**).

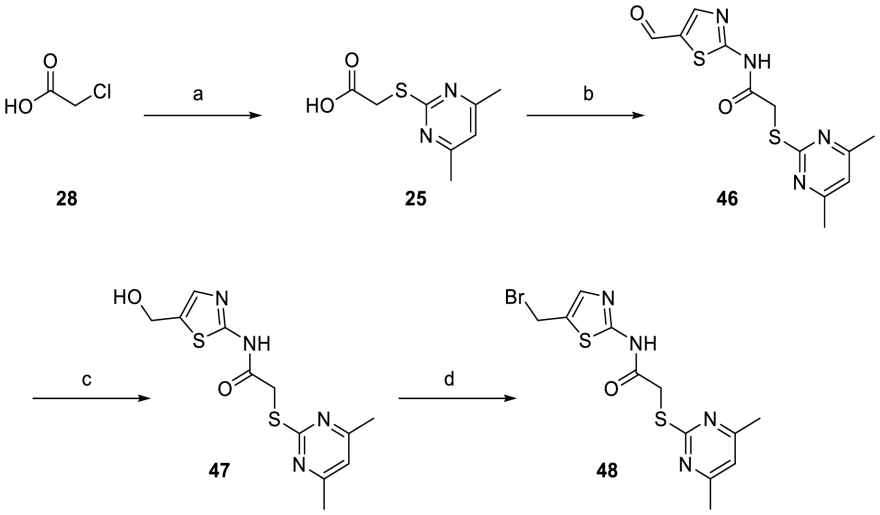

Scheme 21: Synthesis of alkyl bromide **48** as essential precursor for envisaged Williamson ether synthesis. Conditions: a) 4,6-dimethylpyrimidine-2-thiol, NEt_3, acetonitrile, rt, 24 h, 81%; b) 2-aminothiazole-5-carbaldehyde (**45**), DMAP, EDC·HCl, DMF, rt, 16 h, 46%, c) $NaBH_4$, MeOH, 3 h, 0 °C, 79%; d) PBr_3, DCM, rt, 18 h, quantitative.

The straightforward synthesis of the carboxylic acid **25** (previously established in Chapter 3.2.3.2.3, see **Scheme 11**) from 2-chloroacetyl chloride (**28**) marks the first step in the preparation of the primary alkyl halide required for the intended Williamson ether synthesis. EDC·HCl mediated amidation with 2-aminothiazole-5-carbaldehyde (**45**) provides the aldehyde **46**, which was reduced to the corresponding alcohol **39** using sodium borohydride.

Subsequently, the alcohol obtained is converted to the desired alkyl bromide **48** using phosphorus tribromide.

3.3.3.3 Williamson ether synthesis of aryloxymethylthiazolamides: scope and limitations

3.3.3.3.1 Fundamental chemical difficulties and initial adjustments of reaction conditions

The envisaged Williamson ether synthesis for the preparation of **FM345** should in fact be unproblematic, as a general feasibility already has been demonstrated in the synthesis of related boronic acid modifications of lead compound **28a** (see Chapter 3.2.3.2.3, **Scheme 11**), allowing theoretically simple transfer to the other desired hybrid candidates. Unfortunately, however, the establishment of the respective Williamson ether synthesis revealed major difficulties in the preparation of the so far uninvestigated class of 5-(aryloxymethyl)thiazoles of type **FM345** (see **Table 5**).

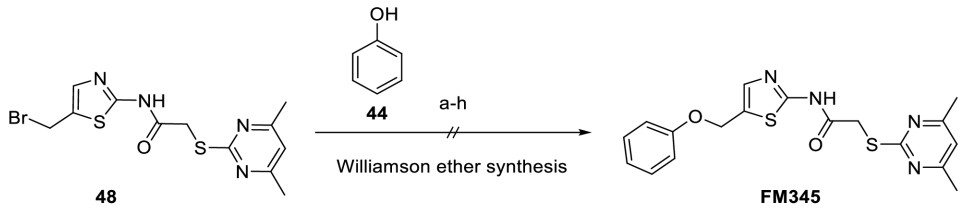

entry	base (1-2 eq)	solvent	condition	outcome description
a	*t*-BuOK	DMF	rt, 3 h	(bromomethyl)thiazole reactant no longer detectable, the desired product was not generated, other products were non-isolatable
b	K_2CO_3	acetonitrile	rt, 5 h	
c	K_2CO_3	DMF	rt, 24 h	
d	Cs_2CO_3	DMF	rt, 24 h	
e	NEt_3	DMF	rt, 24 h	
f	NaH	DMF	rt, 24 h	
h	K_2CO_3	DCM	rt, 24 h	undesired alkylation products
i	-	phenol (**44**)	40 °C, 24 h	

Table 5: Unsuccessful Williamson ether synthesis attempts using various reaction conditions. If reactant was still present after 12 h, a further equivalent of the appropriate base was added. K_2CO_3/DCM attempt h) and base-free phenol melting entry i) led to unwanted alkylation products (see **Figure 29**).

Despite applying the established reaction conditions of previously successfully performed ether syntheses (see Chapter 3.2.3.2.3, **Scheme 11**) the desired product **FM345** was not obtained using potassium *tert*-butanolate in DMF or potassium carbonate in acetonitrile. Further reactions in DMF with triethylamine, potassium carbonate, caesium carbonate, as well as sodium hydride as a base, were unsuccessful. These experiments were performed in consideration of favorable William ether synthesis reaction conditions, such as solvent requirements (aprotic polar solvents stabilize the phenolate anion) and base specifications (sufficient basicity, appropriate nucleophilicity and steric requirements).

The utilization of K_2CO_3 in DCM (**Table 5**, entry h) and a base-free melting experiment (**Table 5**, entry i) initially gave misleading positive results, as a reaction product with the matching high resolution mass spectrum could be isolated, which was however later identified as a *para*-alkylated phenolic product by further comprehensive NMR spectroscopic structural analysis (see **Figure 29**).

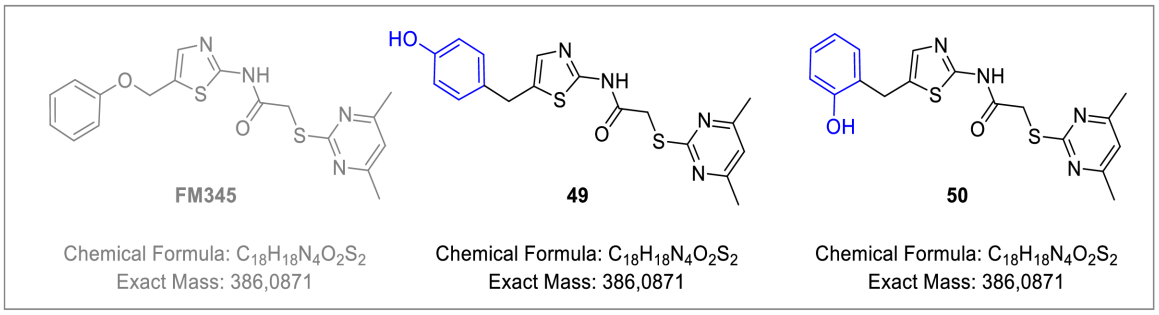

Figure 29: Undesired alkylation products observed (entry h and i) contributed to the further understanding of unwanted side reactions under subsequent Williamson ether synthesis conditions. In contrast to the *para*-substituted compound **49** (yield: 24% obtained from entry h), *ortho* variant **50** was assumed based on TLC-MS analysis but could not be separated and therefore characterized.

A reasonable competing reaction to the proposed Williamson ether synthesis with phenolates represents an electrophilic aromatic substitution, since the +M-effect of the corresponding phenolate anion concentrates the electron density within the aromatic ring and less at the oxygen atom, favoring an attack in *ortho*-, preferably in *para*-position[121]. In contrast to the *para*-alkylation product **49**, the corresponding *ortho*-substituted product **50** was detected only by TLC-MS analysis and not isolated, as the monitored yield was negligible. Nevertheless, the experiments revealed valuable chemical properties of the previously unknown 5-(bromomethyl)thiazol-2-amide **48** suggesting further synthesis adjustments. The undesired alkylation side reactions observed under Williamson ether conditions revealed the strong electrophilic properties of the previously unknown alkyl bromide **48**, represents a possible explanation for the fundamental difficulties in synthesizing 5-(aryloxymethyl)thiazolamides of the type (**FM345**). Consequently, the reaction behavior of **48** was further investigated, and the strategy for the Williamson ether synthesis was reconsidered.

3.3.3.3.2 Electrophilic property of the (bromomethyl)thiazole precursor and related synthetic adjustments

The exceptionally strong electrophilic properties of the alkyl bromide **48** became evident in the presence of water and methanol (see **Scheme 22**), leading to the corresponding alcohol **47** and methylether **51,** whereas the related benzyl bromide **25** (described in Chapter 3.2.3.2.3, **Scheme 11**) remains unaffected under similar conditions. The chemical property of phenol and the extremely strong electrophilic property of the alkyl bromide **48** may be responsible for this

undesirable side reaction described in the previous Chapter, so further experiments were carried out using the theoretically less reactive respective alkyl chloride **52** instead of the alkyl bromide **48**.

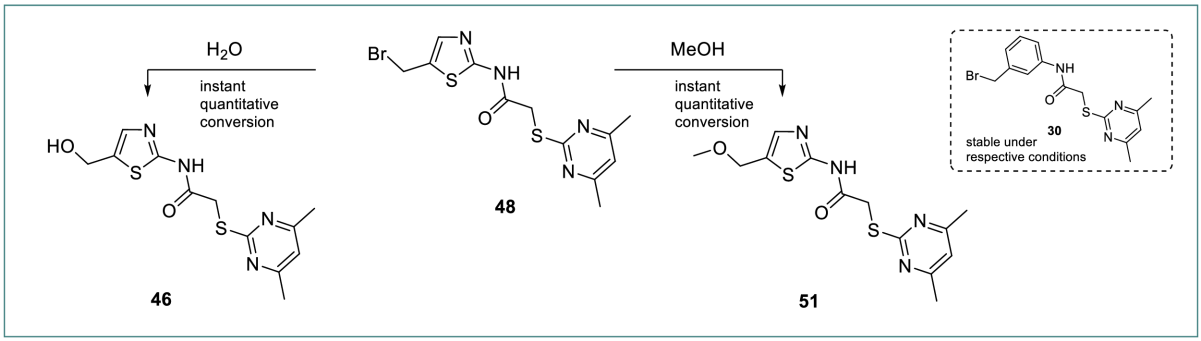

Scheme 22: Spontaneous reactions of alkyl bromide **48** with solvent traces indicate high electrophilic reactivity.

Therefore, alcohol **47** was converted to the corresponding alkyl chloride **52** using thionyl chloride. Additionally, to circumvent the alkylation reactions previously observed with phenol (**44**), 1-naphthol (**53**), the precursor for **FM368** was used for further attempts (see **Scheme 23**).

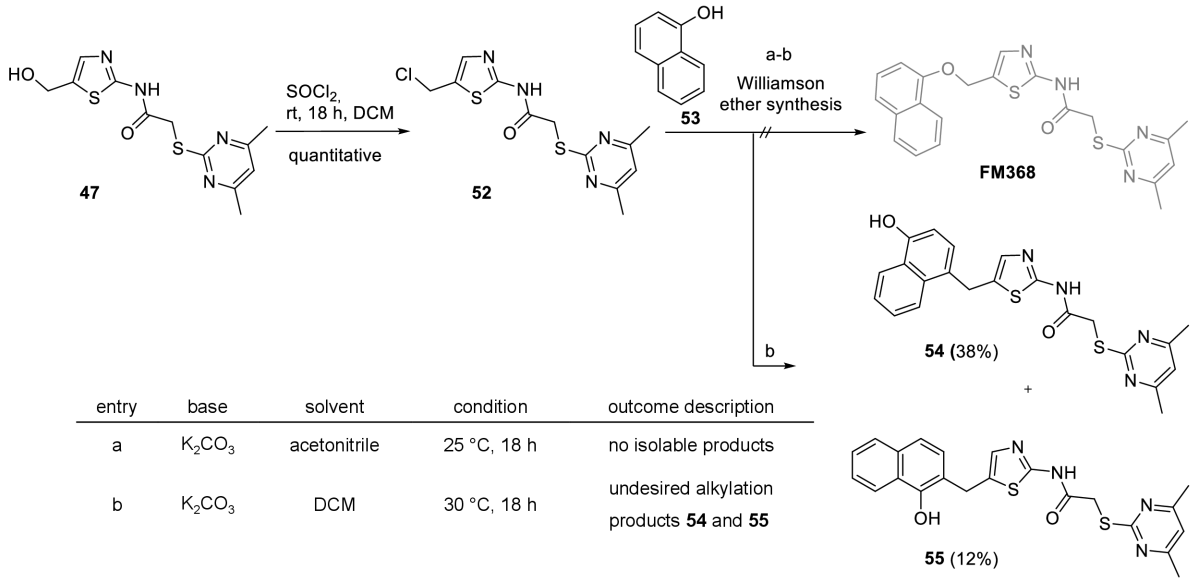

entry	base	solvent	condition	outcome description
a	K_2CO_3	acetonitrile	25 °C, 18 h	no isolable products
b	K_2CO_3	DCM	30 °C, 18 h	undesired alkylation products **54** and **55**

Scheme 23: Preparation of alkyl chloride **52** and unsuccessful Williamson ether synthesis attempts with 1-naphthol (**53**) confirmed alkylation tendency using DCM as solvent, whereas an acetonitrile-based attempt led to unspecific non-isolable products.

Unfortunately, the alkyl chloride **52**, prepared from the corresponding alcohol (**47**) using thionyl chloride, showed no significant improvement in its electrophilic properties compared to the bromine compound (**48**) and exhibited similar reaction behavior and instabilities in solvent traces (see **Scheme 22**). Furthermore, replacing phenol (**44**) with 1-naphthol (**53**) did not successfully yield the desired **FM368**, instead leading to similar undesired *ortho*- and *para*-substituted C-alkylated products **54** and **55**.

3.3.3.3.3 Strategy change: alternative ether synthesis approach via Mitsunobu-based reactions

Due to the large number of unsuccessful Williamson ether synthesis approaches, no further attempts were made at this point and an alternative strategy using Mitsunobu reaction starting from alcohol **47** was pursued to achieve the required ether synthesis to **FM368** (see **Scheme 24**).

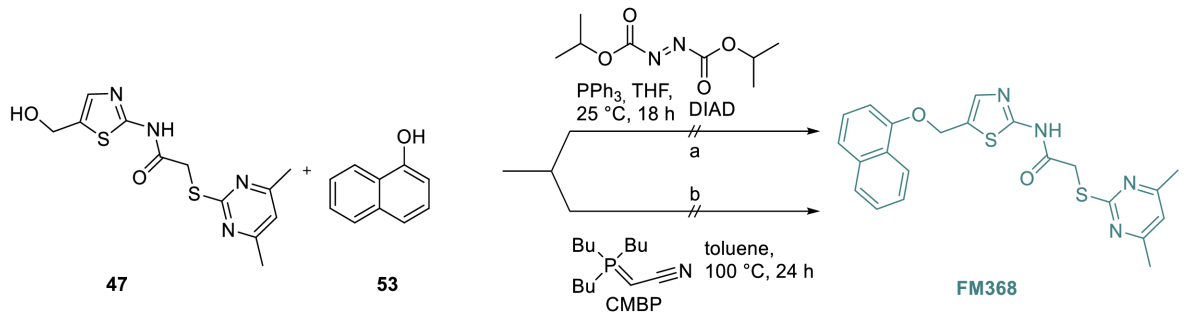

Scheme 24: Mitsunobu-based ether synthesis attempts of **FM368** remained unsuccessful. a) Typical Mitsunobu setup using diisopropyl azodicarboxylate (DIAD) and triphenylphosphine (PPh_3) and b) alternative attempt using CMBP (cyanomethylenetributylphosphorane, Tsunoda reagent).

Since an initial literature-inspired Mitsunobu reaction attempt[122] with DIAD and PPh_3 was unsuccessful due to unreacted starting materials, another experiment was made using CMBP, which is known to deprotonate weakly acidic pronucleophiles and tolerate higher reaction temperatures[123-124].

CMBP, acting as a phosphorane ylide, integrates the redox functions of DIAD and PPh_3 into a single reagent, facilitating the activation of the alcohol **47**, deprotonates the pronucleophile 1-napthol, and mediates the formation of the ether[125].

Unfortunately, this alternative application of the Mitsunobu reaction resulted in the previously observed *ortho/para*-alkylation products **54** and **55**, which is why no further synthetic efforts were undertaken in this direction.

3.3.3.3.4 The return to the Williamson ether synthesis: Successful achievement of the preparation of 5-(aryloxymethyl)thiazole-2-amides using sodium phenolates

After this series of setbacks, one final attempt was made returning to the Williamson ether synthesis using a variation without an additional base but solely with the addition of the appropriate phenolate salt to exclude the potential disadvantageous effects of the base addition. This purist approach, reduced to the absolute minimum, consists only of the alkyl halide electrophile, respective phenolate and solvent to minimize the extent of possible side reactions. Fortunately, using sodium 1-naphtholate (**56**) and alkyl chloride **52** the very first synthesis of the previously unknown substance class of 5-(aryloxymethyl)thiazole-2-amides **with FM345** was achieved (see **Scheme 25**).

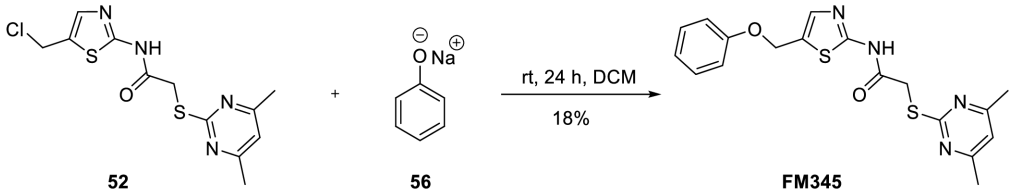

Scheme 25: First successful synthesis of representative **FM345** of the previously unknown structural class of 5-(aryloxymethyl)thiazol-2-amides using a Williamson ether synthesis.

Conveniently, sodium 1-naphtholate (**56**) was commercially available, whereas other phenolates (**59**, **61** and **62**) had to be prepared from the corresponding phenols to apply the newly discovered approach to the other target inhibitors.
Whereas sodium 1-naphtholate (**62**) can be prepared directly from 1-naphthol (**53**, see **Table 6**), the remaining amid-based substrate channel moieties of **FM352** and **FM358** require prior amidation starting from 4-aminophenol (**57**, see **Scheme 26**). Based on 4-aminophenol (**57**) the synthesis of **58**, was achieved in a yield of 69% using thiophene-2-carbonyl chloride, whereas the HATU-mediated amidation with 1-methyl-1*H*-pyrazole-4-carboxylic acid only yielded 21% of **60**, due to the substantial unwanted esterification observed in this case. Subsequently, the appropriate phenols **58** and **60** were treated with an equimolar amount of sodium methanolate and remaining liquid residues were removed by high vacuum to obtain phenol salts **59** and **61** in powder form without the necessity of purification. Finally, the desired **FM352** and **FM358** were prepared according to the previously modified Williamson ether synthesis protocol, combining the corresponding phenolate salts **59** and **61** with the respective alkyl chloride **52** in DCM.

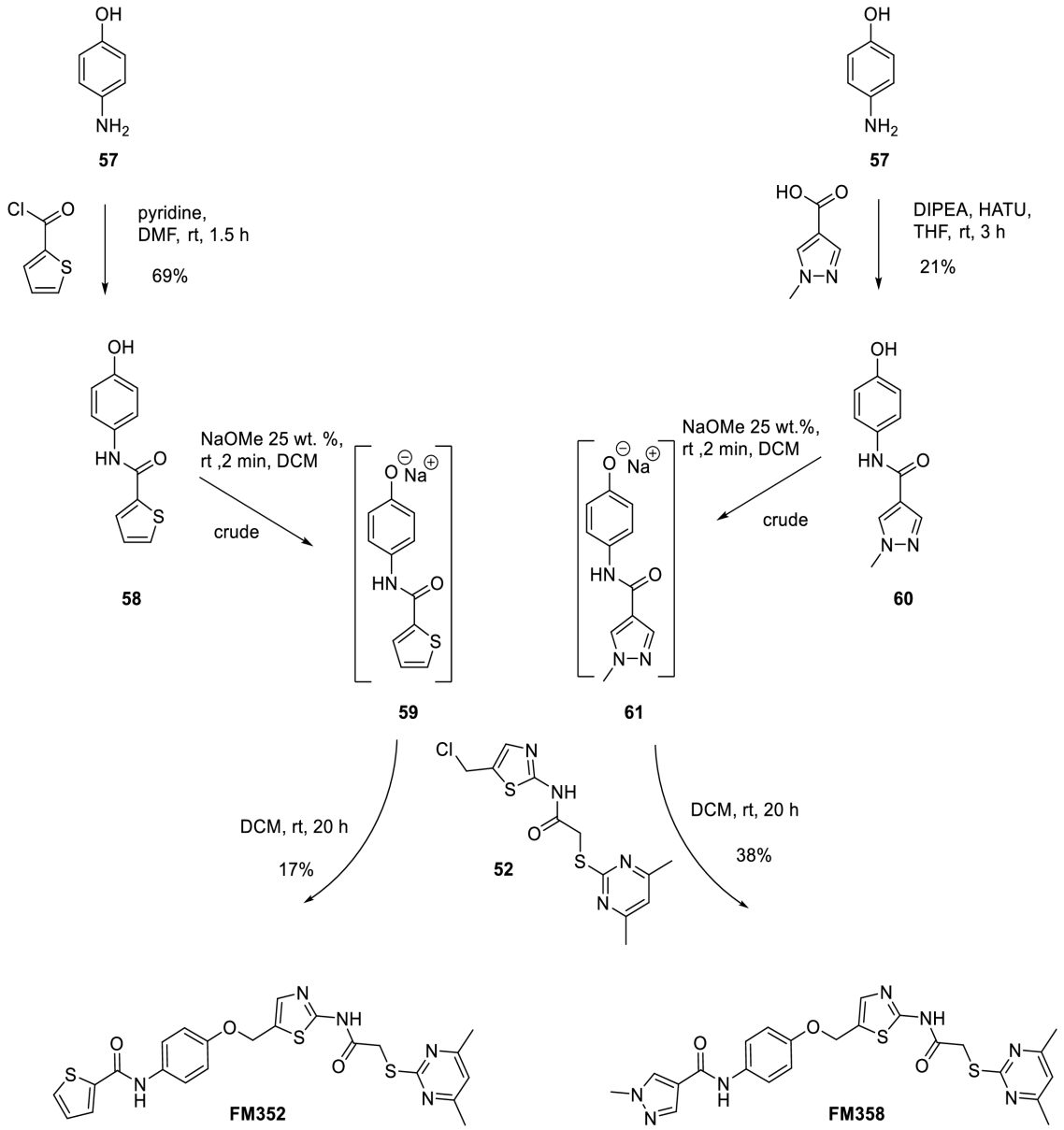

Scheme 26: Synthesis of hybrid candidates **FM352** and **FM358** comprising initial amidation step followed by preparation of the corresponding phenolate salt and final Williamson ether synthesis using previously described alkyl chloride **44**.

By using an appropriate phenolate salt and the associated absence of an external base additive, the reaction conditions of the Williamson ether synthesis could be successfully modified to get access to the desired target ether compounds, without, in contrast to the initial preparation attempts of hybrid candidate **FM345**, detecting any undesired C-alkylation products. Starting from 1-naphthol (**53**), sodium 1- naphtholate (**62**) was prepared using sodium methanolate according to the previous procedure, for subsequent Williamson ether synthesis in DCM using alkyl chloride **52** (see **Table 6**). Contrary to expectations, by applying these exact adjustments to the synthesis of the last remaining target compound **FM368**, the intended ether synthesis was not achieved using sodium 1-naphtholate, instead only the

previously described corresponding *ortho/para*-C-alkylation products **54** and **55** (see Chapter 3.3.3.3.2, see **Scheme 23**) were observed once more.

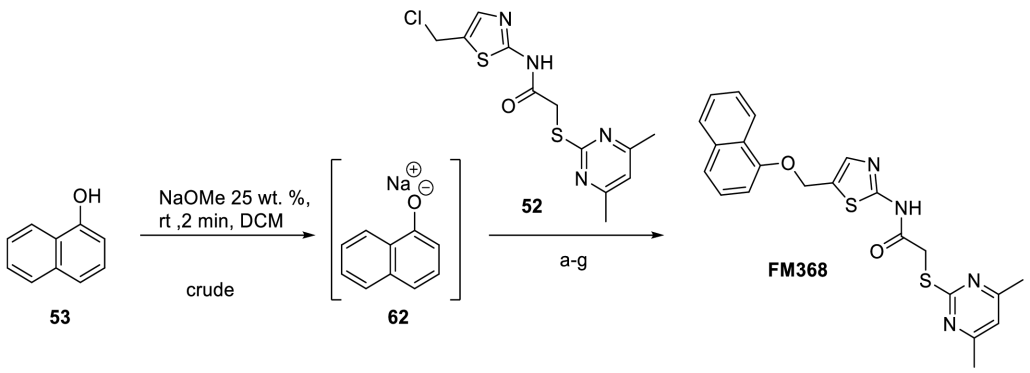

entry	solvent	conditions	outcome description
a	DCM	rt, 24 h	C-alkylation products (**54** and **55**)
a	THF		
b	EtOAc		
c	toluene		
d	dioxan		
e	acetonitrile		C-alkylation products (**54** and **55**) + **FM368** traces
f	DMSO		
g	acetone	rt, 5 h	C-alkylation products (**54** and **55**) + **FM368** (14%)

Table 6: The Williamson ether synthesis strategy previously established did not allow the synthesis of **FM368**, so various solvents were attempted to finally identify acetone as most suitable.

In a further screening (see **Table 6**), various solvents were examined, and the corresponding undesired C-alkylation products **54** and **55** were detected in all entries. In addition, the desired product **FM368** was found in acetonitrile, DMSO and acetone, and in the latter case not only traces but in a sufficient isolated yield of 14%.

The synthesis of the desired target compounds was associated with a series of challenges. Particularly surprising was the unexpected and extensive need to modify the Williamson ether synthesis. With the successful synthesis of the target inhibitors, the previously unknown structural class of 5-(aryloxymethyl)thiazol-2-amides has been described for the first time, and its previously unexplored potential is now available for general research. Subsequently, the synthesized inhibitor candidates were examined for their biological activity with respect to inhibition of Sirtuin 2 and corresponding subtypes.

3.3.4 Biological evaluation and SAR-analysis of synthesized hybrid target inhibitors

3.3.4.1 Sirt2 inhibitory activity examination (IC_{50} value determination) and subtype (Sirt1, Sirt3 and Sirt5) selectivity screening

Based on previously used procedures for the determination of IC_{50} values on Sirt2 and respective subtype selectivity screening on Sirt1, Sirt3 and Sirt5, the biological activity of the synthesized target compounds were determined by Reaction Biology Corporation (Malvern, USA). The detailed description of the respective assay conditions and specific values are provided in Chapter 5.3.3. The application of the lead structure-based hybridization drug design strategy distinctly reveals the successful achievement of the desired highly selective Sirt2 inhibitors with increased potency by combining relevant structural features of the respective lead compounds (see **Figure 30**).

The strongest inhibitory effect on Sirt2 is achieved by compound **FM358** with an IC_{50} = 66 nM, which even surpasses the most potent lead compounds **24a** (IC_{50} = 79 nM) by a factor of 1.2 and its analogue **28e** (IC_{50} = 87 nm) by a factor of 1.3 in this screening.
Therefore, lead compounds **28e** and **24a** were both synthesized according to literature[53, 80].
These results elevate compound **FM358**, together with the remarkable **28e** and **24a**, into the league of the most potent Sirt2 inhibitors published to date, even outperforming the original gold standard **SirReal2** (IC_{50} = 235 nM, Sirt2) in terms of inhibitory potency by a factor of 3.6. **FM352** displays outstanding inhibitory activity as well (IC_{50} = 94 nM, Sirt2), but is however less potent than the corresponding lead compounds **28e** and **24a**, but still shows considerably stronger inhibition in comparison to **SirReal2** (IC_{50} = 235 nM, Sirt2). Unfortunately, **FM345** (IC_{50} = 5.3 µM, Sirt2) and **FM368** (IC_{50} = 6.5 µM, Sirt2) fall significantly below expectations and do not demonstrate convincing biological activity compared to the tested lead compounds. Comprehensive SAR-analysis of the tested hybrid compounds is presented in the following Chapter 3.3.4.2.

Subtype selectivity analysis (see **Figure 30**) revealed that none of the tested compounds showed significant activity on other closely related isoforms of Sirt2 (Sirt1, Sirt3 and Sirt5) compared to the highly potent inhibitory effect of synthesized target compounds. For this purpose, enzyme activity of the investigated isoforms was measured at 50 µM. The resulting percentage values indicate residual enzyme activity after treatment with the corresponding inhibitor. Considering the strong inhibitory properties of the synthesized lead structure-based hybrid target inhibitors against Sirt2, the determined enzyme activities on related subtypes are considered to be negligible (residual enzyme activity indicates IC_{50} > 50 µM), as expected.

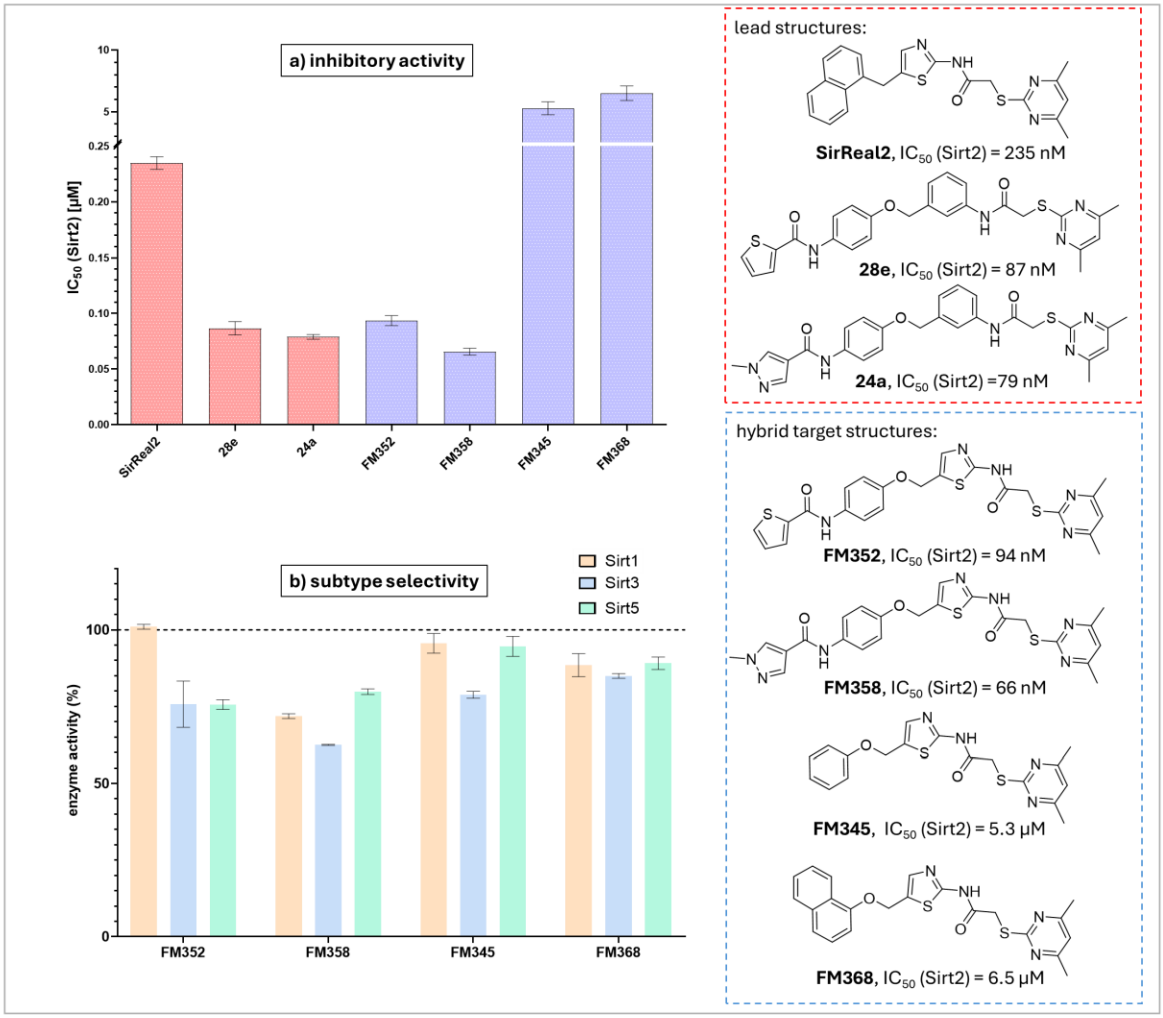

Figure 30: Determination of the inhibitory activity of the test substances on the corresponding sirtuin enzymes, based on a fluorescence-based assay (for details see Chapter 5.3.3) by Reaction Biology Corporation (Malvern, USA). Inhibitory activity (IC_{50}) on Sirt2 of lead compounds **SirReal2**, **28e** and **24a** as well as the synthesized hybrid target compounds **FM352**, **FM358**, **FM345** and **FM368**. For each serially diluted replicate of the triplet, an IC_{50} value was determined by sigmoidal curve fitting and the presented mean and standard deviation (displayed as error bars) were then calculated from the three resulting IC_{50} values. b) Subtype selectivity screening of synthesized hybrid target compounds. The percentage enzyme activity of Sirt1, Sirt3 and Sirt5 in the presence of the corresponding test substances was determined at 50 µM in duplicate, giving the presented mean and corresponding standard deviation (displayed as error bars).

3.3.4.2 SAR-analysis of lead structure-based hybridized inhibitors

Based on the structural variations carried out as part of the lead structure-based hybridization drug design approach, relevant conclusions and assertions can be formulated.

Assumptions that the introduction of the ether group and the associated increase in molecular flexibility by expanding the degree of spatial freedom leads to an increase in inhibitory activity, inspired by the lead compounds **28e** and **24a**, cannot be applied ubiquitously. A closer view at **FM345** and **FM368**, considered to be ether-modified SirReal2-based variations respectively, shows significant disadvantages regarding the inhibitory effect on Sirt2 (see **Figure 31**).

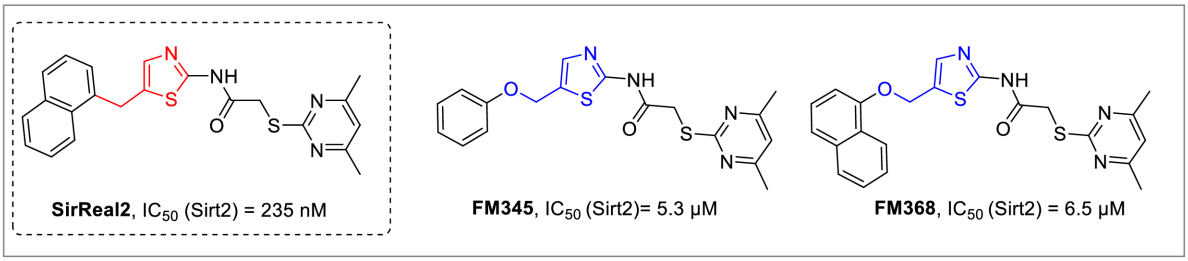

Figure 31: Hybridization strategy evaluation and SAR-display of **FM345** and **FM368** with its corresponding lead compounds **SirReal2**.

Although the additional ether group of **FM368** increases geometric flexibility, the molecule is also lengthened by one atom, potentially resulting in an unfavorable effect regarding the positioning of the naphthalene residue in the respective substrate channel of Sirt2. More differentiated interpretations are conceivable in the case of **FM345**, as although inhibitory activity was initially lost compared to **SirReal2**, the biological effect on Sirt2 was enormously increased by further amide substitution on the benzene ring with **FM352** and **FM358** (see **Figure 32**).

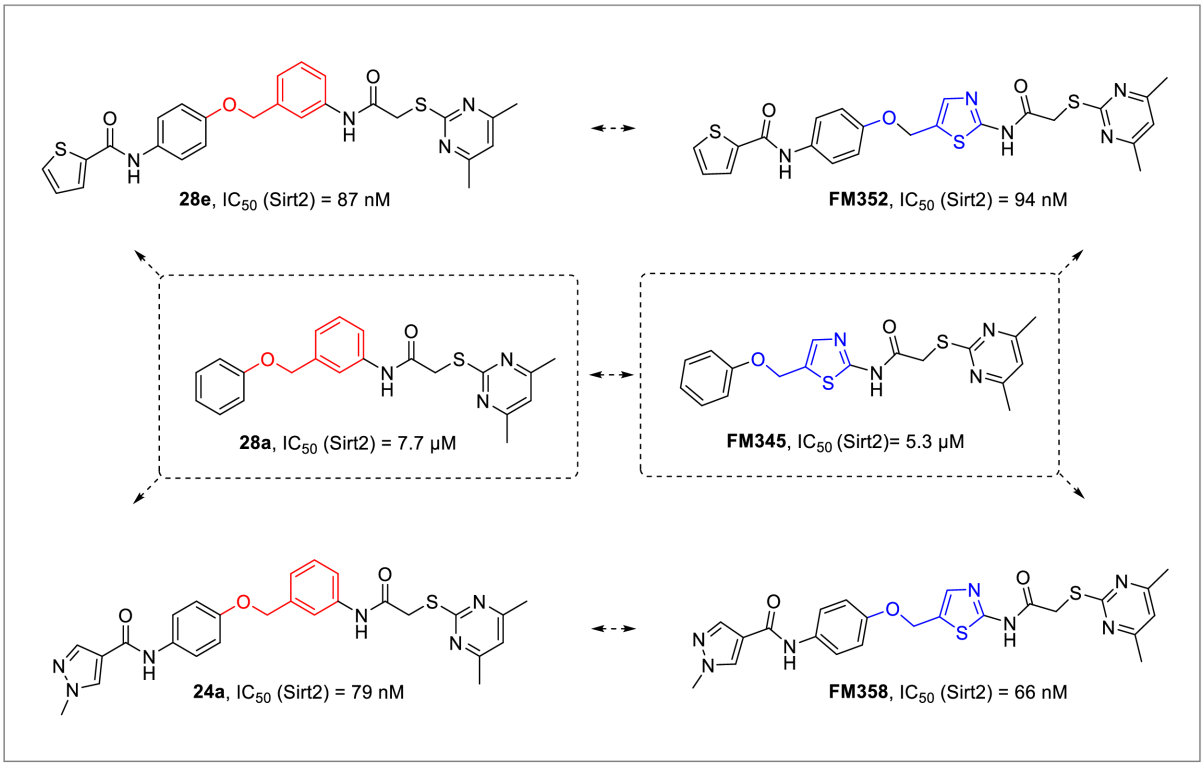

Figure 32: Hybridization strategy evaluation and SAR-display of **FM352** and **FM358** and corresponding lead compounds **24a**, **28a** and **28e**. Additional visualization of **28a** and **FM345**, representing their corresponding predecessor reference compounds, provides a comprehensive interpretation of the structural design.

Depending on the respective substrate channel residue, the expected adjustment of the angled orientation caused by the thiazole ring can increase the inhibitory effect compared to the benzene ring congeners. As a result, the position of the inhibitor in the binding pocket changes

slightly, causing an altered structural environment leading to beneficial interactions in case of **FM358** and **FM345**. Nevertheless, the replacement of a benzene ring by a thiazole does not necessarily guarantee an increase in potency. Although positive effects were observed in the case of **FM345** and **FM358**, a slight decrease in inhibitory activity on Sirt2 was determined for **FM352**. To conclude, no general statement concerning a thiazole-based structural modification is possible. However, particularly decisive correlations are identified when analyzing the effects of the respective substrate channel residues towards the inhibitory potential on Sirt2.
The experimental data clearly proves the significant impact of individual substrate channel residues on the corresponding inhibitory activities. The benzene and naphthalene-substituted compounds (**FM345** and **FM368**) are noticeably inferior compared to the amide-substituted analogues (**FM352** and **FM358**).

In consensus with Yang *et al.*[80], thiophene-2-carboxamide and especially 1-methyl-1*H*-pyrazole-4-carboxamide can be confirmed as highly potent substrate channel residues that crucially contribute to an outstanding inhibitory effect on Sirt2 within the respective lead compounds **28e** and **24a** and the synthesized target compounds **FM352** and **FM358**. Considering **FM345** as a reference compound, its potency is increased through corresponding molecular extension in the form of amide substitution. This is attributed to additional possible hydrogen-bonding and π-π stacking interactions, as already confirmed crystallographically for **24a**.

With an IC_{50} value of 66 nM on Sirt2, **FM358** has an exceptional potency in the nanomolar range and thus clearly exceeds the efficacy of corresponding reference substances. **FM358** is characterized not only by its outstanding inhibitory effect, which exceeds the lead compounds, but also by its high selectivity towards Sirt2. **FM358** is therefore an excellent candidate with ideal prerequisites for further studies and improvements, especially regarding additional polar modifications within the respective amide-based substrate channel residue.

3.4 Additional biological characterization

In addition to determining the efficacy on sirtuin enzymes, the synthesized compounds were examined using MTT and an agar diffusion test, routinely performed by Martina Stadler (research group of Prof. Bracher), to characterize further biological effects.

3.4.1 Cytotoxicity

For future investigations of the synthesized compounds in cellular assays, the evaluation of cytotoxicity is essential. Therefore, all final substances tested on Sirt2 activity were characterized using the MTT assay. Based on the method developed by Mosmann[126] (principle and assay conditions outlined in Chapter 5.3.1), the MTT assay typically utilizes living HL-60 (human leukemia) cells and provides general information on the cytotoxic activity of the substances. This activity is represented by the corresponding IC_{50} value, which indicates the concentration of the test substance at which cell viability is reduced to 50% compared to untreated control cells. Cisplatin (IC_{50} = 5 µM), an approved cytostatic drug, was included as a reference in this MTT experiment to assess and correlate corresponding cytotoxic effects. IC_{50} values below 50 µM are considered cytotoxic, while IC_{50} values below 5 µM indicate a higher level of cytotoxicity than Cisplatin and are therefore classified as highly toxic. IC_{50} values above 50 µM are regarded as non-toxic.

Of all 31 final test compounds evaluated against Sirt2, only three exhibited cytotoxic activity, with compound **FM206** showing an IC_{50} of 0.26 µM, demonstrating particularly high cytotoxicity - nearly 20 times stronger than Cisplatin. Each of the test substances classified as cytotoxic in the respective MTT assay shares one common structural feature: the boronic acid group. The cytotoxic effects of boronic acid-containing substances have been demonstrated, for instance, with the proteasome inhibitor Bortezomib, which has been used to advantage in the treatment of multiple myeloma (covered in Chapter 3.2.1). Bortezomib also induces apoptosis in HL-60 cells, through a different cytotoxic mechanism involving protein phosphatase 2A, discussed in this context[127].

Other boronic acids, such as various arylboronic acids, are reported to exhibit cytotoxic and antiproliferative effects, however it is becoming apparent that the exact causes and particular modes of action are largely undefined, though they seem to involve specific molecular targets rather than general toxicity[128-130].

Fundamentally, and as demonstrated by the present test results, it appears that boronic acid function alone is not solely responsible for the observed cytotoxicity. Rather, the specific positioning of this group and the overall molecular structure plays a crucial role. Whereas lead compound **28a** (IC_{50} > 50 µM) and the *para*-substituted boronic acid **FM161** (IC_{50} > 50 µM)

show no significant cytotoxic effects, the *meta*-substituted boronic acid **FM167** (IC_{50} = 17.8) and the *ortho*-substituted boronic acid **FM166** (IC_{50} = 28.6 µM) display measurable cytotoxicity (see **Figure 33**).

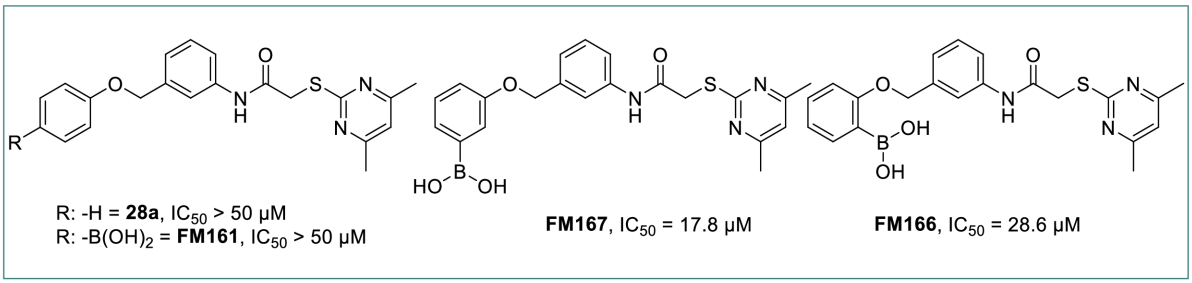

Figure 33: *Meta*- and *ortho*-substituted phenylboronic acids **FM167** and **FM166** show no significant cytotoxic activity, whereas lead compound **28a** and *para*-substituted phenylboronic acid **FM161** are considered non-toxic.

The structure-activity relationships of the highly toxic SirReal2-boronic acid (**FM206**, IC_{50} = 0.26 µM) are particularly interesting. Given that **SirReal2** (IC_{50} > 50 µM) has been identified as a lead compound with no cytotoxic effect, the exceptional cytotoxicity of **FM206** must be attributed to the presence of the boronic acid group. However, when considering boronic acid **40** (IC_{50} > 50 µM), a synthetic precursor of **FM206**, turned out to be non-toxic, it becomes evident that the presence of the selectivity pocket binder motif (2-((4,6-dimethylpyrimidin-2-yl)thio)acetamide moiety) is also crucial for the cytotoxic effect. Therefore, **FM206** exhibits its extreme cytotoxic activity due to the simultaneous presence of both the boronic acid group and the selectivity pocket binder motif (see **Figure 34**).

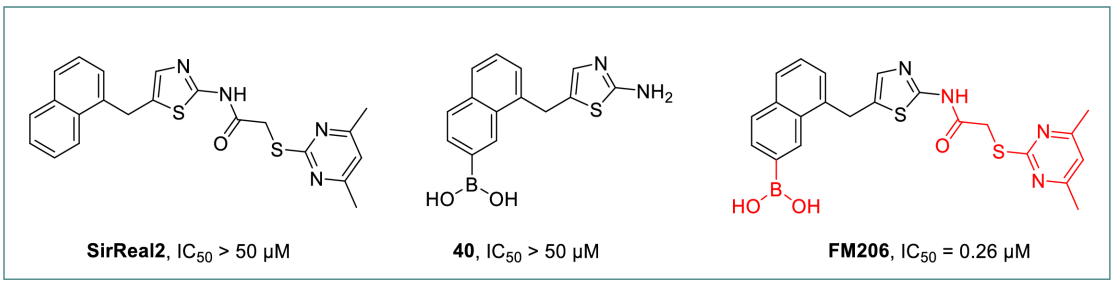

Figure 34: SirReal2-boronic acid **FM206** shows high cytotoxic potential in contrast to lead compound **SirReal2** and precursor **40**.

Taking everything into consideration, the cytotoxic effect of the test substances indicates that a specific molecular design combined with appropriate boronic acid substitution is necessary. This high structural requirement supports the hypothesis that additional molecular targets may be involved. Notably, **FM206** (IC_{50} = 0.26 µM), which exhibits cytotoxicity 20 times greater than Cisplatin (IC_{50} = 5 µM) against HL-60 cells, offers significant potential for further investigation into the cause of this cytotoxicity and for identifying a specific target, providing valuable insights for the future development of anticancer drugs.

3.4.2 Antimicrobial effects

Furthermore, all the synthesized compounds were investigated by Martina Stadler (research group of Prof. Bracher) regarding their antibiotic activity against *Escherichia coli*, *Pseudomonas marginalis*, *Staphylococcus equorum*, *Streptococcus entericus* as well as their antifungal activity against the yeasts *Yarrowia lipolytica* and *Saccharomyces cerevisiae* using agar diffusion experiments (detailed assay conditions and test procedures are presented in Chapter 5.3.2).

None of the final target compounds tested on Sirt2 exhibit noticeable antimicrobial effects. Despite the cytotoxic effects of various boronic acid-containing substances on human cells, these effects did not appear to translate to the examined bacteria and fungi, likely due to fundamental differences in cell structure, membranes, cycles, and proteins between human and microbial cells.

4 Summary

The objective of this thesis was the lead structure-based optimization of SirReal-type Sirtuin 2, inhibitors focusing on three main strategies: rigidization, reversible covalent binding warhead modification and hybridization. Guided by docking studies, a comprehensive compound library was designed, synthesized and biologically evaluated, providing valuable insights into structure-activity relationships. In this process, highly potent and selective novel Sirt2 inhibitors were developed, including compounds that represent a considerable improvement on the lead compounds.

4.1 Rigidization approach of lead compound 28e

Based on the lead compound **28e** published by Yang et al.[53] a rigidization potential was examined in docking studies and naphthalene and benzothiazole were selected as central rigid elements for the conformational restriction of the benzyl ether structure. Further structural variations (see **Scheme 27**) formed a comprehensive compound library (composed of 10 naphthalene- and 10 benzothiazole-based compounds) with a total of 20 test substances.

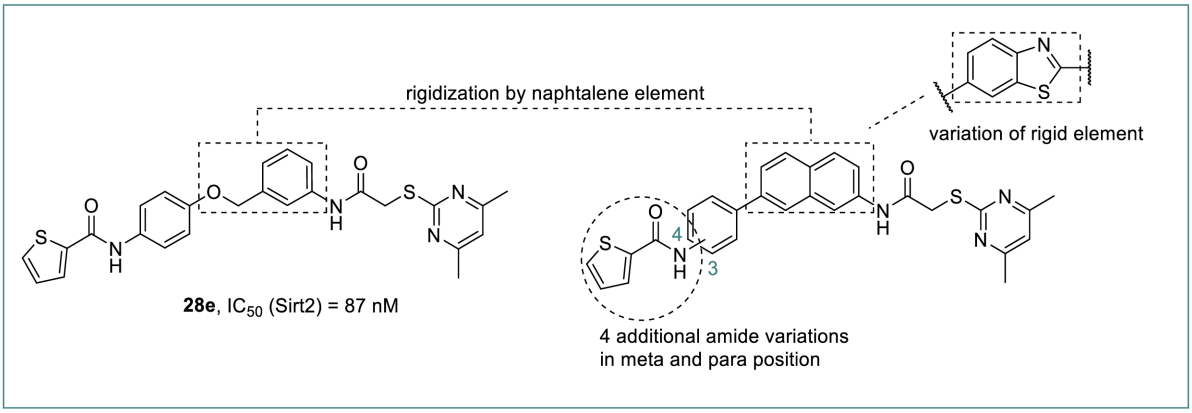

Scheme 27: Rigidization strategy applied to lead compound **28e** (IC_{50} value taken from the assay utilized in this thesis).

The preparation of the final rigid target compounds was achieved in 6 steps in each case, generally arranged in a naphthalene-based (see **Scheme 28**) and benzothiazole-based (see **Scheme 29**) synthesis route. The conversion of 7-bromonaphtalene-2-ol (**1**) to 7-bromo-naphthalene-2 amine (**2**) *via* Bucherer reaction represented the first step in the synthesis of the naphthalene-derived target compounds (see **Scheme 28**). Suzuki coupling with appropriate nitrophenylboronic acids yielded *meta*-substituted amine **7** and *para*-substituted amine **8**. Initial cross coupling difficulties were circumvented by changing the synthesis sequence (first Suzuki reaction then construction of the selectivity pocket binder motif).

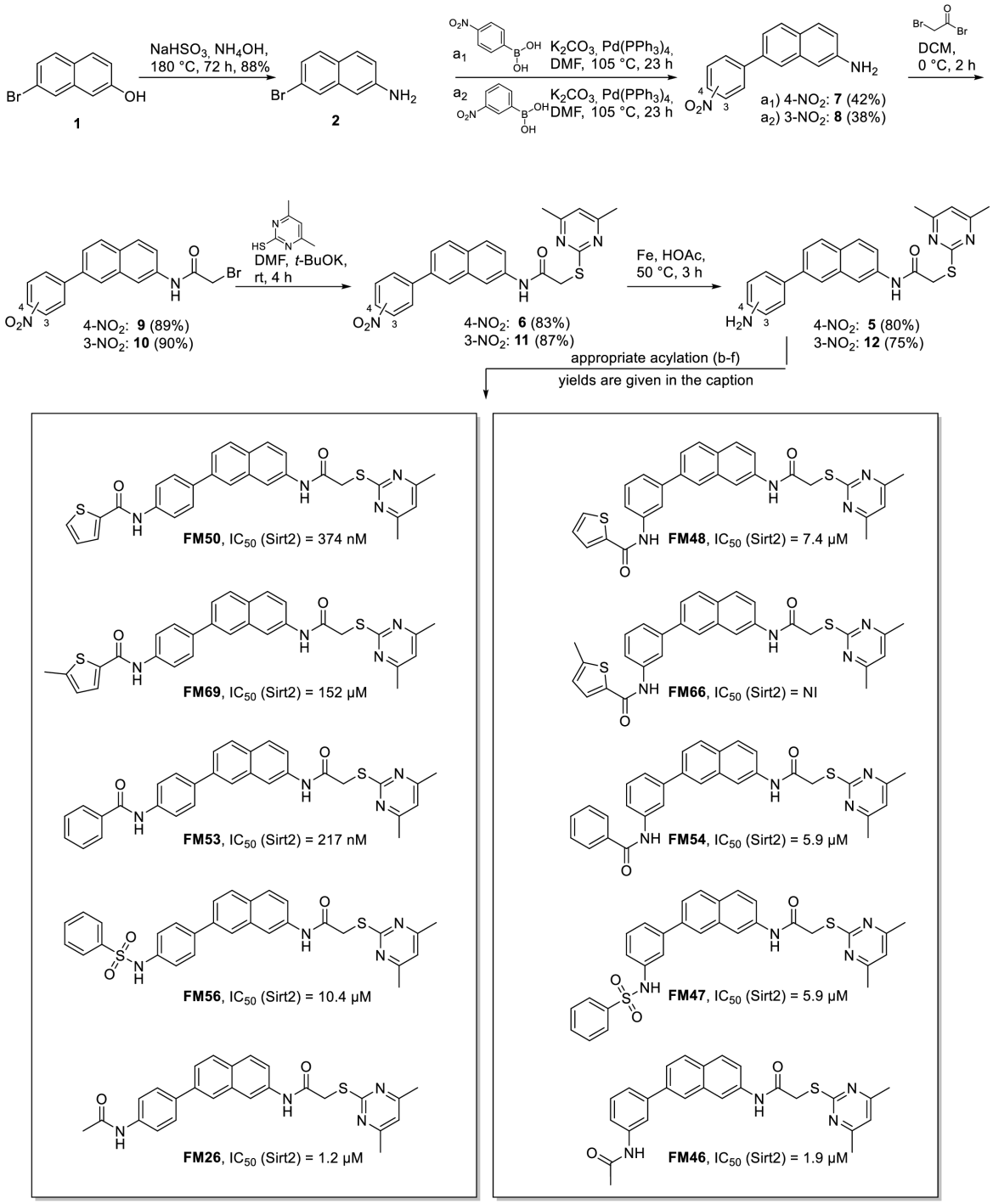

Scheme 28: Full description of the synthesis route for naphthalene-based rigid target compounds and display of determined IC_{50} values on Sirt2. Last step acylation conditions (yields are given in the legend): b) 2-thiophenecarbonyl chloride, NEt_3, DCM, rt, 2 h, 31% (**FM48**), 53% (**FM50**); c_1) 5-methylthiophene-2-carbonyl chloride, NEt_3, DCM, rt, 5 h, 83% (**FM66**); c_2) 5-methylthiophene-2-carbonyl chloride, NEt_3, DCM, 40 °C, 3 h, 74% (**FM69**); d) benzoyl chloride, NEt_3, DCM, rt, 2 h, 87% (**FM54**), 78% (**FM53**); e_1) benzenesulfonyl chloride, NEt_3, DCM, rt, 4 h, 47% (**FM47**); e_2) benzenesulfonyl chloride, NEt_3, DCM, 40 °C, 7 h, 40% (**FM56**); f) acetic anhydride, NEt_3, DCM, rt, 2 h, 91% (**FM46**), 72% (**FM26**).

The selectivity pocket-binding motif (2-((4,6-dimethylpyrimidin-2-yl)thio)acetamide moiety) was introduced in two steps *via* acylation with 2-bromoacetyl bromide to compounds **9** and **10**, followed by the subsequent thioether synthesis with 4,6-dimethylpyrimidin-2-thiol to compounds **6** and **11.** The following reduction of the nitro group with iron/acetic acid led to the primary amines **22** and **23**, which then finally provided the ten desired *meta*- and *para*-substituted naphthalene-based target compounds *via* acylation using various carboxylic and sulfonic acid chlorides and acetic anhydride.

In analogy to the naphthalene-based rigid target substances, the synthesis of the benzothiazole-based rigid compounds (see **Scheme 29**) was also realized in a 6-step synthesis starting from 4-bromoaniline (**13**) by intramolecular cyclization using potassium thiocyanate and bromine in acetic acid to 2-amino-6-bromobenzothiazole (**14**).
Initial challenges with the Suzuki reaction were overcome by changing the base from potassium carbonate to caesium carbonate and switching the solvent from DMF to dioxane/water. In addition, 4-(Boc-amino)phenylboronic acid was favored to improve solubility and yield, while 3-(amino)phenylboronic acid was retained. Subsequently, two steps were performed to introduce the selectivity pocket binding motif (2-((4,6-dimethylpyrimidin-2-yl)thio)acetamide moiety) into the Suzuki coupling products **15** and **17**. Acylation with 2-bromoacetyl bromide in DCM/DMF (for compound **18**) or EtOAc (for compound **19**) was carried out at 40 °C to address solubility issues. Subsequently, thioether synthesis using 4,6-dimethylpyrimidine-2-thiol yielded compounds **20** and **21**, which were then converted into the corresponding amines **22** and **23**. Therefore, the nitro group of **20** was reduced with Fe/NH_4Cl in MeOH/water to avoid extraction problems related to solubility, and the Boc protecting group of **21** was removed with trifluoroacetic acid. Finally, the resulting amines **22** and **23** were acylated to the desired benzothiazole-based target compounds using various acid chlorides and acetic anhydride.

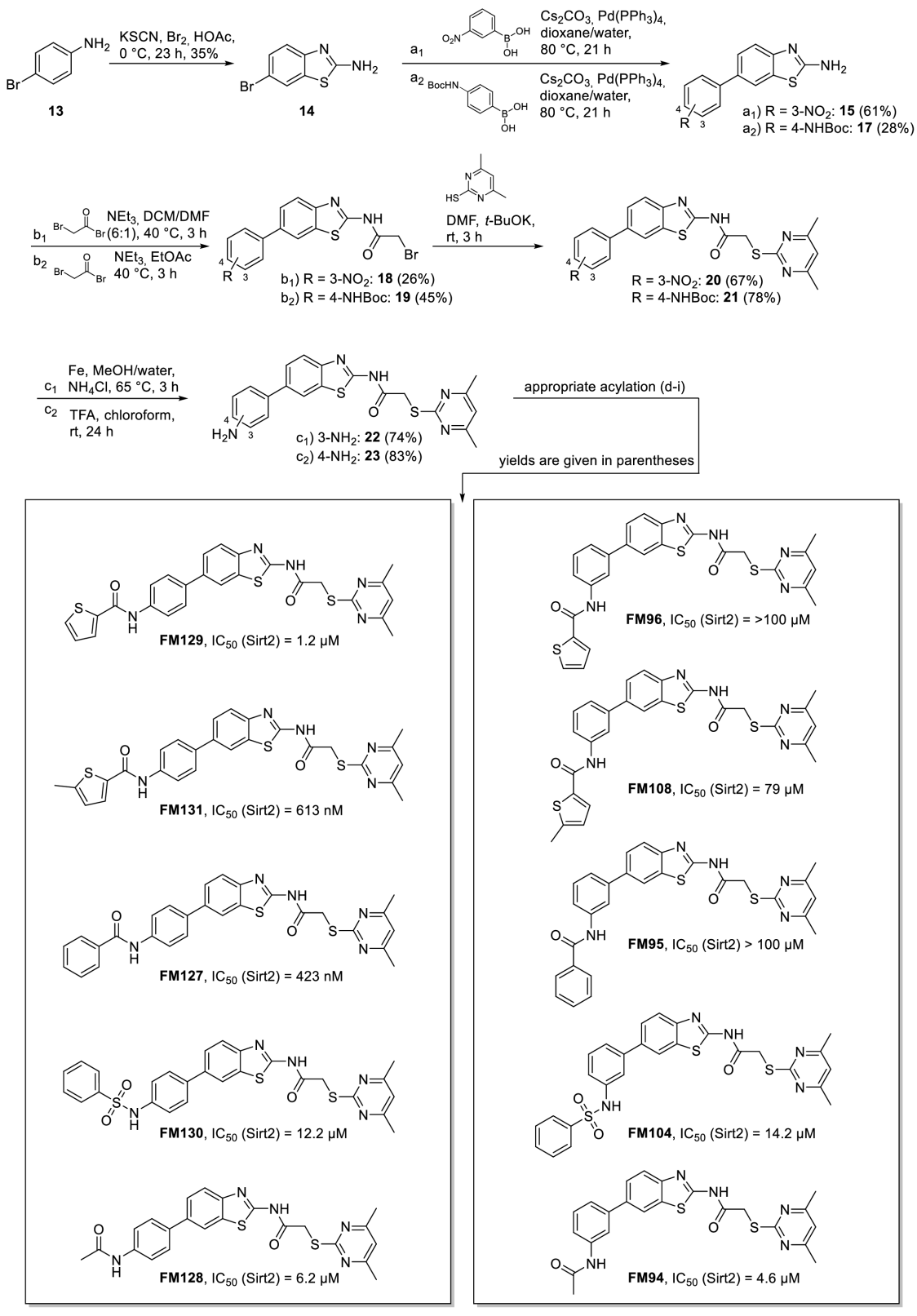

Scheme 29: Full description of the synthesis route for benzothiazole-based rigid target structures and display of determined IC_{50} values on Sirt2. Last step acylation conditions (yields are given in the legend.): d) 2-thiophenecarbonyl chloride, NEt_3, DCM, rt, 1 h, 81% (**FM96**), 77% (**FM129**); e) 5-methylthiophene-2-carbonyl chloride, NEt_3, DCM, rt, 2 h, 46% (**FM108**), 45% **FM131**); f) benzoyl chloride, NEt_3, DCM, rt, 3 h, 66% (**FM95**), 46% (**FM127**); g_1) benzenesulfonyl chloride, NEt_3, DCM, rt, 8 h, 15% (**FM104**); g_2) benzenesulfonyl chloride, NEt_3, DCM, 40 °C, 8 h, 59% (**FM130**); i) acetic anhydride, NEt_3, DCM, rt, 3 h, 96% (**FM94**), 60% (**FM128**).

Biological evaluation on Sirt2 and related subtypes Sirt1, Sirt3 and Sirt5 revealed extended structure-activity relationships, including several selective and potent Sirt2 inhibitors, 5 of them displaying IC_{50} values in the submicromolar range (see **Figure 35**).

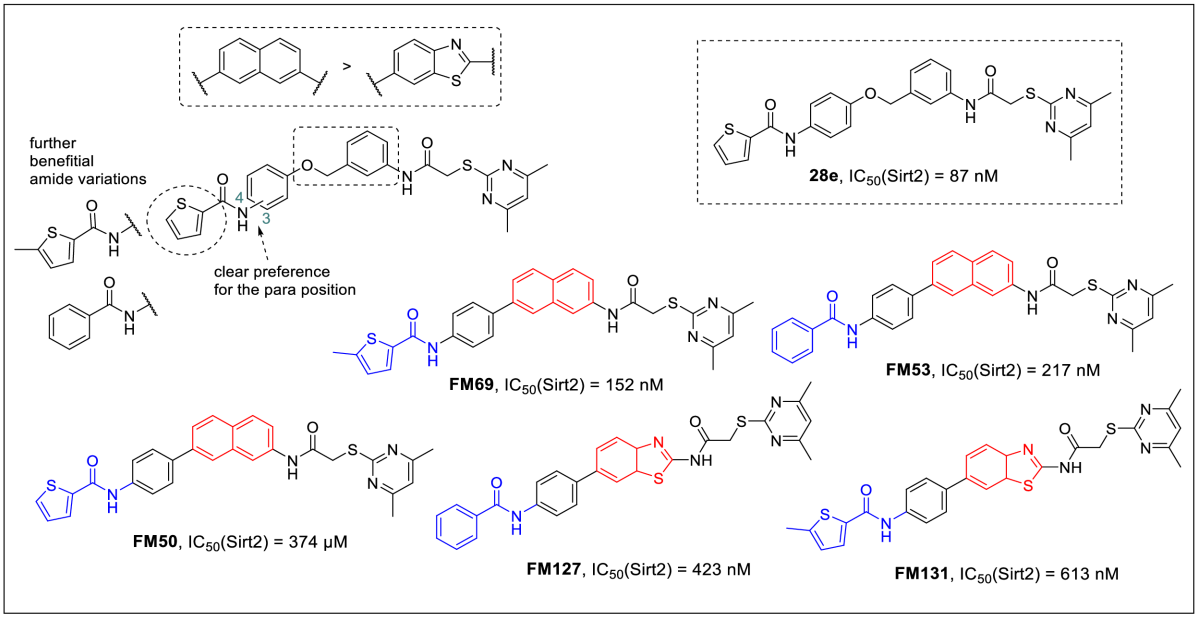

Figure 35: SAR-analysis and illustration of the most potent rigidized target compounds, including lead inhibitor **28e**.

Fundamentally, a *meta* substitution of the amide residue is significantly disadvantageous compared to a *para* position and naphthalene as a rigid structural element is generally preferred over a benzothiazole. In addition to the major influence of the substitution pattern, the specific amide substitution also has a decisive effect on the activity of the amide-based substrate channel residue. Thus, advantageous prerequisites for rigidization could be determined and, potent and selective conformally restricted Sirt2 inhibitors were successfully developed, although the activity of the lead compound **28e** (IC_{50} = 87 nM, Sirt2) was not exceeded. However, **FM69** (IC_{50}= 152 nM, Sirt2) and **FM53** (IC_{50} = 217 nM, Sirt2) showed strong selective inhibitory potential on Sirt2 surpassing the original first-generation lead compound **SirReal2** (IC_{50} = 235 nM, Sirt2). Consequently, the investigated structure-activity relationships concerning rigidization provide a promising foundation for the development of further conformation-restricted inhibitors.

4.2 Warhead-based Sirt2 inhibitor modification targeting the NAD$^+$ cofactor *via* reversible covalent binding principle

The introduction of a boronic acid, nitrile, and aldehyde-based warhead, first in lead compound **28a** (published by Yang *et al.*[53]) and subsequently in lead compound **SirReal2** (published by Rumpf *et al.*[42]), was intended to specifically target the sirtuin cofactor NAD$^+$ by forming a reversible covalent interaction with the corresponding ribose diol structure. This innovative strategy should specifically deactivate the cofactor necessary for catalysis purposes and strengthen the binding of the inhibitor in the active center, resulting in advanced potency. Docking-guided boronic acid equipped analogues of lead compound **28a** with different substitution patterns were synthesized in order to develop the inhibitory potential in a proof of concept study and thus apply the corresponding findings to the more synthetically complex lead compound **SirReal2**.

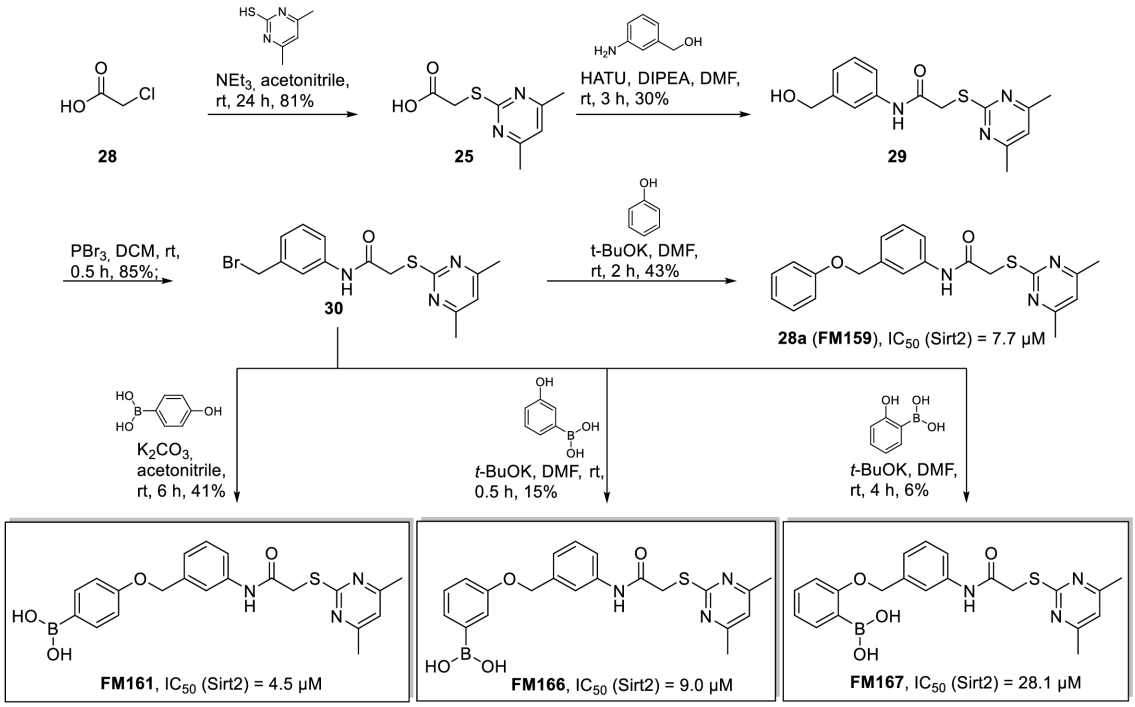

Scheme 30: Full description of the synthesis route of boronic acid modification (**FM161**, **FM166** and **FM167**) of **28a** as warheads of reversible covalent binding mechanisms. Determined inhibitory activity displayed as IC_{50} values.

The synthesis of the corresponding target compounds was realized in 4 steps (see **Scheme 30**), starting with thioether synthesis to carboxylic acid **25** using 2-chloroacetyl chloride (**18**) and 4,6-dimethylpyrimidine-2-thiol, followed by subsequent HATU-mediated amidation of 3-(hydroxymethyl)aniline to alcohol **29.** An initially considered 3-step synthesis approach failed due to the unsuccessful reduction of 3-nitrobenzyl bromide to 3-(bromomethyl)aniline (**27**). Using PBr_3, alcohol **29** is converted into the corresponding benzyl halide **30**, which served as a starting material for the subsequent Williamson ether synthesis, whereby appropriate

hydroxyphenyl boronic acids for the synthesis of desired target compounds **FM161**, **FM166** and **FM167** as well as phenol for the preparation of reference lead compound **28a** were utilized.

Compared to the lead compound **28a** (IC_{50} = 7.7 µM, Sirt2), the *para*-substituted phenylboronic acid **FM161** (IC_{50} = 4.5 µM, Sirt2) showed a promising 1.7-fold increase in inhibitory activity, which encouraged the following optimization of **SirReal2** with appropriate warheads with expected reversible covalent binding mode. The *ortho*- and *para*-substituted phenylboronic acids, **FM167** (IC_{50} = 28.1 µM, Sirt2) and **FM166** (IC_{50} = 9.0 µM, Sirt2), however, proved to be disadvantageous variations, which is why particular attention, along with corresponding docking studies, was given to the favorable positioning of the nitrile, aldehyde, and boronic acid modifications of **SirReal2**: the 7-position of the naphthalene subunit.

The synthesis of SirReal2-boronic acid **FM206** comprised a total of 8 steps (see **Scheme 31**), starting with the oxime synthesis from 7-bromo-1-tetralone (**31**) and hydroxylamine hydrochloride to oxime **32**, which was subsequently aromatized in a Semmler Wolf reaction to 7-bromonaphtalene-1-amine (**33**). Thereby the 5-step nitration-based literature-known synthesis of 7-bromonaphtalene-1-amine (**33**) in two steps with a threefold higher yield was substituted. A subsequent modified Meerwein-arylation approach yielded the aminothiazole **35** according to literature, which served as the central starting point for further boronic acid, nitrile and aldehyde modifications. The boronic acid was introduced as a pinacol ester via Miyaura-borylation, however, which was only successful after prior Boc protection of the amine to **37** in order to realize compound **38**. Thus, both protecting groups had to be removed again in the next two steps, which was achieved solely by initial oxidative pinacol ester cleavage to **39** followed by Boc cleavage to **40**, since the other way around, pinacol ester cleavage with the amine **36** was not successful. Boronic acid amine **40** was then subjected to EDC-mediated amidation to give the target compound SirReal2-boronic acid **FM206**. Suitable model reactions for aryl cyanation were initially carried out with the Boc-protected variant **37** as a precaution and the proven palladium-catalyzed cyanation using zinc cyanide was successfully transferred to the unprotected aminothiazole **35**. For the preparation of the arylacetonitrile **43**, a one-pot palladium-catalyzed cyanomethylation method was applied, similarly starting from aminothiazole **35**. Both nitriles **42** and **43** were finally subjected to HATU-mediated amidation to give the target compounds SirReal2-nitrile **FM295** and SirReal2-acetonitrile **FM302**. To avoid the simultaneous presence of a primary aromatic amine and an aldehyde, aminothiazole was first amidated to yield **7-bromo-SirReal2** (**FM315**) using HATU, to introduce the aldehyde moiety in the final step *via* palladium-catalyzed reductive carbonylation with N-formylsaccharin, resulting in SirReal2-aldehyde **FM316**.

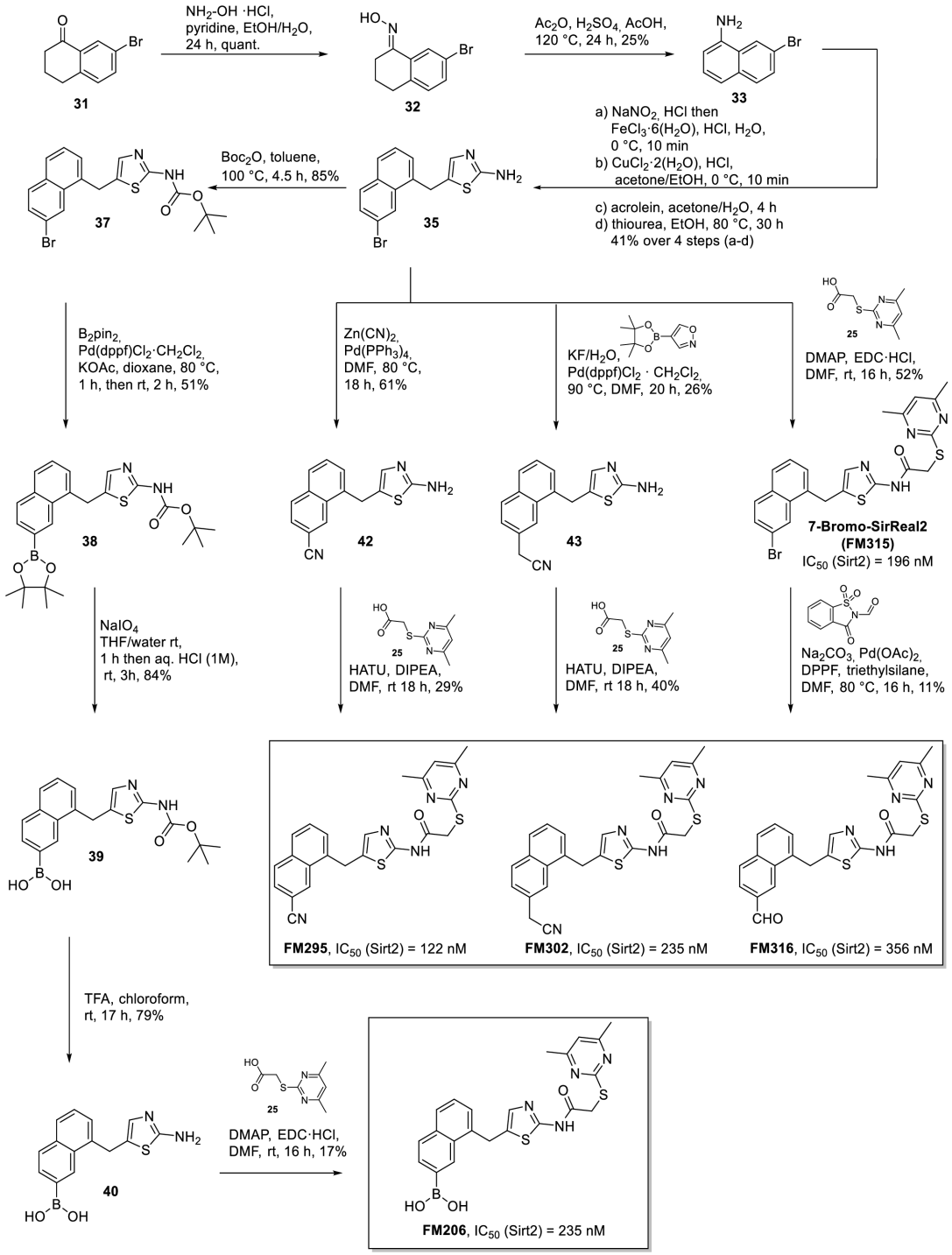

Scheme 31: Full description of the synthesis route of boronic acid, nitrile and aldehyde-based modification of **SirReal2**, as warheads of reversible covalent binding mechanisms. Determined Inhibitory activity displayed as IC_{50} values.

The synthesized target compounds were evaluated for their inhibitory activity against Sirt2 and subtype selectivity towards Sirt1, Sirt3 and Sirt5 and all test compounds showed selective and potent inhibition of Sirt2 (see **Figure 36**). Lead compound **SirReal2** was included into the respective screening and determined with an IC_{50} value of 235 nM on Sirt2. Most remarkable is SirReal2-nitrile **FM295** (IC_{50} = 122 nM, Sirt2), showing almost twice as strong inhibitory effect

as **SirReal2**. SirReal2-boronic acid **FM206** (IC_{50} = 235 nM, Sirt2) and SirReal2-acetonitrile **FM302** (IC_{50} = 235 nM, Sirt2) were equipotent and SirReal2-aldehyde **FM316** (IC_{50} = 356 nM, Sirt2) displayed slightly lower inhibitory activity compared to **SirReal2**.

The exceptionally strong cytotoxicity (IC_{50} determined *via* MTT assay: 0.26 µM, 20 times more toxic than Cisplatin) of SirReal2-boronic acid **FM206** is particularly noteworthy, as the other **SirReal2** modifications did not display cytotoxic effects. The observed toxicity is attributed to the simultaneous presence of the boronic acid functional group in combination with the structural motif of the selectivity pocket binder (2-((4,6-dimethylpyrimidin-2-yl)thio)acetamide moiety), suggesting a specific mode of action rather than a general toxicity, therefore the underlying mode of action is worth investigating.

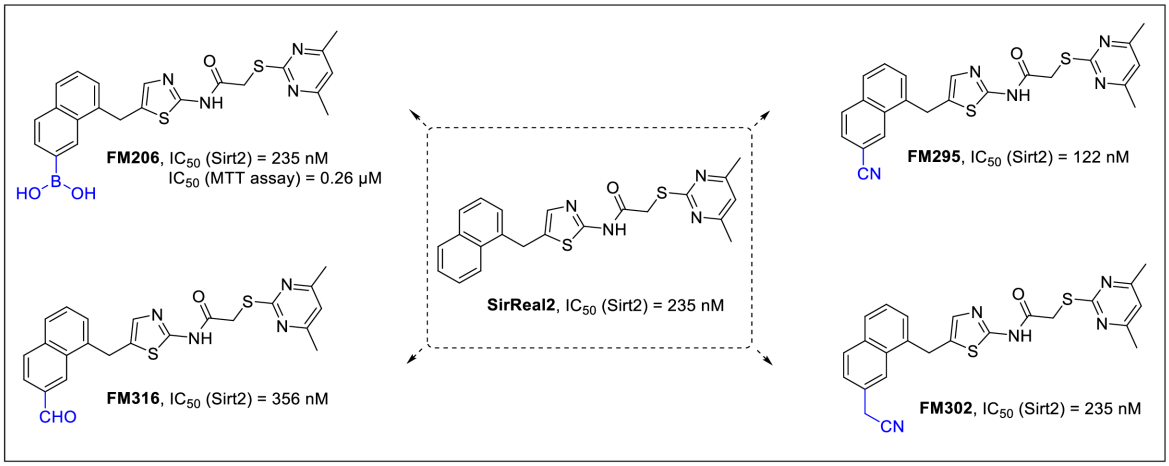

Figure 36: Chemical structures and determined inhibitory activity of synthesized **SirReal2** modifications (**FM320**, **FM316**, **FM295**, **FM302**) and the corresponding lead compound **SirReal2** on Sirt2. Additionally, SirReal2-boronic acid **FM320** shows exceptional cytotoxic potential determined *via* MTT assay.

All compounds exhibit high and selective inhibitory properties towards Sirt2, therefore the envisaged reversible covalent binding mode should be investigated by crystallographic studies.

A cocrystal was achieved in low resolution so far with SirReal2-boronic acid **FM206**, and intensive work is continuing on the other target compounds. The crystal structure of SirReal2-boronic acid **FM206** indicated a binding mode in accordance with the previous prediction, wherein the boronic acid is aligned in the direction of the physiological position of the ribose diols of NAD^+. However, NAD^+ was absent in the crystal structure, therefore a reversible covalent mode could not be verified with the scope of this first crystallographic experiment. Unfortunately, further crystallization of the remaining **SirReal2** modifications had not been accomplished prior to the finalization of this thesis. Examining whether the twofold potency

increase of SirReal2-nitrile **FM295** is linked to a reversible covalent binding mechanism would be of particular interest.

In summary, a synthesis strategy for the targeted introduction of warheads with reversible covalent binding potential was successfully developed, providing potent and selective **SirReal2** modifications. SirReal2-nitrile **FM295** with an IC_{50} of 122 nM against Sirt2 significantly surpasses the **SirReal2** lead compound and thus represents a highly potent and selective structural optimization. With the clarification of the specific binding mode and the cause of potency enhancement, **FM295** offers ideal conditions for developing additional highly effective and selective Sirt2 inhibitors based on the derived structure-activity relationships.

4.3 Lead structure-based hybridization drug design approach

Based on the crystal structure analysis of the lead compounds **SirReal2** (Rumpf *et al.*[42]) and **24a** (Yang *et al.*[80]) the respective binding modes were evaluated and pharmacophoric structural features were combined to generate four optimized hybrid 5-(aryloxymethyl)thiazole-2-amides inhibitors (see **Scheme 32**) whose structure-activity relationships was further characterized.

A general synthetic approach was developed for the previously unexplored structural class of 5-(aryloxymethyl)thiazole-2-amides, providing an effective Williamson ether synthesis strategy as the key step in the preparation, which turned out to be unexpectedly challenging.

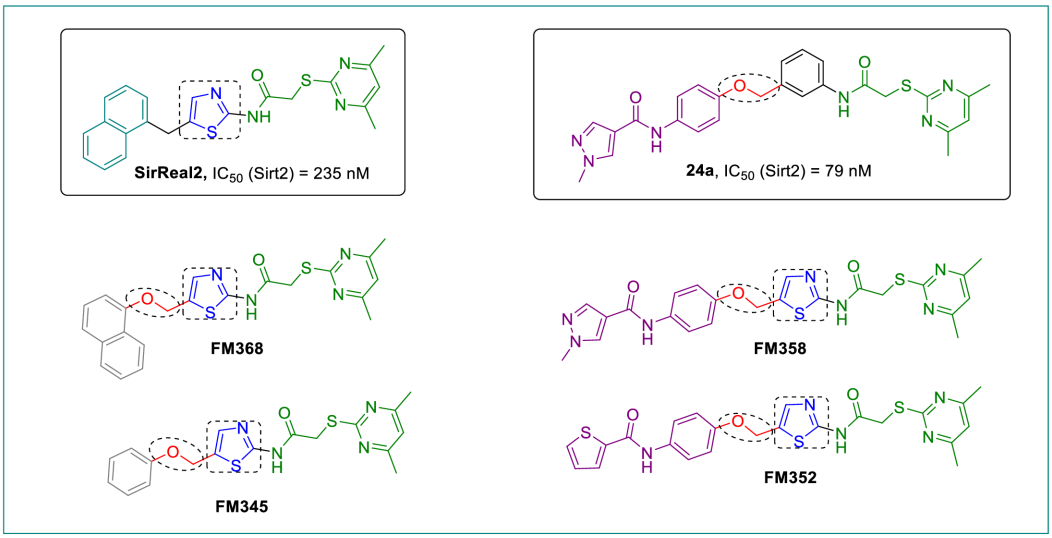

Scheme 32: Illustration of the hybridization concept. Promising structural elements (arylmethyl ether and thiazole) were selected as to design **FM368** and **FM358** through hybridization of lead compounds **SirReal2** and **24a**. Additional hybrid candidates **FM345** und **FM352** complemented the respective SAR-study. IC_{50} values of respective lead compounds **SirReal2** and **24a** originate from biological evaluation within the thesis setting for comparability purposes.

The hybrid target compounds were prepared in five steps (see **Scheme 33**), whereby the carboxylic acid **25** was first synthesized by thioether synthesis using 2-chloroacetyl chloride (**28**) and 4,6-dimethylpyrimidine-2-thiol, which was amidated with 2-aminothiazole-5-carbaldehyde (**37**) using EDC·HCl to obtain aldehyde **46**. After aldehyde **46** was reduced to the corresponding primary alcohol **47** using sodium borohydride, thionyl chloride was utilized to generate alkyl chloride **52.**

The subsequent Williamson ether synthesis of alkyl chloride **44** with an appropriate phenol revealed major difficulties under standard conditions due to the strong alkylation tendency of the halogen compound, presumably a major reason for the absence of a so far published synthetic approach to 5-(aryloxymethyl)thiazole-2-amides. After investigating various reaction conditions, a general method for synthesizing 5-(aryloxymethyl)thiazole-2-amides was

successfully established, enabling the preparation of the desired hybrid target substances using alkyl chloride **52** with appropriate sodium phenolate salts and a suitable solvent.

The required phenolate salts (**59, 61 and 62**) were prepared in crude form from the corresponding phenols (**58**, **60** and **53**) using sodium methanolate, whereby **58** and **60** first had to be prepared from 4-aminophenol (**57**) by acylation by means of thiophene-2-carbonyl chloride and HATU-mediated amidation 1-methyl-1*H*-pyrazole-4-carboxylic acid respectively.

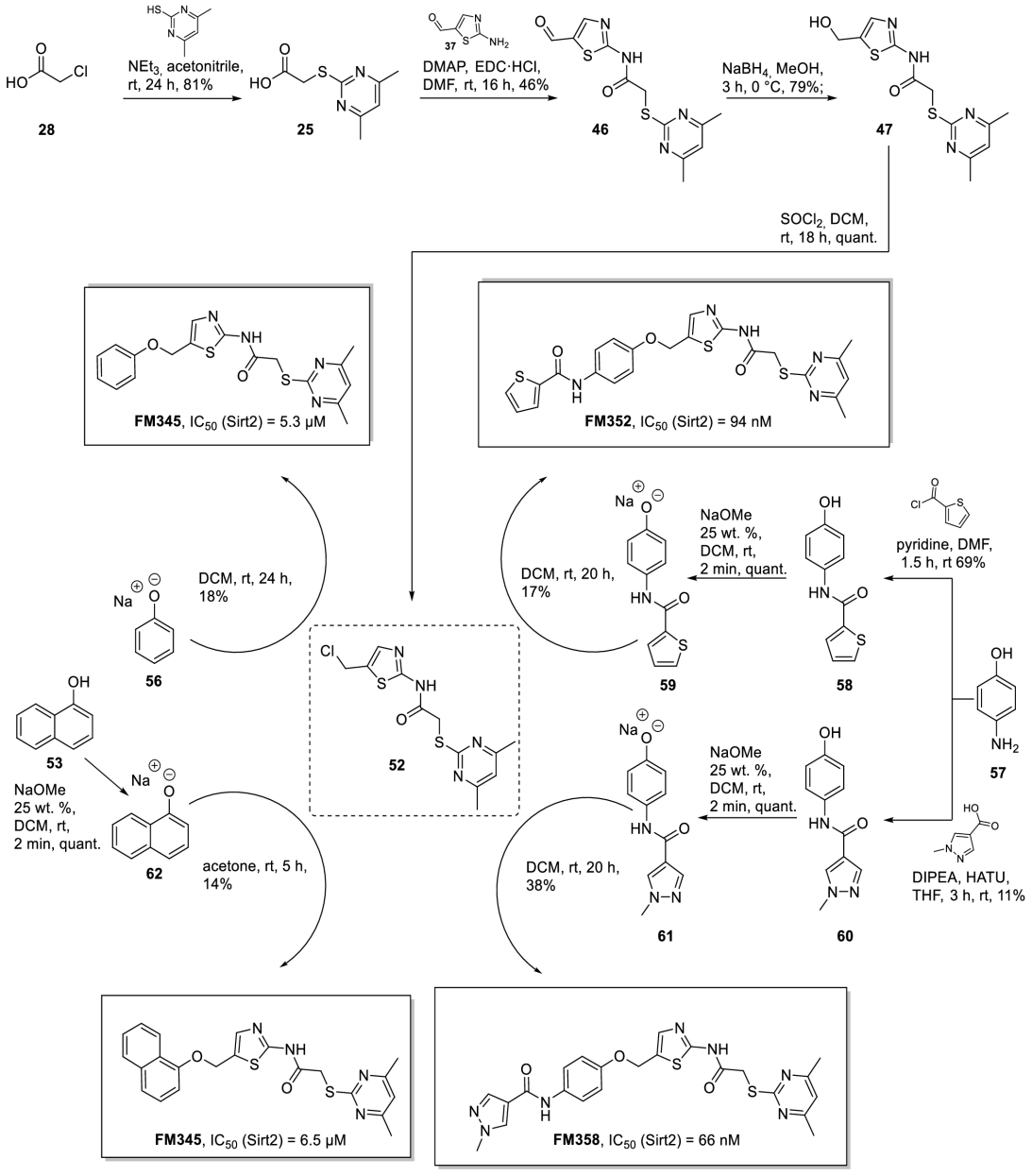

Scheme 33: Full description of the synthesis route of hybrid target inhibitors **FM345**, **FM368**, **FM352**, **FM358**. Determined inhibitory activity displayed as IC_{50} values.

Biological evaluation (see **Figure 37**) of inhibitory activity on Sirt2 and subtype selectivity (Sirt1, Sirt3 and Sirt5) revealed **FM358** (IC_{50} = 66 nM, Sirt2) as a highly potent structural optimization achieved by hybridization of lead compound **SirReal2** (IC_{50} = 235 nM, Sirt2) and **24a** (IC_{50} =

79 nM, Sirt2). The remaining hybrid target compounds are Sirt2 selective, **FM352** (IC_{50} = 94 nM, Sirt2) showed slightly lower potency, **FM345** (IC_{50} = 5.3 µM, Sirt2) and **FM369** (IC_{50} = 6.5 µM, Sirt2) are considerably less effective.

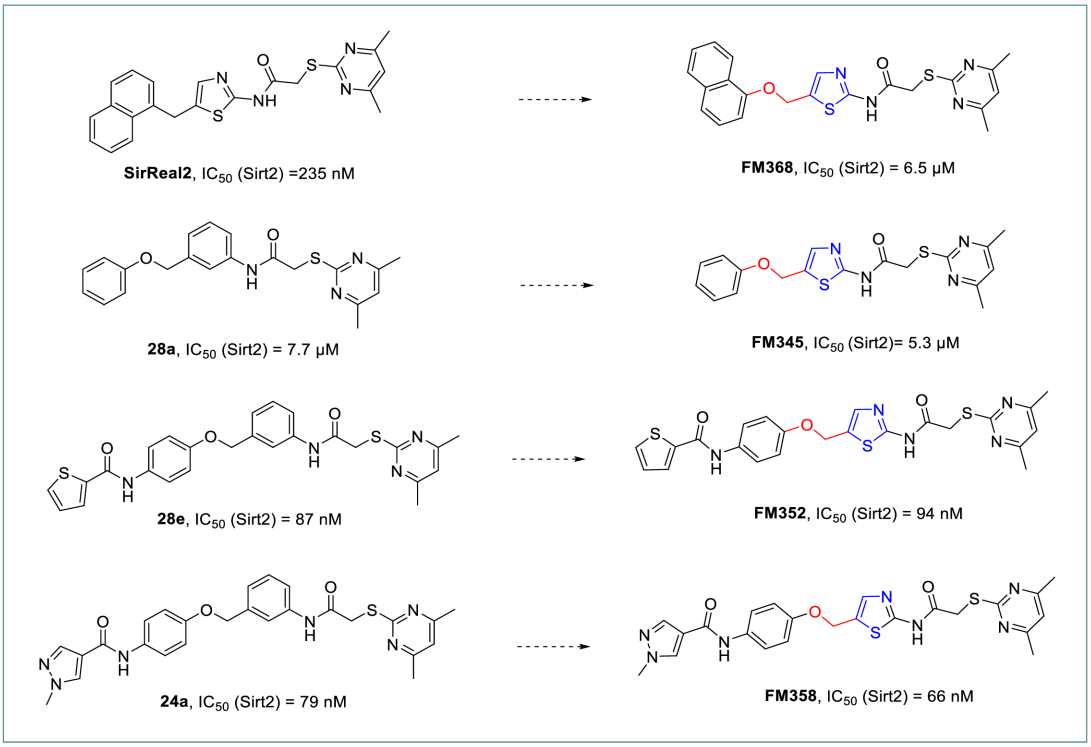

Figure 37: Chemical structures and determined inhibitory potential of the final hybrid target compounds, as well as their corresponding lead compounds. The (aryloxymethyl)aminothiazole moiety represents the central hybridization principle.

Valuable structure-activity relationships can be derived, as the application of a hybridization strategy is associated with high structural requirements for the binding pocket, demonstrated by **FM358** (IC_{50} = 66 nM, Sirt2), outperforming respective lead compounds.

Therefore, **FM358** represents one of the most highly effective and selective small molecule-based Sirt2 inhibitors with favorable prerequisites and high potential for further development.

4.4 Conclusion and outlook

Based on multiple medicinal chemistry approaches (rigidization, warhead-based modification for reversible covalent binding mode and hybridization) 31 final target substances were synthesized and biologically evaluated regarding their inhibitory potential and selectivity on Sirt2. Of these, 11 were identified as sub-micromolar potent and selective Sirt2 inhibitors, 5 outperformed the first-generation lead compound **SirReal2** in terms of inhibitory activity. The comprehensive compound library established in this thesis intensified insight into structure-activity relationships with respect to SirReal-type inhibitors and closes previous knowledge gaps. With the results from ongoing crystallographic studies and the determination of respective binding modes, the impact of the advantageous structural features on the activity can be specifically characterized, in particular using the top substances described in the various approaches of this work (see **Figure 38**).

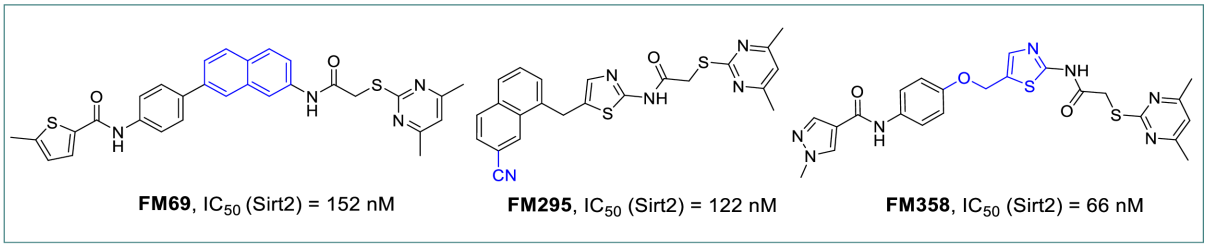

Figure 38: The respective top inhibitors of the applied lead compound optimization strategies based on rigidization (**FM69**), warhead modification (**FM295**) and hybridization (**FM358**) demonstrate selectivity and high potency towards Sirt2.

Based on the promising results and findings of this thesis, further research projects have been initiated to expand the applied strategies and advance the development of highly potent and selective Sirt2 inhibitors, thus providing the pharmaceutical tools required to investigate the physiological and pathophysiological role of sirtuins.

5 Experimental part

5.1 General materials and methods

5.1.1 Laboratory supplies and fundamental procedural methods

Required chemicals and reagents were purchased from commercial sources: Sigma-Aldrich/Merck (Darmstadt, Germany), VWR (Darmstadt, Germany), TCI Chemicals (Eschborn, Germany), abcr (Karlsruhe, Germany) or BLD Pharmatech (Reinbek, Germany). Solvents used for purification were HPLC grade or purified by distillation.

Thin layer chromatography (TLC) based on polyester Polygram SIL G/UV254 plates (SiO_2-coating thickness: 0,20 mm, size 4 × 8 cm), from Machery-Nagel (Düren, Germany), was used to determine retardation factors (R_f, reported in cm) and to monitor reaction and purification processes. TLC results were visualized using UV light (254 nm or 365 nm) or appropriate TLC stains: CAM (ceric ammonium molybdate), $KMNO_4$, DNPH (1,3-dinitrophenylhydrazine) and $FeCl_3$. Reaction control was additionally carried out *via* TLC-MS analysis by compact mass spectrometer Interchim Scientific's expression and Plate Express device from Advion (New York city, USA), using atmospheric pressure chemical ionization (APCI) method.

Purification was performed by flash column chromatography using silica gel 60 (0.040 - 0.063 mm, 230-400 mesh ASTM, from Merck (Darmstadt, Germany) and preparative layer chromatography (PLC) using 1 mm PLC silica gel 60 F_{254} plates (20 x 20 cm) with concentrating zone from Merk (Darmstadt, Germany).

5.1.2 Structural analysis, molecular characterization and purity determination

Nuclear magnetic resonance (NMR) spectra (^{1}H NMR, ^{13}C NMR, DEPT, COSY, HSQC and HMBC) were recorded at room temperature with spectrometers by Bruker Corporation (Billerica, USA): Avance III HD 400 MHz Bruker BioSpin (^{1}H-NMR: 400 MHz; ^{13}C-NMR: 101 MHz) and Avance III HD 500 MHz Bruker BioSpin (^{1}H-NMR: 500 MHz; 126 MHz). The chemical shifts (ppm, parts per million) provided were referenced using MestreNova 14.3.0 (Mestrelab Research S.L., Santiago de Compostela, Spain), to the respective deuterated solvent peak (DMSO-d_6: δH = 2.50 ppm, δC = 39.52 ppm; $CDCl_3$: δH = 7.26 ppm, δC = 77.16 ppm). Coupling constants *J* are reported in Hz and multiplicities are displayed as: s (singulett), d (doublet), t (triplet), q (quartet), respective derivatives thereof or m (multiplet). The NMR spectroscopy was technically performed by Dr. Lars Allmendinger and Claudia Glas at NMR Analytics Department Pharmacy LMU Munich.

High-resolution mass spectrometry (HRMS) was performed by Dr. Werner Spahl and Sonja Kosak at LMU Mass Spectrometry Service Department Chemistry.
Electron impact ionization (EI) was carried out using Jeol JMS-700 MStation device (Akishima, Japan) or Jeol JMS GC Mate II (Akishima, Japan) spectrometer and electron spray ionization (ESI) was conducted with Thermo Finnigan LTQ FT (Thermo Fisher Scientific, Waltham, USA). The molecular ions detected were displayed in corresponding spectra as m/z values.

Infrared spectroscopy was performed using a Perkin Elmer FT-IR BXII/1000 spectrometer (Waltham, USA) combined with DuraSamp IR II Diamond ATR sensor (Smiths Detection, London, England). Characteristic absorption bands were assigned at the wavenumbers (cm^{-1}) reportet.

Melting points were measured using melting point meter Büchi B-540 (Fawil, Swiss) and reported in °C.

HPLC purity was determined on a HP Agilent 1100 system (Agilent Technologies, Santa Clara, USA) using G1311A QuatPump system, 1100/1200 diode array detector and a G1316A ColComp column oven, detecting at 210 nm and 254 nm. HPLC purity (%) was determined *via* Chromeleon 7.2.9 software (Thermo Fisher Scientific Dionex, Waltham, USA) for processing and analysis of HPLC spectra. HPLC-analysis was performed by Anna Niedrig (research group of Prof. Bracher) using following methods:

Method 1
Column: Zorbax Eclipse Plus® C18 5µm (4.6 x 150 mm), flow rate 1.0-1.5 mL/min, temp. 30-50°C. Eluent:
a) Acetonitrile/water (70:30)
b) Acetonitrile/water (50:50)

Method 2
Column: Zorbax Eclipse Plus® C18 5µm (4.6 x 150 mm), flow rate 1.0-1.2 mL/min, temp. 30-50°C. Eluent:
a) Acetonitrile/water (30:70) + 0.1% formic acid
b) Acetonitrile/phosphate buffer pH = 5 (50:50)
c) Acetonitrile/phosphate buffer pH = 5 (70:30)

5.2 Synthetic procedures and analytical data

The numbering of the compounds used is generally based on IUPAC rules. However, the respective levels/hierarchies for the assignment of NMR signals (shown as apostrophes) were chosen differently for simplification and standardization based on the chronological synthesis sequence.

2-Bromo-*N*-(7-bromonaphthalen-2-yl)acetamide (3)

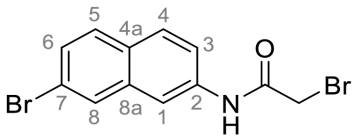

$C_{12}H_9Br_2NO$

M_w = 343.02 g/mol

At 0 °C bromoacetyl bromide (3.63 mL, 41.6 mmol, 8.00 eq) was added dropwise to a stirred solution of 7-bromonaphthalene-2-amine (**2**, 1.16 g, 5.20 mmol, 1.00 eq) and NEt_3 (5.80 mL, 41.6 mmol, 8.00 eq) in anhydrous DCM (200 mL). After 2 h, water (100 mL) and brine (200 mL) were added, and the reaction mixture was extracted with DCM (4 x 100 mL). The combined organic layers were dried over sodium sulfate. After evaporating the solvent *in vacuo*, the crude product was purified *via* flash column chromatography using pure DCM as eluent to yield the title compound as a white solid (1.46 g, 4.24 mmol, 82%).

R_f: 0.25 (DCM).
m.p.: 175-177 °C.

^{1}H NMR (400 MHz, DMSO-d_6) δ [ppm] = 10.66 (s, 1H, NHCO), 8.24 (d, *J* = 2.1 Hz, 1H, 1-H), 8.14 (d, *J* = 2.0 Hz, 1H, 8-H), 7.92 (d, *J* = 8.9 Hz, 1H, 4-H), 7.82 (d, *J* = 8.7 Hz, 1H, 5-H), 7.63 (dd, *J* = 8.9, 2.1 Hz, 1H, 3-H), 7.53 (dd, *J* = 8.7, 2.0 Hz, 1H, 6-H), 4.10 (s, 2H, CH_2).

^{13}C NMR (101 MHz, DMSO-d_6) δ [ppm] = 165.2 (NHCO), 137.2 (C-2), 134.7 (C-8a), 129.8 (C-5), 129.2 (C-8), 128.8 (C-4), 128.4 (C-4a), 127.8 (C-6), 120.3 (C-3), 119.9 (C-7), 114.6 (C-1), 30.4 (CH_2).

IR (ATR) $\tilde{\nu}$ [cm^{-1}] = 3279, 1681, 1652, 1580, 1554, 1495, 1428, 1414, 1360, 1326, 1287, 1216, 1198, 1169, 1104, 1063, 966, 930, 902, 867, 837, 797, 767, 702, 656.

HRMS (EI): *m/z* = $[M]^{\bullet+}$ calculated for $C_{12}H_9{}^{79}Br_2NOS^{\bullet+}$: 340.9045; found: 340.9045.

Purity (HPLC): > 99% (210 nm), > 99% (254 nm), (method 1b).

N-(7-Bromonaphthalen-2-yl)-2-((4,6-dimethylpyrimidin-2-yl)thio)acetamide (4)

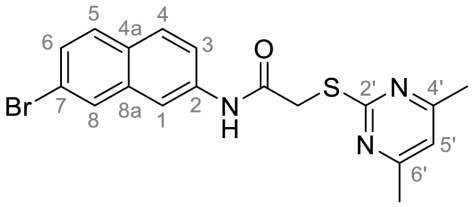

$C_{18}H_{16}BrN_3OS$

M_w = 402.31 g/mol

At room temperature potassium *tert*-butoxide (0.944 g, 8.41 mmol, 2.00 eq) was added to a stirred solution of 2-bromoacetamide **3** (1.44 g, 4.21 mmol, 1.00 eq) and 4,6-dimethylpyrimidine-2-thiol (0.708 mg, 5.05 mmol, 1.20 eq) in anhydrous DMF (15 mL). After 3 h, water (150 mL) and brine (100 mL) were added, and the reaction mixture was extracted with EtOAc (4 x 100 mL). The combined organic layers were dried over sodium sulfate. After evaporating the solvent *in vacuo*, the crude product was purified *via* flash column chromatography (DCM/EtOAc 10:1) to yield the title compound as a white solid (1.50 g, 3.74 mmol, 89%).

R_f: 0.35 (DCM/EtOAc 10:1).
m.p.: 132-134 °C.

^{1}H NMR (400 MHz, DMSO-d_6) δ [ppm] = 10.52 (s, 1H, NHCO), 8.23 (m, 1H, 1-H), 8.09 (d, *J* = 1.7 Hz, 1H, 8-H), 7.89 (d, *J* = 8.9 Hz, 1H, 4-H), 7.80 (d, *J* = 8.7 Hz, 1H, 5-H), 7.66 (d, *J* = 8.9, 2.1 Hz, 1H, 3-H), 7.50 (dd, *J* = 8.7, 2.0 Hz, 1H, 6-H), 6.96 (s, 1H, 5'-H), 4.10 (s, 2H, CH_2), 2.32 (s, 6H, 4-CH_3, 6-CH_3).

^{13}C NMR (101 MHz, DMSO-d_6) δ [ppm] = 169.3 (C-2'), 167.98 (NHCO), 166.97 (C-4', C-6'), 137.7 (C-2), 134.8 (C-8a), 129.7 (C-5), 129.0 (C-8), 128.6 (C-4), 128.2 (C-4a), 127.5 (C-6), 120.4 (C-3), 119.8 (C-7), 116.1 (C-5'), 114.2 (C-1), 35.6 (CH_2), 23.3 (s, 6H, 4'-CH_3, 6'-CH_3).

IR (ATR) $\tilde{\nu}$ [cm^{-1}] = 3250, 1666, 1627, 1599, 1578, 1534, 1497, 1429, 1406, 1365, 1333, 1255, 1227, 1168, 1143, 1062, 985, 950, 899, 868, 837, 830, 735.

HRMS (EI): *m/z* = $[M]^{\bullet+}$ calculated for $C_{18}H_{16}{}^{79}BrNOS^{\bullet+}$: 401.0192; found: 401.0193.

Purity (HPLC): > 99% (210 nm), > 99% (254 nm), (method 1b).

7-(3-Nitrophenyl)naphthalen-2-amine (8)

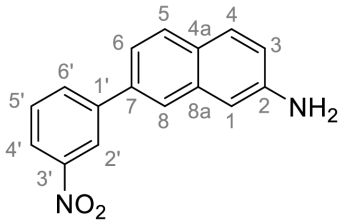

$C_{16}H_{12}N_2O_2$

M_w = 264.28 g/mol

At room temperature, 7-bromonaphthalene-2-amine (**2**, 3.40 g, 15.8 mmol, 1.00 eq), 3-nitrophenyl boronic acid (3.16 g, 18.9 mmol, 1.20 eq), K_2CO_3 (6.32 g, 38.3 mmol, 2.50 eq) and $Pd(PPh_3)_4$ (0.991 g, 0.788 mmol, 0.0500 eq) were weighed out into a flask, which was put under nitrogen afterwards. Degassed anhydrous DMF (15 mL) was added *via* syringe and the reaction mixture was stirred for 23 h at 105 °C and then for another 2 hours at room temperature under nitrogen atmosphere. Subsequently the mixture was diluted with water (100 mL) and brine (200 mL) and extracted with EtOAc (4 x 100 mL). The combined organic layers were dried over sodium sulfate. After evaporating the solvent *in vacuo*, the crude product was purified *via* flash column chromatography (hexanes/EtOAc 7:3 → 3:7) to yield the title compound as a pink-red solid (1.61 g, 6.07 mmol, 38%).

R_f: 0.23 (hexanes/EtOAc 7:3).
m.p.: 160 °C.

^{1}H NMR (400 MHz, DMSO-d_6) δ [ppm] = 8.52 (t, *J* = 2.1 Hz, 1H, 2'-H), 8.26 – 8.18 (m, 2H, 4'-H, 6'-H), 7.94 (d, *J* = 1.9 Hz, 1H, 8-H), 7.82 – 7.73 (m, 2H, 5-H, 5'-H), 7.65 (d, *J* = 8.7 Hz, 1H, 4-H), 7.48 (dd, *J* = 8.4, 1.9 Hz, 1H, 6-H), 6.98 (dd, *J* = 8.7, 2.2 Hz, 1H, 3-H), 6.94 (d, *J* = 2.2 Hz, 1H, 1-H), 5.50 (s, 2H, NH_2).

^{13}C NMR (101 MHz, DMSO-d_6) δ [ppm] = 148.5 (C-3'), 147.3 (C-2), 142.3 (C-1'), 135.3 (C-7), 135.1 (C-8a), 133.4 (C-6'), 130.4 (C-5'), 128.6 (C-5), 128.3 (C-4), 126.0 (C-4a), 123.4 (C-8), 121.9 (C-4'), 121.1 (C-2'), 119.6 (C-6), 119.2 (C-3), 106.2 (C-1).

IR (ATR) $\tilde{\nu}$ [cm^{-1}] = 3450, 3372, 1631, 1526, 1513, 1485, 1460, 1388, 1340, 1308, 1269, 1224, 1190, 1138, 1101, 1082, 890, 870, 838, 814, 776, 738, 716, 682, 659.

HRMS (EI): *m*/*z* = [M]$^{\bullet+}$ calculated for $C_{16}H_{12}N_2O_2^{\bullet+}$: 264.0893; found: 264.0897.

Purity (HPLC): > 99% (210 nm), > 99% (254 nm), (method 1a).

2-Bromo-*N*-(7-(3-nitrophenyl)naphthalen-2-yl)acetamide (10)

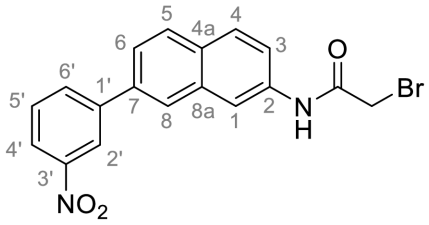

$C_{18}H_{13}BrN_2O_3$

M_w = 385.22 g/mol

At 0 °C bromoacetyl bromide (736 µL, 8.45 mmol, 3.00 eq) was added dropwise to a stirred suspension of amine **8** (745 mg, 2.82 mmol, 1.00 eq) in anhydrous DCM (100 mL). After 2 h, water (50 mL) and brine (150 mL) were added, and the reaction mixture was extracted with DCM (4 x 100 mL). The combined organic layers were dried over sodium sulfate. After evaporating the solvent *in vacuo*, the crude product was purified *via* flash column chromatography (hexanes/EtOAc 7:3 → 1:9) to yield the title compound as a dark yellow solid (981 mg, 2.55 mmol, 90%).

R_f: 0.20 (hexanes/EtOAc 7:3).
m.p.: 200 °C.

^{1}H NMR (500 MHz, CD_2Cl_2) δ [ppm] = 8.58 (t, *J* = 2.0 Hz, 1H, 2'-H), 8.34 (d, *J* = 2.2 Hz, 1H, 1-H), 8.27 (s, 1H, NHCO), 8.23 (ddd, *J* = 8.2, 2.3, 1.0 Hz, 1H, 4'-H), 8.11 (dd, *J* = 1.8, 0.8 Hz, 1H, 8-H), 8.08 (ddd, *J* = 7.7, 1.9, 1.0 Hz, 1H, 6'-H), 7.96 (d, *J* = 8.5 Hz, 1H, 5-H), 7.90 (d, *J* = 8.7 Hz, 1H, 4-H), 7.74 (dd, *J* = 8.5, 1.9 Hz, 1H, 6-H), 7.68 (t, *J* = 8.0 Hz, 1H, 5'-H), 7.55 (dd, *J* = 8.8, 2.2 Hz, 1H, 3-H), 4.09 (s, 2H, CH_2).

^{13}C NMR (126 MHz, CD_2Cl_2) δ [ppm] = 164.3 (NHCO), 149.4 (C-3'), 143.1 (C-1'), 137.4 (C-7), 136.1 (C-8a), 134.4 (C-2), 133.9 (C-6'), 131.1 (C-4a), 130.5 (C-5'), 129.3 (C-4), 129.2 (C-5), 126.7 (C-8), 125.0 (C-6), 122.7 (C-4'), 122.6 (C-2'), 121.0 (C-3), 117.6 (C-1), 30.2 (CH_2).

IR (ATR) $\tilde{\nu}$ [cm^{-1}] = 3266, 3078, 1687, 1662, 1632, 1611, 1528, 1516, 1463, 1398, 1334, 1271, 1243, 1227, 1187, 1172, 1098, 984, 953, 885, 866, 842, 804, 741, 830, 680.

HRMS (ESI): *m/z* = [M-H]$^-$ calculated for $C_{16}H_{12}{}^{79}BrN_2O_3^-$: 383.0037; found: 383.0035.

Purity (HPLC): ≥ 99% (210 nm), > 99% (254 nm), (method 1a).

2-((4,6-Dimethylpyrimidin-2-yl)thio)-*N*-(7-(3-nitrophenyl) naphthalen-2-yl)acetamide (11)

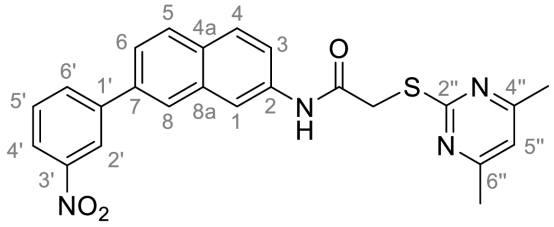

$C_{24}H_{20}N_4O_3S$

M_w = 444.51 g/mol

At room temperature potassium *tert*-butoxide (522 mg, 4.65 mmol, 2.00 eq) was added to a stirred solution of 2-bromoacetamide **10** (896 mg, 2.32 mmol, 1.00 eq) and 4,6-dimethylpyrimidine-2-thiol (391 mg, 2.79 mmol, 1.20 eq) in anhydrous DMF (10 mL). After 3 h, water (150 mL) and brine (100 mL) were added, and the reaction mixture was extracted with EtOAc (4 x 100 mL). The combined organic layers were dried over sodium sulfate. After evaporating the solvent *in vacuo*, the crude product was purified *via* flash column chromatography (hexanes/EtOAc 6:4) to yield the title compound as a white-pink solid (895 mg, 2.01 mmol, 87%).

R_f: 0.17 (hexanes/EtOAc 6:4).
m.p.: 94-98 °C.

^{1}H NMR (500 MHz, DMSO-d_6) δ [ppm] = 10.51 (s, 1H, NHCO), 8.60 (t, *J* = 2.1 Hz, 1H, 2'-H), 8.42 (d, *J* = 2.1 Hz, 1H, 1-H), 8.34 – 8.28 (m, 2H, 8-H, 6'-H), 8.25 (ddd, *J* = 8.0, 2.3, 0.9 Hz, 1H, 4'-H), 7.99 (d, *J* = 8.5 Hz, 1H, 5-H), 7.93 (d, *J* = 8.8 Hz, 1H, 4-H), 7.86 – 7.77 (m, 2H, 6-H, 5'-H), 7.65 (dd, *J* = 8.8, 2.1 Hz, 1H, 3-H), 6.97 (s, 1H, 5''-H), 4.12 (s, 2H, CH_2), 2.33 (s, 6H, 4''-CH_3, 6''-CH_3).

^{13}C NMR (126 MHz, DMSO-d_6) δ [ppm] = 169.3 (C-2''), 167.0 (C-4'', C-6''), 166.9 (NHCO), 148.5 (C-3'), 141.7 (C-1'), 137.3 (C-2), 135.6 (C-7), 133.7 (C-8a), 133.6 (C-6'), 130.5 (C-5'), 129.4 (C-4a), 128.5 (C-5), 128.3 (C-4), 125.7 (C-8), 123.5 (C-6), 122.2 (C-4'), 121.4 (C-2'), 120.6 (C-3), 116.1 (C-5''), 115.7 (C-1), 35.6 (CH_2), 23.3 (4''-CH_3, 6''-CH_3).

IR (ATR) $\tilde{\nu}$ [cm^{-1}] = 3289, 3066, 1688, 1582, 1527, 1512, 1433, 1341, 1266, 1240, 893, 841, 806, 737, 685.

HRMS (ESI): *m/z* = $[M+H]^+$ calculated for $C_{24}H_{21}N_4O_3S^+$: 445.1329; found: 445.1324.

Purity (HPLC): > 99% (210 nm), > 99% (254 nm), (method 1a).

N-(7-(3-Aminophenyl)naphthalen-2-yl)-2-((4,6-dimethylpyrimidin-2-yl)thio)acetamide (12)

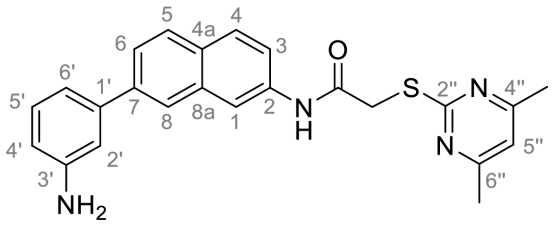

$C_{24}H_{22}N_4OS$

M_w = 414.53 g/mol

Under nitrogen atmosphere nitro compound **11** (0.684 g, 1.54 mmol, 1.00 eq) was suspended in acetic acid (5 mL) and iron powder (3.01 g, 53.9 mmol, 35.0 eq) was added. After the reaction mixture was stirred at 50 °C for 3 h, it was filtered and then diluted with water (50 mL) and brine (100 mL). The mixture was extracted with EtOAc (4 x 50 mL) and the combined organic layers were dried over sodium sulfate. After evaporating the solvent *in vacuo*, the crude product was purified *via* flash column chromatography (hexanes/EtOAc 1:1) to yield the title compound as a yellow solid (480 mg, 1.16 mmol, 75%).

R_f: 0.11 (hexanes/EtOAc 1:1).
m.p.: 167 °C.

^{1}H NMR (500 MHz, DMSO-d_6) δ [ppm] = 10.47 (s, 1H, NHCO), 8.30 (d, *J* = 2.1 Hz, 1H, 1-H), 7.95 (d, *J* = 1.8 Hz, 1H, 8-H), 7.92 – 7.85 (m, 2H, 4-H, 5-H) 7.66 – 7.58 (m, 2H, 3-H, 6-H), 7.14 (t, *J* = 7.8 Hz, 1H, 5'-H), 6.99 (t, *J* = 2.0 Hz, 1H. 2'-H), 6.98 (s, 1H, 5''-H) 6.92 (ddd, *J* = 7.6,

1.8, 1.0 Hz, 1H, 6'-H), 6.60 (ddd, *J* = 7.9, 2.2, 0.9 Hz, 1H, 4'-H), 5.18 (s, 2H, NH_2), 4.12 (s, 2H, CH_2), 2.34 (s, 6H, 4''-CH_3, 6''-CH_3).

^{13}C NMR (126 MHz, DMSO-d_6) δ [ppm] = 169.3 (C-2''), 170.0 (C-4'', C-6'') (166.8 (NHCO), 149.2 (3'-H), 140.7 (1'-H), 138.9 (C-7), 137.0 (C-2), 133.7 (C-8a), 129.5 (C-5'), 128.9 (C-4a), 128.2 (C-5), 128.0 (C-4), 124.2 (C-8), 123.9 (C-6), 119.8 (C-3), 116.1 (C-5''), 115.4 (C-1), 114.6 (C-6'), 113.3 (C-4'), 112.4 (C-2'), 35.6 (CH_2), 23.3 (4''-CH_3, 6''-CH_3).

IR (ATR) $\tilde{\nu}$ [cm^{-1}] = 3430, 3224, 3097, 1656, 1631, 1611, 1584, 1546, 1516, 1493, 1404, 1341, 1322, 1272, 1236, 922, 940, 904, 886, 858, 840, 774, 749, 691.

HRMS (ESI): *m/z* = $[M-H]^-$ calculated for $C_{24}H_{21}N_4OS^-$: 413.1442; found: 413.1440.

Purity (HPLC): > 99% (210 nm), > 99% (254 nm), (method 1a).

N-(7-(3-Acetamidophenyl)naphthalen-2-yl)-2-((4,6-dimethylpyrimidin-2-yl)thio)acetamide (FM46)

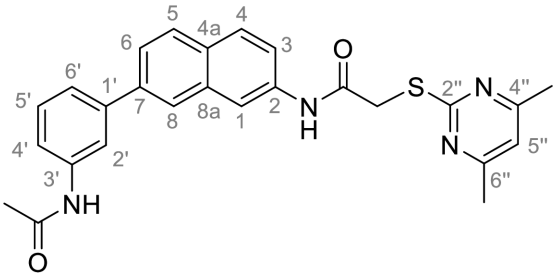

$C_{26}H_{24}N_4O_4S$

M_w = 446.57 g/mol

At room temperature acetic anhydride (36.5 µL, 0.386 mmol, 2.00 eq) was added dropwise to a stirred solution of amine **12** (80.1 mg, 0.193 mmol, 1.00 eq) and NEt_3 (53.9 µL, 0.386 mmol, 2.00 eq) in anhydrous DCM (5 mL). After 2 h, water (25 mL) and brine (25 mL) were added, and the reaction mixture was extracted with EtOAc (3 x 25 mL). The combined organic layers were dried over sodium sulfate. After evaporating the solvent *in vacuo*, the crude product was purified *via* flash column chromatography (hexanes/EtOAc 3:7) to yield the title compound as a white solid (80.2 mg, 0.176 mmol, 91%).

R_f: 0.12 (hexanes/EtOAc 3:7).
m.p.: 213 °C.

^{1}H NMR (500 MHz, DMSO-d_6) δ [ppm] = 10.48 (s, 1H. 2-NHCO), 10.05 (s, 1H, 3'-NHCO), 8.33 (d, *J* = 2.1 Hz, 1H, 1-H), 8.01 (d, *J* = 1.8 Hz, 1H, 8-H), 8.00 (t, *J* = 2.0 Hz, 1H, 2'-H), 7.93 (d, *J* = 8.6 Hz, 1H, 5-H), 7.90 (d, *J* = 8.8 Hz, 1H, 4-H), 7.66 (dd, *J* = 8.5, 1.8 Hz, 1H, 6-H), 7.64 – 7.59 (m, 2H, 3-H, 4'-H), 7.47 (dt, *J* = 7.7, 1.5 Hz, 1H, 6'-H), 7.41 (t, *J* = 7.8 Hz, 1H, 5'-H), 6.97 (s, 1H, 5''-H), 4.12 (s, 2H, CH_2), 2.34 (s, 6H, 4''-CH_3, 6''-CH_3), 2.08 (s, 3H, CH_3).

^{13}C NMR (126 MHz, DMSO-d_6) δ [ppm] = 169.3 (C-2''), 168.4 (3'-NHCO), 167.0 (C-4'', C-6''), 166.9 (2-NHCO), 140.5 (C-1'), 139.9 (C-3'), 138.1 (C-7), 137.1 (C-2), 133.7 (C-8a), 129.4 (C-5'), 129.0 (C-4a), 128.3 (C-4), 128.2 (C-5), 124.7 (C-8), 123.7 (C-6), 121.7 (C-6'), 120.1 (C-3), 118.2 (C-4'), 117.6 (C-2'), 116.1 (C-5''), 115.4 (C-1), 35.6 (CH_2), 24.1 (4''-CH_3, 6''-CH_3), 23.3 (CH_3).

IR (ATR) $\tilde{\nu}$ [cm^{-1}] = 3290, 2923, 2854, 1665, 1609, 1584, 1559, 1542, 1489, 1433, 1394, 1372, 1320, 1268, 1218, 1194, 1172, 1150, 1022, 970, 901, 885, 838, 679, 778, 720, 692.

HRMS (ESI): *m/z* = $[M-H]^-$ calculated for $C_{26}H_{23}N_4O_2S^-$: 445.1547; found: 445.1542.

Purity (HPLC): > 99% (210 nm), > 99% (254 nm), (method 1a).

N-(3-(7-(2-((4,6-Dimethylpyrimidin-2-yl)thio)acetamido)naphthalen-2-yl)phenyl)thiophene-2-carboxamide (FM48)

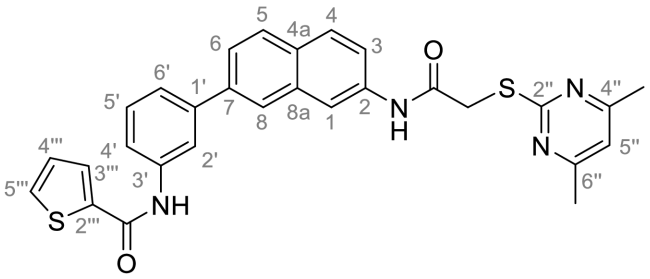

$C_{29}H_{24}N_4O_2S_2$

M_w = 524.67 g/mol

At room temperature 2-thiophenecarbonyl chloride (21.9 µL, 0.205 mmol, 2.00 eq) was added dropwise to a stirred solution of amine **12** (42.4 mg, 0.102 mmol, 1.00 eq) and NEt_3 (28.5 µL, 0.205 mmol, 2.00 eq) in anhydrous DCM (5 mL). After 2 h, water (25 mL) and brine (25 mL) were added, and the reaction mixture was extracted with DCM (3 x 25 mL). The combined organic layers were dried over sodium sulfate. After evaporating the solvent *in vacuo*, the crude

product was purified *via* flash column chromatography (hexanes/EtOAc 1:1) to yield the title compound as a white solid (16.3 mg, 0.0313 mmol, 31%).

R_f: 0.21 (hexanes/EtOAc 1:1).
m.p.: 180 °C.

^{1}H NMR (500 MHz, DMSO-d_6) δ [ppm] = 10.49 (s, 1H, 2-NHCO), 10.33 (s, 1H, 3'-NHCO), 8.36 (d, *J* = 2.1 Hz, 1H, 1-H), 8.15 (t, *J* = 1.9 Hz, 1H, 2'-H), 8.09 – 8.05 (m, 2H, 8-H, 3'''-H), 7.96 (d, *J* = 8.5 Hz, 1H, 5-H), 7.91 (d, *J* = 8.9 Hz, 1H, 4-H), 7.88 (dd, *J* = 5.0, 1.2 Hz, 1H, 5'''-H), 7.81 (ddd, *J* = 8.0, 2.2, 1.1 Hz, 1H, 4-H), 7.72 (dd, *J* = 8.5, 1.8 Hz, 1H, 6-H), 7.63 (dd, *J* = 8.8, 2.1 Hz, 1H, 3-H), 7.56 (dt, *J* = 7.8, 1.4 Hz, 1H, 6'-H), 7.49 (t, *J* = 7.9 Hz, 1H, 5'-H), 7.25 (dd, *J* = 5.0, 3.7 Hz, 1H, 4'''-H), 6.97 (s, 1H, 5''-H), 4.12 (s, 2H, CH_2), 2.34 (s, 6H, 4''-CH_3, 6''-CH_3).

^{13}C NMR (126 MHz, DMSO-d_6) δ [ppm] = 169.3 (C-2''), 167.0 (C-4'', C-6''), 166.9 (2-NHCO), 160.0 (3'-NHCO), 140.5 (C-1'), 140.0 (C-2'''), 139.4 (C-3'), 137.9 (C-7), 137.2 (C-2), 133.8 (C-8a), 132.0 (C-5'''), 129.4 (C-5'), 129.2 (C-3'''), 129.1 (C-4a), 128.3 (C-5), 128.2 (C-4), 128.1 (C-4'''), 124.7 (C-8), 123.7 (C-6), 122.4 (C-6'), 120.1 (C-4), 119.4 (C-4'), 118.9 (C-2'), 116.1 (C-5''), 115.5 (C-1), 35.6 (CH_2), 23.3 (4''-CH_3, 6''-CH_3).

IR (ATR) $\tilde{\nu}$ [cm^{-1}] = 3299, 3078, 2957, 1660, 1634, 1608, 1583, 1538, 1487, 1428, 1335, 1306, 1265, 1227, 891, 841, 786, 718, 698.

HRMS (ESI): *m/z* = $[M-H]^-$ calculated for $C_{29}H_{23}N_4O_2S_2^-$: 525.1268; found: 523.1263.

Purity (HPLC): > 99% (210 nm), ≥ 99% (254 nm), (method 1a).

_N_-(3-(7-(2-((4,6-Dimethylpyrimidin-2-yl)thio)acetamido)naphthalen -2-yl)phenyl)benzamide (FM54)

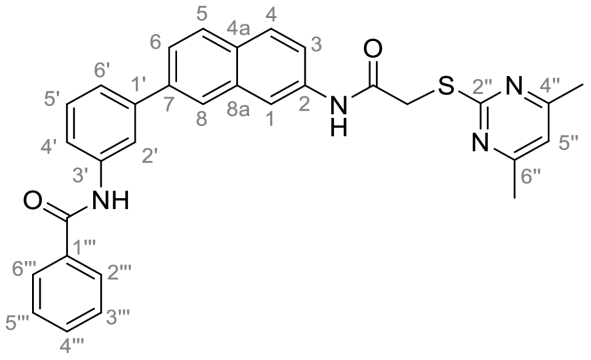

$C_{31}H_{26}N_4O_2S$

M_w = 518.64 g/mol

At room temperature benzoyl chloride (34.7 µL, 0.299 mmol, 2.00 eq) was added dropwise to a stirred solution of amine **12** (62.0 mg, 0.150 mmol, 1.00 eq) and NEt_3 (41.7 µL, 0.299 mmol, 2.00 eq) in anhydrous DCM (5 mL). After 2 h, water (25 mL) and brine (25 mL) were added, and the reaction mixture was extracted with DCM (3 x 25 mL). The combined organic layers were dried over sodium sulfate. After evaporating the solvent *in vacuo*, the crude product was purified *via* flash column chromatography (hexanes/EtOAc 1:1) to yield the title compound as a white solid (68.0 mg, 0.131 mmol, 87%).

R_f: 0.20 (hexanes/EtOAc 1:1).
m.p.: 192 °C.

^{1}H NMR (500 MHz, DMSO-d_6) δ [ppm] = 10.49 (s, 1H, 2-NHCO), 10.35 (s, 1H, 3'-NHCO), 8.36 (d, *J* = 2.1 Hz, 1H, 1-H), 8.23 (t, *J* = 1.9 Hz, 1H, 2'-H), 8.07 (d, *J* = 1.8 Hz, 1H, 8-H), 8.02 – 7.99 (m, 2H, 2'''-H, 6'''-H), 7.96 (d, *J* = 8.6 Hz, 1H, 5-H), 7.91 (d, *J* = 8.8 Hz, 1H, 4-H), 7.87 (ddd, *J* = 8.1, 2.2, 1.1 Hz, 1H, 4'-H), 7.72 (dd, *J* = 8.5, 1.8 Hz, 1H, 6-H), 7.65 – 7.59 (m, 2H, 3-H, 4'''-H), 7.58 – 7.54 (m, 3H, 6'-H, 3'''-H, 5'''-H), 7.49 (t, *J* = 7.9 Hz, 1H, 5'-H), 6.97 (s, 1H, 5''-H), 4.12 (s, 2H, CH_2), 2.34 (s, 6H, 4''-CH_3, 6''-CH_3).

^{13}C NMR (126 MHz, DMSO-d_6) δ [ppm] = 169.3 (C-2''), 167.0 (C-4'', C-6''), 166.9 (2-NHCO), 165.6 (3'-NHCO), 140.4 (C-1'), 139.7 (C-3'), 138.0 (C-7), 137.2 (C-2), 134.8 (C-1'''), 133.8 (C-8a), 131.7 (C-4'''), 129.3 (C-5'), 129.1 (C-4a), 128.4 (C-3''', C-5'''), 128.3 (C-4), 128.2 (C-5), 127.7 (C-2''', C-6'''), 124.7 (C-8), 123.7 (C-6), 122.3 (C-6'), 120.1 (C-3), 119.4 (C-4'), 118.9 (C-2'), 116.1 (C-5''), 115.5 (C-1), 35.6 (CH_2), 23.3 (4''-CH_3, 6''-CH_3).

IR (ATR) $\tilde{\nu}$ [cm^{-1}] = 3282, 3059, 1667, 1649, 1608, 1581, 1537, 1487, 1438, 1396, 1370, 1333, 1299, 1265, 1222, 1027, 889, 838, 787, 697.

HRMS (ESI): *m/z* = [M-H]$^-$ calculated for $C_{31}H_{25}N_4O_2S^-$: 517.1704; found: 517.1701.

Purity (HPLC): > 99% (210 nm), > 99% (254 nm), (method 1a).

2-((4,6-Dimethylpyrimidin-2-yl)thio)-*N*-(7-(3-(phenylsulfonamido)phenyl)naphthalen-2-yl)acetamide (FM47)

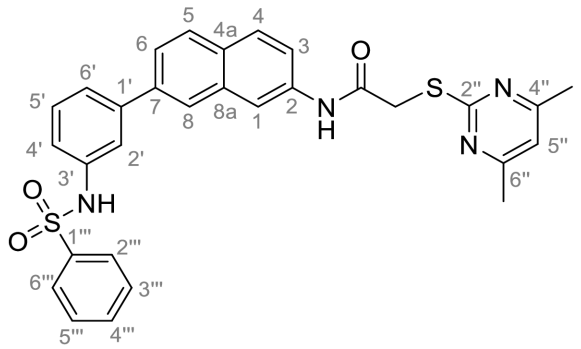

$C_{30}H_{26}N_4O_3S_2$

M_w = 554.69 g/mol

At room temperature benzenesulfonyl chloride (49.3 µL, 0.386 mmol, 2.00 eq) was added dropwise to a stirred solution of amine **12** (80.1 mg, 0.193 mmol, 1.00 eq) and NEt_3 (53.9 µL, 0.193 mmol, 2.00 eq) in anhydrous DCM (5 mL). After 4h, water (25 mL) and brine (25 mL) were added, and the reaction mixture was extracted with EtOAc (4 x 25 mL). The combined organic layers were dried over sodium sulfate. After evaporating the solvent *in vacuo*, the crude product was purified *via* flash column chromatography (hexanes/EtOAc 1:1) to yield the title compound as a white solid (119 mg, 0.0899 mmol, 47%).

R_f: 0.19 (hexanes/EtOAc 1:1).
m.p.: 176 °C (decomposition).

^{1}H NMR (500 MHz, DMSO-d_6) δ [ppm] = 10.49 (s, 1H, NHCO), 10.42 (s, 1H, $NHSO_2$), 8.32 (d, *J* = 2.1 Hz, 1H, 1-H), 7.93 – 7.87 (m, 3H, 4-H, 5-H, 8-H), 7.85 – 7.79 (m, 2H, 2'''-H, 6'''-H), 7.64 – 7.55 (m, 4H, 3-H, 3'''-H, 4'''-H, 5'''-H), 7.54 (dd, *J* = 8.4, 1.8 Hz, 1H, 6-H), 7.46 (dt, *J* = 8.0, 1.1 Hz, 1H, 6'-H), 7.44 (t, *J* = 2.0 Hz, 1H, 2'-H) 7.35 (t, *J* = 7.9 Hz, 1H, 5'-H), 7.12 (ddd, *J*

= 8.1, 2.2, 1.0 Hz, 1H, 4'-H), 6.97 (s, 1H, 5''-H), 4.11 (s, 2H, CH_2), 2.34 (s, 6H, 4''-CH_3, 6''-CH_3).

^{13}C NMR (126 MHz, DMSO-d_6) δ [ppm] = 169.3 (C-2''), 167.0 (C-4'', C-6''), 166.9 (NHCO), 141.0 (C-1'), 139.5 (C-1'''), 138.3 (C-3'), 137.4 (C-7), 137.2 (C-2), 133.6 (C-8a), 133.0 (C-4'''), 129.8 (C-5'), 129.3 (C-3''', C-5'''), 129.1 (C-4a), 128.3 (C-5), 128.2 (C-4), 126.8 (C-2''', C-6'''), 124.7 (C-8), 123.5 (C-6), 122.9 (C-6'), 120.2 (C-3), 119.2 (C-4'), 118.6 (C-2'), 116.1 (C-5''), 115.4 (C-1), 35.6 (CH_2), 23.3 (4''-CH_3, 6''-CH_3).

IR (ATR) $\tilde{\nu}$ [cm^{-1}] = 3294, 3211, 2912, 1670, 1581, 1530, 1511, 1489, 1446, 1385, 1330, 1309, 1265, 1226, 1165, 1094, 944, 906, 893, 846, 839, 786, 758, 737, 685.

HRMS (ESI): *m/z* = [M-H]$^-$ calculated for $C_{30}H_{25}N_4O_3S_2^-$: 553.1374; found: 553.1370.

Purity (HPLC): > 99% (210 nm), > 99% (254 nm), (method 1a).

N-(3-(7-(2-((4,6-Dimethylpyrimidin-2-yl)thio)acetamido)naphthalen-2-yl)phenyl)-5-methylthiophene-2-carboxamide (FM66)

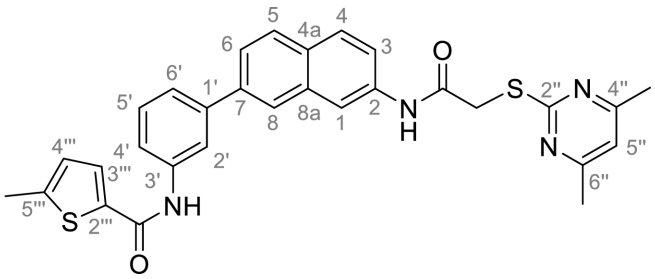

$C_{30}H_{26}N_4O_2S_2$

M_w = 538.69 g/mol

At room temperature previously prepared 5-methylthiophene-2-carbonyl chloride (27.7 µL, 0.228 mmol, 2.00 eq) was added dropwise to a stirred solution of amine **12** (47.2 mg, 0.114 mmol, 1.00 eq) and NEt_3 (31.7 µL, 0.228 mmol, 2.00 eq) in anhydrous DCM (5 mL). After 5 h, water (25 mL) and brine (25 mL) were added, and the reaction mixture was extracted with DCM (3 x 25 mL). The combined organic layers were dried over sodium sulfate. After evaporating the solvent *in vacuo*, the crude product was purified *via* flash column chromatography (hexanes/EtOAc 1:1) to yield the title compound as a white solid (51.0 mg, 0.0947 mmol, 83%).

R_f: 0.28 (hexanes/EtOAc 1:1).

m.p.: 122 °C (decomposition).

^{1}H NMR (500 MHz, DMSO-d_6) δ [ppm] = 10.49 (s, 1H, 2-NHCO), 10.20 (s, 1H, 3'-NHCO), 8.35 (d, *J* = 2.0 Hz, 1H, 1-H), 8.14 (t, *J* = 2.0 Hz, 1H, 2'-H), 8.07 (d, *J* = 1.8 Hz, 1H, 8-H), 7.95 (d, *J* = 8.6 Hz, 1H, 5-H), 7.91 (d, *J* = 8.9 Hz, 1H, 4-H), 7.87 (d, *J* = 3.7 Hz, 1H, 3'''-H), 7.79 (ddd, *J* = 8.0, 2.1, 1.0 Hz, 1H, 4'-H), 7.71 (dd, *J* = 8.5, 1.8 Hz, 1H, 6-H), 7.63 (dd, *J* = 8.8, 2.0 Hz, 1H, 3-H), 7.54 (dt, *J* = 7.9, 1.4 Hz, 1H, 6'-H), 7.47 (t, *J* = 7.9 Hz, 1H, 5'-H), 6.97 (s, 1H, 5''-H), 6.95 (dd, *J* = 3.8, 1.2 Hz, 1H, 4'''-H), 4.12 (s, 2H, CH_2), 2.51 (s, 3H, CH_3), 2.34 (s, 6H, 4''-CH_3, 6''-CH_3).

^{13}C NMR (126 MHz, DMSO-d_6) δ [ppm] = 169.3 (2''-H), 167.0 (C-4'', C-6''), 166.9 (2-NHCO), 159.9 (3'-NHCO), 146.0 (C-5'''), 140.5 (C-1'), 139.5 (C-3'), 137.9 (C-7), 137.4 (C-2'''), 137.1 (C-2), 133.8 (C-8a), 129.4 (C-3'''), 129.3 (C-5'), 129.1 (C-4a), 128.3 (C-5), 128.2 (C-4), 126.7 (C-4'''), 124.7 (C-8), 123.7 (C-6), 122.2 (C-6'), 120.1 (C-3), 119.3 (C-4'), 118.8 (C-2'), 116.1 (C-5''), 115.5 (C-1), 35.6 (CH_2), 23.3 (4''-CH_3, 6''-CH_3), 15.3 (CH_3).

IR (ATR) $\tilde{\nu}$ [cm^{-1}] = 3287, 3059, 2920, 1633, 1607, 1582, 1531, 1510, 1486, 1459, 1428, 1398, 1336, 1303, 1263, 1171, 1085, 1032, 891, 839, 801, 785, 730, 697.

HRMS (EI): *m/z* = $[M]^{\bullet+}$ calculated for $C_{30}H_{26}N_4O_2S_2^{\bullet+}$: 538.1492; found: 538.1500.

Purity (HPLC): > 97% (210 nm), > 96% (254 nm), (method 1a).

7-(4-Nitrophenyl)naphthalen-2-amine (7)

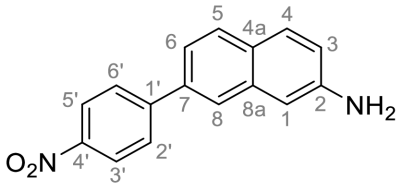

$C_{16}H_{12}N_2O_2$

M_w = 264.28 g/mol

At room temperature, 7-bromonaphthalene-2-amine (**2**, 3.40 g, 15.3 mmol, 1.00 eq), 4-nitrophenyl boronic acid (3.06 g, 18.4 mmol, 1.20 eq), K_2CO_3 (6.32 g, 38.3 mmol, 2.50 eq) and $Pd(PPh_3)_4$ (0.884 g, 0.765 mmol, 0.0500 eq) were weighed out into a flask, which was put under nitrogen afterwards. Degassed anhydrous DMF (15 mL) was added *via* syringe and the

reaction mixture was stirred for 23 h at 105 °C and then for another 2 hours at room temperature under nitrogen atmosphere. Subsequently the mixture was diluted with water (100 mL) and brine (200 mL) and extracted with EtOAc (4 x 100 mL). The combined organic layers were dried over sodium sulfate. After evaporating the solvent *in vacuo*, the crude product was purified *via* flash column chromatography (hexanes/EtOAc 7:3 → 3:7) to yield the title compound as red orange solid (1.70 g, 6.44 mmol, 42%).

R_f: 0.16 (hexanes/EtOAc 7:3).
m.p.: 233 °C.

^{1}H NMR (400 MHz, DMSO-d_6) δ [ppm] = 8.34 – 8.29 (m, 2H, 3'-H, 5'-H), 8.08 – 8.02 (m, 2H, 2'-H, 6'-H), 7.95 (d, *J* = 1.9 Hz, 1H, 8-H), 7.77 (d, *J* = 8.5 Hz, 1H, 5-H), 7.65 (d, *J* = 8.7 Hz, 1H, 4-H), 7.48 (dd, *J* = 8.4, 1.9 Hz, 1H, 6-H), 7.00 (dd, *J* = 8.7, 2.2 Hz, 1H, 3-H), 6.93 (d, *J* = 2.2 Hz, 1H, 1-H), 5.52 (s, 2H, NH_2).

^{13}C NMR (101 MHz, DMSO-d_6) δ [ppm] = δ 147.4 (C-2), 147.2 (C-1'), 146.4 (C-4'), 135.2 (C-7), 135.0 (C-8a), 128.6 (C-5), 128.3 (C-4), 127.9 (C-2', C-6'), 126.2 (C-4a), 124.04 (C-3', C-5'), 123.97 (C-8), 119.6 (C-6), 119.5 (C-3), 106.3 (C-1).

IR (ATR) $\tilde{\nu}$ [cm^{-1}] = 3442, 3355, 1630, 1588, 1501, 1462, 1392, 1340, 1279, 1248, 1108, 895, 855, 835, 750, 696.

HRMS (EI): *m/z* = $[M]^{\bullet+}$ calculated for $C_{16}H_{12}N_2O_2^{\bullet+}$: 264.0893; found: 264.0899.

Purity (HPLC): > 99% (210 nm), > 99% (254 nm), (method 1a).

2-Bromo-*N*-(7-(4-nitrophenyl)naphthalen-2-yl)acetamide (9)

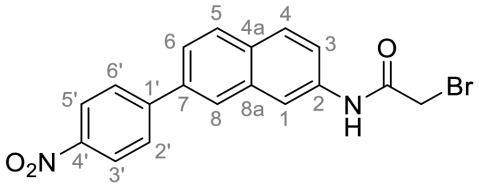

$C_{18}H_{13}BrN_2O_3$

M_w = 385.22 g/mol

At 0 °C bromoacetyl bromide (1.38 mL, 15.9 mmol, 8.00 eq) was added dropwise to a stirred suspension of amine **7** (525 mg, 1.99 mmol, 1.00 eq) in anhydrous DCM (100 mL). After 2 h, water (50 mL) and brine (150 mL) were added, and the reaction mixture was extracted with DCM (4 x 100 mL). The combined organic layers were dried over sodium sulfate. After evaporating the solvent *in vacuo*, the crude product was purified *via* flash column chromatography (hexanes/EtOAc 7:3 → 1:9) to yield the title compound as a yellow orange solid (684 mg, 1.78 mmol, 89%).

R_f: 0.20 (hexanes/EtOAc 7:3).
m.p.: 189 °C.

^{1}H NMR (400 MHz, CD_2Cl_2) δ [ppm] = 8.35 (d, *J* = 1.9 Hz, 1H, 1-H), 8.35 – 8.31 (m, 2H, 3'-H, 5'-H), 8.26 (bs, 1H, NHCO), 8.12 (d, *J* = 2.3 Hz, 1H, 8-H), 7.95 (d, *J* = 8.5 Hz, 1H, 4-H), 7.93 – 7.87 (m, 3H, 5-H, 2'-H, 6'-H), 7.74 (dd, *J* = 8.5, 1.9 Hz, 1H, 6-H), 7.55 (dd, *J* = 8.8, 2.2 Hz, 1H, 3-H), 4.09 (s, 2H, CH_2).

^{13}C NMR (101 MHz, CD_2Cl_2) δ [ppm] = 164.3 (NHCO), 147.83 (C-1'), 147.80 (C-4'), 137.4 (C-2), 136.1 (C-7), 134.4 (C-8a), 131.3 (C-4a), 129.3 (C-4), 129.2 (C-5), 128.6 (C-2', C-6'), 127.2 (C-8), 125.0 (C-6), 124.7 (C-3', C-5'), 121.2 (C-3), 117.7 (C-1), 30.2 (CH_2).

IR (ATR) $\tilde{\nu}$ [cm^{-1}] = 3302, 2926, 1670, 1590, 1561, 1548, 1506, 142, 1397, 1334, 1287, 1214, 1108, 903, 850, 833, 750, 716, 690, 657.

HRMS (ESI): *m/z* = $[M-H]^-$ calculated for $C_{16}H_{12}{}^{79}BrN_2O_3^-$: 383.0037; found: 383.0041.

Purity (HPLC): > 99% (210 nm), > 99% (254 nm), (method 1a).

2-((4,6-Dimethylpyrimidin-2-yl)thio)-*N*-(7-(4-nitrophenyl) naphthalen-2-yl)acetamide (6)

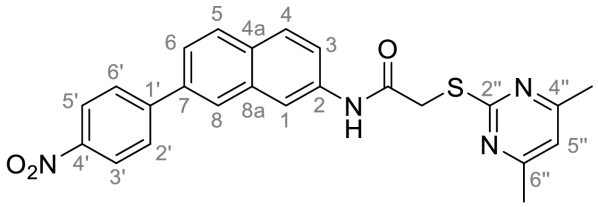

$C_{24}H_{20}N_4O_3S$

M_w = 444.51 g/mol

At room temperature potassium *tert*-butoxide (346 mg, 3.08 mmol, 2.00 eq) was added to a stirred solution of 2-bromoacetamide **9** (594 mg, 1.54 mmol, 1.00 eq) and 4,6-dimethylpyrimidine-2-thiol (260 mg, 1.85 mmol, 1.20 eq) in anhydrous DMF (10 mL). After 3 h, water (150 mL) and brine (100 mL) were added, and the reaction mixture was extracted with EtOAc (4 x 100 mL). The combined organic layers were dried over sodium sulfate. The combined organic layers were dried over sodium sulfate. After evaporating the solvent *in vacuo*, the crude product was purified *via* flash column chromatography (hexanes/EtOAc 6:4) to yield the title compound as a yellow orange solid (684 mg, 1.78 mmol, 89%).

R_f: 0.18 (hexanes/EtOAc 6:4).
m.p.: 185 °C.

^{1}H NMR (500 MHz, DMSO-d_6) δ [ppm] = 10.53 (s, 1H, NHCO), 8.42 (d, *J* = 2.2 Hz, 1H, 1-H), 8.37 – 8.30 (m, 2H, 3'-H, 5'-H), 8.29 (d, *J* = 1.9 Hz, 1H, 8-H), 8.15 – 8.10 (m, 2H, 2'-H, 6'-H), 7.99 (d, *J* = 8.5 Hz, 1H, 5-H), 7.94 (d, *J* = 8.8 Hz, 1H, 4-H), 7.82 (dd, *J* = 8.5, 1.9 Hz, 1H, 6-H), 7.67 (dd, *J* = 8.8, 2.1 Hz, 1H, 3-H), 6.96 (s, 1H, 5''-H), 4.12 (s, 2H, CH_2), 2.33 (s, 6H, 4''-CH_3, 6''-CH_3).

^{13}C NMR (126 MHz, DMSO-d_6) δ [ppm] = 169.3 (C-2''), 166.98 (C-4'', C-6''), 166.94 (NHCO), 146.7 (C-4'), 146.5 (C-1'), 137.3 (C-2), 135.6 (C-7), 133.6 (C-8a), 129.6 (C-4a), 128.6 (C-5), 128.3 (C-4), 128.1 (C-2', C-6'), 126.2 (C-8), 124.1 (C-3', C-5'), 123.5 C-6), 120.9 (C-3), 116.1 (C-5''), 115.8 (C-1), 35.6 (CH_2), 23.3 (4''-CH_3, 6''-CH_3).

IR (ATR) $\tilde{\nu}$ [cm^{-1}] = 3240, 3078, 1667, 1584, 1560, 1512, 1428, 1393, 1344, 1315, 1268, 1221, 1175, 1152, 1107, 904, 884, 847, 752, 696.

HRMS (ESI): *m/z* = $[M+H]^+$ calculated for $C_{24}H_{21}N_4O_3S^+$: 445.1329; found: 445.1329.

Purity (HPLC): > 99% (210 nm), > 99% (254 nm), (method 1a).

***N*-(7-(4-Aminophenyl)naphthalen-2-yl)-2-((4,6-dimethylpyrimidin-2-yl)thio)acetamide (5)**

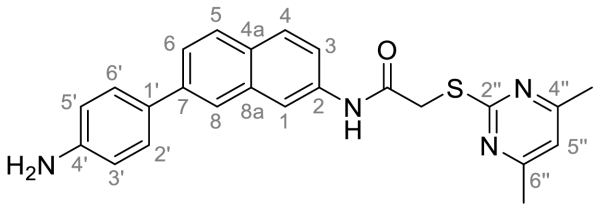

$C_{24}H_{22}N_4OS$

M_w = 414.53 g/mol

Under nitrogen atmosphere nitro compound **6** (0.533 g, 1.20 mmol, 1.00 eq) was suspended in acetic acid (5 mL) and iron powder (2.34 g, 42.0 mmol, 35.0 eq) was added. After the reaction mixture was stirred at 50 °C for 3 h, it was filtered and then diluted with water (50 mL) and brine (100 mL). The mixture was extracted with EtOAc (4 x 50 mL) and the combined organic layers were dried over sodium sulfate. After evaporating the solvent *in vacuo*, the crude product was purified *via* flash column chromatography (hexanes/EtOAc 1:1) to yield the title compound as a yellow solid (397 mg, 0.957 mmol, 80%).

R_f: 0.10 (hexanes/EtOAc 1:1).
m.p.: 202 °C.

^{1}H NMR (500 MHz, DMSO-d_6) δ [ppm] = 10.42 (s, 1H, NHCO), 8.25 (d, *J* = 2.0 Hz, 1H, 1-H), 7.91 (d, *J* = 1.9 Hz, 1H, 8-H), 7.84 – 7.79 (m, 2H, 4-H, 5-H), 7.64 (dd, *J* = 8.6, 1.8 Hz, 1H, 6-H), 7.53 (dd, *J* = 8.7, 2.1 Hz, 1H, 3-H), 7.52 – 7.49 (m, 2H, 2'-H, 6'-H), 6.97 (s, 1H, 5''-H), 6.70 – 6.64 (m, 2H, 3'-H, 5'-H), 5.27 (s, 2H, NH_2), 4.10 (s, 2H, CH_2), 2.34 (s, 6H, 4''-CH_3, 6''-CH_3).

^{13}C NMR (126 MHz, DMSO-d_6) δ [ppm] = 169.4 (C-2''), 167.0 (C-4'', C-6''), 166.8 (NHCO), 148.6 (C-4'), 138.5 (C-7), 136.8 (C-2), 134.0 (C-8a), 128.2 (C-4a), 128.0 (C-4), 127.8 (C-5), 127.5 (C-2', C-6'), 127.0 (C-1'), 123.3 (C-6), 122.4 (C-8), 119.1 (C-3), 116.1 (C-5''), 115.3 (C-1), 114.3(C-3', C-5'), 35.6 (CH_2), 23.3 (4''-CH_3, 6''-CH_3).

IR (ATR) $\tilde{\nu}$ [cm^{-1}] = 3439, 3355, 3248, 2968, 2911, 1660, 1618, 1606, 1577, 1532, 1506, 1338, 1264, 1248, 1228, 1190, 1168, 984, 952, 896, 851, 828, 802, 728, 706.

HRMS (ESI): *m/z* = $[M-H]^-$ calculated for $C_{24}H_{21}N_4OS^-$: 413.1442; found: 413.1442.

Purity (HPLC): > 99% (210 nm), > 99% (254 nm), (method 1a).

N-(7-(4-Acetamidophenyl)naphthalen-2-yl)-2-((4,6-dimethylpyrimidin-2-yl)thio)acetamide (FM29)

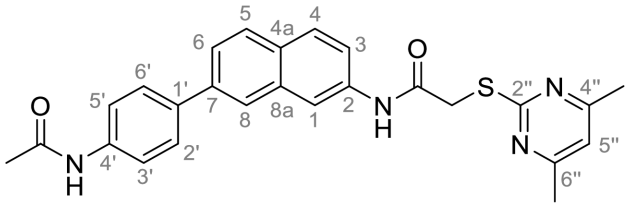

$C_{26}H_{24}N_4O_4S$

M_w = 446.57 g/mol

At room temperature acetic anhydride (9.03 µL, 0.0955 mmol, 2.00 eq) was added dropwise to a stirred solution of amine **5** (19.8 mg, 0.0478 mmol, 1.00 eq) and NEt_3 (13.3 µL, 0.0955 mmol, 2.00 eq) in anhydrous DCM (5 mL). After 2 h, water (25 mL) and brine (25 mL) were added, and the reaction mixture was extracted with EtOAc (3 x 25 mL). The combined organic layers were dried over sodium sulfate. After evaporating the solvent *in vacuo*, the crude product was purified *via* flash column chromatography (hexanes/EtOAc 2:8) to yield the title compound as a white solid (15.6 mg, 0.0342 mmol, 72%).

R_f: 0.23 (hexanes/EtOAc 2:8).
m.p.: 194 °C.

^{1}H NMR (500 MHz, DMSO-d_6) δ [ppm] = 10.46 (s, 1H, 2'-NHCO), 10.05 (s, 1H, 4'-NHCO), 8.32 (d, *J* = 2.0 Hz, 1H, 8-H), 8.06 (d, *J* = 1.8 Hz, 1H, 1-H), 7.89 (d, *J* = 8.6 Hz, 1H, 5-H), 7.87 (d, *J* = 8.8 Hz, 1H, 4-H), 7.80 – 7.73 (m, 2H, 2'-H, 6'-H), 7.73 – 7.68 (m, 3H. 3-H, 3'-H, 5'-H), 7.59 (dd, *J* = 8.8, 2.1 Hz, 1H, 6-H), 6.97 (s, 1H, 5''-H), 4.11 (s, 2H, CH_2), 2.33 (s, 6H, 4''-CH_3, 6''-CH_3), 2.08 (s, 3H, CH_3).

^{13}C NMR (126 MHz, DMSO-d_6) δ [ppm] = 169.4 (C-2''), 168.4 (4'-NHCO), 167.0 (C-4'', C-6''), 166.8 (2''-NHCO), 138.9 (C-4'), 137.5 (C-7), 137.0 (C-2), 134.4 (C-1'), 133.8 (C-8a), 128.8 (C-4a), 128.2 (C-4), 128.1 (C-5), 127.2 (C-2', C-6'), 124.0 (C-8), 123.5 (C-6), 119.8 (C-3), 119.3 (C-3', C-5'), 116.1 (C-5''), 115.5 (C-1), 35.6 (CH_2), 24.1 (CH_3), 23.3 (4''-CH_3, 6''-CH_3).

IR (ATR) $\tilde{\nu}$ [cm^{-1}] = 3250, 3050, 2926, 1658, 1578, 1521, 1504, 1424, 1400, 1369, 1337, 1316, 1291, 1266, 1239, 1224, 1180, 1164, 1015, 984, 956, 892, 836, 826, 804, 713.

HRMS (ESI): *m/z* = $[M-H]^-$ calculated for $C_{26}H_{23}N_4O_2S^-$: 445.1547; found: 445.1546.

Purity (HPLC): ≥ 98% (210 nm), ≥ 98% (254 nm), (method 1a).

N-(4-(7-(2-((4,6-Dimethylpyrimidin-2-yl)thio)acetamido)naphthalen-2-yl)phenyl)thiophene-2-carboxamide (FM50)

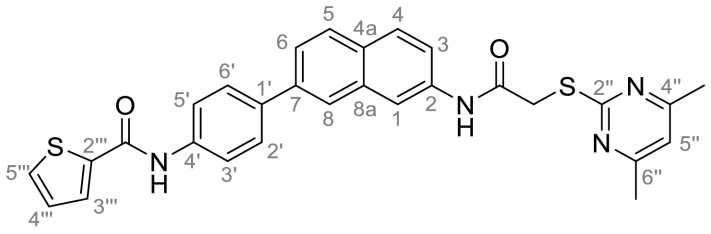

$C_{29}H_{24}N_4O_2S_2$

M_w = 524.67 g/mol

At room temperature 2-thiophenecarbonyl chloride (17.6 µL, 0.165 mmol, 2.00 eq) was added dropwise to a stirred solution of amine **5** (34.1 mg, 0.0823 mmol, 1.00 eq) and NEt_3 (22.9 µL, 0.165 mmol, 2.00 eq) in anhydrous DCM (5 mL). After 2 h, water (25 mL) and brine (25 mL) were added, and the reaction mixture was extracted with EtOAc (3 x 25 mL). The combined organic layers were dried over sodium sulfate. After evaporating the solvent *in vacuo*, the crude product was purified *via* flash column chromatography (hexanes/EtOAc 1:1) to yield the title compound as a white solid (53.3 mg, 0.0438 mmol, 53%).

R_f: 0.25 (hexanes/EtOAc 1:1).
m.p.: 195-198 °C.

^{1}H NMR (500 MHz, DMSO-d_6) δ [ppm] = 10.47 (s, 1H, 2-NHCO), 10.34 (s, 1H, 4'-NHCO), 8.33 (d, *J* = 2.0 Hz, 1H, 1-H), 8.11 (d, *J* = 1.9 Hz, 1H, 8-H), 8.06 (dd, *J* = 3.8, 1.2 Hz, 1H, 3'''-H), 7.91 (d, *J* = 8.6 Hz, 1H, 5-H), 7.90 – 7.85 (m, 4H, 4-H, 3'-H, 5'-H, 5'''-H), 7.84 (d, *J* = 8.9 Hz, 2H, 2'-H, 6'-H), 7.76 (dd, *J* = 8.5, 1.8 Hz, 1H, 6-H), 7.61 (dd, *J* = 8.8, 2.1 Hz, 1H, 3-H), 7.25 (dd, *J* = 5.0, 3.7 Hz, 1H, 4'''-H), 6.97 (s, 1H, 5''-H), 4.12 (s, 2H, CH_2), 2.34 (s, 6H, 4''-CH_3, 6''-CH_3).

^{13}C NMR (126 MHz, DMSO-d_6) δ [ppm] = 169.4 (C-2''), 167.0 (C-4'', C-6''), 166.8 (2-NHCO), 159.9 (4'-NHCO), 140.0 (C-2'''), 138.4 (C-4'), 137.4 (C-7), 137.0 (C-2), 135.1 (C-1'), 133.9 (C-8a), 132.0 (C-5'''), 129.2 (C-3'''), 128.9 (C-4a), 128.2 (C-5), 128.14 (C-4), 128.11 (C-4'''), 127.2

(C-2', C-6'), 124.1 (C-8), 123.5 (C-6), 120.6 (C-3', C-5'), 119.9 (C-3), 116.1 (C-5''), 115.5 (C-1), 35.6 (CH_2), 23.3 (4''-CH_3, 6''-CH_3).

IR (ATR) $\tilde{\nu}$ [cm^{-1}] = 3509, 3242, 1665, 1632, 1584, 1529, 1507, 1424, 1355, 1339, 1264, 1250, 1229, 1191, 984, 952, 901, 865, 834, 801, 732, 718.

HRMS (ESI): *m/z* = $[M+H]^+$ calculated for $C_{29}H_{25}N_4O_2S_2^+$: 525.1413; found: 525.1408.

Purity (HPLC): ≥ 98% (210 nm), ≥ 98% (254 nm), (method 1a).

N-(4-(7-(2-((4,6-Dimethylpyrimidin-2-yl)thio)acetamido)naphthalen-2-yl)phenyl)benzamide (FM53)

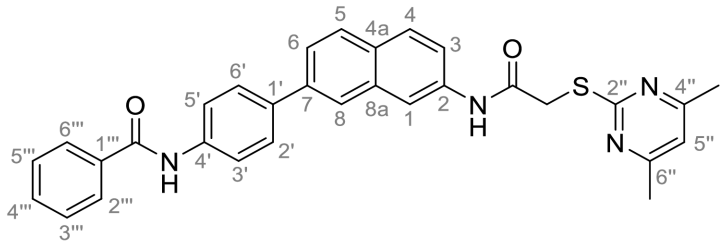

$C_{31}H_{26}N_4O_2S$

M_w = 518.64 g/mol

At room temperature benzoyl chloride (36.7 µL, 0.316 mmol, 2.00 eq) was added dropwise to a stirred solution of amine **5** (65.5 mg, 0.158 mmol, 1.00 eq) and NEt_3 (44.0 µL, 0.316 mmol, 2.00 eq) in anhydrous DCM (5 mL). After 2 h, water (25 mL) and brine (25 mL) were added, and the reaction mixture was extracted with EtOAc (3 x 25 mL). The combined organic layers were dried over sodium sulfate. After evaporating the solvent *in vacuo*, the crude product was purified *via* flash column chromatography (DCM/MeOH 100:2) to yield the title compound as a white solid (64.1 mg, 0.124 mmol, 78%).

R_f: 0.24 (DCM/MeOH 100:2).
m.p.: 207 °C.

^{1}H NMR (500 MHz, DMSO-d_6) δ [ppm] = 10.47 (s, 1H, 2-NHCO), 10.37 (s, 1H, 4'-NHCO), 8.34 (d, *J* = 2.0 Hz, 1H, 1-H), 8.11 (d, *J* = 1.9 Hz, 1H, 8-H), 8.01 – 7.97 (m, 2H, 2'''-H, 6'''-H), 7.96 – 7.90 (m, 3H, 5-H, 3'-H, 5'-H), 7.88 (d, *J* = 8.9 Hz, 1H, 4-H), 7.85 – 7.82 (m, 2H, 2'-H, 6'-H), 7.76 (dd, *J* = 8.5, 1.9 Hz, 1H, 6-H), 7.63 – 7.59 (m, 2H, 3-H, 4'''-H), 7.57 – 7.53 (m, 2H, 3'''-H, 5'''-H), 6.97 (s, 1H, 5''-H), 4.12 (s, 2H, CH_2), 2.34 (s, 6H, 4''-CH_3, 6''-CH_3).

^{13}C NMR (126 MHz, DMSO-d_6) δ [ppm] = 169.4 (C-2''), 167.0 (C-4'', C-6''), 166.8 (2-NHCO), 165.6 (4'-NHCO), 138.8 (C-4'), 137.5 (C-7), 137.0 (C-2), 135.0 (C-1'), 134.9 (C-1'''), 133.9 (C-8a), 131.6 (C-4'''), 128.8 (C-4a), 128.4 (C-3''', C-5'''), 128.2 (C-4), 128.1 (C-5), 127.7 (C-2''', C-6'''), 127.1 (C-2', C-6'), 124.1 (C-8), 123.6 (C-6), 120.6 (C-3', C-5'), 119.8 (C-3), 116.1 (C-5''), 115.5 (C-1), 35.6 (CH_2), 23.3 (4''-CH_3, 6''-CH_3).

IR (ATR) $\tilde{\nu}$ [cm^{-1}] = 3283, 3038, 1680, 1645, 1581, 1521, 1504, 1426, 1323, 1263, 892, 823, 795, 688.

HRMS (ESI): *m/z* = [M-H]$^-$ calculated for $C_{31}H_{25}N_4O_2S^-$: 517.1704; found: 517.1701.

Purity (HPLC): > 99% (210 nm), > 99% (254 nm), (method 1a).

2-((4,6-Dimethylpyrimidin-2-yl)thio)-*N*-(7-(4-(phenylsulfonamido)phenyl)naphthalen-2-yl)acetamide (FM56)

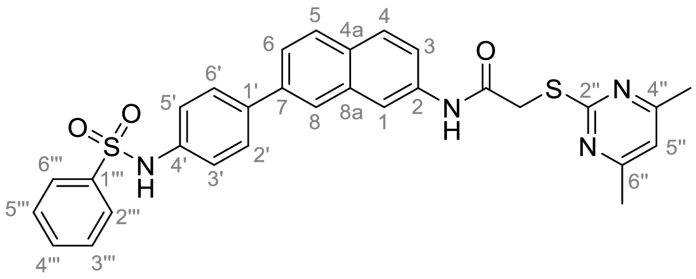

$C_{30}H_{26}N_4O_3S_2$

M_w = 554.69 g/mol

At room temperature benzenesulfonyl chloride (19.9 µL, 0.156 mmol, 0.95 eq) was added dropwise to a stirred solution of amine **5** (67.9 mg, 0.164 mmol, 1.00 eq) and NEt_3 (21.7 µL, 0.156 mmol, 0.95 eq) in anhydrous DCM (5 mL). After heating to reflux for 7h, water (25 mL) and brine (25 mL) were added, and the reaction mixture was extracted with DCM (3 x 25 mL). The combined organic layers were dried over sodium sulfate. After evaporating the solvent *in vacuo*, the crude product was purified *via* flash column chromatography (DCM/MeOH 120:1) to yield the title compound as a white solid (39.5 mg, 0.0617 mmol, 40%).

R_f: 0.04 (DCM/MeOH 120:1).
m.p.: 135 °C (decomposition).

^{1}H NMR (500 MHz, DMSO-d_6) δ [ppm] = 10.45 (s, 2H, NHCO, $NHSO_2$), 8.29 (d, *J* = 2.0 Hz, 1H, 1-H), 8.00 (d, *J* = 1.8 Hz, 1H, 8-H), 7.87 (d, *J* = 6.0 Hz, 1H, 5-H), 7.85 (d, *J* = 6.2 Hz, 1H, 4-H), 7.83 – 7.80 (m, 2H, 2'''-H, 6'''-H), 7.71 – 7.68 (m, 2H, 2'-H, 6'-H), 7.65 (dd, *J* = 8.6, 1.9 Hz, 1H, 6-H), 7.63 – 7.55 (m, 4H, 3-H, 3'''-H, 4'''-H, 5'''-H), 7.24 – 7.19 (m, 2H, 3'-H, 5'-H), 6.97 (s, 1H, 5''-H), 4.10 (s, 2H, CH_2), 2.33 (s, 6H, 4''-CH_3, 6''-CH_3).

^{13}C NMR (126 MHz, DMSO-d_6) δ [ppm] = 169.3 (C-2''), 167.0 (C-4'', C-6''), 166.8 (NHCO), 139.6 (C-1'''), 137.2 (C-4'), 137.1 (C-7), 137.0 (C-2), 135.5 (C-1'), 133.7 (C-8a), 133.0 (C-4'''), 129.4 (C-3''', C-5'''), 128.8 (C-4a), 128.14 (C-5), 128.11 (C-4), 127.7 (C-2', C-6'), 126.6 (C-2''', C-6'''), 124.2 (C-8), 123.5 (C-6), 120.2 (C-3', C-5'), 119.9 (C-3), 116.1 (C-5''), 115.4 (C-1), 35.6 (CH_2), 23.3 (4''-CH_3, 6''-CH_3).

IR (ATR) $\tilde{\nu}$ [cm^{-1}] = 3056, 2923, 2854, 1668, 1583, 1532, 1502, 1329, 1265, 1158, 1091, 902, 830, 720, 687.

HRMS (ESI): *m/z* = $[M-H]^-$ calculated for $C_{30}H_{25}N_4O_3S_2^-$: 553.1374; found: 553.1373.

Purity (HPLC): > 99% (210 nm), > 99% (254 nm), (method 1a).

N-(4-(7-(2-((4,6-Dimethylpyrimidin-2-yl)thio)acetamido)naphthalen-2-yl)phenyl)-5-methylthiophene-2-carboxamide (FM69)

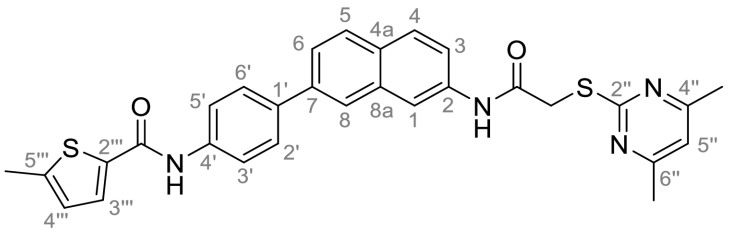

$C_{30}H_{26}N_4O_2S_2$

M_w = 538.69 g/mol

At room temperature previously prepared 5-methylthiophene-2-carbonyl chloride (24.5 µL, 0.201 mmol, 2.00 eq) was added dropwise to a stirred solution of amine **5** (41.7 mg, 0.101 mmol, 1.00 eq) and NEt_3 (28.0 µL, 0.201 mmol, 2.00 eq) in anhydrous DCM (5 mL). After heating to reflux for 3 h, water (25 mL) and brine (25 mL) were added, and the reaction mixture was extracted with DCM (3 x 25 mL). The combined organic layers were dried over sodium sulfate. After evaporating the solvent *in vacuo*, the crude product was purified *via* flash column

chromatography (DCM/MeOH 120:1) to yield the title compound as a white solid (40.2 mg, 0.0746 mmol, 74%).

R_f: 0.07 (DCM/MeOH 120:1)
m.p.: 191-193 °C.

^{1}H NMR (500 MHz, DMSO-d_6) δ [ppm] = 10.47 (s, 1H, 2-NHCO), 10.22 (s, 1H, 4'-NHCO), 8.33 (d, *J* = 2.0 Hz, 1H, 1-H), 8.10 (d, *J* = 1.8 Hz, 1H, 8-H), 7.91 (d, *J* = 8.6 Hz, 1H, 5-H), 7.89 – 7.79 (m, 6H, 4-H, 2'-H, 3'-H, 5'-H, 6'-H, 3'''-H), 7.75 (dd, *J* = 8.5, 1.8 Hz, 1H, 6-H), 7.60 (dd, *J* = 8.8, 2.1 Hz, 1H, 3-H), 6.97 (s, 1H, 5''-H), 6.95 – 6.93 (m, 1H, 4'''-H), 4.11 (s, 2H, CH_2), 2.51 (s, 3H, CH_3), 2.34 (s, 6H, 4''-CH_3, 6''-CH_3).

^{13}C NMR (126 MHz, DMSO-d_6) δ [ppm] = 169.4 (C-2''), 167.0 (C-4'', C-6''), 166.8 (2-NHCO), 159.8 (4'-NHCO), 146.0 (C-5'''), 138.5 (C-4'), 137.43 (C-7, C-2'''), 137.0 (C-2), 134.9 (C-1'), 133.9 (C-8a), 129.5 (C-3'''), 128.8 (C-4a), 128.2 (C-5), 128.1 (C-4) 127.1 (C-2', C-6'), 126.7 (C-4'''), 124.1 (C-8), 123.5 (C-6), 120.5 (C-3', C-5'), 119.8 (C-3), 116.1 (C-5''), 115.5 (C-1), 35.6 (CH_2), 23.3 (4''-CH_3, 6''-CH_3), 15.3 (CH_3).

IR (ATR) $\tilde{\nu}$ [cm^{-1}] = 3446, 3241, 2914, 1663, 1613, 1583, 1526, 1505, 1458, 1398, 1338, 1320, 1264, 1249, 1228, 1190, 1170, 1093, 984, 952, 901, 873, 832, 802, 741.

HRMS (EI): *m/z* = $[M]^{\bullet+}$ calculated for $C_{30}H_{26}N_4O_2S_2^{\bullet+}$: 538.1492; found: 538.1494.

Purity (HPLC): > 98% (210 nm), > 98% (254 nm), (method 1a).

6-(3-Nitrophenyl)benzo[d]thiazol-2-amine (15)

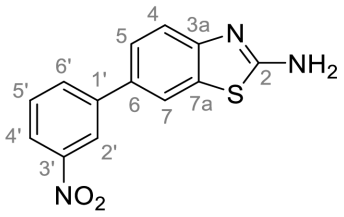

$C_{13}H_9N_3O_2S$
M_w = 271.30 g/mol

2-Amino-6-bromobenzothiazole (**14**, 1.86 g, 8.14 mmol, 1.00 eq and $Pd(PPh_3)_4$ (0.941 g, 0.814 mmol, 0.100 eq) were weighed out into a flask, which was put under nitrogen afterwards. Degassed 1-4 dioxane (40 mL) was added *via* syringe and the mixture was stirred for 10 min

at room temperature before 3-nitrophenyl boronic acid (1.63 g, 9.77 mmol, 1.20 eq), Cs_2CO_3 (13.3 g, 40.7 mmol, 5.00 eq) and degassed water (17.5 mL) was added under nitrogen atmosphere. The reaction mixture was stirred for 21 h at 80 °C, cooled to room temperature, diluted with water (200 mL) and extracted with EtOAc (4 x 100 mL). The combined organic layers were dried over sodium sulfate. After evaporating the solvent *in vacuo*, the crude product was purified *via* flash column chromatography (hexanes/EtOAc 7:3) to yield the title compound as an orange solid (1.35 g, 4.97 mmol, 61%).

R_f: 0.05 (hexanes/EtOAc 7:3).
m.p.: 218-219 °C (decomposition).

^{1}H NMR (500 MHz, $CDCl_3$) δ [ppm] = 8.46 (t, *J* = 2.1 Hz, 1H, 2'-H), 8.18 (ddd, *J* = 8.2, 2.3, 1.0 Hz, 1H, 4'-H), 7.92 (ddd, *J* = 7.7, 1.9, 1.0 Hz, 1H, 6'-H), 7.87 (d, *J* = 2.1 Hz, 1H, 7-H), 7.67 – 7.56 (m, 3H, 4-H, 5-H, 5'-H), 5.30 (s, 2H, NH_2).

^{13}C NMR (126 MHz, DMSO-d_6) δ [ppm] = 166.5 (C-2), 152.6 (C-3a), 148.9 (C-3'), 142.8 (C-1'), 133.3 (C-6), 133.1 (C-7a), 133.0 (C-6'), 129.9 (C-5'), 125.5 (C-5), 121.9 (C-2'), 121.9 (C-4'), 119.9 (C-4), 119.7 (C-7).

IR (ATR) $\tilde{\nu}$ [cm^{-1}] = 3422, 3290, 3066, 1638, 1599, 1530, 1512, 1486, 1456, 1345, 1304, 1275, 1094, 1064, 906, 876, 862, 801, 742, 728, 714, 685, 674.

HRMS (EI): *m/z* = $[M]^{\bullet+}$ calculated for $C_{13}H_9N_3O_2S^{\bullet+}$: 271.0410; found: 271.0411.

Purity (HPLC): > 99% (210 nm), > 99% (254 nm), (method 1b).

2-Bromo-*N*-(6-(3-nitrophenyl)benzo[d]thiazol-2-yl)acetamide (18)

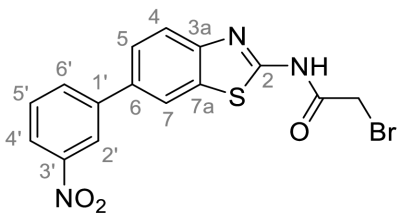

$C_{15}H_{10}BrN_3O_3S$
M_w = 392.23 g/mol

At 0 °C bromoacetyl bromide (851 µL, 9.77 mmol, 1.20, eq) was added dropwise to a stirred suspension of amine **15** (2.21 g, 8.14 mmol, 1.00 eq) and NEt_3 (1.36 mL, 9.77 mmol, 1.20 eq)

in anhydrous DCM/DMF (6:1, 35 mL). After heating to reflux for 3 h, water (150 mL) and brine (50 mL) were added, and the reaction mixture was extracted with EtOAc (4 x 100 mL). The combined organic layers were dried over sodium sulfate. After evaporating the solvent *in vacuo*, the crude product was purified *via* flash column chromatography (hexanes/EtOAc 8:2) to yield the title compound as a light yellow solid (827 mg, 2.11 mmol, 26%).

R_f: 0.07 (hexanes/EtOAc 8:2).
m.p.: 186 °C.

^{1}H NMR (500 MHz, DMSO-d_6) δ [ppm] = 9.74 (s, 1H, NHCO), 8.51 (t, *J* = 2.0 Hz, 1H, 2'-H), 8.23 (ddd, *J* = 8.2, 2.2, 1.0 Hz, 1H, 4'-H), 8.09 (dd, *J* = 1.9, 0.6 Hz, 1H, 7-H), 7.97 (ddd, *J* = 7.7, 1.8, 1.0 Hz, 1H, 6'-H), 7.92 (dd, *J* = 8.4, 0.6 Hz, 1H, 4-H), 7.73 (dd, *J* = 8.5, 1.9 Hz, 1H, 5-H), 7.65 (t, *J* = 8.0 Hz, 1H, 5'-H), 4.15 (s, 2H, CH_2).

^{13}C NMR (126 MHz, DMSO-d_6) δ [ppm] = 164.2 (NHCO), 157.9 (C-2), 149.0 (C-3'), 148.7 (C-3a), 142.5 (C-1'), 135.4 (C-6), 133.6 (C-7a), 133.3 (C-6'), 130.1 (C-5'), 126.1 (C-5), 122.3 (C-4'), 122.3 (C-2'), 122.1 (C-4), 120.3 (C-7), 27.9 (CH_2).

IR (ATR) $\tilde{\nu}$ [cm^{-1}] = 2968, 1653, 1610, 1574, 1548, 1530, 1452, 1342, 1320, 1281, 1111, 1000, 874, 863, 825, 799, 770, 746, 730, 718, 679.

HRMS (EI): *m/z* = $[M]^{\bullet+}$ calculated for $C_{15}H_{10}{}^{79}BrN_3O_3S^{\bullet+}$: 390.9621; found: 390.9615.

Purity (HPLC): > 99% (210 nm), > 99% (254 nm), (method 1a).

2-((4,6-Dimethylpyrimidin-2-yl)thio)-*N*-(6-(3-nitrophenyl)benzo[d]thiazol-2-yl)acetamide (20)

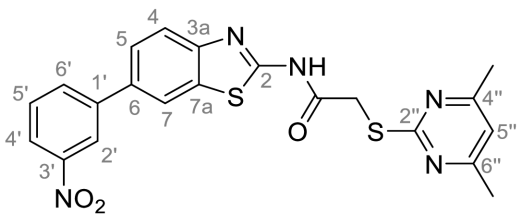

$C_{21}H_{17}N_5O_3S_2$
M_w = 451.53 g/mol

At room temperature potassium *tert*-butoxide (236 mg, 2.10 mmol, 2.00 eq) was added to a stirred solution of 2-bromoacetamide **18** (413 mg, 1.05 mmol, 1.00 eq) and 4,6-

dimethylpyrimidine-2-thiol (177 mg, 1.26 mmol, 1.20 eq) in anhydrous DMF (5 mL). After 3 h, water (50 mL) and brine (100 mL) were added, and the reaction mixture was extracted with EtOAc (3 x 100 mL). The combined organic layers were dried over sodium sulfate. The combined organic layers were dried over sodium sulfate. After evaporating the solvent *in vacuo*, the crude product was purified *via* flash column chromatography (hexanes/EtOAc 7:3) to yield the title compound as a yellow solid (319 mg, 0.707 mmol, 67%).

R_f: 0.09 (hexanes/EtOAc 7:3).
m.p.: 205 °C.

^{1}H NMR (400 MHz, DMSO-d_6) δ [ppm] = 12.75 (s, 1H, NHCO), 8.51 (t, *J* = 2.1 Hz, 1H, 2'-H), 8.49 – 8.44 (m, 1H, 7-H), 8.24 – 8.19 (m, 2H, 4'-H, 6'-H), 7.90 – 7.85 (m, 2H, 4-H, 5-H), 7.78 (t, *J* = 8.0 Hz, 1H, 5'-H), 6.97 (s, 1H, 5''-H), 4.20 (s, 2H, CH_2), 2.29 (s, 6H, 4''-CH_3, 6''-CH_3).

^{13}C NMR (101 MHz, DMSO-d_6) δ [ppm] = 168.8 (NHCO), 168.3 (C-2''), 167.1 (C-4'', C-6''), 159.1 (C-2), 148.9 (C-3a), 148.5 (C-3'), 141.6 (C-1'), 133.3 (C-6'), 133.2 (C-6), 132.6 (C-7a), 130.5 (C-5'), 125.4 (C-5), 121.9 (C-4'), 121.1 (C-2'), 121.0 (C-4), 120.5 (C-7), 116.2 (C-5''), 34.5 (CH_2), 23.2 (4''-CH_3, 6''-CH_3).

IR (ATR) $\tilde{\nu}$ [cm^{-1}] = 2985, 1694, 1666, 1608, 1564, 1526, 1452, 1342, 1304, 1262, 1156, 893, 864, 800, 745, 730, 716, 676.

HRMS (EI): *m/z* = $[M]^{\bullet+}$ calculated for $C_{21}H_{17}N_5O_3S_2^{\bullet+}$: 451.0767; found: 451.0762.

Purity (HPLC): > 99% (210 nm), > 99% (254 nm), (method 1a).

_N_-(6-(3-Aminophenyl)benzo[d]thiazol-2-yl)-2-((4,6-dimethylpyrimidin-2-yl)thio)acetamide (22)

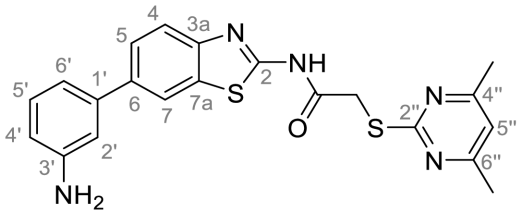

$C_{21}H_{19}N_5OS_2$

M_w = 421.55 g/mol

Under nitrogen atmosphere nitro compound **20** (317 mg, 0.808 mmol, 1.00 eq) was suspended in MeOH/water (10:1, 2.2 mL) and iron powder (266 mg, 4.04 mmol, 5.00 eq) and ammonium chloride (216 mg, 4.04 mmol, 5.00 eq) was added. The reaction mixture was heated to reflux for 3 h and after cooling it was diluted with water (100 mL). Subsequently the mixture was extracted with EtOAc (4 x 50 mL) and the combined organic layers were dried over sodium sulfate. After evaporating the solvent *in vacuo*, the crude product was purified *via* flash column chromatography (hexanes/EtOAc 1:1) to yield the title compound as a light yellow solid (251 mg, 0.596 mmol, 74%).

R_f: 0.12 (hexanes/EtOAc 1:1).
m.p.: 118-122 °C.

^{1}H NMR (400 MHz, DMSO-d_6) δ [ppm] = 12.65 (s, 1H, NHCO), 8.14 (d, *J* = 1.8 Hz, 1H, 7-H), 7.79 (d, *J* = 8.4 Hz, 1H, 4-H), 7.62 (dd, *J* = 8.5, 1.9 Hz, 1H, 5-H), 7.10 (t, *J* = 7.8 Hz, 1H, 5'-H), 6.96 (s, 1H, 5''-H), 6.88 (t, *J* = 2.0 Hz, 1H, 2'-H), 6.82 (ddd, *J* = 7.6, 1.8, 1.0 Hz, 1H, 6'-H), 6.56 (ddd, *J* = 7.9, 2.2, 1.0 Hz, 1H, 4'-H), 5.15 (s, 2H, NH_2), 4.19 (s, 2H, CH_2), 2.29 (s, 6H, 4''-CH_3, 6''-CH_3).

^{13}C NMR (101 MHz, DMSO-d_6) δ [ppm] = 168.8 (NHCO), 168.1 (C-2''), 167.0 (C-4'', C-6''), 158.1 (C-2), 149.1 (C-3'), 147.9 (C-3a), 140.7 (C-1'), 136.8 (C-6), 132.3 (C-7a), 129.4 (C-5'), 125.0 (C-5), 120.6 (C-4), 119.4 (C-7), 116.1 (C-5''), 114.5 (C-6'), 113.0 (C-4'), 112.3 (C-2'), 34.5 (CH_2), 23.3 (4''-CH_3, 6''-CH_3).

IR (ATR) $\tilde{\nu}$ [cm^{-1}] = 2921, 1693, 1602, 1583, 1560, 1532, 1453, 1265, 1135, 864, 824, 782, 733, 694.

HRMS (EI): *m/z* = $[M]^{\bullet+}$ calculated for $C_{21}H_{19}N_5OS_2^{\bullet+}$: 421.1026; found: 421.1011.

Purity (HPLC): > 98% (210 nm), > 99% (254 nm), (method 1a).

N-(6-(3-Acetamidophenyl)benzo[d]thiazol-2-yl)-2-((4,6-dimethylpyrimidin-2-yl)thio)acetamide (FM94)

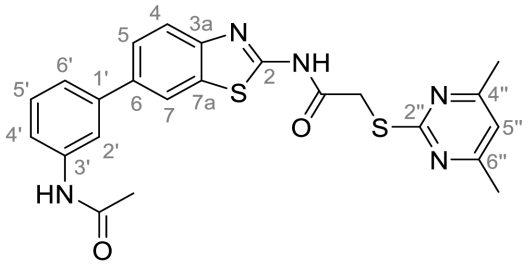

$C_{23}H_{21}N_5O_2S_2$

M_w = 463.58 g/mol

At room temperature acetic anhydride (22.3 µL, 0.237 mmol, 2.00 eq) was added dropwise to a stirred solution of amine **22** (50.0 mg, 0.119 mmol, 1.00 eq) and NEt_3 (33.1 µL, 0.237 mmol, 2.00 eq) in anhydrous DCM (2 mL). After 3 h, water (50 mL) was added, and the reaction mixture was extracted with DCM (4 x 50 mL). The combined organic layers were dried over sodium sulfate. After evaporating the solvent *in vacuo*, the crude product was purified *via* flash column chromatography (DCM/MeOH 100:1) to yield the title compound as a white solid (53.0 mg, 0.114 mmol, 96%).

R_f: 0.03 (DCM/MeOH 100:1).
m.p.: 162 °C (decomposition).

^{1}H NMR (500 MHz, DMSO-d_6) δ [ppm] = 12.68 (s, 1H, 2-NHCO), 10.03 (s, 1H, 3'-NHCO), 8.21 (d, *J* = 1.9 Hz, 1H, 7-H), 7.93 (t, *J* = 1.9 Hz, 1H, 2'-H), 7.83 (d, *J* = 8.4 Hz, 1H, 4-H), 7.66 (dd, *J* = 8.5, 1.9 Hz, 1H, 5-H), 7.56 (dt, *J* = 7.2, 2.1 Hz, 1H, 4'-H), 7.44 – 7.32 (m, 2H, 5'-H, 6'-H), 6.96 (s, 1H, 5''-H), 4.20 (s, 2H, CH_2), 2.29 (s, 6H, 4''-CH_3, 6''-CH_3), 2.07 (s, 3H, CH_3).

^{13}C NMR (126 MHz, DMSO-d_6) δ [ppm] = 168.8 (C-2''), 168.4 (3'-NHCO), 168.2 (2-NHCO), 167.1 (C-4'', C-6''), 162.3 (C-2'), 158.4 (C-2), 148.2 (C-3a), 140.5 (C-1'), 139.9 (C-3'), 135.9 (C-6), 132.4 (C-7a), 129.3 (C-5'), 125.1 (C-5), 121.6 (C-6'), 120.8 (C-4), 119.7 (C-7), 117.9 (C-4'), 117.4 (C-2'), 116.2 (C-5''), 34.5 (CH_2), 24.1 (CH_3), 23.3 (4''-CH_3, 6''-CH_3).

IR (ATR) $\tilde{\nu}$ [cm^{-1}] = 2922, 1694, 1605, 1583, 1537, 1456, 1428, 1314, 1263, 1146, 1033, 874, 824, 790, 696.

HRMS (EI): *m*/*z* = $[M]^{\bullet+}$ calculated for $C_{23}H_{21}N_5O_2S_2^{\bullet+}$: 463.1131; found: 463.1128.

Purity (HPLC): > 99% (210 nm), > 99% (254 nm), (method 1b).

N-(3-(2-(2-((4,6-Dimethylpyrimidin-2-yl)thio)acetamido)benzo[d]thiazol -6-yl)phenyl)thiophene-2-carboxamide (FM96)

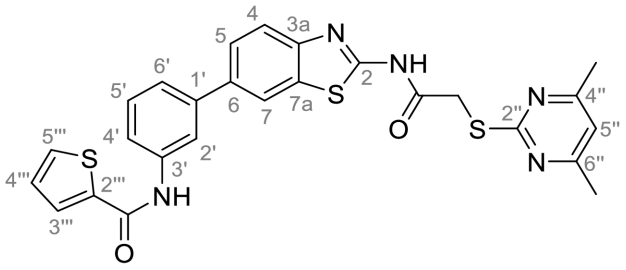

$C_{29}H_{24}N_4O_2S_2$

M_w = 531.68 g/mol

At room temperature 2-thiophenecarbonyl chloride (15.6 µL, 0.145 mmol, 1.10 eq) was added dropwise to a stirred solution of amine **22** (55.7 mg, 0.132 mmol, 1.00 eq) and NEt_3 (20.3 µL, 0.145 mmol, 1.10 eq) in anhydrous DCM (2 mL). After 1 h, water (50 mL) was added, and the reaction mixture was extracted with DCM (4 x 50 mL). The combined organic layers were dried over sodium sulfate. After evaporating the solvent *in vacuo*, the crude product was purified *via* flash column chromatography (hexanes/EtOAc 6:4) to yield the title compound as a white solid (57.0 mg, 0.107 mmol, 81%).

R_f: 0.25 (hexanes/EtOAc 6:4).
m.p.: 226 °C.

^{1}H NMR (400 MHz, DMSO-d_6) δ [ppm] = 12.70 (s, 1H, 2-NHCO), 10.32 (s, 1H, 3'-NHCO), 8.27 (d, *J* = 1.9 Hz, 1H, 7-H), 8.10 (s, 1H, 2'-H), 7.93 – 7.81 (m, 2H, 4-H, 5'''-H), 7.81 – 7.68 (m, 2H, 5-H, 6'-H), 7.51 – 7.42 (m, 2H, 4'-H, 5'-H), 7.25 (dd, *J* = 5.0, 3.7 Hz, 1H, 4'''-H), 6.97 (s, 1H, 5''-H), 4.20 (s, 2H, CH_2), 2.30 (s, 6H, 4''-CH_3, 6''-CH_3).

^{13}C NMR (126 MHz, DMSO-d_6) δ [ppm] = δ 168.8 (2-NHCO), 168.2 (C-2'''), 167.1 (C-4'', C-6''), 156.0 (3'-NHCO), 158.5 (C-2), 148.3 (C-3a), 140.4 (C-1'), 140.0 (C-2'''), 139.3 (C-3'),

135.7 (C-6), 132.5 (C-7a), 132.0 (C-5'''), 129.4 (C-5'), 129.2 (C-3'''), 128.1 (C-4'''), 125.1 (C-5), 122.2 (C-4'), 120.9 (C-4), 119.7 (C-7), 119.1 (C-6'), 118.8 (C-2'), 116.2 (C-5''), 34.5 (CH_2), 23.3 (4''-CH_3, 6''-CH_3).

IR (ATR) $\tilde{\nu}$ [cm^{-1}] = 2964, 1704, 1657, 1605, 1583, 1544, 1491, 1454, 1313, 1266, 1212, 1152, 875, 837, 792, 732, 696.

HRMS (EI): *m/z* = $[M]^{\bullet+}$ calculated for $C_{26}H_{21}N_5O_2S_3^{\bullet+}$: 531.0852; found: 531.0843.

Purity (HPLC): > 99% (210 nm), > 99% (254 nm), (method 1b).

N-(3-(2-(2-((4,6-Dimethylpyrimidin-2-yl)thio)acetamido)benzo[d]thiazol-6-yl)phenyl)benzamide (FM95)

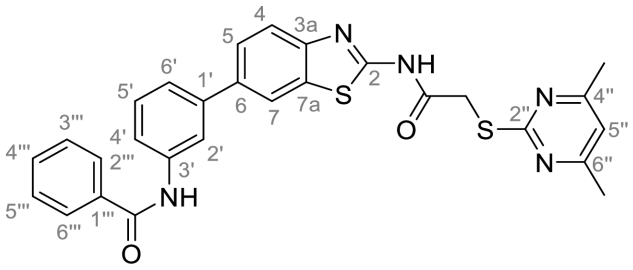

$C_{28}H_{23}N_5O_2S_2$

M_w = 525.66 g/mol

At room temperature benzoyl chloride (26.6 µL, 0.229 mmol, 2.00 eq) was added dropwise to a stirred solution of amine **22** (48.3 mg, 0.115 mmol, 1.00 eq) and NEt_3 (31.9 µL, 0.229 mmol, 2.00 eq) in anhydrous DCM (2 mL). After 3 h, water (50 mL) was added, and the reaction mixture was extracted with DCM (4 x 50 mL). The combined organic layers were dried over sodium sulfate. After evaporating the solvent *in vacuo*, the crude product was purified *via* flash column chromatography (DCM/MeOH 120:1) to yield the title compound as a white solid (39.7 mg, 0.0755 mmol, 66%).

R_f: 0.17 (DCM/MeOH 120:1).
m.p.: 262 °C.

^{1}H NMR (500 MHz, DMSO-d_6) δ [ppm] = 12.70 (s, 1H, 2-NHCO), 10.34 (s, 1H, 3'-NHCO), 8.27 (d, *J* = 1.8 Hz, 1H, 7-H), 8.17 (t, *J* = 1.5 Hz, 1H, 2'-H), 8.02 – 7.97 (m, 2H, 2'''-H, 6'''-H), 7.86 (d, *J* = 8.4 Hz, 1H, 4-H), 7.85 – 7.79 (m, 1H, 4'-H), 7.73 (dd, *J* = 8.5, 1.9 Hz, 1H, 5-H),

7.63 – 7.59 (m, 1H, 4'''-H), 7.58 – 7.53 (m, 2H, 3'''-H, 5'''-H), 7.49 – 7.44 (m, 2H, 5'-H, 6'-H), 6.96 (s, 1H, 5''-H), 4.20 (s, 2H, CH_2), 2.30 (s, 6H, 4''-CH_3, 6''-CH_3).

^{13}C NMR (126 MHz, DMSO-d_6) δ [ppm] = 168.8 (C-2''), 168.2 (2-NHCO), 167.1 (C-4'', C-6''), 165.6 (3'-NHCO), 158.4 (C-2), 148.2 (C-3a), 140.4 (C-1'), 139.8 (C-3'), 135.8 (C-6), 134.9 (C-1'''), 132.5 (C-7a), 131.6 (C-4'''), 129.3 (C-5'), 128.4 (C-3''', C-5'''), 127.7 (C-2''', C-6'''), 125.1 (C-5), 122.1 (C-6'), 120.9 (C-4), 119.7 (C-7), 119.1 (C-4'), 118.7 (C-2'), 116.2 (C-5'), 34.5 (CH_2), 23.3 (4''-CH_3, 6''-CH_3).

IR (ATR) $\tilde{\nu}$ [cm^{-1}] = 3295, 2956, 1718, 1647, 1582, 1526, 1464, 1432, 1389, 1368, 1307, 1264, 1152, 884, 876, 884, 892, 762, 706, 694.

HRMS (EI): *m/z* = $[M]^{\bullet+}$ calculated for $C_{28}H_{23}N_5O_2S_2^{\bullet+}$: 525.1288; found: 525.1294.

Purity (HPLC): > 99% (210 nm), > 99% (254 nm), (method 1b).

2-((4,6-Dimethylpyrimidin-2-yl)thio)-*N*-(6-(3-(phenylsulfonamido)phenyl)benzo[d]thiazol-2-yl)acetamide (FM104)

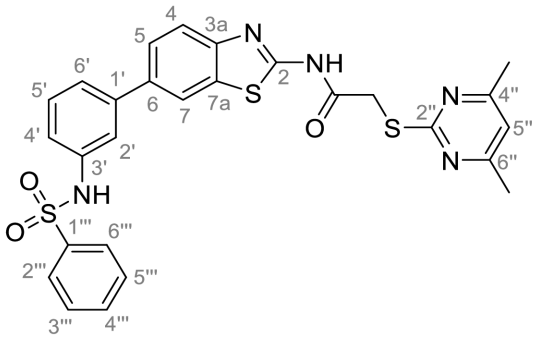

$C_{27}H_{23}N_5O_3S_3$

M_w = 561.71 g/mol

At room temperature benzenesulfonyl chloride (23.4 µL, 0.184 mmol, 0.95 eq) was added dropwise to a stirred solution of amine **22** (81.5 mg, 0.193 mmol, 1.00 eq) and NEt_3 (25.6 µL, 0.184 mmol, 0.95 eq) in anhydrous DCM (5 mL). After 1h, water (25 mL) and brine (25 mL) were added, and the reaction mixture was extracted with DCM (3 x 50 mL). The combined organic layers were dried over sodium sulfate. After evaporating the solvent *in vacuo*, the crude product was purified *via* flash column chromatography (DCM/MeOH 100:1) to yield the title compound as a white solid (16.3 mg, 0.0290 mmol, 15%).

R_f: 0.06 (DCM/MeOH 100:1).

m.p.: 204-209 °C.

^{1}H NMR (500 MHz, DMSO-d_6) δ [ppm] = 12.69 (s, 1H, NHCO), 10.40 (s, 1H, $NHSO_2$), 8.13 (d, *J* = 1.9 Hz, 1H, 7-H), 7.85 – 7.78 (m, 3H, 4-H, 2'''-H, 6'''-H), 7.63 – 7.59 (m, 1H, 4'''-H), 7.58 – 7.53 (m, 3H, 5-H, 3'''-H, 5'''-H), 7.41 – 7.35 (m, 2H, 2'-H, 6'-H), 7.32 (t, *J* = 7.8 Hz, 1H, 5'-H), 7.07 (ddd, *J* = 7.8, 2.2, 1.1 Hz, 1H, 4'-H), 6.96 (s, 1H, 5''-H), 4.19 (s, 2H, CH_2), 2.29 (s, 6H, 4''-CH_3, 6''-CH_3).

^{13}C NMR (126 MHz, DMSO-d_6) δ [ppm] = 168.8 (C-2''), 168.2 (NHCO), 167.1 (C-4'', C-6''), 158.6 (C-2), 148.3 (C-3a), 141.0 (C-1'), 139.4 (C-1'''), 138.3 (C-3'), 135.2 (C-6), 133.0 (C-4'''), 132.5 (C-7a), 129.8 (C-5'), 129.3 (C-3''', C-5'''), 126.7 (C-2''', C-6'''), 125.0 (C-5), 122.7 (C-6'), 120.9 (C-4), 119.7 (C-7), 118.8 (C-4'), 118.4 (C-2'), 116.2 (C-5''), 34.5 (CH_2), 23.3 (4''-CH_3, 6''-CH_3).

IR (ATR) $\tilde{\nu}$ [cm^{-1}] = 3186, 2965, 1720, 1602, 1580, 1454, 1331, 1309, 1265, 1154, 1088, 955, 882, 836, 794, 751, 714, 685.

HRMS (EI): *m/z* = $[M]^{\bullet+}$ calculated for $C_{27}H_{23}N_5O_3S_3^{\bullet+}$: 561.0958; found: 561.0956.

Purity (HPLC): > > 99% (210 nm), > 99% (254 nm), (method 1b).

N-(3-(2-(2-((4,6-Dimethylpyrimidin-2-yl)thio)acetamido)benzo[d]thiazol-6-yl)phenyl)-5-methylthiophene-2-carboxamide (FM131)

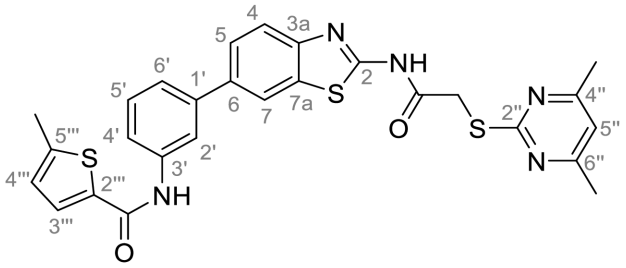

$C_{27}H_{23}N_5O_2S_3$

M_w = 545.71 g/mol

At room temperature previously prepared 5-methylthiophene-2-carbonyl chloride (26.8 µL, 0.220 mmol, 2.00 eq) was added dropwise to a stirred solution of amine **22** (46.4 mg, 0.110

mmol, 1.00 eq) and NEt_3 (30.7 µL, 0.220 mmol, 2.00 eq) in anhydrous DCM (5 mL). After 2 h, water (50 mL) was added, and the reaction mixture was extracted with DCM (3 x 50 mL). The combined organic layers were dried over sodium sulfate. After evaporating the solvent *in vacuo*, the crude product was purified *via* flash column chromatography (DCM/MeOH 100:2) to yield the title compound as a white solid (27.6 mg, 0.0506 mmol, 46%)

R_f: 0.04 (DCM/MeOH 100:2).
m.p.: 122 °C (decomposition).

^{1}H NMR (500 MHz, DMSO-d_6) δ [ppm] = 12.69 (s, 1H, 2-NHCO), 10.19 (s, 1H, 3'-NHCO), 8.26 (d, *J* = 1.9 Hz, 1H, 7-H), 8.09 (t, *J* = 1.3 Hz, 1H, 2'-H), 7.89 – 7.83 (m, 2H, 4-H, 3'''-H), 7.75 – 7.70 (m, 2H, 5-H, 4'-H), 7.48 – 7.40 (m, 2H, 5'-H, 6'-H), 6.97 (s, 1H, 5''-H), 6.94 (dd, *J* = 3.7, 1.1 Hz, 1H, 4'''-H), 4.20 (s, 2H, CH_2), 2.51 (s, 3H, CH_3), 2.30 (s, 6H, 4''-CH_3, 6''-CH_3).

^{13}C NMR (126 MHz, DMSO-d_6) δ [ppm] = 168.8 (C-2''), 168.2 (2-NHCO), 167.1 (C-4'', C-6''), 159.9 (3'-NHCO), 158.4 (C-2), 148.2 (C-3a), 146.0 (C-5'''), 140.4 (C-1'), 139.5 (C-3'), 137.4 (C-2'''), 135.7 (C-6), 132.5 (C-7a), 129.4 (C-3'''), 129.3 (C-5'), 126.7 (C-4'''), 125.1 (C-5), 122.1 (C-6'), 120.9 (C-4), 119.7 (C-7), 119.0 (C-4'), 118.6 (C-2'), 116.2 (C-5''), 34.5 (CH_2), 23.3 (4''-CH_3, 6''-CH_3), 15.3 (CH_3).

IR (ATR) $\tilde{\nu}$ [cm^{-1}] = 3268, 2956, 1720, 1626, 1581, 1544, 1525, 1486, 1455, 1422, 1307, 1264, 1212, 1152, 1095, 978, 881, 852, 834, 816, 790, 756, 742, 698, 664.

HRMS (EI): *m/z* = $[M]^{\bullet+}$ calculated for $C_{30}H_{26}N_4O_2S_2^{\bullet+}$: 545.1008; found: 545.1005.

Purity (HPLC): > 99% (210 nm), > 99% (254 nm), (method 1b).

6-(4-Nitrophenyl)benzo[d]thiazol-2-amine (16)

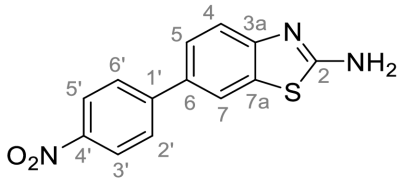

$C_{13}H_9N_3O_2S$

M_w = 271.30 g/mol

2-Amino-6-bromobenzothiazole (**14**, 978 mg, 4.27 mmol, 1.00 eq) and $Pd(PPh)_4$ (493 mg, 0.427 mmol, 0.100 eq) were weighed out into a flask, which was put under nitrogen afterwards. Degassed 1-4 dioxane (25 mL) was added *via* syringe and the mixture was stirred for 10 min at room temperature before 4-nitrophenyl boronic acid (855 mg, 5.12 mmol, 1.20 eq), Cs_2CO_3 (6.95 g, 21.3 mmol, 5.00 eq) and degassed water (8.5 mL) was added under nitrogen atmosphere. The reaction mixture was stirred for 21 h at 80 °C, cooled to room temperature, diluted with water (200 mL) and extracted with EtOAc (4 x 100 mL). The combined organic layers were dried over sodium sulfate. After evaporating the solvent *in vacuo*, the crude product was purified *via* flash column chromatography (hexanes/EtOAc 6:4) to yield the title compound as an orange solid (94.9 mg, 0.350 mmol, 8%).

R_f: 0.09 (hexanes/EtOAc 6:4).
m.p.: 283 °C.

^{1}H NMR (400 MHz, DMSO-d_6) δ [ppm] = 8.32 – 8.23 (m, 2H, 3'-H, 5'-H), 8.17 (d, *J* = 2.0 Hz, 1H, 7-H), 7.99 – 7.91 (m, 2H, 2'-H, 6'-H), 7.70 (s, 2H, NH_2), 7.66 (dd, *J* = 8.4, 2.0 Hz, 1H, 5-H), 7.44 (d, *J* = 8.4 Hz, 1H, 4-H).

^{13}C NMR (101 MHz, DMSO-d_6) δ [ppm] = 167.9 (C-2), 153.8 (C-3a), 146.8 (C-1'), 145.9 (C-4'), 132.3 (C-7a), 130.2 (C-6), 127.1 (C-2', C-6'), 124.9 (C-5) 124.1 (C-3', C-5'), 119.8 (C-7), 118.0 (C-4).

IR (ATR) $\tilde{\nu}$ [cm^{-1}] = 3432, 3079, 1639, 1591, 1527, 1498, 1456, 1396, 1330, 1274, 1259, 1199, 1109, 898, 850, 810, 751, 685.

HRMS (EI): *m/z* = $[M]^{\bullet+}$ calculated for $C_{13}H_9N_3O_2S^{\bullet+}$: 271.0410; found: 271.0377.

Purity (HPLC): ≥ 95% (210 nm), ≥ 98% (254 nm), (method 1b).

tert-Butyl (4-(2-aminobenzo[d]thiazol-6-yl)phenyl)carbamate (17)

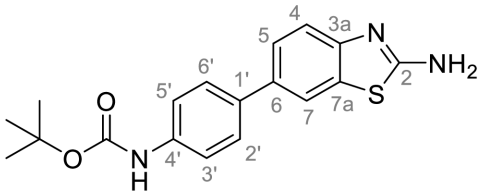

$C_{18}H_{19}N_3O_2S$

M_w = 341.43 g/mol

2-Amino-6-bromobenzothiazole (**14**, 1.21 g, 5.28 mmol, 1.00 eq) and $Pd(PPh_3)_4$ (610 mg, 0.528 mmol, 0.100 eq) were weighed out into a flask, which was put under nitrogen afterwards. Degassed 1-4 dioxane (30 mL) was added *via* syringe and the mixture was stirred for 10 min at room temperature before 4-(*N*-boc-amino)phenylboronic acid pinacol ester (2.02 g, 6.34 mmol, 1.20 eq), Cs_2CO_3 (8.60 g, 26.4 mmol, 5.00 eq) and degassed water (10 mL) was added under nitrogen atmosphere. The reaction mixture was stirred for 20 h at 80 °C, cooled to room temperature, diluted with water (250 mL) and extracted with EtOAc (4 x 100 mL). The combined organic layers were dried over sodium sulfate. After evaporating the solvent *in vacuo*, the crude product was purified *via* flash column chromatography (hexanes/EtOAc 1:1) to yield the title compound as a light yellow solid (498 mg, 1.46 mmol, 28%).

R_f: 0.16 (hexanes/EtOAc 1:1).
m.p.: 320 °C (decomposition).

^{1}H NMR (500 MHz, DMSO-d_6) δ [ppm] = 9.40 (s, 1H, NHCO), 7.92 (d, *J* = 1.9 Hz, 1H, 7-H), 7.57 – 7.54 (m, 2H, 2'-H, 6'-H), 7.53 – 7.48 (m, 4H, 3'-H, 5'-H, NH_2), 7.47 (dd, *J* = 8.4, 1.9 Hz, 1H, 5-H), 7.36 (d, *J* = 8.3 Hz, 1H, 4-H), 1.49 (s, 9H, $C(CH_3)_3$).

^{13}C NMR (126 MHz, DMSO-d_6) δ [ppm] = 166.6 (NHCO), 152.8 (C-2), 151.8 (C-3a), 138.4 (C-4'), 133.9 (C-1'), 132.9 (C-6), 131.8 (C-7a), 126.5 (C-2', C-6'), 123.8 (C-5), 118.43 (C-7), 118.38 (C-3', C-5'), 117.8 (C-4), 79.1 ($\underline{C}(CH_3)_3$), 28.1 ($C(CH_3)_3$).

IR (ATR) $\tilde{\nu}$ [cm^{-1}] = 3351, 2981, 2932, 1699, 1635, 1588, 1522, 1504, 1459, 1417, 1389, 1367, 1314, 1301, 1233, 1160, 1110, 1053, 1023, 835, 812, 772, 762.

HRMS (EI): *m/z* = $[M]^{\bullet+}$ calculated for $C_{18}H_{19}N_3O_2S^{\bullet+}$: 341.1192; found: 341.1193.

Purity (HPLC): > 99% (210 nm), > 99% (254 nm), (method 1b).

tert-Butyl (4-(2-(2-bromoacetamido)benzo[d]thiazol-6-yl)phenyl)carbamate (19)

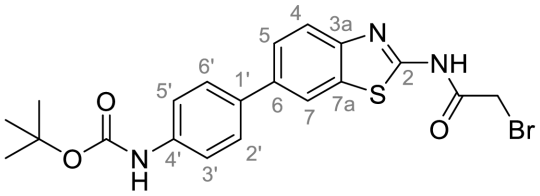

$C_{20}H_{20}BrN_3O_3S$

M_w = 462.37 g/mol

At 0 °C bromoacetyl bromide (206 µL, 2.37 mmol, 1.00, eq) was added dropwise to a stirred suspension of amine **17** (809 mg, 2.37 mmol, 1.00 eq) and NEt_3 (661 µL, 4.74 mmol, 2.00 eq) in anhydrous EtOAc (20 mL). After heating to reflux for 3 h, water (100 mL) and brine (50 mL) were added, and the reaction mixture was extracted with EtOAc (4 x 100 mL). The combined organic layers were dried over sodium sulfate. After evaporating the solvent *in vacuo*, the crude product was purified *via* flash column chromatography (hexanes/EtOAc 7:3) to yield the title compound as a light yellow solid (495 mg, 1.07 mmol, 45%).

R_f: 0.28 (hexanes/EtOAc 7:3).
m.p.: 300 °C (decomposition).

^{1}H NMR (500 MHz, $CDCl_3$) δ [ppm] = δ 8.00 (d, *J* = 1.8 Hz, 1H, 7-H), 7.85 (d, *J* = 8.4 Hz, 1H, 4-H), 7.68 (dd, *J* = 8.5, 1.8 Hz, 1H, 5-H), 7.60 – 7.55 (m, 2H, 2'-H, 6'-H), 7.50 – 7.43 (m, 2H, 3'-H, 5'-H), 7.26 (s, 1H, 4-NHCO), 6.59 (bs, 1H, 4'-NHCO), 4.14 (s, 2H, CH_2), 1.55 (s, 9H, $C(CH_3)_3$).
^{13}C NMR (126 MHz, $CDCl_3$)) δ [ppm] = 164.2 (2-NHCO), 157.5 (4'-NHCO), 152.9 (C-2), 146.7 (C-3a), 138.1 (C-4'), 137.8 (C-6), 135.3 (C-1'), 132.9 (C-7a), 128.0 (C-2', C-6'), 126.1 (C-5), 121.3 (C-4), 119.5 (C-7), 119.1 (C-3', C-5'), 80.9 ($\underline{C}(CH_3)_3$), 28.5 ($C(CH_3)_3$), 27.9 (CH_2).

IR (ATR) $\tilde{\nu}$ [cm^{-1}] = 3370, 3215, 1687, 1602, 1543, 1524, 1502, 1454, 1393, 1368, 1329, 1299, 1272, 1234, 1158, 1058, 982, 834, 812, 754, 720.

HRMS (EI): *m/z* = $[M-H]^-$ calculated for $C_{20}H_{19}{}^{79}BrN_3O_3S^-$: 460.0338; found: 460.0336.

Purity (HPLC): > 99% (210 nm), > 99% (254 nm), (method 1b).

tert-Butyl (4-(2-(2-((4,6-dimethylpyrimidin-2-yl)thio)acetamido)benzo[d]thiazol-6-yl)phenyl)carbamate (21)

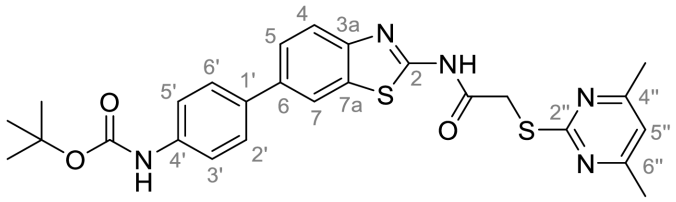

$C_{26}H_{27}N_5O_3S_2$

M_w = 521.66 g/mol

At room temperature potassium *tert*-butoxide (274 mg, 2.44 mmol, 2.00 eq) was added to a stirred solution of 2-bromoacetamide **19** (564 mg, 1.22 mmol, 1.00 eq) and 4,6-dimethylpyrimidine-2-thiol (205 mg, 1.46 mmol, 1.20 eq) in anhydrous DMF (5 mL). After 3 h, water (50 mL) and brine (100 mL) were added, and the reaction mixture was extracted with EtOAc (4 x 100 mL). The combined organic layers were dried over sodium sulfate. The combined organic layers were dried over sodium sulfate. After evaporating the solvent *in vacuo*, the title compound was yielded as a yellow solid (499 mg, 0.956 mmol, 78%).

R_f: 0.10 (hexanes/EtOAc 7:3).
m.p.: 220 °C.

^{1}H NMR (400 MHz, DMSO-d_6) δ [ppm] = δ 12.64 (s, 1H, 2-NHCO), 9.44 (s, 1H, 4'-NHCO), 8.23 (d, *J* = 1.8 Hz, 1H, 7-H), 7.78 (d, *J* = 8.5 Hz, 1H, 4-H), 7.70 (dd, *J* = 8.5, 1.9 Hz, 1H, 5-H), 7.65 – 7.60 (m, 2H, 2'-H, 6'-H), 7.59 – 7.51 (m, 2H, 3'-H, 5'-H), 6.96 (s, 1H, 5''-H), 4.19 (s, 2H, CH_2), 2.29 (s, 6H, 4''-CH_3, 6''-CH_3), 1.49 (s, 9H, $C(CH_3)_3$).

^{13}C NMR (101 MHz, DMSO-d_6) δ [ppm] = 168.8 (C-2''), 168.1 (2-NHCO), 167.0 (C-4'', C-6''), 158.0 (C-2), 152.7 (4'-NHCO), 147.7 (C-3a), 138.9 (C-4'), 135.5 (C-6), 133.5 (C-1'), 132.4 (C-7a), 126.9 (C-2', C-6'), 124.7 (C-5), 120.7 (C-4), 119.0 (C-7), 118.4 (C-3', C-5'), 116.2 (C-5''), 79.1 ($\underline{C}(CH_3)_3$), 34.4 (CH_2), 28.13 ($C(CH_3)_3$), 23.2 (4''-CH_3, 6''-CH_3).

IR (ATR) $\tilde{\nu}$ [cm^{-1}] = 2976, 1720, 1700, 1583, 1536, 1458, 1367, 1326, 1264, 1233, 1154, 1119, 1053, 1024, 846, 819, 779, 478.

HRMS (EI): *m/z* = $[M]^{\bullet+}$ calculated for $C_{26}H_{27}N_5O_3S_2^{\bullet+}$: 521.1550; found: 521.1550.

Purity (HPLC): > 91% (210 nm), > 93% (254 nm), (method 1b).

_N_-(6-(4-Aminophenyl)benzo[d]thiazol-2-yl)-2-((4,6-dimethylpyrimidin-2-yl)thio)acetamide (23)

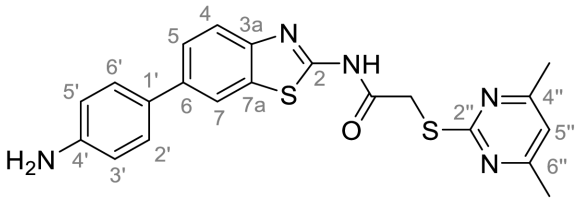

$C_{21}H_{19}N_5OS_2$

M_w = 421.55 g/mol

At room temperature boc-protected amine **21** (1.12 g, 2.15 mmol, 1.00 eq) was suspended in chloroform (10 mL) and TFA (3.22 mL, 42.9 mmol, 25.0 eq) was added. After the reaction mixture was stirred for 24 h, it was alkalized with saturated $NaHCO_3$ solution and extracted with DCM (4 x 50 mL). The combined organic layers were dried over sodium sulfate. After evaporating the solvent *in vacuo*, the crude product was purified *via* flash column chromatography (hexanes/EtOAc 1:1) to yield the title compound as a beige solid (755 mg, 1.79 mmol, 83%).

R_f: 0.12 (hexanes/EtOAc 1:1).
m.p.: 146 °C (decomposition).

^{1}H NMR (500 MHz, DMSO-d_6) δ [ppm] = 12.58 (s, 1H, NHCO), 8.11 (d, *J* = 1.8 Hz, 1H, 7-H), 7.72 (d, *J* = 8.4 Hz, 1H, 4-H), 7.61 (dd, *J* = 8.5, 1.9 Hz, 1H, 5-H), 7.44 – 7.37 (m, 2H, 2'-H, 6'-H), 6.97 (s, 1H, 5''-H), 6.68 – 6.61 (m, 2H, 3'-H, 5'-H), 5.22 (s, 2H, NH_2), 4.18 (s, 2H, CH_2), 2.30 (s, 6H, 4''-CH_3, 6''-CH_3).

^{13}C NMR (101 MHz, DMSO-d_6) δ [ppm] = δ 168.9 (C-2''), 168.0 (NHCO), 167.1 (C-4'', C-6''), 157.4 (C-2), 148.3 (C-4'), 146.8 (C-3a), 136.6 (C-6), 132.4 (C-7a), 127.7 (C-2', C-6'), 127.3 (C-1'), 124.9 (C-5), 124.1 (C-4), 120.6 (C-7), 117.9 (C-5''), 116.2 (C-3', C-5'), 34.4 (CH_2), 23.3 (4''-CH_3, 6''-CH_3).

IR (ATR) $\tilde{\nu}$ [cm^{-1}] = 2922, 1692, 1603, 1583, 1536, 1455, 1265, 1184, 1136, 818.

HRMS (EI): *m/z* = $[M]^{\bullet+}$ calculated for $C_{21}H_{19}N_5OS_2^{\bullet+}$: 421.1026; found: 421.1024.

Purity (HPLC): > 99% (210 nm), > 99% (254 nm), (method 1b).

_N_-(6-(4-Acetamidophenyl)benzo[d]thiazol-2-yl)-2-((4,6-dimethylpyrimidin-2-yl)thio)acetamide (FM128)

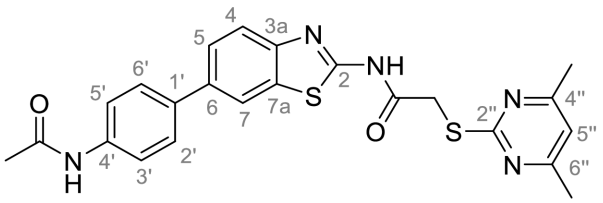

$C_{23}H_{21}N_5O_2S_2$

M_w = 463.58 g/mol

At room temperature acetic anhydride (23.7 µL, 0.253 mmol, 2.00 eq) was added dropwise to a stirred solution of amine **23** (53.3 mg, 0.126 mmol, 1.00 eq) and NEt_3 (35.2 µL, 0.253 mmol, 2.00 eq) in anhydrous DCM (2 mL). After 3 h, water (50 mL) was added, and the reaction mixture was extracted with DCM (4 x 50 mL). The combined organic layers were dried over sodium sulfate. After evaporating the solvent *in vacuo*, the crude product was purified *via* flash column chromatography (hexanes/EtOAc 4:6) to yield the title compound as a white solid (35.1 mg, 0.0757 mmol, 60%).

R_f: 0.06 (hexanes/EtOAc 4:6).
m.p.: 255 °C.

^{1}H NMR (500 MHz, DMSO-d_6) δ [ppm] = 12.65 (s, 1H, 2-NHCO), 10.02 (s, 1H, 4'-NHCO), 8.24 (d, *J* = 1.8 Hz, 1H, 7-H), 7.79 (d, *J* = 8.4 Hz, 1H, 4-H), 7.71 (dd, *J* = 8.5, 1.9 Hz, 1H, 5-H), 7.69 – 7.64 (m, 4H, 2'-H, 3'-H, 5'-H, 6'-H), 6.96 (s, 1H, 5''-H), 4.19 (s, 2H, CH_2), 2.29 (s, 6H, 3''-CH_3, 4''-CH_3), 2.07 (s, 3H, CH_3).

^{13}C NMR (126 MHz, DMSO-d_6) δ [ppm] = 168.8 (C-2''), 168.3 (4'-NHCO), 168.1 (2-NHCO), 167.1 (C-4'', C-6''), 158.1 (C-2), 147.8 (C-3a), 138.7 (C-4'), 135.5 (C-6), 134.4 (C-1'), 132.4 (C-7a), 127.0 (C-2', C-6'), 124.8 (C-5), 120.8 (C-4), 119.3 C-3', C-5'), 119.1 (C-7), 116.2 (C-5''), 34.4 (CH_2), 24.1 (CH_3), 23.3 (3''-CH_3, 4''-CH_3).

IR (ATR) $\tilde{\nu}$ [cm^{-1}] = 3361, 1679, 1658, 1600, 1551, 1531, 1460, 1394, 1340, 1330, 1292, 1275, 1264, 1225, 1192, 1128, 1092, 830, 807, 799, 748, 734, 692.

HRMS (EI): *m/z* = $[M]^{\bullet+}$ calculated for $C_{23}H_{21}N_5O_2S_2^{\bullet+}$: 463.1131; found: 463.1132.

Purity (HPLC): > 99% (210 nm), > 99% (254 nm), (method 1b).

_N_-(4-(2-(2-((4,6-Dimethylpyrimidin-2-yl)thio)acetamido)benzo[d]thiazol -6-yl)phenyl)thiophene-2-carboxamide (FM129)

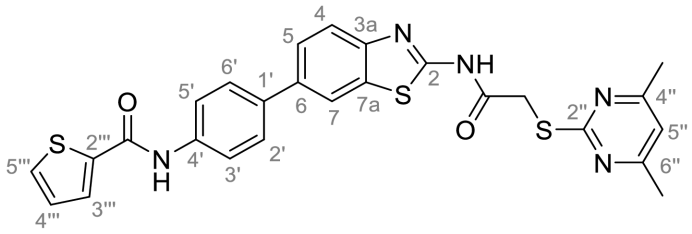

$C_{29}H_{24}N_4O_2S_2$

M_w = 531.68 g/mol

At room temperature 2-thiophenecarbonyl chloride (23.8 µL, 0.222 mmol, 1.20 eq) was added dropwise to a stirred solution of amine **23** (78.1 mg, 0.185 mmol, 1.00 eq) and NEt_3 (23.8 µL, 0.222 mmol, 1.20 eq) in anhydrous DCM (5 mL). After 1 h, water (50 mL) was added, and the reaction mixture was extracted with DCM (4 x 50 mL). The combined organic layers were dried over sodium sulfate. After evaporating the solvent *in vacuo*, the crude product was purified *via* flash column chromatography (DCM/MeOH 100:1) to yield the title compound as a white solid (75.7 mg, 0.142 mmol, 77%).

R_f: 0.29 (DCM/MeOH 100:1).
m.p.: 280-284 °C.

^{1}H NMR (400 MHz, DMSO-d_6) δ [ppm] = 12.68 (s, 1H, 2-NHCO), 10.33 (s, 1H, 4'-NHCO), 8.30 (d, *J* = 1.8 Hz, 1H, 7-H), 8.05 (dd, *J* = 3.8, 1.2 Hz, 1H, 3'''-H), 7.88 (dd, *J* = 5.0, 1.1 Hz, 1H, 5'''-H), 7.86-7.79 (m, 3H, 4-H, 3'-H, 5'-H), 7.79 – 7.72 (m, 3H, 5-H, 2'-H, 6'-H), 7.24 (dd, *J* = 5.0, 3.8 Hz, 1H, 4'''-H), 6.97 (s, 1H, 5''-H), 4.20 (s, 2H, CH_2), 2.29 (s, 6H, 4''-CH_3, 6''-CH_3).

^{13}C NMR (101 MHz, DMSO-d_6) δ [ppm] = 168.8 (C-2''), 168.2 (2-NHCO), 167.0 (C-4'', C-6''), 159.9 (4'-NHCO), 158.2 (C-2), 147.9 (C-3a), 140.0 (C-2'''), 138.1 (C-4'), 135.3 (C-6), 135.1 (C-1'), 132.5 (C-7a), 132.0 (C-5'''), 129.2 (C-3'''), 128.1 (C-4'''), 127.0 (C-2', C-6')), 124.8 (C-5), 120.8 (C-4), 120.7 (C-3', C-5'), 119.2 (C-7), 116.2 (C-5''), 34.5 (CH_2), 23.3 (4''-CH_3, 6''-CH_3).

IR (ATR) $\tilde{\nu}$ [cm^{-1}] = 3371, 1682, 1659, 1600, 1531, 1457, 1421, 1326, 1263, 1228, 1188, 1091, 864, 832, 805, 750, 722.

HRMS (EI): *m/z* = $[M]^{\bullet+}$ calculated for $C_{26}H_{21}N_5O_2S_3^{\bullet+}$: 531.0852; found: 531.0860.

Purity (HPLC): > 99% (210 nm), > 99% (254 nm), (method 1a).

N-(4-(2-(2-((4,6-Dimethylpyrimidin-2-yl)thio)acetamido)benzo[d]thiazol-6-yl)phenyl)benzamide (FM127)

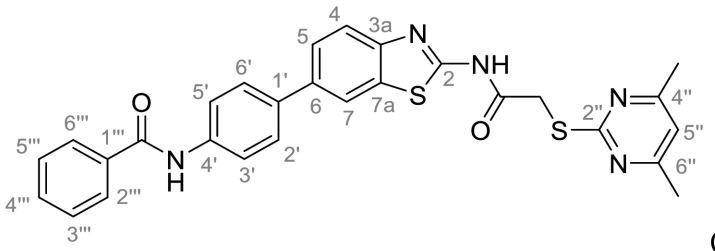

$C_{28}H_{23}N_5O_2S_2$

M_w = 525.66 g/mol

At room temperature benzoyl chloride (43.0 µL, 0.371 mmol, 2.00 eq) was added dropwise to a stirred solution of amine **23** (78.1 mg, 0.185 mmol, 1.00 eq) and NEt_3 (51.6 µL, 0.371 mmol, 2.00 eq) in anhydrous DCM (5 mL). After 3 h, water (50 mL) was added, and the reaction mixture was extracted with DCM (4 x 50 mL). The combined organic layers were dried over sodium sulfate. After evaporating the solvent *in vacuo*, the crude product was purified *via* flash column chromatography (hexanes/EtOAc 1:1) to yield the title compound as a white solid (44.3 mg, 0.0843 mmol, 46%).

R_f: 0.14 (hexanes/EtOAc 1:1).
m.p.: 262 °C.

^{1}H NMR (400 MHz, DMSO-d_6) δ [ppm] = 12.67 (s, 1H, 2-NHCO), 10.35 (s, 1H, 4'-NHCO), 8.30 (d, *J* = 1.8 Hz, 1H, 7-H), 8.02 – 7.94 (m, 2H, 2'''-H, 6'''-H), 7.94 – 7.88 (m, 2H, 3'-H, 5'-H), 7.82 (d, *J* = 8.5 Hz, 1H, 4-H), 7.78 – 7.71 (m, 3H, 5-H, 2'-H, 6'-H), 7.64 – 7.52 (m, 3H, 3'''-H, 4'''-H, 5'''-H), 6.97 (s, 1H, 5''-H), 4.20 (s, 2H, CH_2), 2.30 (s, 6H, 4''-CH_3, 6''-CH_3).

^{13}C NMR (101 MHz, DMSO-d_6) δ [ppm] = δ 168.9 (C-2''), 168.2 (2-NHCO), 167.1 (C-4'', C-6''), 165.6 (4'-NHCO), 158.2 (C-2), 147.9 (C-3a), 138.6 (C-4'), 135.4 (C-6), 135.0 (C-1'''), 134.9 (C-1'), 132.5 (C-7a), 131.6 (C-4'''), 128.4 (C-3''', C-5'''), 127.7 (C-2''', C-6'''), 126.9 (C-5), 124.8 (C-4), 120.7 (C-3', C-5'), 119.2 (C-7), 116.2 (C-5''), 34.5 (CH_2), 23.3 (4''-CH_3, 6''-CH_3).

IR (ATR) $\tilde{\nu}$ [cm^{-1}] = 3367, 1684, 1673, 1604, 1566, 1550, 1527, 1493, 1455, 1394, 1342, 1324, 1298, 1267, 1245, 1227, 1189, 1129, 1031, 897, 870, 834, 808, 750, 702, 690, 676.

HRMS (EI): *m/z* = $[M]^{\bullet+}$ calculated for $C_{28}H_{23}N_5O_2S_2^{\bullet+}$: 525.1288; found: 525.1281.

Purity (HPLC): > 99% (210 nm), > 99% (254 nm), (method 1b).

2-((4,6-Dimethylpyrimidin-2-yl)thio)-*N*-(6-(3-(phenylsulfonamido)phenyl)benzo[d]thiazol-2-yl)acetamide (FM130)

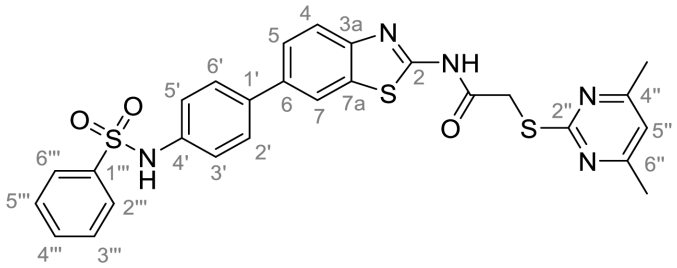

$C_{27}H_{23}N_5O_3S_3$

M_w = 561.71 g/mol

At room temperature benzenesulfonyl chloride (26.1 µL, 0.204 mmol, 0.95 eq) was added dropwise to a stirred solution of amine **23** (90.6 mg, 0.215 mmol, 1.00 eq) and NEt_3 (28.5 µL, 0.204 mmol, 0.95 eq) in anhydrous DCM (5 mL). After heating to reflux for 8 h, water (25 mL) and brine (25 mL) were added, and the reaction mixture was extracted with DCM (3 x 50 mL). The combined organic layers were dried over sodium sulfate. After evaporating the solvent *in vacuo*, the crude product was purified *via* flash column chromatography (DCM/MeOH/AcOH 100:0.5:0.25) to yield the title compound as a white solid (68.0 mg, 0.121 mmol, 59%).

R_f: 0.07 (DCM/MeOH/AcOH 100:0.5:0.25).
m.p.: 233 °C.

^{1}H NMR (500 $CDCl_3$) δ [ppm] = 11.86 (s, 1H, NHCO), 7.91 (d, *J* = 1.8 Hz, 1H, 7-H), 7.84 – 7.78 (m, 2H, 2'''-H, 6'''-H), 7.74 (d, *J* = 8.4 Hz, 1H, 4-H), 7.57 – 7.52 (m, 2H, 5-H, 4'''-H), 7.52 – 7.48 (m, 2H, 2'-H, 6'-H), 7.48 – 7.43 (m, 2H, 3'''H, 5'''-H), 7.18 – 7.12 (m, 2H, 3'-H, 5'-H), 6.88 (s, 1H, 5''-H), 6.78 (s, 1H, $NHSO_2$), 3.98 (s, 2H, CH_2), 2.57 (s, 6H, 4''-CH_3, 6''-CH_3).

^{13}C NMR (126 MHz, $CDCl_3$) δ [ppm] = 169.9 (C-2''), 168.4 (NHCO), 168.3 (C-4'', C-6''), 158.0 (C-2), 148.4 (C-3a), 139.2 (C-1'''), 138.2 (C-1'), 136.2 (C-6), 135.6 (C-4'), 133.4 (C-7a), 133.2 (C-4'''), 129.2 (C-3''', C-5'''), 128.2 (C-2', C-6'), 127.4 (C-2''', C-6''')), 125.5 (C-5), 122.4 (C-3', C-5'), 121.3 (C-4), 119.6 (C-7), 117.3 (C-5''), 34.8 (CH_2), 24.0 (4''-CH_3, 6''-CH_3).

IR (ATR) $\tilde{\nu}$ [cm^{-1}] = 3260, 2918, 1695, 1604, 1583, 1560, 1540, 1517, 1464, 1407, 1332, 1312, 1295, 1274, 1227, 1151, 1090, 1031, 929, 847, 824, 754, 718, 687.

HRMS (EI): *m/z* = $[M]^{\bullet+}$ calculated for $C_{27}H_{23}N_5O_3S_3^{\bullet+}$: 561.0958; found: 561.0954.

Purity (HPLC): > 99% (210 nm), > 99% (254 nm), (method 1b).

N-(4-(2-(2-((4,6-Dimethylpyrimidin-2-yl)thio)acetamido)benzo[d]thiazol-6-yl)phenyl)-5-methylthiophene-2-carboxamide (FM131)

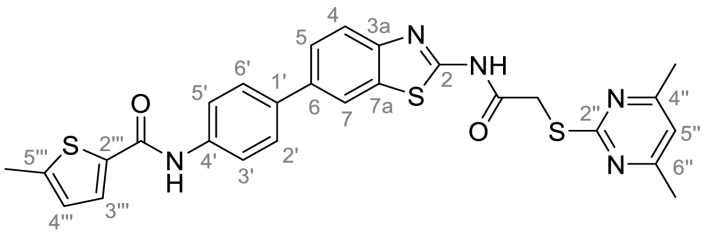

$C_{27}H_{23}N_5O_2S_3$

M_w = 545.71 g/mol

At room temperature previously prepared 5-methylthiophene-2-carbonyl chloride (25.2 µL, 0.202 mmol, 1.10 eq) was added dropwise to a stirred solution of amine **23** (77.4 mg, 0.184 mmol, 1.10 eq) and NEt_3 (28.2 µL, 0.202 mmol, 1.10 eq) in anhydrous DCM (5 mL). After 2 h, water (50 mL) was added, and the reaction mixture was extracted with DCM (3 x 50 mL). The combined organic layers were dried over sodium sulfate. After evaporating the solvent *in vacuo*, the crude product was purified *via* flash column chromatography (hexanes/EtOAc 6:4) to yield the title compound as a white solid (45.3 mg, 0.083 mmol, 45%).

R_f: 0.10 (hexanes/EtOAc 6:4).
m.p.: 294 °C.

^{1}H NMR (400 MHz, DMSO-d_6) δ [ppm] = 12.66 (s, 1H, 2-NHCO), 10.19 (s, 1H, 4'-NHCO), 8.29 (d, *J* = 1.8 Hz, 1H, 7-H), 7.87 – 7.78 (m, 4H, 4-H, 3'-H, 5'-H, 3'''-H), 7.78 – 7.70 (m, 3H, 2'-H, 6'-H, 5-H), 6.97 (s, 1H, 5''-H), 6.94 (dd, *J* = 3.7, 1.2 Hz, 1H, 4'''-H), 4.20 (s, 2H, CH_2), 2.30 (s, 6H, 4''-CH_3, 6''-CH_3).

^{13}C NMR (126 MHz, DMSO-d_6) δ [ppm] = 168.8 (C-2''), 168.1 (2-NHCO), 167.1 (C-4'', C-6''), 159.8 (4'-NHCO), 158.1 (C-2), 147.9 (C-3a), 145.9 (C-5'''), 138.2 (C-4'), 137.4 (C-2'''), 135.4 (C-6), 134.9 (C-1'), 132.5 (C-7a), 129.4 (C-3'''), 126.9 (C-2', C-6'), 126.7 (C-4'''), 124.8 (C-5),

120.8 (C-4), 120.5 (C-3', C-5'), 119.2 (C-7), 116.2 (C-5''), 34.4 (CH_2), 23.3 (4''-CH_3, 6''-CH_3), 15.3 (CH_3).

IR (ATR) $\tilde{\nu}$ [cm^{-1}] = 3361, 1679, 1658, 1600, 1551, 1531, 1460, 1394, 1340, 1330, 1292, 1275, 1264, 1255, 1192, 1128, 1092, 899, 863, 830, 807, 799, 748, 734, 692.

HRMS (EI): *m*/*z* = $[M]^{\bullet+}$ calculated for $C_{30}H_{26}N_4O_2S_2^{\bullet+}$: 545.1008; found: 545.1008.

Purity (HPLC): > 99% (210 nm), > 99% (254 nm), (method 1a).

2-((4,6-Dimethylpyrimidin-2-yl)thio)acetic acid (25)

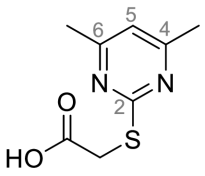

$C_8H_{10}N_2O_2S$

M_w = 198.25 g/mol

2-Chloroacetyl chloride (**28**, 3.07 g, 32.5 mmol, 1.20 eq) and 2-thiopyrimidine (3.80 g, 27.1 mmol, 1.00 eq) and were suspended in acetonitrile (25 mL) at room temperature. After addition of NEt_3 (15.1 mL, 108 mmol, 4.00 eq), the reaction mixture was stirred for 24 h. After evaporating the solvent, the crude product was purified *via* flash column chromatography (DCM/MeOH/AcOH 100:1:1) to yield the title compound as a light-beige solid (4.33 g, 21.8 mmol, 81%).

R_f: 0.11 (DCM/MeOH/AcOH 100:1:1).
m.p.: 128 °C.

^{1}H NMR (400 MHz, DMSO-d_6) δ [ppm] = 12.73 (s, 1H, COOH), 6.97 (s, 1H, 5-H), 3.90 (s, 2H, CH_2), 2.33 (s, 6H, 4-CH_3, 6-CH_3).

^{13}C NMR (101 MHz, DMSO-d_6) δ [ppm] = 170.2 (COOH), 169.0 (C-2), 167.0 (C-4, C-6), 116.0 (C-5), 32.9 (CH_2), 23.3 (4-CH_3, 6-CH_3).

IR (ATR) $\tilde{\nu}$ [cm^{-1}] = 3474, 2942, 2534, 1924, 1716, 1584, 1538, 1309, 1267, 1208, 1172, 984, 862, 791, 661.

HR-MS (ESI): *m/z* = $[M-H]^-$ calculated for $C_8H_9N_2O_2S^-$: 197.0390; found: 197.0390.

Purity (HPLC): > 99% (210 nm), > 99% (254 nm) (method 2a).

Literature-known compound[96] was prepared using an optimized synthesis procedure.

2-((4,6-Dimethylpyrimidin-2-yl)thio)-*N*-(3-(hydroxymethyl)phenyl)acetamide (29)

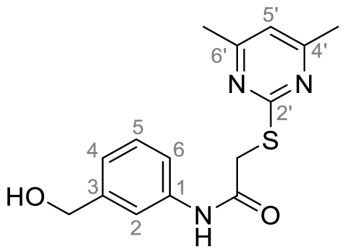

$C_{15}H_{17}N_3O_2S$

M_w = 303.39 g/mol

DIPEA (4.21 mL, 24.4 mmol, 3.00 eq) and HATU (4.63 g, 12.2 mmol, 1.50 eq) were added to a solution of carboxylic acid **25** (2.41 g, 12.2 mmol, 1.50 eq) in anhydrous DMF (8 mL) and the reaction mixture was stirred at room temperature for 1 h. 3-Aminobenzyl alcohol (800 mg, 7.33 mmol, 1.00 eq) was added and the reaction mixture was stirred for another 3 h. Then the mixture was diluted with brine (250 mL) and extracted with EtOAc (4 x 100 mL). The combined organic layers were dried over sodium sulfate. After evaporating the solvent *in vacuo*, the crude product was purified *via* flash column chromatography (hexanes/EtOAc 4:6) to yield the title compound as a white solid (731 mg, 2.41 mmol, 30%).

R_f: 0.16 (hexanes/EtOAc 4:6).
m.p.: 138-140 °C.

^{1}H NMR (400 MHz, DMSO-d_6) δ [ppm] = δ 10.20 (s, 1H, NHCO), 7.56 (t, *J* = 2.0 Hz, 1H, 2-H), 7.44 (d, *J* = 7.9, 1.5 Hz, 1H, 6-H), 7.24 (t, *J* = 7.8 Hz, 1H, 5-H), 7.02 – 6.94 (m, 2H, 4-H, 5'-H), 5.18 (t, *J* = 5.7 Hz, 1H, $CH_2O\underline{H}$), 4.45 (d, *J* = 5.7 Hz, 2H, CH_2OH), 4.03 (s, 2H, CH_2S), 2.33 (s, 6H, 4-CH_3, 6-CH_3).

^{13}C NMR (101 MHz, DMSO-d_6) δ [ppm] = 169.3 (C-2'), 167.0 (C-4', C-6'), 166.4 (NHCO), 143.3 (C-3), 138.9 (C-1), 128.4 (C-5), 121.3 (C-4), 117.4 (C-6), 117.2 (C-2), 116.1 (C-5'), 62.8 (CH_2OH) 35.5 (CH_2S), 23.3 (4-CH_3, 6-CH_3).

IR (ATR) $\tilde{\nu}$ [cm^{-1}] = 3276, 1668, 1587, 1558, 1486, 1436, 1670, 1339, 1271, 1205, 1143, 1070, 960, 940, 882, 846, 789, 755, 736.

HRMS (EI): *m/z* = $[M]^{\bullet+}$ calculated for $C_{15}H_{17}N_3O_2S^{\bullet+}$: 303.1036; found: 303.1036.

Purity (HPLC): > 99% (210 nm), > 99% (254 nm), (method 1b).

N-(3-(Bromomethyl)phenyl)-2-((4,6-dimethylpyrimidin-2-yl)thio)acetamide (30)

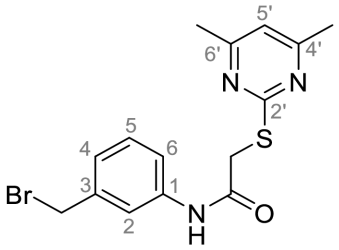

$C_{15}H_{16}BrN_3OS$

M_w = 366.28 g/mol

PBr_3 (249 µL, 2.65 mmol, 1.10 eq) was diluted in anhydrous DCM (20 mL) and added dropwise to a solution of primary alcohol **29** (730 mg, 2.41 mmol, 1.00 eq) dissolved in anhydrous DCM (50 mL) under nitrogen atmosphere. After the reaction mixture was stirred for 30 min, water (50 mL) was added, and it was extracted with DCM (4 x 50 mL). The combined organic layers were dried over sodium sulfate. After evaporating the solvent *in vacuo*, the crude product was purified *via* flash column chromatography (DCM/MeOH 100:2) to yield the title compound as a light brown solid (748 mg, 2.04 mmol, 85%).

R_f: 0.25 (DCM/MeOH 100:2).
m.p.: 119 °C.

^{1}H NMR (400 MHz, $CDCl_3$) δ [ppm] = 9.57 (s, 1H, NHCO), 7.56 (t, *J* = 1.9 Hz, 1H), 7.35 (ddd, *J* = 8.2, 2.2, 1.1 Hz, 1H, 6-H), 7.26 (m, 1H, 5-H), 7.10 (dt, *J* = 7.7, 1.4 Hz, 1H, 4-H), 6.84 (s, 1H, 5'-H), 4.45 (s, 2H, CH_2Br), 3.89 (s, 2H, CH_2S), 2.50 (s, 6H, 4-CH_3, 6-CH_3).

^{13}C NMR (101 MHz, $CDCl_3$) δ [ppm] = δ 170.3 (C-2'), 168.0 (NHCO), 167.8 (C-4', C-6'), 138.8 (C-3), 138.6 (C-1), 129.6 (C-5), 124.8 (C-4), 120.3 (C-2), 119.7 (C-6), 116.9 (C-5'), 35.7 (CH_2S), 33.4 (CH_2Br), 24.1 (4-CH_3, 6-CH_3).

IR (ATR) $\tilde{\nu}$ [cm^{-1}] = 3263, 1669, 1613, 1580, 1558, 1492, 1428, 1366, 1334, 1264, 1200, 1031, 983, 893, 880, 850, 823, 795, 751.

HRMS (ESI): *m/z* = [M-H]$^-$ calculated for $C_{15}H_{15}{}^{79}BrN_3O_3S^-$: 364.0125; found: 364.0127.

Purity (HPLC): > 97% (210 nm), > 98% (254 nm), (method 1a).

2-((4,6-Dimethylpyrimidin-2-yl)thio)-*N*-(3-(phenoxymethyl)phenyl)acetamide (28a, FM159)

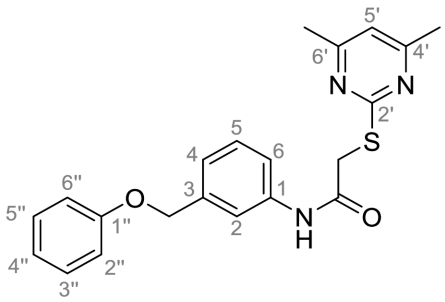

$C_{21}H_{21}N_3O_2S$

M_w = 379.48 g/mol

Under nitrogen atmosphere alkyl bromide **30** (79.2 mg, 0.216 mmol, 1.00 eq), phenol (24.4 mg, 0.259 mmol, 1.20 eq) and potassium *tert*-butoxide (48.5 mg, 0.432 mmol, 2.00 eq) were dissolved in anhydrous DMF (0.5 mL). After the reaction mixture was stirred for 2 h at room temperature, brine (25 mL) was added, and it was extracted with EtOAc (4 x 50 mL). The combined organic layers were dried over sodium sulfate and the solvent was evaporated *in vacuo*. The crude product was purified *via* flash column chromatography (hexanes/EtOAc 7:3) to yield the title compound as a white solid (35.6 mg, 0.0938 mmol, 43%).

R_f: 0.32 (hexanes/EtOAc 7:3).
m.p.: 141-142 °C.

^{1}H NMR (400 MHz, DMSO-d_6) δ [ppm] = 10.28 (s, 1H, NHCO), 7.68 (d, *J* = 1.9 Hz, 1H. 2-H), 7.52 (d, *J* = 8.2 Hz, 1H, 6-H), 7.36 – 7.24 (m, 5-H, 3''-H, 5''-H), 7.12 (d, *J* = 7.4 Hz, 1H, 4-H), 7.03 – 6.89 (m, 4H, 5'-H, 2''-H, 4''-H, 6''-H), 5.07 (s, 2H, CH_2O), 4.03 (s, 2H, CH_2S), 2.32 (s, 6H, 4-CH_3, 6-CH_3).

^{13}C NMR (101 MHz, DMSO-d_6) δ [ppm] = 169.3 (C-2'), 167.0 (C-4', C-6'), 166.6 (NHCO), 158.3 (C-1''), 139.2 (C-1), 137.9 (C-3), 129.5 (C-3'', C-5''), 128.9 (C-5), 122.4 (C-4), 120.7 (C-

4''), 118.5 (C-6), 118.0 (C-2), 116.1 (C-5'), 114.8 (C-2''. C-6''), 69.0 (CH_2O), 35.5 (CH_2S), 23.3 (4-CH_3, 6-CH_3).

IR (ATR) $\tilde{\nu}$ [cm^{-1}] = 3266, 1671, 1618, 1598, 1584, 1561, 1493, 1382, 1338, 1266, 1240, 1226, 1208, 1174, 1031, 1014, 888, 851, 842, 792, 764, 694.

HRMS (ESI): *m/z* = $[M+H]^+$ calculated for $C_{21}H_{22}N_3O_2S^+$: 380.1427; found: 380.1430.

Purity (HPLC): > 99% (210 nm), > 99% (254 nm), (method 1a).

Literature-known compound[53] was prepared using an alternate synthesis procedure.

(3-((3-(2-((4,6-Dimethylpyrimidin-2-yl)thio)acetamido) benzyl)oxy)phenyl)boronic acid (FM166)

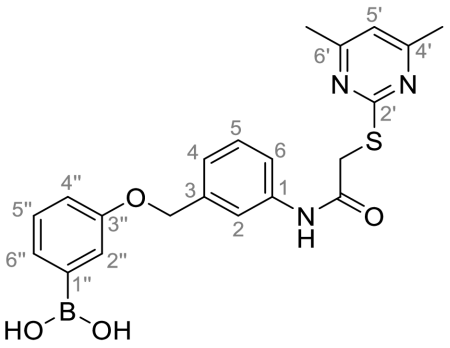

$C_{21}H_{22}BN_3O_4S$

M_w = 423.30 g/mol

Under nitrogen atmosphere alkyl bromide **30** (130 mg, 0.354 mmol, 1.00 eq), 3-hydroxyphenylboronic acid (58.7 mg, 0.354 mmol, 1.00 eq) and potassium carbonate (176 mg, 1.06 mmol, 3.00 eq) were suspended in anhydrous acetonitrile (10 mL). After the reaction mixture was stirred for 6 h at room temperature, brine (25 mL) and aq. HCl (2 M, 25 mL) was added, and it was extracted with DCM (4 x 50 mL). The combined organic layers were dried over sodium sulfate and the solvent was evaporated *in vacuo*. The crude product was purified *via* flash column chromatography (hexanes/EtOAc/FA 4:6:0.1 → DCM/MeOH/FA 100:1:1) to yield the title compound as a white solid (61.7 mg, 0.146 mmol, 41%).

R_f: 0.25 (hexanes/EtOAc/FA 4:6:0.1).

m.p.: 190-193 °C.

^{1}H NMR (500 MHz, DMSO-d_6) δ [ppm] = 10.28 (s, 1H, NHCO), 8.18 (s, 2H, $B(OH)_2$), 7.68 (t, *J* = 1.9 Hz, 1H, 2-H), 7.52 (dt, *J* = 8.2, 1.6 Hz, 1H, 6-H), 7.41 (dd, *J* = 2.9, 0.9 Hz, 1H, 2''-H), 7.38 – 7.34 (m, 1H, 4''-H), 7.32 (t, *J* = 7.8 Hz, 1H, 5-H), 7.28 – 7.19 (m, 1H, 5''-H), 7.13 (dt, *J* = 7.6, 1.3 Hz, 1H, 4-H), 7.01 (ddd, *J* = 8.1, 2.8, 1.0 Hz, 1H, 6''-H), 6.95 (s, 1H, 5'-H), 5.06 (s, 2H, CH_2O), 4.02 (s, 2H, CH_2S), 2.31 (s, 6H, 4-CH_3, 6-CH_3).

^{13}C NMR (126 MHz, DMSO-d_6) δ [ppm] = 169.4 (C-2'), 167.1 (C-4', C-6'), 166.7 (NHCO), 157.7 (C-1''), 139.2 (C-1), 138.1 (C-3), 135.9 (C-3''), 128.9 (C-5), 128.6 (C-5''), 126.7 (C-4''), 122.5 (C-4), 120.1 (C-2''), 118.5 (C-6), 118.1 (C-2), 116.5 (C-6''), 116.1 (C-5''), 68.9 (CH_2O), 35.5 (CH_2S), 23.4 (4-CH_3, 6-CH_3).

IR (ATR) $\tilde{\nu}$ [cm^{-1}] = 3264, 1671, 1600, 1583, 1554, 1488, 1432, 1341, 1268, 1206, 1024, 896, 876, 791, 727, 701.

HRMS (ESI): *m/z* = $[M+H]^+$ calculated for $C_{21}H_{23}BN_3O_4S^+$: 424.1497; found: 424.1498.

Purity (HPLC): > 99% (210 nm), > 99% (254 nm), (method 1b).

(4-((3-(2-((4,6-Dimethylpyrimidin-2-yl)thio)acetamido)benzyl) oxy)phenyl)boronic acid (FM161)

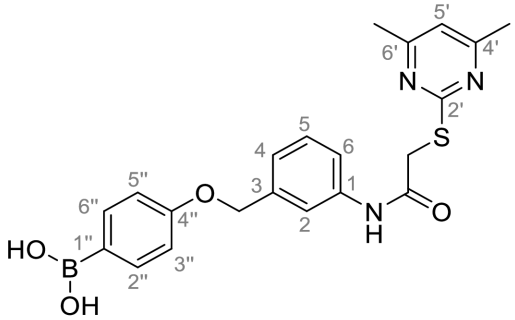

$C_{21}H_{22}BN_3O_4S$

M_w = 423.30 g/mol

Under nitrogen atmosphere alkyl bromide **30** (112 mg, 0.307 mmol, 1.00 eq), 4-hydroxyphenylboronic acid (50.8 mg, 0.368 mmol, 1.20 eq) and potassium *tert*-butoxide (68.9 mg, 0.614 mmol, 2.00 eq) were dissolved in anhydrous DMF (0.5 mL). After the reaction mixture was stirred for 30 min at room temperature, brine (25 mL) and aq. HCl (2 M, 25 mL) was added, and it was extracted with DCM (4 x 50 mL). The combined organic layers were dried over sodium sulfate and the solvent was evaporated *in vacuo*. The crude product was

purified *via* flash column chromatography (DCM/MeOH/AcOH 100:2:1) to yield the title compound as a white solid (19.8 mg, 0.0468 mmol, 15%).

R_f: 0.30 (DCM/MeOH/AcOH 100:2:1).
m.p.: 189-194 °C.

^{1}H NMR (500 MHz, DMSO-d_6) δ [ppm] = 10.28 (s, 1H, NHCO), 7.95 (s, 2H, $B(OH)_2$), 7.76 – 7.68 (m, 2H, 3''-H, 5''-H), 7.67 (t, *J* = 1.9 Hz, 1H, 2-H), 7.52 (dt, *J* = 8.1, 1.5 Hz, 1H, 6-H), 7.31 (t, *J* = 7.8 Hz, 1H, 5-H), 7.12 (dt, *J* = 7.7, 1.3 Hz, 1H, 4-H), 6.99 – 6.88 (m, 3H, 5'-H, 2''-H, 6''-H), 5.08 (s, 2H, CH_2O), 4.02 (s, 2H, CH_2S), 2.31 (s, 6H, 4-CH_3, 6-CH_3).

^{13}C NMR (126 MHz, DMSO-d_6) δ [ppm] = 169.4 (C-2'), 167.1 (C-4', C-6'), 166.7 (NHCO), 160.0 (C-1''), 139.2 (C-1), 137.9 (C-3), 135.9 (C-3'', C-5''), 129.0 (C-5), 125.9 (C-4''), 122.6 (C-4), 118.6 (C-6), 118.2 (C-2), 116.2 (C-5'), 113.9 (C-2'', C-6''), 68.9 (CH_2O), 35.5 (CH_2S), 23.4 (4-CH_3, 6-CH_3).

IR (ATR) $\tilde{\nu}$ [cm^{-1}] = 1695, 1603, 1570, 1444, 1414, 1359, 1309, 1271, 1244, 1171, 994, 892, 830, 776, 744, 686.

HRMS (ESI): *m/z* = $[M+H]^+$ calculated for $C_{21}H_{23}BN_3O_4S^+$: 424.1497; found: 424.1496.

Purity (HPLC): > 99% (210 nm), > 99% (254 nm), (method 1b).

(2-((3-(2-((4,6-Dimethylpyrimidin-2-yl)thio)acetamido)benzyl) oxy)phenyl)boronic acid (FM167)

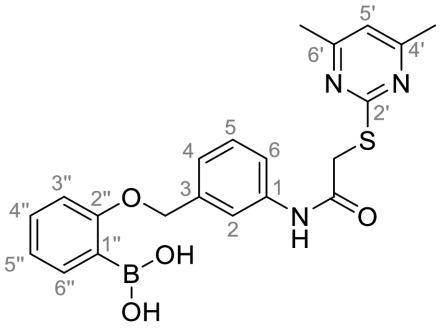

$C_{21}H_{22}BN_3O_4S$

M_w = 423.30 g/mol

Under nitrogen atmosphere alkyl bromide **30** (142 mg, 0.387 mmol, 1.00 eq), 2-hydroxyphenylboronic acid (53.4 mg, 0.387 mmol, 1.00 eq) and potassium *tert*-butoxide (86.9 mg, 0.775 mmol, 2.00 eq) were dissolved in anhydrous DMF (0.5 mL). After the reaction mixture was stirred for 4 h at room temperature aq. HCl (2 M, 75 mL) was added, and it was extracted with EtOAc (4 x 50 mL). The combined organic layers were dried over sodium sulfate and the solvent was evaporated *in vacuo*. The crude product was purified *via* flash column chromatography (hexanes/EtOAc/FA 4:6:0.1 → DCM/MeOH/FA 100:1:1) to yield the title compound as a white solid (9.50 mg, 0.0224 mmol, 6 %).

R_f: 0.20 (hexanes/EtOAc/FA 6:4:0.1).
m.p.: 98 °C (decomposition).

^{1}H NMR (500 MHz, DMSO-d_6) δ [ppm] = 10.29 (s, 1H, NHCO), 7.70 (s, 2H, $B(OH)_2$), 7.66 (t, *J* = 1.9 Hz, 1H, 2-H), 7.58 (dd, *J* = 7.2, 1.9 Hz, 1H, 3''-H), 7.54 (d, *J* = 8.1 Hz, 1H, 6-H), 7.38 – 7.31 (m, 2H, 5-H, 5''-H), 7.18 (d, *J* = 7.6 Hz, 1H, 4-H), 7.02 (d, *J* = 8.1 Hz, 1H, 6''-H), 6.97 – 6.91 (m, 2H, 5'-H, 4''-H), 5.14 (s, 2H, CH_2O), 4.03 (s, 2H, CH_2S), 2.31 (s, 6H, 4-CH_3, 6-CH_3).

^{13}C NMR (126 MHz, DMSO-d_6) δ [ppm] = 169.3 (C-2'), 167.0 (C-4', C-6'), 166.7 (NHCO), 162.5 (C-1''), 139.3 (C-1), 137.8 (C-3), 135.5 (C-3''), 131.6 (C-5''), 129.1 (C-5), 122.6 (C-4) 122.0 (C-2''), 120.7 (C-4''), 118.7 (C-6), 118.1 (C-2), 116.1 (C-5'), 111.9 (C-6''), 69.5 (CH_2O), 35.5 (CH_2S), 23.4 (4-CH_3, 6-CH_3).

IR (ATR) $\tilde{\nu}$ [cm^{-1}] = 1677, 1599, 1576, 1488, 1447, 1339, 1264, 1134, 1020, 842, 760.

HRMS (ESI): *m/z* = $[M+H]^+$ calculated for $C_{21}H_{23}BN_3O_4S^+$: 424.1497; found: 424.1499.

Purity (HPLC): > 99% (210 nm), > 99% (254 nm), (method 1b).

tert-Butyl (5-((7-bromonaphthalen-1-yl)methyl)thiazol-2-yl)carbamate (37)

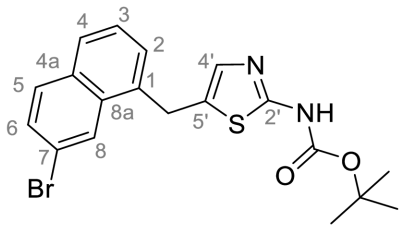

$C_{19}H_{19}BrN_2O_2S$

M_w = 419.34 g/mol

At room temperature, aminothiazole **35** (0.738 g, 2.31 mmol, 1 eq) was dissolved in toluene (75 mL) and di-*tert*-butyl dicarbonate (1.98 mL, 9.24 mmol, 4 eq) was added dropwise. After the reaction mixture was stirred at 100 °C for 4.5 h, the solvent was evaporated *in vacuo*. The crude product was purified *via* flash column chromatography (hexanes/EtOAc 8:2) to yield the title compound as a beige solid (828 mg, 1.98 mmol, 85%).

R_f: 0.22 (hexanes/EtOAc 8:2).
m.p.: 296 -299 °C.

^{1}H NMR (400 MHz, DMSO-d_6) δ [ppm] = 11.25 (s, 1H, NHCO), 8.32 (d, J = 2.0 Hz, 1H, 8-H), 7.93 (d, J = 8.8 Hz, 1H, 5-H), 7.87 (m, 1H, 4-H), 7.65 (dd, J = 8.8, 1.9 Hz, 1H, 6-H), 7.56 – 7.48 (m, 2H, 2-H, 3-H), 7.19 (s, 1H, 4'-H), 4.52 (s, 2H, CH_2), 1.41 (s, 9H, $C(CH_3)_3$).

^{13}C NMR (126 MHz, DMSO-d_6) δ [ppm] = 158.4 (C-2'), 152.7 (NHCO), 135.7 (C-1), 134.9 (C-4'), 132.3 (C-8a), 132.1 (C-4a), 130.9 (C-5), 130.4 (C-5'), 128.9 (C-6), 127.8 (C-2), 127.4 (C-4), 126.4 (C-3), 126.0 (C-8), 119.8 (C-7), 80.9 ($\underline{C}(CH_3)_3$), 29.3 (CH_2), 27.8 ($C(CH_3)_3$).

IR (ATR) $\tilde{\nu}$ [cm^{-1}] = 2726, 1710, 1579, 1546, 1495, 1447, 1391, 1368, 1321, 1297, 1251, 1236, 1080, 1056, 1028, 880, 860, 844, 825, 809, 763, 750, 683.

HRMS (ESI): *m/z* = $[M-H]^-$ calculated for $C_{19}H_{18}{}^{79}BrN_2S^-$: 417.0278; found: 417.0285.

Purity (HPLC): > 98% (210 nm), > 99% (254 nm), (method 1a).

tert-Butyl (5-((7-(4,4,5,5-tetramethyl-1,3,2-dioxaborolan-2-yl) naphthalene-1-yl)methyl)thiazol-2-yl)carbamate (38)

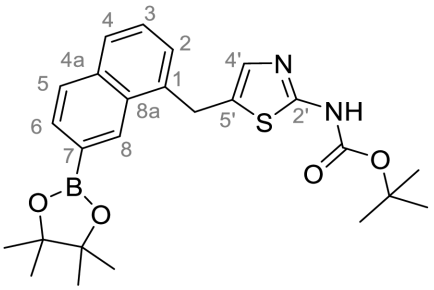

$C_{25}H_{31}BN_2O_4S$

M_w = 466.41 g/mol

At room temperature, bromo compound **37** (804 mg, 1.92 mmol, 1.00 eq), B_2Pin_2 (1.46 g, 5.75 mmol, 3.00 eq), KOAc (753 mg, 7.67 mmol, 4.00 eq) and Pd(dppf)Cl_2 · CH_2Cl_2 (281 mg, 0.383 mmol, 0.200 eq) were weighed out into a flask, which was put under nitrogen afterwards. Degassed anhydrous 1, 4-dioxane (15 mL) was added *via* syringe and the reaction mixture was stirred for 1 h at 80 °C and then for another 2 hours at room temperature under nitrogen atmosphere. Subsequently the mixture was diluted with water (100 mL) and brine (100 mL) and extracted with EtOAc (3 x 100 mL). The combined organic layers were dried over sodium sulfate. After evaporating the solvent *in vacuo*, the crude product was purified *via* flash column chromatography (hexanes/EtOAc 10:0 → 10:2) to yield the title compound as a beige solid (456 mg, 0.978 mmol, 51%).

R_f: 0.33 (hexanes/EtOAc 10:2).
m.p.: 203 °C.

^{1}H NMR (400 MHz, DMSO-d_6) δ [ppm] = 11.24 (s, 1H, NHCO), 8.49 (s, 1H, 8-H), 7.93 (d, *J* = 8.2 Hz, 1H, 5-H), 7.85 (d, *J* = 8.1 Hz, 1H, 4-H), 7.73 (dd, *J* = 8.2, 1.0 Hz, 1H, 6-H), 7.53 (dd, *J* = 8.2, 7.0 Hz, 1H, 3-H), 7.45 (d, *J* = 7.0 Hz 1H, 2-H), 7.13 (s, 1H, 4'-H), 4.55 (s, 2H, CH_2), 1.41 (s, 9H, $C(CH_3)_3$), 1.33 (s, 12H, $O_2C_2(CH_3)_4$).

^{13}C NMR (101 MHz, DMSO-d_6) δ [ppm] = 158.4 (C-2'), 152.7 (NHCO), 136.8 (C-1), 135.1 (C-4a), 134.9 (C-4), 131.3 (C-8), 130.34 (C-5'), 130.31 (C-8a), 130.0 (C-6), 128.0 (C-5), 127.2 (C-4), 126.8 (C-3), 126.7 (C-2), 125.4 (C-7), 83.8 ($O_2\underline{C}_2(CH_3)_4$), 80.9 ($\underline{C}(CH_3)_3$), 29.3 ($CH_2$), 27.8 ($C(CH_3)_3$), 24.7 ($O_2C_2(CH_3)_4$).

IR (ATR) $\tilde{\nu}$ [cm^{-1}] = 2975, 1719, 1624, 1568, 1457, 1369, 1341, 1309, 1251, 1240, 1142, 1090, 1059, 1009, 982, 962, 836, 804, 768, 755, 690.

HRMS (ESI): *m/z* = [M-H]$^-$ calculated for $C_{25}H_{30}BN_2O_4S^-$: 465.2025; found: 465.2033.

Purity (HPLC): > 98% (210 nm), > 99% (254 nm), (method 1a).

5-((7-(4,4,5,5-Tetramethyl-1,3,2-dioxaborolan-2-yl)naphthalene -1-yl)methyl)thiazol-2-amine (36)

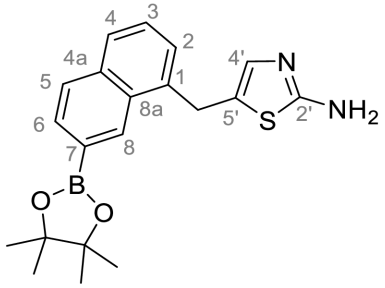

$C_{20}H_{23}BN_2O_2S$

M_w = 366.29 g/mol

At room temperature, dioxaborolane **38** (89.9 mg, 0.193 mmol, 1.00 eq) was dissolved in chloroform and TFA (1.43 mL, 19.3 mmol, 100 eq) was added and the reaction mixture was stirred for 17 h. After the mixture was allowed to cool to room temperature it was alkalized using NaOH (aq., 2 M, 100 mL), diluted with brine (50 mL) and extracted with DCM (4x 50 mL). The combined organic layers were dried over sodium sulfate. After evaporating the solvent *in vacuo*, the crude product was purified *via* flash column chromatography (DCM/MeOH 100:2) to yield the title compound as a light beige solid (23.3 mg, 0.0636 mmol, 79%).

R_f: 0.13 (DCM/MeOH 100:2).
m.p.: 87 °C.

^{1}H NMR (400 MHz, DMSO-d_6) δ [ppm] = 8.49 (s, 1H, 8-H), 7.92 (d, *J* = 8.2 Hz, 1H, 5-H), 7.83 (d, *J* = 8.2 Hz, 1H, 4-H), 7.73 (dd, *J* = 8.1, 1.0 Hz, 1H, 6-H), 7.51 (dd, *J* = 8.0, 7.0 Hz, 1H, 3-H), 7.42 (dd, *J* = 7.1, 1.3 Hz, 1H, 2-H), 6.67 (s, 2H, NH_2), 6.66 (s, 1H, 4'-H), 4.39 (s, 2H, CH_2), 1.34 (s, 12H, $O_2C_2(CH_3)_4$).

^{13}C NMR (101 MHz, DMSO-d_6) δ [ppm] = 167.7 (C-2'), 137.1 (C-1), 135.6 (C-4'), 135.0 (C-4a), 131.2 (C-8), 130.4 (C-8a), 130.0 (C-6), 127.9 (C-5), 127.0 (C-3), 126.5 (C-2), 125.2 (C-7), 124.2 (C-5'), 83.8 ($O_2\underline{C}_2(CH_3)_4$), 29.6 ($CH_2$), 24.7 ($O_2C_2(CH_3)_4$).

IR (ATR) $\tilde{\nu}$ [cm^{-1}] = 2976, 1623, 1519, 1458, 1372, 1343, 1298, 1272, 1233, 1212, 1141, 1092, 963, 887, 878, 837, 755, 693.

HRMS (ESI): *m/z* = $[M+H]^+$ calculated for $C_{20}H_{24}BN_2O_2S^+$: 367.1646; found: 367.1647.

Purity (HPLC): > 82% (210 nm), > 88% (254 nm), (method 1b).

(8-((2-((*tert*-Butoxycarbonyl)amino)thiazol-5-yl)methyl) naphthalen-2-yl)boronic acid (39)

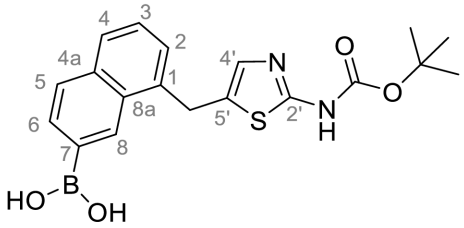

$C_{19}H_{21}BN_2O_4S$

M_w = 384.26 g/mol

At room temperature, dioxaborolane **38** (541 mg, 1.16 mmol, 1.00 eq) was dissolved in THF/water (3:1, 6 mL), subsequently sodium periodate (744 mg, 3.48 mmol, 3.00 eq) was added and the reaction mixture was stirred for 1 h. After aq. HCl (1 M, 1.16 mL, 1.00 eq) was added and the reaction was continued for another 3 h, then the mixture was extracted with EtOAc (3 x 50 mL). The combined organic layers were dried over sodium sulfate. After evaporating the solvent *in vacuo*, the crude product was purified *via* flash column chromatography (DCM/MeOH 100:2) to yield the title compound as a white solid (376 mg, 0.978 mmol, 84%).

R_f: 0.28 (DCM/MeOH 100:2).
m.p.: 194 °C (decomposition).

^{1}H NMR (400 MHz, DMSO-d_6) δ [ppm] = 11.21 (s, 1H, NHCO), 8.68 (s, 1H, 8-H), 8.23 (s, 2H, $B(OH)_2$), 7.88 – 7.86 (m, 2H, 5-H, 6-H), 7.80 (d, *J* = 8.1 Hz, 1H, 4-H), 7.48 (dd, *J* = 8.1, 7.0 Hz, 1H, 3-H), 7.42 (dd, *J* = 7.0, 1.3 Hz, 1H, 2-H), 7.19 (s, 1H, 4'-H), 4.54 (s, 2H, CH_2), 1.41 (s, 9H, $C(CH_3)_3$).

^{13}C NMR (126 MHz, DMSO-d_6) δ [ppm] = 158.3 (C-2'), 152.7 (NHCO), 137.0 (C-1), 134.8 (C-4), 134.6 (C-4a), 131.7 (C-7), 130.74 (C-6, C-8a), 130.6 (C-8), 130.5 (C-5'), 127.3 (C-5), 127.0 (C-4), 126.4 (C-3), 126.3 (C-2), 80.9 ($\underline{C}(CH_3)_3$), 29.2 (CH_2), 27.9 ($C(CH_3)_3$).

IR (ATR) $\tilde{\nu}$ [cm^{-1}] = 2976, 1716, 1624, 1558, 1458, 1368, 1346, 1306, 1250, 1151, 1094, 1061, 1024, 837, 755, 697.

HRMS (ESI): *m/z* = $[M+H]^+$ calculated for $C_{19}H_{22}BN_2O_4S^+$: 385.1388; found: 358.1388.

Purity (HPLC): > 99% (210 nm), > 99% (254 nm), (method 1a).

(8-((2-Aminothiazol-5-yl)methyl)naphthalen-2-yl)boronic acid (40)

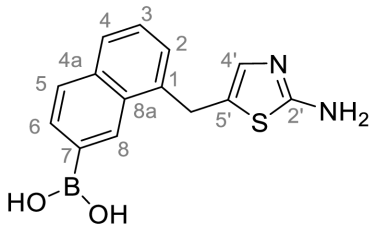

$C_{14}H_{13}BN_2O_2S$

M_w = 284.15 g/mol

At room temperature, boc-protected aminothiazole **39** (407 mg, 1.06 mmol, 1.00 eq) was dissolved in chloroform (10 mL) and TFA (3.98 mL, 53.0 mmol, 50.0 eq) and the reaction mixture was stirred for 17 h. Subsequently brine (15 mL) was added, and the solution was alkalized using NaOH (2.33 g, 58.3 mmol, 55.0 eq). After collecting the organic phase, the aqueous phase was extracted using DCM/isopropanol (3 x 30 mL, 4:1) and EtOAc/isopropanol (3 x 30 mL, 4:1). The combined organic layers were dried over sodium sulfate and the solvent was evaporated *in vacuo* to yield the title compound as a light grey-white solid (302 mg, 1.06 mmol, quantitative).

R_f: 0.04 (DCM/MeOH 100:5).
m.p.: 286-281 °C (decomposition).

^{1}H NMR (500 MHz, DMSO-d_6) δ [ppm] = 8.69 (d, *J* = 1.1 Hz, 1H, 8-H), 8.21 (s, 2H, $B(OH)_2$), 7.90 – 7.82 (m, 2H, 5-H, 6-H), 7.77 (d, *J* = 8.1 Hz, 1H, 4-H), 7.46 (dd, *J* = 8.2, 7.0 Hz, 1H, 3-H), 7.37 (dd, *J* = 7.0, 1.2 Hz, 1H, 2-H), 6.74 (s, 1H, 4'-H), 6.64 (s, 2H, NH_2), 4.40 (s, 2H, CH_2).

^{13}C NMR (126 MHz, DMSO-d_6) δ [ppm] = 167.7 (C-2'), 137.3 (C-1), 135.6 (C-4'), 134.5 (C-4a), 131.6 (C-7) 130.8 (C-8), 130.5 (C-8a), 130.4 (C-6), 127.2 (C-5), 126.7 (C-4), 126.3 (C-3), 125.9 (C-2), 124.5 (C-5'), 29.6 (CH_2).

IR (ATR) $\tilde{\nu}$ [cm^{-1}] = 2929, 1599, 1554, 1515, 1456, 1379, 1315, 1256, 1157, 1051, 834, 754, 699.

HRMS (ESI): *m/z* = $[M+H]^+$ calculated for $C_{14}H_{14}BN_2O_2S^+$: 285.0864; found: 285.0863.

Purity (HPLC): ≥ 95% (210 nm), > 95% (254 nm), (method 1c).

(8-((2-(2-((4,6-Dimethylpyrimidin-2-yl)thio)acetamido)thiazol-5-yl) methyl)naphthalen-2-yl)boronic acid (FM206)

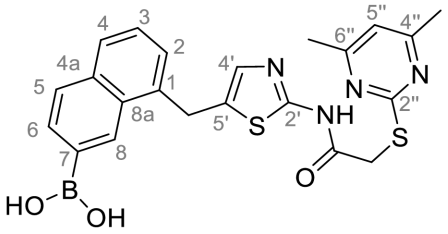

$C_{22}H_{21}BN_4O_3S_2$

M_w = 464.38 g/mol

Carboxylic acid **25** (212 mg, 1.07 mmol, 1.00 eq) was dissolved in anhydrous DMF (1 mL) and the solution was added *via* syringe to a previously prepared mixture of boronic acid **40** (304 mg, 1,07 mmol, 1.00 eq), DMAP (65.4 mg, 0.535 mmol, 0.500 eq) and EDC·HCl (251 mg, 1.28 mmol, 1.20 eq) in anhydrous DMF (5 mL). After reacting for 16 h at room temperature, water (100 mL) and brine (50 mL) was added, and the mixture was extracted with EtOAc (3 x 100 mL). After the combined organic layers were dried over sodium sulfate, the solvent was evaporated *in vacuo* and the crude product was purified *via* flash column chromatography (DCM/MeOH/NH_3 (aq., 25%) 100:5:0.05) to yield the title compound as a white solid (82.5 mg, 0.178 mmol, 17%).

R_f: 0.10 (DCM/MeOH/NH_3 (aq., 25%) 100:5:0.05).
m.p.: 153-157 °C (decomposition).

^{1}H NMR (500 MHz, DMSO-d_6) δ [ppm] = 12.17 (s, 1H, NHCO), 8.68 (s, 1H, 8-H), 8.20 (s, 2H, $B(OH)_2$), 7.88 – 7.84 (m, 2H, 5-H, 6-H), 7.79 (d, *J* = 8.1 Hz, 1H, 4-H), 7.47 (dd, *J* = 8.2, 7.0 Hz,

1H, 3-H), 7.41 (dd, *J* = 7.0, 1.3 Hz, 1H, 2-H), 7.27 (s, 1H, 4'-H), 6.92 (s, 1H, 5''-H), 4.57 (s, 2H, CH_2), 4.05 (s, 2H, CH_2S), 2.26 (s, 6H, 4-CH_3, 6-CH_3).

^{13}C NMR (126 MHz, DMSO-d_6) δ [ppm] = 168.9 (C-2''), 167.0 (C-4'', C-6''), 166.8 (NHCO), 156.6 (C-2'), 136.8 (C-1), 134.8 (C-4'), 134.5 (C-4a), 131.7 (C-7), 131.2 (C-5'), 130.7 (C-8), 130.5 (C-6), 130.4 (C-8a), 127.2 (C-5), 127.0 (C-4), 126.33 (C-3), 126.27 (C-2), 116.1 (C-5''), 34.0 (CH_2S), 29.1 (CH_2), 23.2 (4-CH_3, 6-CH_3).

IR (ATR) $\tilde{\nu}$ [cm^{-1}] = 2928, 1691, 1623, 1583, 1533, 1438, 1385, 1313, 1265, 1163, 1030, 972, 893, 837, 758, 668.

HRMS (ESI): *m/z* = $[M+H]^+$ calculated for $C_{22}H_{22}BN_4O_3S_2^-$: 465.1221; found: 465.1220.

Purity (HPLC): > 98% (210 nm), > 98% (254 nm), (method 1a).

tert-Butyl (5-((7-cyanonaphthalen-1-yl)methyl)thiazol-2-yl)carbamate (41)

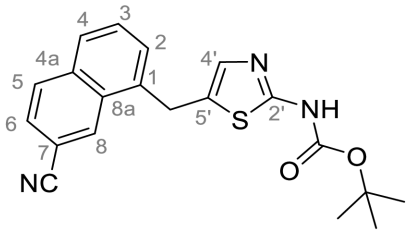

$C_{20}H_{19}N_3O_2S$

M_w = 365.46 g/mol

Under nitrogen atmosphere boc-protected aminothiazole **37** (50 mg, 0.119 mmol, 1.00 eq) was dissolved in anhydrous DMF (1 mL) and zinc cyanide (8.40 mg, 0.0715 mmol, 0.60 eq) as well as $Pd(PPh_3)_4$ (13.8 mg, 0.0119 mmol, 0.100 eq) were added. After the reaction mixture was stirred for 18 h at 80 °C, it was diluted with water (15 mL) and extracted with EtOAc (3 x 25 mL). After the combined organic layers were dried over sodium sulfate, the solvent was evaporated *in vacuo* and the crude product was purified *via* flash column chromatography (DCM/MeOH 100:0.5) to yield the title compound as a white solid (15.0 mg, 0.0410 mmol, 35%).

R_f: 0.15 (DCM/MeOH 100:0.5).

m.p.: 321-324 °C (decomposition).

^{1}H NMR (400 MHz, $CDCl_3$) δ [ppm] = 10.82 (s, 1H, NHCO), 8.39 (s, 1H, 8-H), 7.93 (d, *J* = 8.5 Hz, 1H, 5-H), 7.81 (d, *J* = 8.1 Hz, 1H, 4-H), 7.61 (dd, *J* = 8.5, 1.6 Hz, 1H, 6-H), 7.58 (dd, *J* = 8.2, 7.1 Hz, 1H, 3-H), 7.52 (dd, *J* = 7.1, 1.1 Hz, 1H, 2-H), 4.50 (s, 2H, CH_2), 1.44 (s, 9H, $C(CH_3)_3$).

^{13}C NMR (126 MHz, $CDCl_3$) δ [ppm] = 160.4 (C-2'), 152.8 (NHCO), 136.1 (C-1), 135.5 (C-4a), 134.5 (C-4'), 130.9 (C-8a), 130.21 (C-5), 130.20 (C-8), 129.8 (C-5'), 129.0 (C-3), 128.8 (C-2), 128.0 (C-4), 126.5 (C-6), 119.5 (CN), 109.9 (C-7), 82.2 ($\underline{C}(CH_3)_3$), 30.5 (CH_2), 28.3 ($C(CH_3)_3$).

IR (ATR) $\tilde{\nu}$ [cm^{-1}] = 2930, 2788, 2227, 1715, 1575, 1547, 1477, 1452, 1422, 1384, 1369, 1322, 1294, 1252, 1238, 1164, 1061, 1030, 972, 874, 862, 831, 808, 778, 769, 752.

HRMS (ESI): *m/z* = $[M-H]^-$ calculated for $C_{20}H_{18}N_3O_2S^-$: 364.1125; found: 364.1127.

Purity (HPLC): ≥ 92% (210 nm), > 92% (254 nm), (method 2c).

8-((2-Aminothiazol-5-yl)methyl)-2-naphthonitrile (42)

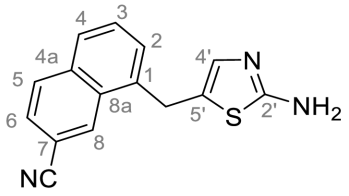

$C_{15}H_{11}N_3S$

M_w = 265.34 g/mol

Under nitrogen atmosphere nitrile **42** (500 mg, 1.57 mmol, 1.00 eq) was dissolved in anhydrous DMF (5 mL) and zinc cyanide (110 mg, 0.940 mmol, 0.600 eq) as well as $Pd(PPh_3)_4$ (181 mg, 0.157 mmol, 0.100 eq) were added. After the reaction mixture was stirred for 18 h at 80 °C, it was diluted with water (50 mL) and extracted with EtOAc (3 x 100 mL). After the combined organic layers were dried over sodium sulfate, the solvent was evaporated *in vacuo* and the crude product was purified *via* flash column chromatography (hexanes/EtOAc/NEt_3 3:7:0.1) to yield the title compound as a light yellow solid (254 mg, 0.957 mmol, 61%).

R_f: 0.29 (hexanes/EtOAc/NEt_3 3:7:0.1).

m.p.: 216-219 °C.

^{1}H NMR (500 MHz, DMSO-d_6) δ [ppm] = 8.75 (d, *J* = 1.6 Hz 1H, 8-H), 8.13 (d, *J* = 8.4 Hz, 1H, 5-H), 7.95 (d, *J* = 8.2 Hz, 1H, 4-H), 7.80 (dd, *J* = 8.5, 1.5 Hz, 1H, 6-H), 7.67 (dd, *J* = 8.2, 7.0 Hz, 1H, 3-H), 7.57 (dd, *J* = 7.2, 1.2 Hz, 1H, 2-H), 6.77 (s, 1H, 4'-H), 6.69 (s, 2H, NH_2), 4.46 (s, 2H, CH_2).

^{13}C NMR (126 MHz, DMSO-d_6) δ [ppm] = 167.8 (C-2'), 137.9 (C-1), 135.9 (C-4'), 134.94 (C-4a), 130.6 (C-8), 130.14 (C-8a), 130.13 (C-5), 129.1 (C-3), 128.0 (C-2), 127.3 (C-4), 126.2 (C-6), 124.0 (C-5'), 119.4 (CN), 108.5 (C-7), 29.5 (CH_2).

IR (ATR) $\tilde{\nu}$ [cm^{-1}] = 3397, 3283, 3116, 2221, 1629, 1517, 1438, 1377, 1326, 1310, 1270, 1204, 1160, 1120, 1052, 889, 861, 835, 794, 749, 721, 688.

HRMS (ESI): *m/z* = $[M+H]^+$ calculated for $C_{15}H_{12}N_3S^+$: 266.0746; found: 266.0745.

Purity (HPLC): > 93% (210 nm), ≥ 94% (254 nm), (method 2c).

N-(5-((7-Cyanonaphthalen-1-yl)methyl)thiazol-2-yl)-2-((4,6-dimethylpyrimidin-2-yl)thio)acetamide (FM295)

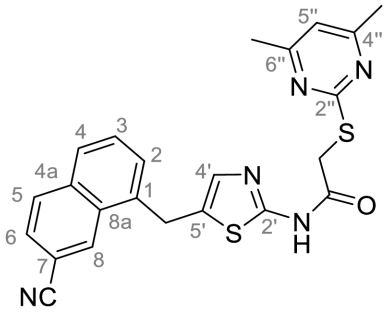

$C_{23}H_{19}N_5OS_2$

M_w = 445.57 g/mol

DIPEA (429 µL, 2.44 mmol, 3.00 eq) and HATU (371 mg, 0.976 mmol, 1.20 eq) were added to a solution of carboxylic acid **25** (194 mg, 0.976 mmol, 1.20 eq) in anhydrous DMF (3 mL) and the reaction mixture was stirred at room temperature for 1 h. Nitrile **25** (216 mg, 0.814 mmol, 1.00 eq) was added and the reaction mixture was stirred for another 18 h. Then the mixture was diluted with water (150 mL) and extracted with EtOAc (4 x 100 mL). The combined organic layers were dried over sodium sulfate. After evaporating the solvent *in vacuo*, the crude product was purified *via* flash column chromatography (hexanes/EtOAc 4:6) to yield the title compound as a white solid (105 mg, 0.235 mmol, 29%).

R_f: 0.42 (hexanes/EtOAc 4:6).

m.p.: 218-224 °C.

^{1}H NMR (500 MHz, DMSO-d_6) δ [ppm] = 12.20 (s, 1H, CONH), 8.75 (d, *J* = 1.6 Hz, 1H, 8-H), 8.13 (d, *J* = 8.4 Hz, 1H, 5-H), 7.97 (d, *J* = 8.2 Hz, 1H, 4-H), 7.80 (dd, *J* = 8.5, 1.5 Hz, 1H, 6-H), 7.68 (dd, *J* = 8.2, 7.0 Hz, 1H, 3-H), 7.61 (dd, *J* = 7.1, 1.3 Hz, 1H, 2-H), 7.33 (s, 1H, 4'-H), 6.92 (s, 1H, CH_2), 4.64 (s, 2H, CH_2S), 4.05 (s, 2H, CH_2S), 2.25 (s, 6H, 4-CH_3, 6-CH_3).

^{13}C NMR (126 MHz, DMSO-d_6) δ [ppm] = 168.9 (C-2''), 167.0 (C-4'', C-6''), 166.9 (NHCO), 156.8 (C-2'), 137.5 (C-1), 135.1 (C-4'), 135.0 (C-4a), 130.7 (C-5'), 130.6 (C-8), 130.2 (C-5), 130.1 (C-8a), 129.1 (C-3), 128.3 (C-2), 127.5 (C-4), 126.3 (C-6), 119.3 (CN), 116.1 (C-5''), 108.7 (C-7), 34.0 (CH_2S), 29.0 (CH_2), 23.2 (4-CH_3, 6-CH_3).

IR (ATR) $\tilde{\nu}$ [cm^{-1}] = 2897, 2221, 1687, 1581, 1530, 1429, 1374, 1322, 1258, 1243, 1161, 966, 876, 841, 819, 755, 715.

HRMS (ESI): *m/z* = $[M-H]^-$ calculated for $C_{23}H_{18}N_5OS_2^-$: 444.0958; found: 444.0956.

Purity (HPLC): > 98% (210 nm), > 98% (254 nm), (method 2b).

2-(8-((2-aminothiazol-5-yl)methyl)naphthalen-2-yl)acetonitrile (43)

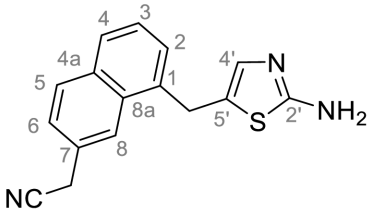

$C_{16}H_{13}N_3S$

M_w = 279.37 g/mol

Aminothiazole **35** (323 mg, 1.01 mmol, 1.00 eq) and 4-(4,4,5,5-tetramethyl-1,3,2-dioxaborolan-2-yl)isoxazole (237 mg, 1.22 mmol, 1.20 eq) were dissolved in DMF (1.21 mL). Subsequently a previously prepared aqueous solution (1 M, 513 µL) of potassium fluoride (29.8 mg, 0.513 mmol, 3.00 eq) was added and the mixture was degassed in an ultrasondic bath under nitrogen atmosphere. $Pd(dppf)Cl_2 \cdot CH_2Cl_2$ (12.5 mg, 0.0171 mmol, 0.100 eq) was added under nitrogen counterflow and the reaction mixture was stirred at 90 °C for 20 h. After the mixture was allowed to cool to room temperature it was diluted with water (50 mL) and brine (50 mL) and

extracted with EtOAc (3 x 50 mL). The combined organic layers were dried over sodium sulfate. After evaporating the solvent *in vacuo*, the crude product was purified *via* flash column chromatography (hexanes/EtOAc 1:1) to yield the title compound as a light brown solid (74.4 mg, 0.266 mmol, 26%).

R_f: 0.08 (hexanes/EtOAc 1:1).
m.p.: 220-203 °C.

^{1}H NMR (400 MHz, DMSO-d_6) δ [ppm] = 8.14 (d, *J* = 1.6 Hz, 1H, 8-H), 7.98 (d, *J* = 8.4 Hz, 1H, 5-H), 7.84 (dd, *J* = 8.1 ,1.6 Hz 1H, 4-H), 7.52 – 7.41 (m, 3H, 2-H, 3-H, 6-H), 6.77 (s, 1H, 4'-H), 6.66 (s, 2H, NH_2), 4.37 (s, 2H, CH_2), 4.23 (s, 2H, CH_2CN).

^{13}C NMR (101 MHz, DMSO-d_6) δ [ppm] = 168.2 (C-2'), 136.9 (C-1), 136.2 (C-4'), 133.1 (C-4a), 131.5 (C-8a), 129.9 (C-5), 129.5 (C-7), 127.44 (C-4), 127.37 (C-2), 126.5 (C-3), 126.0 (C-6), 124.7 (C-5'), 123.3 (C-8), 119.7 (CN), 30.2 (CH_2), 23.4 (CH_2CN).

IR (ATR) $\tilde{\nu}$ [cm^{-1}] = 3463, 3112, 1613, 1519, 1403, 1354, 1301, 1195, 1035, 930, 844, 825, 794, 770, 754, 673.

HRMS (ESI): *m/z* = $[M+H]^+$ calculated for $C_{16}H_{14}N_3S^+$: 280.0903; found: 280.0902.

Purity (HPLC): > 99% (210 nm), > 99% (254 nm), (method 2b).

_N_-(5-((7-(Cyanomethyl)naphthalen-1-yl)methyl)thiazol-2-yl)-2-((4,6-dimethylpyrimidin-2-yl)thio)acetamide (FM302)

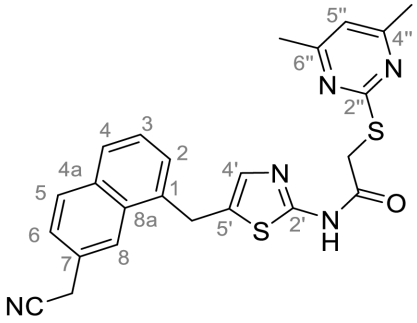

$C_{24}H_{21}N_5OS_2$

M_w = 459.60 g/mol

DIPEA (130 µL, 0.741 mmol, 3.00 eq) and HATU (141 mg, 0.370 mmol, 1.50 eq) were added to a solution of carboxylic acid **25** (73.4 mg, 0.370 mmol, 1.50 eq) in anhydrous DMF (0.5 mL) and the reaction mixture was stirred at room temperature for 1 h. Acetonitrile **43** (69.0 mg, 0.247 mmol, 1.00 eq) was added and the reaction mixture was stirred for another 18 h. Then the mixture was diluted with water (50 mL) and extracted with EtOAc (4 x 50 mL). The combined organic layers were dried over sodium sulfate. After evaporating the solvent *in vacuo*, the crude product was purified *via* flash column chromatography (hexanes/EtOAc 1:1) to yield the title compound as a white solid (45.5 mg, 0.0990 mmol, 40%).

R_f: 0.14 (hexanes/EtOAc 1:1).
m.p.: 179-182 °C.

^{1}H NMR (500 MHz, DMSO-d_6) δ [ppm] = 12.18 (s, 1H, NHCO), 8.13 (s, 1H, 8-H), 7.98 (d, *J* = 8.4 Hz, 1H, 5-H), 7.85 (dd, *J* = 6.5, 3.0 Hz, 1H, 4-H), 7.51 – 7.45 (m, 3H, 2-H, 3-H, 6-H), 7.31 (s, 1H, 4'-H), 6.92 (s, 1H, 5''-H), 4.54 (s, 2H, CH_2), 4.21 (s, 2H, CH_2CN), 4.05 (s, 2H, CH_2S), 2.26 (s, 6H, 4-CH_3, 6-CH_3).

^{13}C NMR (126 MHz, DMSO-d_6) δ [ppm] = 168.9 (C-2''), 168.0 (C-4'', C-6''), 166.8 (NHCO), 156.6 (C-2'), 136.0 (C-1), 134.9 (C-4'), 132.6 (C-4a), 131.0 (C-8a), 130.9 (C-5'), 129.5 (C-5), 129.2 (C-7), 127.20 (C-2, C-4), 126.03 (C-3), 125.95 (C-6), 122.9 (C-8), 119.2 (CN), 116.1 (C-5''), 34.0 (CH_2S), 29.3 (CH_2), 23.2 (4-CH_3, 6-CH_3), 22.9 (CH_2CN).

IR (ATR) $\tilde{\nu}$ [cm^{-1}] = 2925, 1687, 1580, 1549, 1524, 1505, 1434, 1403, 1340, 1280, 1260, 1229, 1177, 1155, 1121, 1035, 951, 932, 891, 845, 823, 792, 757, 717.

HRMS (ESI): *m/z* = $[M-H]^-$ calculated for $C_{24}H_{20}N_5O_4S_2^-$: 458.1115; found: 458.1113.

Purity (HPLC): > > 99% (210 nm), > 99% (254 nm), (method 2b).

N-(5-((7-Bromonaphthalen-1-yl)methyl)thiazol-2-yl)-2-((4,6-dimethylpyrimidin-2-yl)thio)acetamide (7-Bromo-SirReal2, FM315)

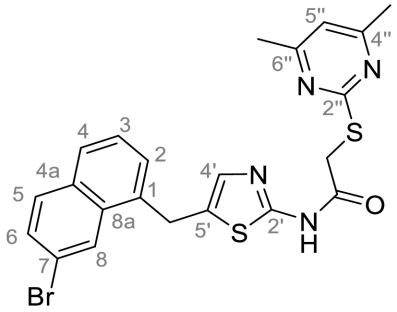

$C_{22}H_{19}BrN_4OS_2$

M_w = 499.46 g/mol

Carboxylic acid **25** (389 mg, 1.96 mmol, 1.00 eq) was dissolved in anhydrous DMF (1 mL) and the solution was added *via* syringe to a previously prepared mixture of aminothiazole **35** (627 mg, 1,96 mmol, 1.00 eq), DMAP (120 mg, 0.982 mmol, 0.500 eq) and EDC·HCl (461 mg, 2.36 mmol, 1.20 eq) in anhydrous DMF (5 mL). After reacting for 16 h at room temperature, water (50 mL) and brine (50 mL) was added, and the mixture was extracted with DCM (3 x 100 mL). After the combined organic layers were dried over sodium sulfate, the solvent was evaporated *in vacuo* and the crude product was purified *via* flash column chromatography (DCM/EtOAc 9:1) to yield the title compound as a white solid (509 mg, 1.02 mmol, 52%).

R_f: 0.41 (DCM/EtOAc 9:1).
m.p.: 209-210 °C.

^{1}H NMR (400 MHz, DMSO-d_6) δ [ppm] = 12.19 (s, 1H, NHCO), 8.31 (d, *J* = 1.9 Hz, 1H, 8-H), 7.93 – 7.85 (m, 2H, 4-H, 5-H), 7.64 (dd, *J* = 8.7, 1.9 Hz, 1H, 6-H), 7.53 – 7.50 (m, 2H, 2-H, 3-H), 7.28 (s, 1H, 4'-H), 6.92 (s, 1H, 5''-H), 4.55 (s, 2H, CH_2), 4.05 (s, 2H, CH_2S), 2.26 (s, 6H, 4-CH_3, 6-CH_3).

^{13}C NMR (101 MHz, DMSO-d_6) δ [ppm] = 168.9 (C-2''), 167.0 (C-4'', C-6''), 166.8 (NHCO), 156.7 (C-2'), 135.6 (C-1), 134.9 (C-4'), 132.3 (C-8a), 132.1 (C-4a), 130.89 (C-5, C-5'), 128.9

(C-6), 127.8 (C-2), 127.4 (C-4), 126.4 (C-3), 126.0 (C-8), 119.8 (C-7), 116.1 (C-5''), 34.0 (CH_2S), 29.2 (CH_2), 23.2 (4-CH_3, 6-CH_3).

IR (ATR) $\tilde{\nu}$ [cm^{-1}] = 2916, 2850, 1691, 1577, 1534, 1495, 1435, 1400, 1366, 1330, 1265, 1178, 1163, 1080, 1030, 1011, 973, 953, 893, 874, 859, 845, 819, 786, 763, 746, 718.

HRMS (ESI): *m/z* = [M-H]$^-$ calculated for $C_{22}H_{18}{}^{79}BrN_4OS_2^-$: 497.0111; found: 497.0107.

Purity (HPLC): > 99% (210 nm), ≥ 99% (254 nm), (method 1b).

Literature-known compound[40] was prepared using an alternate synthesis procedure.

2-((4,6-Dimethylpyrimidin-2-yl)thio)-*N*-(5-((7-formylnaphthalen-1-yl)methyl)thiazol-2-yl)acetamide (FM316)

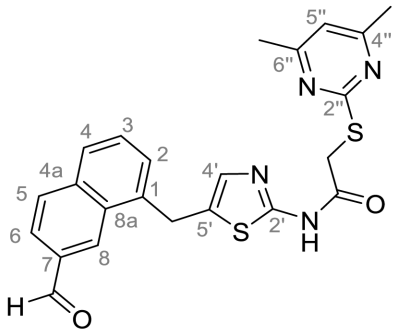

$C_{23}H_{20}N_4O_2S_2$

M_w = 448.57 g/mol

A flask was charged with **7-bromo-SirReal2** (**FM315**) (200 mg, 0.400 mmol, 1.00 eq), N-formylsaccharin (134 mg, 0.601 mmol, 1.5 eq), Na_2CO_3 (63.7 mg, 0.601 mmol, 1.50 eq), $Pd(OAc)_2$ (2.70 mg, 0.0120 mmol, 0.0300 eq) and DPPF (9.99 mg, 0.0180 mmol, 0.0450 eq), which was put under nitrogen afterwards. A degassed solution of triethylsilane (84.1 µL, 0.521 mmol, 1.30 eq) in anhydrous DMF (2 mL) was added dropwise under nitrogen atmosphere and the reaction mixture was stirred for 10 min at room temperature, then it was heated to 80 °C for 16 h. After cooling to room temperature, the mixture was diluted with water (100 mL) and extracted with DCM (3 x 50 mL). After the combined organic layers were dried over sodium sulfate, the solvent was evaporated *in vacuo* and the crude product was purified using two consecutive PTLCs (hexanes/EtOAc/NEt_3 5:5:0.1 and DCM/EtOAc 7:3) to yield the title compound as a white solid (18.8 mg, 0.0419 mmol, 11%).

R_f: 0.32 (DCM/EtOAc 7:3).

m.p.: 219-222 °C.

^{1}H NMR (500 MHz, DMSO-d_6) δ [ppm] = 11.43 (bs, 1H, NHCO), 10.02 (s, 1H, CHO), 8.45 (s, 1H, 8-H), 7.90 (d, *J* = 8.5 Hz, 1H. 5-H), 7.84 (dd, *J* = 8.5, 1.5 Hz, 1H, 6-H), 7.78 (d, *J* = 8.2 Hz, 1H, 4-H), 7.52 (dd, *J* = 8.3, 7.0 Hz, 1H, 3-H), 7.44 (d, *J* = 7.1 Hz, 1H, 2-H), 7.01 (s, 1H, 4'-H), 6.76 (s, 1H, 5''-H), 4.53 (s, 2H, CH_2), 3.76 (s, 2H, CH_2S), 2.40 (s, 6H, 4-CH_3, 6-CH_3).

^{13}C NMR (126 MHz, DMSO-d_6) δ [ppm] = 192.5 (CHO), 170.1 (C-2''), 168.5 (C-4'', C-6''), 167.7 (NHCO), 157.2 (C-2'), 137.9 (C-1), 137.5 (C-4a), 135.6 (C-4'), 134.6 (C-7), 131.9 (C-5'), 131.4 (C-8a), 130.5 (C-8), 130.4 (C-5), 129.3 (C-3), 128.4 (C-4), 128.2 (C-2), 123.0 (C-6), 117.2 (C-5''), 34.7 (CH_2S), 30.7 (CH_2), 23.9 (4-CH_3, 6-CH_3).

IR (ATR) $\tilde{\nu}$ [cm^{-1}] = 2961, 1921, 2852, 1691, 1580, 1533, 1434, 1368, 1341, 1297, 1259, 1231, 1168, 1187, 1168, 1134, 1014, 972, 886, 860, 794, 762, 751, 711.

HRMS (ESI): *m/z* = $[M+Na]^+$ calculated for $C_{23}H_{20}N_4NaO_2S_2^+$: 417.0920; found: 417.0919.

Purity (HPLC): ≥ 95% (210 nm), > 98% (254 nm), (method 2b).

2-((4,6-Dimethylpyrimidin-2-yl)thio)-*N*-(5-formylthiazol-2-yl)acetamide (46)

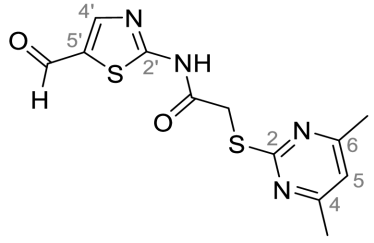

$C_{12}H_{12}N_4O_2S_2$

M_w = 308.39 g/mol

Carboxylic acid **25** (1.55 g, 7.80 mmol, 1.00 eq) was dissolved in DMF (5 mL) and added to a previously prepared solution of 2-aminothiazole-5-carbaldehyde (**45**, 1.00 g, 7.80 mmol, 1.00 eq), DMAP (0.477 g, 3.90 mmol, 0.50 eq) and EDC·HCl (1.83 g, 9.36 mmol, 1.20 eq) in 5 mL DMF. After stirring for 16 h at room temperature, the reaction mixture was diluted with water (400 mL) and extracted with EtOAc (3 x 100 mL). The combined organic layers were dried over sodium sulfate and filtered. After evaporating the solvent, the crude product was purified

via flash column chromatography (DCM/MeOH 100:1) to yield the title compound as a pale yellow solid (1.11 g, 3.61 mmol, 46%).

R_f: 0.22 (DCM/MeOH 100:1).
m.p.: 191-193 °C.

^{1}H NMR (400 MHz, DMSO-d_6) δ [ppm] = 13.02 (s, 1H, NHCO), 9.96 (s, 1H, CHO), 8.44 (s, 1H, 4'-H), 6.97 (s, 1H, 5-H), 4.18 (s, 2H, CH_2), 2.28 (s, 6H, 4-CH_3, 6-CH_3).

^{13}C NMR (101 MHz, DMSO-d_6) δ [ppm] = 184.6 (CHO), 169.2 (C-2), 168.9 (NHCO), 167.5 (C-4, C-6), 164.5 (C-2'), 151.2 (C-4') 132.6 (C-5'), 116.7 (C-5), 34.8 (CH_2), 23.7 (4-CH_3, 6-CH_3).

IR (ATR) $\tilde{\nu}$ [cm^{-1}] = 2924, 2137, 1688, 1664, 1586, 1555, 1516, 1427, 1385, 1311, 1268, 1234, 1173, 1123, 977, 872, 819, 733.

HRMS (ESI): *m/z* = [M-H]$^-$ calculated for $C_{12}H_{11}N_4O_2S_2^-$: 307.0329; found: 307.0330.

Purity (HPLC): > 99% (210 nm), > 99% (254 nm), (method 2b).

2-((4,6-Dimethylpyrimidin-2-yl)thio)-*N*-(5-(hydroxymethyl)thiazol-2-yl)acetamide (47)

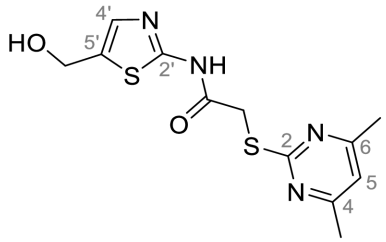

$C_{12}H_{14}N_4O_2S_2$
M_w = 310.40 g/mol

Aldehyde **46** (806 mg, 2.61 mmol, 1.00 eq) was dissolved in anhydrous methanol (5 mL) at 0 °C and sodium borohydride (148 mg, 3.92 mmol, 1.50 eq) was added in portions to the reaction mixture, which was stirred for 3 h. Water (5 mL) was added under stirring and the reaction mixture was allowed to warm to room temperature. After the solvent was removed under reduced pressure, aq. HCl (2 M, 100 mL) was added. The aqueous phase was washed with EtOAc (100 mL) and DCM (100 mL) and neutralized with aq. NaOH (2 M). The resulting precipitate was collected by filtration and washed with water (3 x 20 mL) and acetone (3 x 20 mL) to yield the title compound as a white solid. (635 mg, 2.05 mmol, 79%).

R_f: 0.27 (DCM/MeOH 100:5).
m.p.: 250-252 °C.

^{1}H NMR (400 MHz, DMSO-d_6) δ [ppm] = 12.22 (s, 1H, NHCO), 7.28 (d, *J* = 1.0 Hz, 1H, 4'-H), 6.96 (s, 1H, 5-H), 5.35 (t, *J* = 5.7 Hz, 1H, OH), 4.57 (dd, *J* = 5.7, 0.9 Hz, 2H, CH_2OH), 4.11 (s, 2H, CH_2S), 2.30 (s, 6H, 4-CH_3, 6-CH_3).

^{13}C NMR (101 MHz, DMSO-d_6) δ [ppm] = 168.9 (C-2), 167.02 (C-4, C-6), 166.9 (NHCO), 157.5 (C-2'), 134.5 (C-4') 133.1 (C-5'), 116.1 (C-5), 55.7 (CH_2OH), 34.1 (CH_2S), 23.2 (4-CH_3, 6-CH_3).

IR (ATR) $\tilde{\nu}$ [cm^{-1}] = 3284, 2917, 1696, 1588, 1537, 1323, 1273, 1262, 1161, 1037, 971, 843, 834, 788, 717.

HRMS (ESI): *m/z* = $[M-H]^-$ calculated for $C_{12}H_{13}N_4O_2S_2^-$: 309.0485; found: 309.0486.

Purity (HPLC): ≥ 90% (210 nm), > 96% (254 nm), (method 2b).

N-(5-(Bromomethyl)thiazol-2-yl)-2-((4,6-dimethylpyrimidin-2-yl)thio)acetamide (48)

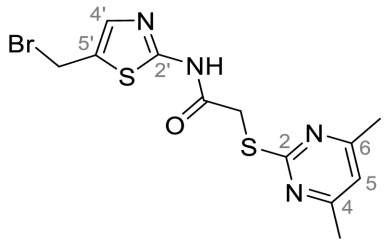

$C_{12}H_{13}BrN_4O_2S_2$
M_w = 373.30 g/mol

Primary alcohol **47** (267 mg, 0.860 mmol, 1.00 eq) was suspended in anhydrous DCM (10 mL) under nitrogen atmosphere and PBr_3 (88.9 µL, 0.946 mmol, 1.10 eq) was added dropwise, while stirring at room temperature. After 18 h the reaction mixture was filtered and the collected precipitate was washed with hexanes (3 x 20 mL) to yield the title compound as a beige solid (321 mg, 0.860 mmol, quantitative).

R_f: not detectable due to instability.
m.p.: 220-225 °C (decomposition).

^{1}H NMR (400 MHz, DMSO-d_6) δ [ppm] = δ 12.21 (s, 1H, NHCO), 7.28 (s, 1H, 4'-H), 6.96 (s, 1H, 5-H), 4.57 (s, 2H, CH_2Br), 4.11 (s, 2H, CH_2S), 2.30 (s, 6H, 4-CH_3, 6-CH_3).

^{13}C NMR (101 MHz, DMSO-d_6) δ [ppm] = δ 168.9 (C-2), 167.0 (C-4, C-6), 166.9 (NHCO), 157.5 (C-2'), 134.5 (C-4'), 133.0 (C-5'), 116.1 (C-5), 55.7 (CH_2Br), 34.1 (CH_2S), 23.3 (4-CH_3, 6-CH_3).

IR (ATR) $\tilde{\nu}$ [cm^{-1}] = 2837, 1707, 1623, 1417, 1363, 1333, 1278, 1147, 1003, 934, 834, 754.

HRMS (ESI): *m/z* = [M-^{79}Br+H_2O-2H]$^-$ calculated for $C_{12}H_{13}N_4O_2S_2^-$: 309.0485; found: 309.0486.

Purity (HPLC): not detectable due to instability.

2-((4,6-Dimethylpyrimidin-2-yl)thio)-*N*-(5-(4-hydroxybenzyl)thiazol-2-yl)acetamide (49)

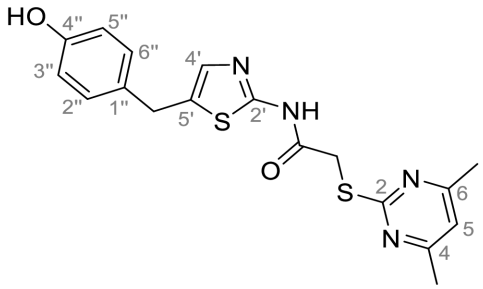

$C_{18}H_{18}N_4O_2S_2$

M_w = 386.50 g/mol

R_f: 0.71 (DCM/MeOH 100:2).

m.p.: 215-219 °C.

Under nitrogen atmosphere bromomethyl compound **48** (148 mg, 0.450 mmol, 1.00 eq), phenol (**44**, 42.4 mg, 0.450 mmol, 1.00 eq) and potassium carbonate (124 mg, 0.900 mmol, 2.00 eq) were suspended in anhydrous acetonitrile (5 mL). After the reaction mixture was stirred for 24 h at room temperature, water (15 mL) and brine (15 mL) were added, and it was extracted with DCM (3 x 50 mL). The combined organic layers were dried over sodium sulfate and the solvent was evaporated *in vacuo*. The crude product was purified *via* flash column chromatography (DCM/MeOH 100:1) to yield the title compound as a red solid (21.1 mg, 0.0546 mmol, 12%).

^{1}H NMR (500 MHz, DMSO-d_6) δ [ppm] = 12.17 (s, 1H, NHCO), 9.26 (s, 1H, OH), 7.20 (s, 1H, 4'-H), 7.06 – 6.99 (m, 2H, 2''-H, 6''-H), 6.96 (s, 1H, 5-H), 6.71 – 6.64 (m, 2H, 3''-H, 5''-H), 4.08 (s, 2H, CH_2S), 3.94 (s, 2H. CH_2), 2.29 (s, 6H, 4-CH_3, 6-CH_3).

^{13}C NMR (126 MHz, DMSO-d_6) δ [ppm] = 169.4 (C-2), 167.5 (C-4, C-6), 167.2 (NHCO), 157.2 (C-2'), 156.3 (C-4''), 134.7 (C-4'), 132.7 (C-5'), 130.8 (C-1''), 129.8 (C-2'', C-6''), 116.6 (C-5), 115.7 (C-3'', C-5''), 34.5 (CH_2S), 31.6 (CH_2), 23.7 (4-CH_3, 6-CH_3).

IR (ATR) $\tilde{\nu}$ [cm^{-1}] = 2921, 2852, 1682, 1588, 1543, 1515, 1453, 1365, 1342, 1286, 1260, 1221, 1156, 1114, 1098, 1030, 894, 855, 839, 821, 798, 763, 716.

HRMS (ESI): *m/z* = [M-H]$^-$ calculated for $C_{18}H_{17}N_4O_2S_2^-$: 385.0798; found: 385.0795.

Purity (HPLC): > 85% (210 nm), > 86% (254 nm), (method 2b).

2-((4,6-Dimethylpyrimidin-2-yl)thio)-*N*-(5-(methoxymethyl)thiazol-2-yl)acetamide (51)

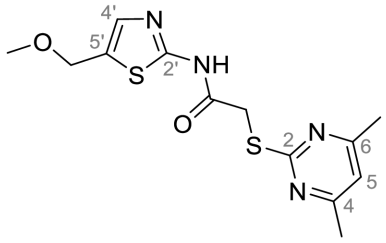

$C_{13}H_{16}N_4O_2S_2$

M_w = 324.43 g/mol

R_f: 0.40 (DCM/MeOH 100:4).

m.p.: 201-203 °C.

At room temperature bromomethyl compound **48** (50.0 mg, 0.134 mmol, 1.00 eq) was dissolved in anhydrous MeOH (500 µL, 12.3 mmol, 91.8 eq). Immediately after, the solvent was concentrated *in vacu* and the crude product was purified *via* flash column chromatography (DCM/MeOH 100:4) to yield the title compound as a white solid (43.4 mg, 0.134 mmol, quantitative).

^{1}H NMR (400 MHz, DMSO-d_6) δ [ppm] = 12.32 (s, 1H, NHCO), 7.40 (s, 1H, 4'-H), 6.96 (s, 1H, 5-H), 4.53 (s, 1H, CH_2O), 4.12 (s, 2H, CH_2S), 3.23 (s, 3H, OCH_3), 2.29 (s, 6H, 4-CH_3, 6-CH_3).

^{13}C NMR (101 MHz, DMSO-d_6) δ [ppm] = 168.9 (C-2), 167.1 (NHCO), 167.0 (C-4, C-6), 158.3 (C-2'), 136.9 (C-4'), 128.0 (C-5'), 116.1 (C-5), 65.6 (CH_2O), 56.9 (OCH_3), 34.1 (CH_2S), 23.2 (4-CH_3, 6-CH_3).

IR (ATR) $\tilde{\nu}$ [cm^{-1}] = 2923, 1686, 1584, 1534, 1327, 1265, 1161, 1086, 971, 948, 867, 837, 792, 722.

HRMS (EI): *m/z* = $[M]^{\bullet+}$ calculated for $C_{13}H_{16}N_4O_2S_2^{\bullet+}$: 324.0709; found: 324.0711.

Purity (HPLC): > 99% (210 nm), > 99% (254 nm), (method 2c).

N-(5-(Chloromethyl)thiazol-2-yl)-2-((4,6-dimethylpyrimidin-2-yl)thio)acetamide (52)

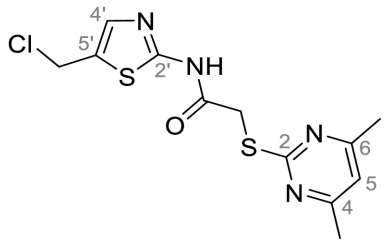

$C_{12}H_{13}ClN_4O_2S_2$

M_w = 328.85 g/mol

Primary alcohol **47** (358 mg, 1.15 mmol, 1.00 eq) was suspended in anhydrous DCM (15 mL) under nitrogen atmosphere and $SOCl_2$ (101 µL, 1.38 mmol, 1.20 eq) was added dropwise, while stirring at room temperature. After 18 h, *n*-hexane (5 mL) was added to the reaction mixture and the precipitate was collected by filtration. Subsequently the product was washed with *n*-hexane/DCM (1:1, 3 x 20 mL) to yield the title compound as a white solid (378 mg, 1.15 mmol, quantitative).

R_f: not detectable due to instability.
m.p.: 226-233 °C (decomposition).

^{1}H NMR (400 MHz, DMSO-d_6) δ [ppm] = 12.46 (s, 1H, NHCO), 7.53 (s, 1H, 3'-H), 6.96 (s, 1H, 5-H), 5.03 (s, 2H, CH_2S), 4.13 (s, 2H, CH_2Cl), 2.29 (s, 6H, 4-CH_3, 6-CH_3).

^{13}C NMR (101 MHz, DMSO-d_6) δ [ppm] = 168.8 (C-2), 167.4 (NHCO), 167.0 (C-4, C-6), 159.2 (C-2'), 138.2 (C-3'), 128.0 (C-4'), 116.2 (C-5), 38.7 (CH_2Cl), 34.1 (CH_2S), 23.2 (4-CH_3, 6-CH_3).

IR (ATR) $\tilde{\nu}$ [cm^{-1}] = 3270, 2421, 1720, 1624, 1602, 1582, 1540, 1417, 1370, 1333, 1307, 1268, 1158, 876, 849, 716, 703, 695 .

HRMS (ESI): *m/z* = [M-Cl+H_2O-2H]$^-$ calculated for $C_{12}H_{13}N_4O_2S_2^-$: 309.0485; found: 309.0483.

Purity (HPLC): not detectable due to instability.

2-((4,6-Dimethylpyrimidin-2-yl)thio)-*N*-(5-((4-hydroxynaphthalen-1-yl)methyl)thiazol-2-yl)acetamide (54)

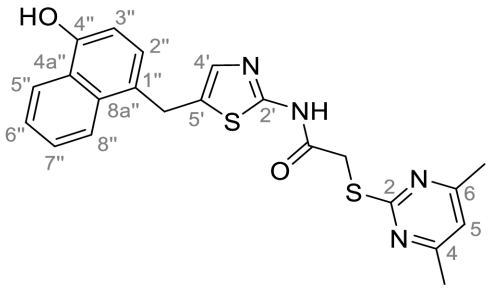

$C_{22}H_{20}N_4O_2S_2$

M_w = 436.56 g/mol

R_f: 0.17 (DCM/MeOH/NH_3 (aq., 25%) 100:3:0.05).

m.p.: 245-249 °C (decomposition).

Under nitrogen atmosphere chloromethyl compound **52** (131 mg, 0.398 mmol, 1.00 eq), 1-naphthol (**53**, 57.3 mg, 0.398 mmol, 1.00 eq) and potassium carbonate (110 mg, 0.795 mmol, 2.00 eq) were suspended in anhydrous DCM (5 mL). After the reaction mixture was stirred for 18 h at room temperature, water (15 mL) and brine (15 mL) were added, and it was extracted with DCM (3 x 50 mL). The combined organic layers were dried over sodium sulfate and the solvent was evaporated in vacuo. The crude product was purified via flash column chromatography (DCM/MeOH 100:1) to yield the title compound as a yellow solid (66 mg, 0.151 mmol, 38%).
In addition, the *ortho*-substituted byproduct **55** (12.1 mg, 0.0481 mmol, 12%) could be isolated as a yellow solid during the purification process. (Characterization of the byproduct is shown in the next entry).

Characterization of **54**:

^{1}H NMR (500 MHz, DMSO-d_6) δ [ppm] = 12.13 (s, 1H, NHCO), 10.06 (s, 1H, OH), 8.15 (dd, *J* = 8.2, 1.5 Hz, 1H, 5''-H), 7.99 (d, *J* = 8.5 Hz, 1H, 8''-H), 7.48 (ddd, *J* = 8.4, 6.8, 1.5 Hz, 1H, 7''-H), 7.43 (ddd, *J* = 8.1, 6.8, 1.3 Hz, 1H, 6''-H), 7.27-7.22 (m, 1H, 2''-H, 4''-H), 7.24 (s, 1H, 4'-H), 6.93 (s, 1H, 5-H), 6.80 (d, *J* = 7.7 Hz, 1H, 3''-H), 4.39 (s, 2H, CH_2), 4.04 (s, 2H, CH_2S), 2.26 (s, 6H, 4-CH_3, 6-CH_3).

^{13}C NMR (126 MHz, DMSO-d_6) δ [ppm] = 168.9 (C-2), 167.0 (C-4, C-6), 166.7 (NHCO), 156.3 (C-2'), 152.5 (C-4''), 134.3 (C-4'), 132.3 (C-5'), 132.1 (8a''), 127.1 (C-2''), 126.2 (C-7''), 126.3 (C-7''), 125.0 (C-4a''), 124.4 (6''), 123.7 (C-8''), 122.6 (C-5''), 116.1 (C-5), 107.4 (C-3''), 34.0 (CH_2S), 29.1 (CH_2), 23.2 (4-CH_3, 6-CH_3).

IR (ATR) $\tilde{\nu}$ [cm^{-1}] = 2923, 2852, 1691, 1583, 1566, 1537, 1413, 1384, 1354, 1304, 1267, 1225, 1167, 1102, 1008, 841, 817, 798, 753, 721.

HRMS (ESI): *m/z* = $[M+H]^+$ calculated for $C_{22}H_{21}N_4O_2S_2^+$: 437.1100; found: 437.1100.

Purity (HPLC): ≥ 97% (210 nm), ≥ 96% (254 nm), (method 2c).

2-((4,6-Dimethylpyrimidin-2-yl)thio)-*N*-(5-((1-hydroxynaphthalen-2-yl)methyl)thiazol-2-yl)acetamide (55)

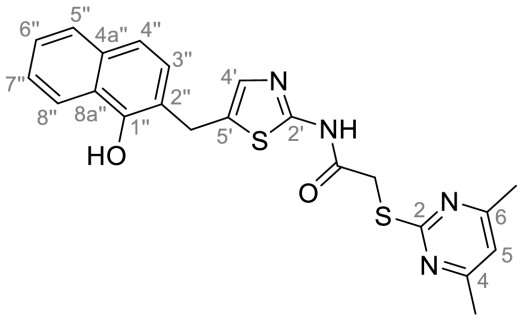

$C_{22}H_{20}N_4O_2S_2$

M_w = 436.56 g/mol

Byproduct of the above reaction.

R_f: 0.18 (DCM/MeOH/NH_3 (aq., 25%) 100:3:0.05).

m.p.: 229-234 °C (decomposition).

^{1}H NMR (500 MHz, DMSO-d_6) δ [ppm] = 12.14 (s, 1H, NHCO), 9.43 (s, 1H, OH), 8.22 (m, 1H, 8''-H), 7.79 (dd, *J* = 7.1, 2.3 Hz, 1H, 5''-H), 7.49 – 7.40 (m, 2H, , 6''-H, 7''-H), 7.36 (d, *J* = 8.3 Hz, 1H, 4''-H), 7.28 (d, *J* = 8.4 Hz, 1H, 3''-H), 7.24 (s, 1H, 4'-H), 6.93 (s, 1H, 5-H), 4.21 (s, 2H, CH_2), 4.06 (s, 2H, CH_2S), 2.27 (s, 6H, 4-CH_3, 6-CH_3).

713C NMR (126 MHz, DMSO-d_6) δ [ppm] = 168.9 (C-2), 167.0 (C-4, C-6), 166.7 (NHCO), 156.7 (C-2'), 149.2 (C-2''), 134.4 (C-4'), 133.3 (C-1''), 131.4 (C-5'), 128.3 (C-3''), 127.5 (C-5''), 125.5 (C-6''), 125.3 (C-4a''), 124.9 (C-7''), 122.0 (C-8''), 121.1 (C-8a''), 119.5 (C-4''), 116.1 (C-5), 34.0 (CH_2), 26.7 (CH_2S), 23.2 (4-CH_3, 6-CH_3).

IR (ATR) $\tilde{\nu}$ [cm^{-1}] = 2923, 2851, 1696, 1578, 1537, 1513, 1433, 1388, 1358, 1322, 1295, 1245, 1218, 1178, 1157, 1081, 1027, 970, 841, 785, 748, 731, 715.

HRMS (ESI): *m/z* = $[M+H]^+$ calculated for $C_{22}H_{21}N_4O_2S_2^+$: 437.1100; found: 437.1100.

Purity (HPLC): > 99% (210 nm), > 99% (254 nm), (method 2c).

2-((4,6-Dimethylpyrimidin-2-yl)thio)-*N*-(5-(phenoxymethyl)thiazol-2-yl)acetamide (FM345)

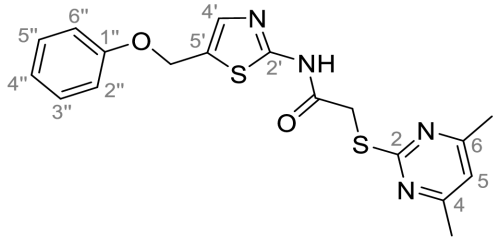

$C_{18}H_{18}N_4O_2S_2$

M_w = 386.50 g/mol

Chloromethyl compound **52** (154 mg, 0.468 mmol, 1.00 eq) and sodium phenolate (**56**, 54.4 mg, 0.468 mmol, 1.00 eq) were suspended in anhydrous DCM (20 mL) under nitrogen atmosphere and the reaction mixture was stirred for 24 h at room temperature. Following TLC monitoring, an additional equivalent of sodium phenolate (**56**, 54.4 mg, 0.468 mmol, 1.00 eq) was added to complete the reaction. After 2 h, the solvent was evaporated under reduced pressure. NaOH (aq., 2 M, 50 mL) was added to the residue and the mixture was extracted with EtOAc (4 x 75 mL). The combined organic layers were dried over sodium sulfate. After evaporating the solvent, the crude product was purified *via* flash column chromatography (DCM/MeOH 100:1) to yield the title compound as a white solid (33.0 mg, 0.0854 mmol, 18%).

R_f: 0.22 (DCM/MeOH 100:1).
m.p.: 160-163 °C.

^{1}H NMR (500 MHz, DMSO-d_6) δ [ppm] = 12.38 (s, 1H, NHCO), 7.54 (s, 1H, 4'-H), 7.33 – 7.25 (m, 2H, 3''-H, 5''-H), 7.03 – 6.98 (m, 2H, 2''-H, 5''-H), 6.98 – 6.91 (m, 2H, 4''-H, 5-H), 5.25 (s, 2H, CH_2O), 4.11 (s, 2H, CH_2S), 2.28 (s, 6H, 4-CH_3, 6-CH_3).

^{13}C NMR (126 MHz, DMSO-d_6) δ [ppm] = 168.9 (C-2), 167.2 (NHCO), 167.0 (C-4, C-6), 158.6 (C-2'), 157.7 (C-1''), 137.7 (C-4'), 129.5 (C-3'', C-5''), 126.6 (C-5'), 121.0 (C-4'), 116.1 (C-5), 115.0 (C-2'', C-6''), 61.8 (CH_2O), 34.1 (CH_2S), 23.2 (4-CH_3, 6-CH_3).

IR (ATR) $\tilde{\nu}$ [cm^{-1}] = 2916, 2159, 1688, 1583, 1539, 1496, 1384, 1312, 1270, 1238, 1171, 1139, 1008, 966, 883, 803, 749, 733, 687.

HRMS (ESI): *m/z* = $[M+H]^+$ calculated for $C_{18}H_{19}N_4O_2S_2^+$: 387.0944;
found: 387.0944.

Purity (HPLC): > 99% (210 nm), > 99% (254 nm), (method 1b).

N-(4-Hydroxyphenyl)thiophene-2-carboxamide (58)

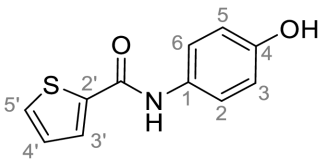

$C_{11}H_9NO_2S$
M_w = 219.26 g/mol

At room temperature, 4-aminophenol (**57**, 9.38 g, 86.0 mmol, 1.00 eq) was dissolved in DMF (30 mL) and pyridine (7.41 mL, 91.7 mmol, 1.07 eq) was added. The stirred reaction mixture was cooled to 0 °C, and 2-thiophenecarbonyl chloride (9.78 mL, 91.4 mmol, 1.06 eq) was subsequently added dropwise. After 1.5 h the reaction mixture was diluted with water (300 mL) and the mixture was extracted using EtOAc (4 x 100 mL). The combined organic layers were dried over sodium sulfate and concentrated *in vacuo* to obtain a viscous oil. The addition of DCM/hexanes (5 mL, 9:1) to the viscous oil induced the crystallization process. The obtained crystals were collected by filtration and washed with DCM/hexanes (9:1, 3 x 50 mL) to yield the title compound as a white-pink solid (13.0 g, 59.1 mmol, 69%).

R_f: 0.43 (hexanes/EtOAc 1:1).
m.p.: 192-195 °C.

^{1}H NMR (400 MHz, DMSO-d_6) δ [ppm] = 10.01 (s, 1H, NHCO), 9.27 (s, 1H, OH), 7.96 (dd, *J* = 3.8, 1.1 Hz, 1H, 3'-H), 7.81 (dd, *J* = 5.0, 1.2 Hz, 1H, 5'-H), 7.50 – 7.44 (m, 2H, 2-H, 6-H), 7.20 (dd, *J* = 5.0, 3.7 Hz, 1H, 4'-H), 6.77 – 6.72 (m, 2H, 3-H, 5-H).

13C NMR (101 MHz, DMSO-d_6) δ [ppm] = 159.4 (NHCO), 153.8 (C-4), 140.4 (C-2'), 131.3 (C-5'), 130.1 (C-1'), 128.5 (C-3'), 128.0 (C-4'), 122.4 (C-2, C-6), 115.0 (C-3, C-5).

IR (ATR) $\tilde{\nu}$ [cm^{-1}] = 3109, 1620, 1598, 1539, 1505, 1438, 1355, 1314, 1264, 1245, 1221, 1173, 1095, 884, 8299, 765, 739, 712.

HRMS (ESI): *m/z* = [M-H]$^-$ calculated for $C_{11}H_8NO_2S^-$: 218.0281; found: 218.0280.

Purity (HPLC): > 99% (210 nm), > 99% (254 nm), (method 1a).

N-(4-Hydroxyphenyl)-1-methyl-1*H*-pyrazole-4-carboxamide (60)

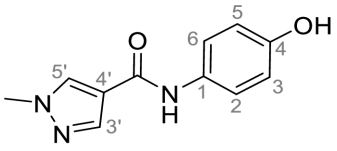

$C_{11}H_{11}N_3O_2$
M_w = 217.23 g/mol

DIPEA (3.80 mL, 22.0 mmol, 3.00 eq) and HATU (2.26 g, 5.95 mmol, 1.50 eq) were added to a solution of 1-methyl-1*H*-pyrazole-4-carboxylic acid (925 mg, 7.33 mmol, 1.00 eq) in anhydrous THF (15 mL) and the reaction mixture was stirred at room temperature for 1 h. 4-Aminophenol (**57**, 800 mg, 7.33 mmol, 1.00 eq) was added and the reaction mixture was stirred for another 3 h. Then the mixture was diluted with water (150 mL) and extracted with DCM (4 x 100 mL). The combined organic layers were dried over sodium sulfate. After evaporating the solvent *in vacuo*, the crude product was purified *via* flash column chromatography (hexanes/EtOAc 2:8) to yield the title compound as a white solid (239 mg, 1.10 mmol, 21%).

R_f: 0.25 (hexanes/EtOAc 2:8).
m.p.: 227-230 °C.

^{1}H NMR (400 MHz, DMSO-d_6) δ [ppm] = 9.57 (s, 1H, NHCO), 9.18 (s, 1H, OH), 8.24 (s, 1H, 5'-H), 7.96 (s, 1H, 3'-H), 7.48 – 7.40 (m, 2H, 2-H, 6-H), 6.75 – 6.67 (m, 2H, 3-H, 5-H), 3.87 (s, 3H, CH_3).

^{13}C NMR (101 MHz, DMSO-d_6) δ [ppm] = 160.0 (NHCO), 153.4 (C-4), 139.1 (C-3'), 132.3 (C-5'), 130.6 (C-1), 121.9 (C-2, C-6), 118.7 (C-4'), 115.0 (C-3, C-5), 38.8 (CH_3).

IR (ATR) $\tilde{\nu}$ [cm^{-1}] = 3347, 2926, 1641, 1601, 1558, 1509, 1430, 1388, 1308, 1273, 1201, 1151, 1099, 1005, 841, 812, 749, 703.

HRMS (ESI): *m/z* = $[M+H]^+$ calculated for $C_{11}H_{12}N_3O_2^+$: 218.0924; found:

Purity (HPLC): not detectable due to instability.

N-(4-((2-(2-((4,6-Dimethylpyrimidin-2-yl)thio)acetamido)thiazol-5-yl)methoxy)phenyl)thiophene-2-carboxamide (FM352)

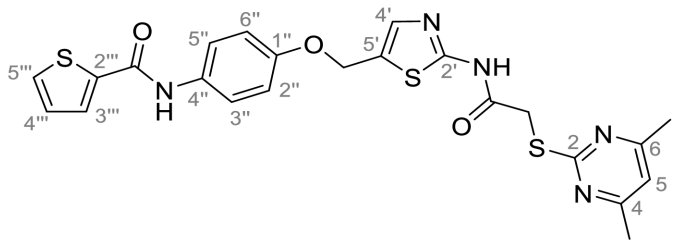

$C_{23}H_{21}N_5O_3S_3$

M_w = 511.65 g/mol

Under nitrogen atmosphere *N*-(4-hydroxyphenyl)thiophene-2-carboxamide (**58**, 268 mg, 1.22 mmol, 1.00 eq) was dissolved in anhydrous methanol (2 mL) and sodium methanolate (25 wt. % in MeOH, 272 µL, 1.22 mmol, 1.00 eq) was added at room temperature. The reaction mixture was stirred for 2 min, subsequently the solvent was evaporated. The residue was dried under high vacuum to yield sodium 4-(thiophene-2-carboxamido)phenolate (**59**) quantitatively, which was used without further purification for the next step. Chloromethyl compound **52** (123 mg, 0.374 mmol, 1.00 eq) and the previously prepared sodium 4-(thiophene-2-carboxamido)phenolate (**59**, 90.2 mg, 0.374 mmol, 1.00 eq) were suspended in anhydrous DCM (15 mL) and the reaction mixture was stirred for 18 h at room temperature. Following TLC monitoring, an additional equivalent of sodium 4-(thiophene-2-carboxamido)phenolate (**59**, 90.2 mg, 0.374 mmol, 1.00 eq) was added to complete the reaction. After 2 h, NaOH (aq., 2 M, 50 mL) was added, and the mixture was extracted with DCM (3 x 50 mL). The combined

organic layers were dried over sodium sulfate. After evaporating the solvent, the crude product was purified *via* flash column chromatography (DCM/MeOH 100:1) to yield the title compound as a white solid (31.5 mg, 0.0616 mmol, 17%).

R_f: 0.29 (DCM/MeOH 100:1).
m.p.: 176-179 °C.

^{1}H NMR (500 MHz, DMSO-d_6) δ [ppm] = 12.38 (s, 1H, 2'-NHCO), 10.11 (s, 1H, 4''-NHCO), 7.97 (d, *J* = 3.7 Hz, 1H, 3'''-H), 7.83 (d, *J* = 4.9 Hz, 1H, 5'''-H), 7.63 – 7.57 (m, 2H, 3''-H, 5''-H), 7.55 (s, 1H, 4'-H), 7.21 (t, *J* = 4.3 Hz, 1H, 4'''-H), 7.03 – 6.98 (m, 2H, 2''-H, 6''-H), 6.95 (s, 1H, 5-H), 5.25 (s, 2H, CH_2O), 4.12 (s, 2H, CH_2S), 2.28 (s, 6H, 4-CH_3, 6-CH_3).

^{13}C NMR (126 MHz, DMSO-d_6) δ [ppm] = 168.9 (C-2) , 167.2 (2'-NHCO), 167.0 (C-4, C-6), 159.6 (4''-NHCO), 158.6 (C-2'), 154.0 (C-1''), 140.2 (C-2'''), 137.8 (C-4'), 132.2 (C-4''), 131.5 (C-5'''), 128.8 (C-3'''), 128.0 (C-4'''), 126.6 (C-5'), 121.9 (C-3'', C-5''), 116.1 (C-5), 115.1 (C-2'', C-6''), 62.1 (CH_2O), 34.1 (CH_2S), 23.2 (4-CH_3, 6-CH_3).

IR (ATR) $\tilde{\nu}$ [cm^{-1}] = 2923, 2164, 1700, 1635, 1578, 1512, 1422, 1323, 1265, 1229, 1159, 1010, 845, 734.

HRMS (ESI): *m/z* = $[M-H]^-$ calculated for $C_{23}H_{20}N_5O_3S_3^-$: 510.0734; found: 510.0733.

Purity (HPLC): > 99% (210 nm), > 99% (254 nm), (method 1b).

N-(4-((2-(2-((4,6-Dimethylpyrimidin-2-yl)thio)acetamido)thiazol-5-yl)methoxy)phenyl)-1-methyl-1*H*-pyrazole-4-carboxamide (FM358)

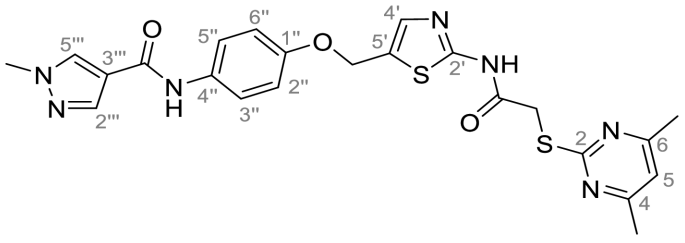

$C_{23}H_{23}N_7O_3S_2$
M_w = 509.61 g/mol

Under nitrogen atmosphere 1-methyl-1*H*-pyrazole-4-carboxylic acid (**60**, 294 mg, 1.35 mmol, 1.00 eq) was dissolved in anhydrous methanol (2 mL) and sodium methanolate (25 wt. % in

MeOH, 302 µL, 1.35 mmol, 1.00 eq) was added at room temperature. The reaction mixture was stirred for 2 min, subsequently the solvent was evaporated. The residue was dried under high vacuum to yield sodium 4-(1-methyl-1*H*-pyrazole-4-carboxamido)phenolate (**61**) quantitatively, which was used without further purification for the next step. Under nitrogen atmosphere chloromethyl compound **52** (150 mg, 0.456 mmol, 1.00 eq) and the previously prepared sodium 4-(1-methyl-1H-pyrazole-4-carboxamido)phenolate (**61**, 109 mg, 0.456 mmol, 1.00 eq) were suspended in anhydrous DCM (15 mL) and the reaction mixture was stirred for 18 h at room temperature. Following TLC monitoring, an additional equivalent of sodium 4-(1-methyl-1*H*-pyrazole-4-carboxamido)phenolate (**61**, 0.456 mmol, 109 mg, 1.00 eq) was added to complete the reaction. After 2 h, MeOH (1 mL) was added, and the reaction mixture was concentrated *in vacuo*. After evaporating the solvent, the crude product was purified *via* flash column chromatography (DCM/MeOH/AcOH 100:3:0.5) to yield the title compound as a white solid (87.1 mg, 0.171 mmol, 38%).

R_f: 0.07 (DCM/MeOH/AcOH 100:3:0.5).
m.p.: 188-191 °C.

^{1}H NMR (500 MHz, DMSO-d_6) δ [ppm] = 12.37 (s, 1H, 2'-NHCO), 9.68 (s, 1H, 4''-NHCO), 8.26 (s, 1H, 4'''-H), 7.97 (s, 1H, 2'''-H), 7.59 (m, 2H, 3''-H, 5''-H), 7.53 (s, 1H, 4'-H), 6.98 (m, 2H, 2''-H), 6.95 (s, 1H, 5-H) 5.23 (s, 2H, CH_2O), 4.11 (s, 2H, CH_2S), 3.88 (s, 3H, NCH_3), 2.28 (s, 6H, 4-CH_3, 6-CH_3).

^{13}C NMR (126 MHz, DMSO-d_6) δ [ppm] = 168.9 (C-2), 167.2 (s, 1H, 2'-NHCO), 167.0 (C-4, C-6), 160.1 (4''-NHCO), 158.8 (C-2'), 153.6 (C-1''), 138.7 (C-2'''), 137.7 (C-4'), 132.7 (C-4''), 132.5 (C-4'''), 126.6 (C-5'), 121.4 (C-3'', C-5''), 118.6 (C-3'''), 116.1 (C-5'''), 115.1 (C-2''', C-6'''), 62.2 (CH_2O), 38.8 (NCH_3), 34.2 (CH_2S), 23.2 (4-CH_3, 6-CH_3).

IR (ATR) $\tilde{\nu}$ [cm^{-1}] = 3285, 2923, 1692, 1640, 1578, 1559, 1512, 1489, 1438, 1413, 1378, 1325, 1268, 1226, 1172, 1158, 1007, 977, 870, 845, 820, 779, 757, 717.

HRMS (ESI): *m/z* = $[M-H]^-$ calculated for $C_{23}H_{22}N_7O_3S_2^-$: 508.1231; found: 508.1231.

Purity (HPLC): > 99% (210 nm), > 99% (254 nm), (method 1b).

2-((4,6-Dimethylpyrimidin-2-yl)thio)-*N*-(5-((naphthalen-1-yloxy)methyl) thiazol-2-yl)acetamide (FM368)

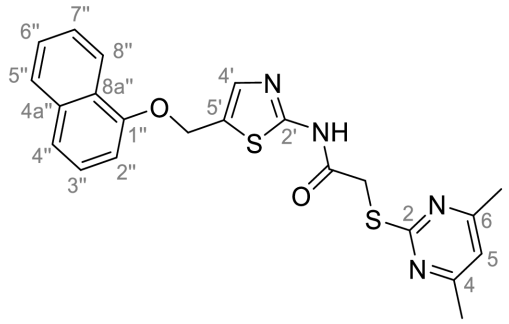

$C_{22}H_{20}N_4O_2S_2$

M_w = 436.56 g/mol

Under nitrogen atmosphere 1-naphthol (**53**, 377 mg, 2.61 mmol, 1.00 eq) was dissolved in anhydrous methanol (2 mL) and sodium methanolate (25 wt. % in MeOH, 583 µL, 2.61 mmol, 1.00 eq) was added at room temperature. The reaction mixture was stirred for 2 min, subsequently the solvent was evaporated. The residue was dried under high vacuum to yield sodium 1-naphtholate (**62**) quantitatively, which was used without further purification for the next step. Under nitrogen atmosphere chloromethyl compound **52** (150 mg, 0.456 mmol, 1.00 eq) and the previously prepared sodium 1-naphtholate (**62**, 75.8 mg, 0.456 mmol, 1.00 eq) were suspended in anhydrous acetone (5 mL) and the reaction mixture was stirred for 3 h at room temperature. Following TLC monitoring, an additional equivalent of sodium 1-naptholate (**62**, 75.8 mg, 0.456 mmol, 1.00 eq) was added to complete the reaction. After 2 h, water (50 mL) was added to the reaction mixture and the mixture was extracted with EtOAc (3 x 100 mL). The combined organic layers were dried over sodium sulfate. After evaporating the solvent *in vacuo*, the crude product was purified *via* flash column chromatography (DCM/MeOH 100:0.5) to yield the title compound as a white solid (28.0 mg, 0.0641 mmol, 14%).

R_f: 0.09 (DCM/MeOH 100:0.5).
m.p.: 181-183 °C.

^{1}H NMR (500 MHz, DMSO-d_6) δ [ppm] = 12.42 (s, 1H; NHCO), 8.09 (d, *J* = 8.1 Hz, 1H, 8''-H), 7.87 (d, *J* = 8.0 Hz, 1H, 5''-H), 7.63 (s, 1H, 4'-H), 7.55 – 7.40 (m, 4H, 3''-H, 4''-H, 6''-H, 7''-H), 7.14 (d, *J* = 7.6 Hz, 1H, 2''-H), 6.95 (s, 1H, 5-H), 5.47 (s, 2H, CH_2O), 4.13 (s, 2H, CH_2S), 2.29 (s, 6H, 4-CH_3, 6-CH_3).

^{13}C NMR (126 MHz, DMSO-d_6) δ [ppm] = 169.0 (C-2), 167.2 (NHCO), 167.0 (C-4, C-6), 158.7 (C-2'), 153.1 (C-1''), 137.6 (C-4'), 134.1 (C-4a''), 127.5 (C-5''), 126.7 (C-5'), 126.5 (C-3''), 126.1 (C-6''), 125.5 (C-7''), 125.0 (C-8a''), 121.4 (C-8''), 120.5 (C-4''), 116.1 (C-5), 106.1 (C-2''), 62.6 (CH_2O), 34.1 (CH_2S), 23.2 (4-CH_3, 6-CH_3).

IR (ATR) $\tilde{\nu}$ [cm^{-1}] = 2907, 1697, 1580, 1552, 1506, 1437, 1396, 1367, 1320, 1264, 1241, 1163, 1099, 1065, 1018, 975, 891, 874, 859, 834, 778, 768, 717.

HRMS (EI): *m*/*z* = $[M]^{\bullet+}$ calculated for $C_{22}H_{20}N_4O_2S_2^{\bullet+}$: 436.1028; found: 436.1032.

Purity (HPLC): > 99% (210 nm), > 99% (254 nm), (method 2c).

5.3 Supplementary data on methods and assays utilized: test procedure, assay condition, background details

5.3.1 MTT assay

Cytotoxicity was determined using a colorimetric MTT assay, following Mosmann's protocol[126] as performed by Martina Stadler (research group of Prof. Bracher) with HL-60 cells. The principle of this assay is to measure cell viability based on metabolic activity, which can be quantified through the NADH/NADPH-dependent reduction of MTT to the corresponding formazan derivative (see **Scheme 34**).

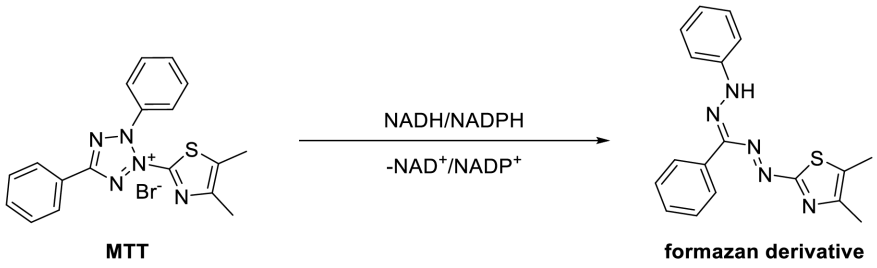

Scheme 34: NADH/NADPH-based reduction of yellow colored MTT (3-(4,5-dimethylthiazol-2-yl)-2,5-diphenyltetrazolium bromide) to blue colored MTT-formazan (1-(4,5-dimethylthiazol-2-yl)-3,5-diphenylformazan).

The amount of formed formazan derivative is proportional to the number of metabolically active cells and is characterized by photometric measurement of absorption at a wavelength of 570 nm. The derived IC_{50} value represents the concentration of the test substance at which cell viability is reduced to 50% compared to untreated control cells. IC_{50} values above 50 µM are considered non-toxic under the respective experimental conditions, providing only a general indication of cytotoxic potential without identifying specific modes of action or targets.

The MTT assay was performed using HL-60 cells (DSMZ number: ACC 3), purchased from DSMZ (German Collection of Microorganisms and Cell Cultures, Deutsche Sammlung von Mikroorganismen und Zellkulturen GmbH, Braunschweig, Germany) and cultivated (37 °C, 5 % CO_2 atmosphere) in RPMI medium supplemented with 10% fetal bovine serum. A cell density of 9 x 10^5 cells per mL was achieved using a Fuchs-Rosenthal counting chamber, and 99 µL of this cell suspension was transferred into the designated wells of a 96-well plate and incubated for 24 h at 37 °C with 5% CO_2.

In addition to the test substances (various final well concentrations prepared from a 10 mM stock solution), a positive control with Triton X-100® (final well concentration 1.00 µg/mL), a negative control with DMSO (final well concentration 1%) acting as reference were included. The final concentrations of the substances are related to the reaction volume of 100 µL per well.

Initially, the substances were pre-screened at a final concentration of 50 µM. If cytotoxic activity suggested an IC_{50} value of less than 50 µM, further testing to determine the respective IC_{50} values was conducted using a dilution series consisting of at least 5 descending 1:2 dilutions starting from 100 µM. To each well containing 99.0 µL of the cell suspension, 1.0 µL of the respective test compound solution, Triton X-100®, or DMSO was added. After an additional 24 hours incubation, 10 µL of MTT solution (5.0 mg/mL in PBS) was added to each well and incubated for another 2 hours. Following this, 190 µL of DMSO was added to dissolve the precipitated MTT-formazan derivative and the plate was shaken for 1 hour under light exclusion. Subsequently, the respective absorbance in each well was then measured at 570 nm using the MRX Microplate Reader (Dynex Technologies, Chantilly, USA) and the corresponding triplicate values were averaged.
The absorbance of the 1% DMSO negative control represented the untreated control cells and was used for normalization to 100% cell viability. Data processing was performed using Prism 8.0.2 (GraphPad Software, Boston, USA) software to perform sigmoid curve fitting for the calculation the respective IC_{50} values.

5.3.2 Agar diffusion assay

The agar diffusion assay was performed by Martina Stadler (research group of Prof. Bracher) using bacteria (*Escherichia coli, Pseudomonas marginalis, Staphylococcus equorum, Streptococcus entericus*) and yeasts (*Yarrowia lipolytica and Saccharomyces cerevisiae*) purchased at DSMZ (German Collection of Microorganisms and Cell Cultures, Deutsche Sammlung von Mikroorganismen und Zellkulturen GmbH, Braunschweig, Germany) and cultivated according to DSMZ specifications. A variety of culture media were prepared to address the individual requirements of the microorganisms (see **Table 7**).

mikroorganism	DSMZ number	culture media [in 1.0 L water]
Escherichia coli	426	agar (20 g), AC agar (35.2 g)
Pseudomonas marginalis	7527	agar (20 g), AC agar (35.2 g)
Staphylococcus equorum	20675	glucose (5.0 g), yeast extract (5.0 g), NaCl (5.0 g), casein peptone (10 g), agar (15 g)
Streptococcus entericus	14446	glucose (5.0 g), yeast extract (5.0 g), NaCl (5.0 g), casein peptone (10 g), agar (15 g)
Yarrowia lipolytica	1345	agar (20 g), AC agar (35.2 g)
Saccharomyces cerevisiae	1333	ac agar (35.2 g)

Table 7: Evaluated microorganisms, corresponding DSMZ number and the respective preparation of culture media. Abbreviation: AC agar (all-culture agar, purchased by Merk, Darmstadt, Germany)

After preparation, the culture media were autoclaved and 15.0 mL of each, still liquid, were directly filled into petri dishes under aseptic conditions and allowed to solidify for 1 h at 8 °C. The Petri dishes were then streaked with the respective microorganisms using cotton swabs and then covered with six substance-containing filter paper discs (d = 6.0 mm, Macherey-Nagel, Düren, Germany). Of the six filter paper discs, four comprise the test substances, one served as a DMSO negative control and one contained the reference substance (Clotrimazole for fungi, Tetracycline for bacteria). The different filter paper discs were previously treated with 3.00 µL of the respective substance (1% w/v solution prepared in DMSO) and stored at room temperature for 24 h. The test substances and the reference substances Clotrimazole and Tetracycline used as positive controls were prepared as a 1% (w/v) stock solution in DMSO. After sealing the agar plates, they were incubated for 36 h at 32 °C (bacteria) or 28 °C (fungi) and finally the diameter (mm) was measured manually. Larger inhibition zones correlate with stronger antimicrobial activity, which can be classified in relation to the respective reference substances. However, the agar diffusion test only provides information on the general antimicrobial activity and offers no information about corresponding mode of actions.

5.3.3 Sirtuin assays

The determination of inhibitory activity on Sirt2 and subtype selectivity (Sirt1, Sirt3 and Sirt5) of synthesized target substances and respective lead compounds was performed by Reaction Biology Corporation (Malvern, USA) using a fluorescence-based enzyme assay. The fundamental principle (see **Scheme 35**) of the assay systems employed, comprise peptide substrates with N-terminally acetylated lysine, which are additionally C-terminally coupled with a fluorophore (in this case 7-amino-4-methylcoumarin), which in this state is non-fluorescent. The deacetylation mediated by the corresponding sirtuins removes the acetyl group from the ε-amino group of the lysine residue in the peptide substrate, so that the now deacetylated substrate is recognized by a protease-based (usually trypsin) developer added in the following.

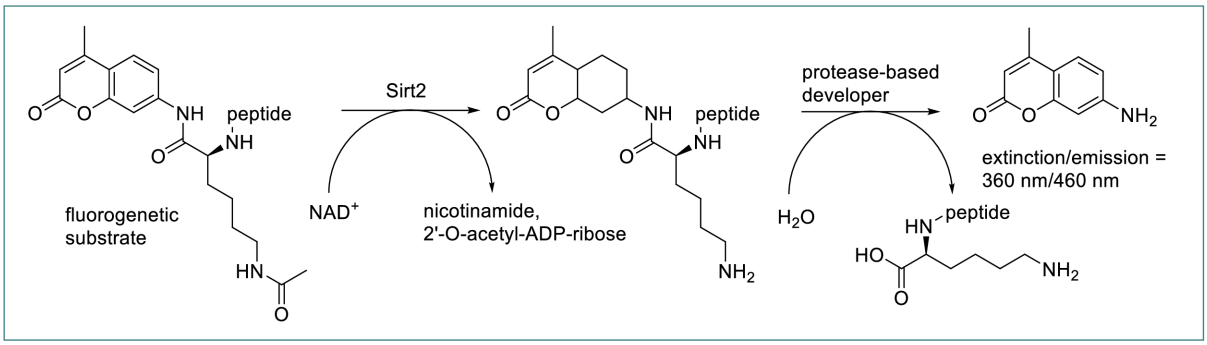

Scheme 35: General principle of inhibitor screening *via* fluorescence-based activity measurement, exemplified by a Sirt2 fluorogenic substrate peptide (cf. lit.[131]).

Proteolytically, the corresponding peptide bond at the C-terminus of lysine is cleaved and the fluorophore element previously bound to the substrate is liberated and can be quantified by its characteristic fluorescence. The enzyme activity is therefore directly proportional to the amount of fluorogenic substrate converted and thus to the fluorescence measured. Conversely, the inhibitor activity is indirectly proportional to the amount of fluorogenic substrate converted and thus to the fluorescence measured. [132-134]

The inhibitor screening was performed by Reaction Biology Corporation (Malvern, USA) according to an internal protocol. Based on the information provided, the test procedure and conditions are briefly outlined in the following.
Test substances were prepared in DMSO, delivered into the respective enzyme mixture (prepared with reaction buffer: Tris-HCl, pH = 8) and incubated for 10 minutes at 30 °C. Subsequently the substrate mixture (NAD^+ and fluorogenic substrate) was added to initiate the deacetylation reaction. After 2 hours incubation at 30 °C, 2 mM Nicotinamide (universal sirtuin inhibitor, to stop the reaction) and developer (to generate fluorescence) was added. At 30 °C 1 hour later, the respective fluorescence was measured (extinction/emission = 360 nm/460 nm). The inhibitory effect of the test compounds is indirectly proportional to the amount of converted fluorescent substrate standardized as 100 % activity of the control without inhibitor. The test substances were tested in 10-dose IC_{50} triplicate mode, with 3-fold serial dilution starting at 50 µM final reaction concentration and if necessary, starting at 100 µM. For each serially diluted replicate of the triplicate, an IC_{50} value was determined by sigmoidal curve fitting, resulting in three IC_{50} values, from which the mean and corresponding standard deviation were subsequently calculated. Data processing was performed based on Prism 8.0.2 software (GraphPad Software, Boston, USA).
Subtype selectivity on Sirt1, Sirt3 and Sirt5 was evaluated in a single dose duplicate mode at 50 µM final test compound concentration according to previous outlined internal protocol of Reaction Biology Cooperation by determining the enzyme activity of the respective sirtuins in % (no inhibitor control as 100% activity).

The following **Table 8** provides detailed measured values and results of the fluorescence-based activity measurements. This includes the IC_{50} values determined on Sirt2, and the enzyme activity determined on Sirt1, Sirt3 and Sirt5, each with corresponding standard deviation.

compound ID	IC_{50} (Sirt2) ± SD [µM]	subtype selectivity (residual enzyme activity [%] at 50 µM inhibitor concentration)		
		Sirt1	Sirt3	Sirt5
SirReal2	0.235 ± 0.008	n.d.	n.d.	n.d.
28a	7.676 ± 0.92	n.d.	n.d.	n.d.
28e	0.0867 ± 0.00853	n.d.	n.d.	n.d.
24a	0.0790 ± 0.00303	105 ± 2.68	86.4 ± 0.831	103 ± 2.29
7-Bromo-SirReal2	0.196 ± 0.0141	85.0 ± 0.0949	97.2 ± 1.81	79.5 ± 2.15
FM 26	1.23 ± 0.205	79.9 ± 0.226	93.6 ± 2.13	89.3 ± 2.07
FM 46	1.96 ± 0.233	99.6 ± 1.54	87.8 ± 0.357	99.0 ± 0.235
FM 47	1.28 ± 0.127	100 ± 0.843	99.6 ± 0.382	84.1 ± 0
FM 48	7.42 ± 2.41	93.9 ± 0.441	98.4 ± 1.19	84.4 ± 0.373
FM 50	0.374 ± 0.0359	92.6 ± 0.872	98.9 ± 0.0639	96.7 ± 0.198
FM 53	0.217 ± 0.0298	102 ± 2.47	102 ± 1.53	101 ± 1.38
FM 54	5.86 ± 1.58	99.4 ± 0.118	97.1 ± 1.32	89.4 ± 4.25
FM 56	10.4 ± 0.657	96.5 ± 0.431	96.2 ± 1.315	88.0 ± 0.142
FM 66	<100	n.d.	n.d.	n.d.
FM 69	0.152 ± 0.00905	106 ± 1.88	126 ± 3.91	103 ± 0.337
FM 94	4.62 ± 1.22	84.1 ± 0.397	81.8 ± 1.30	85.4 ± 0.968
FM 95	<100	n.d.	n.d.	n.d.
FM 96	<100	n.d.	n.d.	n.d.
FM 104	14.2 ± 3.90	86.3 ± 0.817	81.7 ± 0.431	78.0 ± 0.151
FM 108	78.7 ± 22.8	93.8 ± 0.784	91.6 ± 0.161	86.1 ± 0.553
FM 127	0.423 ± 0.0281	95.2 ± 0.966	97.0 ± 0.00261	86.6 ± 1.35
FM 128	6.22 ± 1.26	86.2 ± 0.915	68.0 ± 0.879	89.6 ± 0.0535
FM 129	1.17 ± 0.315	101 ± 4.10	85.5 ± 1.04	83.6 ± 0.218
FM 130	12.2 ± 1.30	83.7 ± 1.32	80.3 ± 0.574	78.4 ± 0.242
FM 131	0.613 ± 0.0292	93.3 ± 0.0500	109 ± 0.879	92.2 ± 0.685
FM161	4.54 ± 0.467	95.9 ± 1.34	85.6 ± 1.62	93.1 ± 0.160
FM166	28.1 ± 1.37	89.2 ± 0.515	90.3 ± 0.578	94.2 ± 0.677
FM167	9.016 ± 0.612	92.5 ± 3.37	92.9 ± 1.82	101 ± 1.97
FM206	0.235 ± 0,0151	99,9 ± 1,17	84,8 ± 1,25	98.1 ± 3.23
FM295	0.122 ± 0.00617	93.6 ± 0.165	90.7 ± 2.17	91.8 ± 2.44
FM302	0.235 ± 0.0151	99.9 ± 1.17	84.8 ± 1.25	98.1 ± 3.23
FM316	0.356 ± 0.0340	89.3 ± 0.511	87.2 ± 0.118	79.0 ± 2.92
FM320	0.235 ± 0.0296	91.3 ± 2.27	88.5 ± 1.45	77.4 ± 1.71
FM345	5.29 ± 0.732	95.6 ± 2.27	78.8 ± 0.800	94.6 ± 2.33

FM352	0.0935 ± 0.00636	101 ± 0.547	75.8 ± 5.33	75.6 ± 1.12
FM358	0.0656 ± 0.00441	71.9 ± 0.566	62.5 ± 0.138	79.8 ± 0.640
FM368	6.51 ± 0.837	88.5 ± 2.66	85.0 ± 0.53	89.1 ± 1.44

Table 8: Detailed overview of screening data, values given to three significant digits. For each serially diluted replicate of the triplicate, an IC_{50} value was determined based on sigmoidal curve fitting, and the mean and standard deviation (SD) were calculated from the three resulting IC_{50} values. The percentage enzyme activity of Sirt1, Sirt3 and Sirt5 in the presence of the corresponding test substances was determined at 50 µM in duplicate, giving the presented mean and corresponding standard deviation. IC_{50} values and enzyme activities of the respective test substances presented in the thesis refer to the averaged values. Values were presented and discussed in the thesis with a reasonable degree of accuracy to allow appropriate comparability with the lead compounds. Abbreviation: n.d. (not determined). Graphical editing and illustration were performed using Prism 8.0.2 software (GraphPad Software, Boston, USA).

5.4 Computational and crystallography methods

5.4.1 Docking simulations

Docking simulations were carried out by Dr. Thomas Wein using the Schrödinger software suite (Schrödinger Inc., New York city, USA, version 2020-3)[135].

Crystal structures of Sirt2 and respective lead structures were imported from the Protein Data Bank (PDB)[136]: (**SirReal2**: PDB ID: 4RMG[42]; **7-Bromo-SirReal2**: PDB ID: 5DY4[40]; **24a**: PDB ID: 5YQO[80]) and prepared with the Protein Preparation Wizard. All ligands were prepared with the Ligand Preparation Wizard using Epik for protonation and charge calculations.[137]

Docking was performed using Glide in standard precision mode SP (all docking parameters left to their default values). Results were inspected and visualized with Pymol 2.5.8 (Schrödinger Inc., New York city, USA). The top-ranking poses were analyzed, considering the favorable spatial orientation in relation to the crystal structures of the corresponding lead compounds.

5.4.2 Crystallographic studies

The implementation and principle of the crystallographic study was based on previously established procedure and conditions of published SirReal-inhibitors[40, 42] and carried out by PD Dr. Eva Huber (research group of Prof. Dr. Michael Groll) at the Center for Functional Protein Assemblies of the Technical University of Munich, Germany.

6 Appendices

6.1 Abbreviations

µM	micromolar
Å	Ångström
AC agar	all-culture agar
Ac_2O	acetic anhydride
AChE	acetylcholinesterase
AcOH	acetic acid
ADP	adenosine diphosphate
ALK2	activin receptor-like kinase-2
APCI	atmospheric pressure chemical ionization
aq.	aqueous
ATR	attenuated total reflexion
BETis	bromo-and extra-terminal domain inhibitors
Boc	*tert*-butoxycarbonyl
CAM	ceric ammonium molybdate
C-C coupling	carbon-carbon bond coupling
cf. lit	confere literature (compare)
CMBP	cyanomethylenetributylphosphoran
CO	carbon monoxide
COSY	correlation spectroscopy
d	doublet (NMR)
dba	dibenzylideneaceton
DCM	dichloromethane
DEPT	distortionless enhancement by polarization transfer
DIAD	diisopropyl azodicarboxylate
DIPEA	*N,N*-diisopropylethylamine
DMAP	4-dimethylaminopyridine

DMF	*N,N*-dimethylformamide
DMSO	dimethyl sulfoxide
DNA	deoxyribonucleic acid
DNMTis	DNA methyltransferase inhibitors
DNMTs	DNA methyltransferases
DNPH	1,3-dinitrophenylhydrazine
dppf	ferrocene-1,1′-diyl)bis(diphenylphosphane)
DSMZ	Deutsche Sammlung von Mikroorganismen und Zellkulturen
e.g.	exempli gratia (for example)
EC_{50}	half maximal effective concentration
ECS	extended C-site
EDC	3-{[(Ethylimino)methylidene]amino-N,N-dimethylpropan-1-amine
EHMTis	euchromatic histone-lysine N-methyltransferase 2 inhibitors
EI	electron impact ionization
eq.	equivalents
ESI	electron spray ionization
et. al.	et alii (and others)
EtOAc	ethylacetate
EtOH	ethanol
EZH2	enhancer of zeste homolog 2
FAD	flavin adenine dinucleotide
FDA	Food and Drug Administration
G	Gibbs energy of binding
H	enthalpy
HATs	Histone acetyltransferases
HATU	O-(7-azabenzotriazol-1-yl)-N,N,N′,N′-tetramethyluronium-hexafluorphosphat
H-bonds	hydrogen bond
HDAC	histone deacetylases

HDACis	histone deacetylase inhibitors
His	histidine
HIV-IN	retroviral integrase of human immunodeficiency viruses
HL-60	human leukemia (cell line)
HMBC	heteronuclear multiple-bond correlation spectroscopy
HMTi	EZH2 methyltransferase inhibitor
HMTs	histone methyltransferases
HPLC	high-performance liquid chromatography
HRMS	high-resolution mass spectrometry
HSQC	heteronuclear single-quantum correlation spectroscopy
IC_{50}	half maximal inhibitory concentration
ID	identifier
Ile	isoleucine
IR	infrared spectroscopy
J	coupling constant
KDMs	general term for lysine demethylases
k_i	inhibition constant
KMTs	general term for lysine methyltransferases
LdNMT	Leishmania N-myristoyltransferase
M	molarity
m	multiplet (NMR)
m.p.	melting point
m/z	mass-to-charge ratio
MAO	monoamine oxidases
MeOH	methanol
MTT	3-(4,5-dimethylthiazol-2-yl)-2,5-diphenyltetrazolium bromide
M_w	molecular weight
n.d.	not determined
NAD	nicotinamide adenine dinucleotide

NADP	nicotinamide adenine dinucleotide phosphate
NaOMe	sodium methoxide
NEt_3	triethylamine
nM	nanomolar
NMP	*N*-methylpyrrolidone
NMR	nuclear magnetic resonance spectroscopy
OAc	acetate
PBS	phosphate buffered saline
PDB	Protein Data Bank
pH	potential of hydrogen
ph	phenyl
pin	pinacol
PLC	preparative layer chromatography
PPh_3	triphenylphosphine
ppm	parts per million
q	quartet (NMR)
quant.	quantitative
RAR	retinoic acid receptors
R_f	retardation factor
RPMI	RPMI 1640 (cell culture medium for mammalian cells)
rt	room temperature
RXR	retinoid X receptor
s	singlet (NMR)
S	entropy
SAR	structure-activity relationship
SD	standard deviation
SirReal	sirtuin-rearranging ligands
sirt	Sirtuin
Sirt2	Sirtuin 2

T	temperature
t	triplett (NMR)
t-BuOK	potassium *tert*-butoxide
temp.	temperature
TETs	ten-eleven translocation enzymes
TFA	trifluoroacetic acid
THF	tetrahydrofuran
TLC	thin layer chromatography
TLC-MS	thin layer chromatography coupled with mass spectrometry
TNSK1	tankyrase 1
Tris	tris(hydroxymethyl)aminomethan
UV	ultraviolet
$\tilde{\nu}$	wavenumber
Val	valine
w/v	mass concentration
wt. %	weight percent
w/w	weight/weight
δ	chemical shift (commonly expressed in ppm)

6.2 References

[1] C. D. Allis, T. Jenuwein, *Nat Rev Genet* **2016**, *17*, 487-500.
[2] Y. Atlasi, H. G. Stunnenberg, *Nat Rev Genet* **2017**, *18*, 643-658.
[3] C. Biemont, *Heredity (Edinb)* **2010**, *105*, 1-3.
[4] K. Maeshima, S. Tamura, J. C. Hansen, Y. Itoh, *Curr Opin Cell Biol* **2020**, *64*, 77-89.
[5] K. Maeshima, S. Ide, M. Babokhov, *Curr Opin Cell Biol* **2019**, *58*, 95-104.
[6] K. Maeshima, R. Imai, S. Tamura, T. Nozaki, *Chromosoma* **2014**, *123*, 225-237.
[7] D. E. Handy, R. Castro, J. Loscalzo, *Circulation* **2011**, *123*, 2145-2156.
[8] S. Biswas, C. M. Rao, *Eur J Pharmacol* **2018**, *837*, 8-24.
[9] C. H. Arrowsmith, C. Bountra, P. V. Fish, K. Lee, M. Schapira, *Nat Rev Drug Discov* **2012**, *11*, 384-400.
[10] J. L. Miller, P. A. Grant, in *Epigenetics: Development and Disease* (Ed.: T. K. Kundu), Springer Netherlands, Dordrecht, **2013**, pp. 289-317.
[11] S. Rosa, P. Shaw, *Biology (Basel)* **2013**, *2,* 1378-410, figure/image adapted: permission link http://creativecommons.org/licenses/by/4.0/.
[12] M. I. Lind, F. Spagopoulou, *Heredity (Edinb)* **2018**, *121*, 205-209.
[13] M. R. Farani, M. Sarlak, A. Gholami, M. Azaraian, M. M. Binabaj, S. Kakavandi, M. M. Tambuwala, A. Taheriazam, M. Hashemi, S. Ghasemi, *Pathol Res Pract* **2023**, *248*, 154688.
[14] S. Heerboth, K. Lapinska, N. Snyder, M. Leary, S. Rollinson, S. Sarkar, *Genet Epigenet* **2014**, *6*, 9-19.
[15] F. Citron, L. Fabris, *Cancers* **2020**, *12,* 682*,* , figure/image adapted: permission link http://creativecommons.org/licenses/by/4.0/.
[16] S. F. Cai, C. W. Chen, S. A. Armstrong, *Mol Cell* **2015**, *60*, 561-570.
[17] T. Feehley, C. W. O'Donnell, J. Mendlein, M. Karande, T. McCauley, *Clin Epigenetics* **2023**, *15*, 6.
[18] M. Campbell, S. Hagemann, O. Heil, F. Lyko, B. Brueckner, *PLoS ONE* **2011**, *6*, e17388.
[19] A. J. Bannister, T. Kouzarides, *Cell Res* **2011**, *21*, 381-395.
[20] Y. Yang, M. Zhang, Y. Wang, *J Natl Cancer Cent* **2022**, *2*, 277-290.
[21] L. L. Marzochi, C. I. Cuzziol, C. Nascimento Filho, J. A. Dos Santos, M. M. U. Castanhole-Nunes, E. C. Pavarino, E. N. S. Guerra, E. M. Goloni-Bertollo, *Eur J Pharmacol* **2023**, *944*, 175590.
[22] V. M. Richon, *British Journal of Cancer* **2006**, *95*, S2-S6.
[23] A. D. Bondarev, M. M. Attwood, J. Jonsson, V. N. Chubarev, V. V. Tarasov, H. B. Schioth, *Br J Clin Pharmacol* **2021**, *87*, 4577-4597.
[24] G. A. Holdgate, C. Bardelle, A. Lanne, J. Read, D. H. O'Donovan, J. M. Smith, N. Selmi, R. Sheppard, *Drug Discov Today* **2022**, *27*, 1088-1098.
[25] R. Parveen, D. Harihar, B. P. Chatterji, *Cancer* **2023**, *129*, 3372-3380.
[26] G. Milazzo, D. Mercatelli, G. Di Muzio, L. Triboli, P. De Rosa, G. Perini, F. M. Giorgi, *Genes (Basel)* **2020**, *11*.
[27] S. Y. Park, J. S. Kim, *Exp Mol Med* **2020**, *52*, 204-212.
[28] Y. Liu, L. Wang, G. Yang, X. Chi, X. Liang, Y. Zhang, *Biomolecules* **2023**, *13,* 1210, figure/image adapted: permission link http://creativecommons.org/licenses/by/4.0/.
[29] Q. J. Wu, T. N. Zhang, H. H. Chen, X. F. Yu, J. L. Lv, Y. Y. Liu, Y. S. Liu, G. Zheng, J. Q. Zhao, Y. F. Wei, J. Y. Guo, F. H. Liu, Q. Chang, Y. X. Zhang, C. G. Liu, Y. H. Zhao, *Signal Transduct Target Ther* **2022**, *7*, 402.
[30] A. M. Curry, D. S. White, D. Donu, Y. Cen, *Front Physiol* **2021**, *12*, 752117.
[31] P.-T. Chen, K. Y. Yeong, *Medicinal Chemistry Research* **2024**, *33*, 1064-1078.
[32] H. Jing, H. Lin, *Chem Rev* **2015**, *115*, 2350-2375.
[33] Y. Wang, J. Yang, T. Hong, X. Chen, L. Cui, *Ageing Res Rev* **2019**, *55*, 100961.
[34] C. Zhu, X. Dong, X. Wang, Y. Zheng, J. Qiu, Y. Peng, J. Xu, Z. Chai, C. Liu, *Genet Res (Camb)* **2022**, *2022*, 9282484.

[35] J. Y. Hong, I. Fernandez, A. Anmangandla, X. Lu, J. J. Bai, H. Lin, *ACS Chem Biol* **2021**, *16*, 1266-1275.
[36] E. Pontiki, D. Hadjipavlou-Litina, *Medicinal Research Reviews* **2011**, *32*, 1-165.
[37] K. L. Bursch, C. J. Goetz, B. C. Smith, *Molecules* **2024**, *29*.
[38] J. Xue, X. Hou, H. Fang, *Pharmaceutical Science Advances* **2023**, *1*, 100010.
[39] W. Yang, W. Chen, H. Su, R. Li, C. Song, Z. Wang, L. Yang, *RSC Adv* **2020**, *10*, 37382-37390.
[40] M. Schiedel, T. Rumpf, B. Karaman, A. Lehotzky, J. Olah, S. Gerhardt, J. Ovadi, W. Sippl, O. Einsle, M. Jung, *J Med Chem* **2016**, *59*, 1599-1612.
[41] D. Robaa, D. Monaldi, N. Wossner, N. Kudo, T. Rumpf, M. Schiedel, M. Yoshida, M. Jung, *Chem Rec* **2018**, *18*, 1701-1707.
[42] T. Rumpf, M. Schiedel, B. Karaman, C. Roessler, B. J. North, A. Lehotzky, J. Oláh, K. I. Ladwein, K. Schmidtkunz, M. Gajer, M. Pannek, C. Steegborn, D. A. Sinclair, S. Gerhardt, J. Ovádi, M. Schutkowski, W. Sippl, O. Einsle, M. Jung, *Nature Communications* **2015**, *6,* 6263*,* image (figure 8, crystal structure SirReal2) permission link http://creativecommons.org/licenses/by/4.0/.
[43] M. Schiedel, T. Rumpf, B. Karaman, A. Lehotzky, S. Gerhardt, J. Ovadi, W. Sippl, O. Einsle, M. Jung, *Angew Chem Int Ed Engl* **2016**, *55*, 2252-2256.
[44] S. Sundriyal, S. Moniot, Z. Mahmud, S. Yao, P. Di Fruscia, C. R. Reynolds, D. T. Dexter, M. J. Sternberg, E. W. Lam, C. Steegborn, M. J. Fuchter, *J Med Chem* **2017**, *60*, 1928-1945.
[45] P. Mellini, Y. Itoh, E. E. Elboray, H. Tsumoto, Y. Li, M. Suzuki, Y. Takahashi, T. Tojo, T. Kurohara, Y. Miyake, Y. Miura, Y. Kitao, M. Kotoku, T. Iida, T. Suzuki, *J Med Chem* **2019**, *62*, 5844-5862.
[46] S. Swyter, M. Schiedel, D. Monaldi, S. Szunyogh, A. Lehotzky, T. Rumpf, J. Ovadi, W. Sippl, M. Jung, *Philos Trans R Soc Lond B Biol Sci* **2018**, *373*.
[47] E. Roshdy, M. Mustafa, A. E. Shaltout, M. O. Radwan, M. A. A. Ibrahim, M. E. Soliman, M. Fujita, M. Otsuka, T. F. S. Ali, *Eur J Med Chem* **2021**, *224*, 113709.
[48] Y. Jiang, J. Liu, D. Chen, L. Yan, W. Zheng, *Trends Pharmacol Sci* **2017**, *38*, 459-472.
[49] N. Djokovic, D. Ruzic, M. Rahnasto-Rilla, T. Srdic-Rajic, M. Lahtela-Kakkonen, K. Nikolic, *J Chem Inf Model* **2022**, *62*, 2571-2585.
[50] D. Kalbas, M. Meleshin, S. Liebscher, M. Zessin, J. Melesina, C. Schiene-Fischer, E. F. Bulbul, F. Bordusa, W. Sippl, M. Schutkowski, *Biochemistry* **2022**, *61*, 1705-1722.
[51] A. B. Penteado, H. Hassanie, R. A. Gomes, F. D. Silva Emery, G. H. Goulart Trossini, *Future Med Chem* **2023**, *15*, 291-311.
[52] S. G. Kaya, G. Eren, *Bioorg Chem* **2024**, *143, 07038, doi: 10.1016/j.bioorg.2023.107038; image/(figure 7) permitted by Elsevier and Copyright Clearance Center, License Number: 5853090718796.*
[53] L. Yang, X. Ma, C. Yuan, Y. He, L. Li, S. Fang, W. Xia, T. He, S. Qian, Z. Xu, G. Li, Z. Wang, *Eur J Med Chem* **2017**, *134, 230-241, doi: 10.1016/j.ejmech.2017.04.010, image (docking 28e, figure 8) permitted by Elsevier and Copyright Clearance Center, License Number: 5873501448336.*
[54] Z. Fang, Y. n. Song, P. Zhan, Q. Zhang, X. Liu, *Future Medicinal Chemistry* **2014**, *6*, 885-901.
[55] A. D. G. Lawson, M. MacCoss, J. P. Heer, *J Med Chem* **2018**, *61*, 4283-4289.
[56] K. Müller, H. Prinz, M. Lehr, *Pharmazeutische/Medizinische Chemie: Arzneistoffe - von der Struktur zur Wirkung*, Wissenschaftliche Verlagsgesellschaft, **2022**.
[57] G. Klebe, *Wirkstoffdesign: Entwurf und Wirkung von Arzneistoffen*, Spektrum Akademischer Verlag, **2009**.
[58] I. V. Komarov, V. A. Bugrov, A. Cherednychenko, O. O. Grygorenko, *The Chemical Record* **2023**, *24*.
[59] H. J. Böhm, G. Klebe, *Angewandte Chemie International Edition in English* **2003**, *35*, 2588-2614.
[60] B. Shroot, S. Michel, *Journal of the American Academy of Dermatology* **1997**, *36*, S96-S103.

[61] M. Lewandowski, M. Carmina, L. Knümann, M. Sai, S. Willems, T. Kasch, J. Pollinger, S. Knapp, J. A. Marschner, A. Chaikuad, D. Merk, **2023**.
[62] T. W. Johnson, S. P. Tanis, S. L. Butler, D. Dalvie, D. M. Delisle, K. R. Dress, E. J. Flahive, Q. Hu, J. E. Kuehler, A. Kuki, W. Liu, G. A. McClellan, Q. Peng, M. B. Plewe, P. F. Richardson, G. L. Smith, J. Solowiej, K. T. Tran, H. Wang, X. Yu, J. Zhang, H. Zhu, *J Med Chem* **2011**, *54*, 3393-3417.
[63] H. González-Álvarez, D. Ensan, T. Xin, J. F. Wong, C. A. Zepeda-Velázquez, J. Cros, M. N. Sweeney, L. Hoffer, T. Kiyota, B. J. Wilson, A. Aman, O. Roberts, M. B. Isaac, A. N. Bullock, D. Smil, R. Al-awar, *Journal of Medicinal Chemistry* **2024**, *67*, 4707-4725.
[64] Y. H. Chen, L. W. Qi, F. Fang, B. Tan, *Angew Chem Int Ed Engl* **2017**, *56*, 16308-16312.
[65] H.T. Bucherer, *J.Prakt. Chem* **1904**, *69*, 49-91.
[66] in *Name Reactions in Organic Synthesis* (Eds.: A. Parikh, H. Parikh, K. Parikh), Foundation Books, **2006**, pp. 82-85.
[67] S. J. Gilani, S. A. Khan, N. Siddiqui, S. P. Verma, P. Mullick, O. Alam, *Journal of Enzyme Inhibition and Medicinal Chemistry* **2010**, *26*, 332-340.
[68] Y. Gull, N. Rasool, M. Noreen, F. U. Nasim, A. Yaqoob, S. Kousar, U. Rasheed, I. H. Bukhari, M. Zubair, M. S. Islam, *Molecules* **2013**, *18*, 8845-8857.
[69] A. Kamlah, F. Bracher, *European Journal of Organic Chemistry* **2020**, *2020*, 2708-2719.
[70] A. Ganesan, *Philos Trans R Soc Lond B Biol Sci* **2018**, *373*.
[71] Y. Fang, G. Liao, B. Yu, *J Hematol Oncol* **2019**, *12*, 129.
[72] R. R. Ramsay, L. Basile, A. Maniquet, S. Hagenow, M. Pappalardo, M. C. Saija, S. D. Bryant, A. Albreht, S. Guccione, *Molecules* **2020**, *25*.
[73] R. Borštnar, M. Repič, M. Kržan, J. Mavri, R. Vianello, *European Journal of Organic Chemistry* **2011**, *2011*, 6419-6433.
[74] R. Poulin, L. Lu, B. Ackermann, P. Bey, A. E. Pegg, *Journal of Biological Chemistry* **1992**, *267*, 150-158.
[75] N. LoGiudice, L. Le, I. Abuan, Y. Leizorek, S. C. Roberts, *Med Sci (Basel)* **2018**, *6*.
[76] T. Asaba, T. Suzuki, R. Ueda, H. Tsumoto, H. Nakagawa, N. Miyata, *Journal of the American Chemical Society* **2009**, *131*, 6989-6996.
[77] B. C. Smith, J. M. Denu, *Biochemistry* **2007**, *46*, 14478-14486.
[78] P. Mellini, Y. Itoh, H. Tsumoto, Y. Li, M. Suzuki, N. Tokuda, T. Kakizawa, Y. Miura, J. Takeuchi, M. Lahtela-Kakkonen, T. Suzuki, *Chem Sci* **2017**, *8*, 6400-6408.
[79] C. Glas, dissertation: Structure-activity relationship analysis of the subtype-selective Sirt5 inhibitor balsalazide, Ludwig-Maximilians-Universität, München, **2021**.
[80] L. L. Yang, H. L. Wang, L. Zhong, C. Yuan, S. Y. Liu, Z. J. Yu, S. Liu, Y. H. Yan, C. Wu, Y. Wang, Z. Wang, Y. Yu, Q. Chen, G. B. Li, *Eur J Med Chem* **2018**, *155*, 806-823.
[81] Faridoon, R. Ng, G. Zhang, J. J. Li, *Med Chem Res* **2023**, *32*, 1039-1062.
[82] J. Schrader, F. Henneberg, R. A. Mata, K. Tittmann, T. R. Schneider, H. Stark, G. Bourenkov, A. Chari, *Science* **2016**, *353*, 594-598.
[83] J. Brayer, R. Baz, *Ther Adv Hematol* **2017**, *8*, 209-220.
[84] W. J. Metzler, J. Yanchunas, C. Weigelt, K. Kish, H. E. Klei, D. Xie, Y. Zhang, M. Corbett, J. K. Tamura, B. He, L. G. Hamann, M. S. Kirby, J. Marcinkeviciene, *Protein Sci* **2008**, *17*, 240-250.
[85] D. Oksenberg, K. Dufu, M. P. Patel, C. Chuang, Z. Li, Q. Xu, A. Silva-Garcia, C. Zhou, A. Hutchaleelaha, L. Patskovska, Y. Patskovsky, S. C. Almo, U. Sinha, B. W. Metcalf, D. R. Archer, *British Journal of Haematology* **2016**, *175*, 141-153.
[86] H. A. Blair, *Drugs* **2020**, *80*, 209-215.
[87] P. Huang, A. Lv, Q. Yan, Z. Jiang, S. Yang, *Acta Crystallogr D Struct Biol* **2022**, *78*, 735-751.
[88] H. Kuramochi, H. Nakata, S.-i. Ushuj, *The Journal of Biochemistry* **1979**, *86*, 1403-1410.
[89] G. F. Whyte, R. Vilar, R. Woscholski, *J Chem Biol* **2013**, *6*, 161-174.

[90] J. Plescia, N. Moitessier, *Eur J Med Chem* **2020**, *195*, 112270.
[91] B. A. Deore, M. S. Freund, *Chemistry of Materials* **2005**, *17*, 2918-2923.
[92] V. Hernandez, X. Li, S. Zhang, T. Akama, Y. Zhang, Y. Liu, J. Plattner, M. Alley, Zhou Y. Yasheen, N. J., WO2011060196, **2011**.
[93] G. Hartmann, Flores, O., WO2013096744A1, **2014**.
[94] P. Wang, H. Zhu, M. Liu, J. Niu, B. Yuan, R. Li, J. Ma, *RSC Adv.* **2014**, *4*, 28922-28927.
[95] S. Eichner, H. G. Floss, F. Sasse, A. Kirschning, *Chembiochem* **2009**, *10*, 1801-1805.
[96] B. Kalluraya, B. Lingappa, S. R. Nooji, *Phosphorus, Sulfur, and Silicon and the Related Elements* **2007**, *182*, 1393-1401.
[97] H. Meerwein, E. Büchner, K. v. Emster, *Journal Fur Praktische Chemie-chemiker-zeitung* **1939**, *152*, 237-266.
[98] M. Obushak, M. Lyakhovich, E. Bilaya, *Russian Journal of Organic Chemistry* **2002**, *38*, 38-46.
[99] D. G. Hall, in *Boronic Acids*, **2005**, pp. 1-99.
[100] S. J. Coutts, J. Adams, D. Krolikowski, R. J. Snow, *Tetrahedron Letters* **1994**, *35*, 5109-5112.
[101] S. Müller, R. Schohe-Loop, H. N. Ortega, F. Süssmeier, E. J. Nunez, T. Brumby, N. Lindner, C. Gerdes, E. Pook, A. Buchmüller, F. Z. Gaugaz, D. Lang, S. Zimmermann, A. H. M. Ehrmann, M. Gerisch, L. Lehmann, A. Timmermann, M. Schäfer, G. Schmidt, K.-H. Schlemmer, M. Follmann, E. Kersten, V. Wang, X. Gao, Y. Wang, WO2019219517A1, **2019**.
[102] L. Bauer, R. E. Hewitson, *The Journal of Organic Chemistry* **1962**, *27*, 3982-3985.
[103] D. A. Vazquez-Molina, G. M. Pope, A. A. Ezazi, J. L. Mendoza-Cortes, J. K. Harper, F. J. Uribe-Romo, *Chem Commun (Camb)* **2018**, *54*, 6947-6950.
[104] Zhou F., Xu X., Zhang L., Liu Z., Hu G., Ding Q., Xie F., Zheng B., Lv Q., L. J., US20220177462A1,
[105] Udo A. B., A. M. Birch, R. J. Butlin, C. Green, J. G. Barlind, R. Hovland, P. Johannesson, J. M. Johansson, A. Leach, A. T. Noeske, A. U. Petersson, WO2009081195, **2009**.
[106] T. Klassmüller, Dissertation: Entwicklung neuer Synthesewege zu den Naturstoffen Cassiarin A und Zephycandidin A, Ludwig-Maximilians-Universität, München, **2024**.
[107] J. Zanon, A. Klapars, S. L. Buchwald, *Journal of the American Chemical Society* **2003**, *125*, 2890-2891.
[108] C. T. Yang, J. Han, J. Liu, M. Gu, Y. Li, J. Wen, H. Z. Yu, S. Hu, X. Wang, *Org Biomol Chem* **2015**, *13*, 2541-2545.
[109] Y. Shi, J. T. Koh, *Journal of the American Chemical Society* **2002**, *124*, 6921-6928.
[110] I. Heisler, B. Buchmann, A. Cleve, M. Heroult, R. Neuhaus, H. Petrul, M. Quanz-Schöffel, C. C. Kopitz, WO2016202935, **2016**.
[111] J. Velcicky, A. Soicke, R. Steiner, H. G. Schmalz, *J Am Chem Soc* **2011**, *133*, 6948-6951.
[112] T. Ueda, H. Konishi, K. Manabe, *Angew Chem Int Ed Engl* **2013**, *52*, 8611-8615.
[113] H. Konishi, M. Kumon, M. Yamaguchi, K. Manabe, *Tetrahedron* **2020**, *76*, 131639.
[114] M. Groll, C. R. Berkers, H. L. Ploegh, H. Ovaa, *Structure* **2006**, *14*, 451-456.
[115] C. Viegas-Junior, A. Danuello, V. da Silva Bolzani, E. J. Barreiro, C. A. Fraga, *Current medicinal chemistry* **2007**, *14*, 1829-1852.
[116] S. Zhang, J. Zhang, P. Gao, L. Sun, Y. Song, D. Kang, X. Liu, P. Zhan, *Drug Discov Today* **2019**, *24*, 805-813.
[117] H. Bregman, N. Chakka, A. Guzman-Perez, H. Gunaydin, Y. Gu, X. Huang, V. Berry, J. Liu, Y. Teffera, L. Huang, B. Egge, E. L. Mullady, S. Schneider, P. S. Andrews, A. Mishra, J. Newcomb, R. Serafino, C. A. Strathdee, S. M. Turci, C. Wilson, E. F. DiMauro, *J Med Chem* **2013**, *56*, 4320-4342.
[118] U. R. Anumala, J. Waaler, Y. Nkizinkiko, A. Ignatev, K. Lazarow, P. Lindemann, P. A. Olsen, S. Murthy, E. Obaji, A. G. Majouga, S. Leonov, J. P. von Kries, L. Lehtio, S. Krauss, M. Nazare, *J Med Chem* **2017**, *60*, 10013-10025.

[119] H. Huang, A. Guzman-Perez, L. Acquaviva, V. Berry, H. Bregman, J. Dovey, H. Gunaydin, X. Huang, L. Huang, D. Saffran, R. Serafino, S. Schneider, C. Wilson, E. F. DiMauro, *ACS Med Chem Lett* **2013**, *4*, 1218-1223.
[120] J. A. Hutton, V. Goncalves, J. A. Brannigan, D. Paape, M. H. Wright, T. M. Waugh, S. M. Roberts, A. S. Bell, A. J. Wilkinson, D. F. Smith, R. J. Leatherbarrow, E. W. Tate, *J Med Chem* **2014**, *57*, 8664-8670.
[121] G. Keglevich, E. Bálint, É. Karsai, A. Grün, M. Bálint, I. Greiner, *Tetrahedron Letters* **2008**, *49*, 5039-5042.
[122] A. Gopalsamy, A. E. Aulabaugh, A. Barakat, K. C. Beaumont, S. Cabral, D. P. Canterbury, A. Casimiro-Garcia, J. S. Chang, M. Z. Chen, C. Choi, R. L. Dow, O. O. Fadeyi, X. Feng, S. P. France, R. M. Howard, J. M. Janz, J. Jasti, R. Jasuja, L. H. Jones, A. King-Ahmad, K. M. Knee, J. T. Kohrt, C. Limberakis, S. Liras, C. A. Martinez, K. F. McClure, A. Narayanan, J. Narula, J. J. Novak, T. N. O'Connell, M. D. Parikh, D. W. Piotrowski, O. Plotnikova, R. P. Robinson, P. V. Sahasrabudhe, R. Sharma, B. A. Thuma, D. Vasa, L. Wei, A. Z. Wenzel, J. M. Withka, J. Xiao, H. G. Yayla, *J Med Chem* **2021**, *64*, 326-342.
[123] S. Fletcher, *Organic Chemistry Frontiers* **2015**, *2*, 739-752.
[124] T. Tsunoda, F. Ozaki, S. Itô, *Tetrahedron Letters* **1994**, *35*, 5081-5082.
[125] I. Sakamoto, H. Kaku, T. Tsunoda, *Chemical and Pharmaceutical Bulletin* **2003**, *51*, 474-476.
[126] T. Mosmann, *Journal of Immunological Methods* **1983**, *65*, 55-63.
[127] C. Y. Liu, C. W. Shiau, H. Y. Kuo, H. P. Huang, M. H. Chen, C. H. Tzeng, K. F. Chen, *Haematologica* **2013**, *98*, 729-738.
[128] Z. Canturk, Y. Tunali, S. Korkmaz, Z. Gulbaş, *Cytotechnology* **2016**, *68*, 87-93.
[129] M. Ortiz-Flores, M. González-Pérez, A. Portilla, M. A. Soriano-Ursúa, J. Pérez-Durán, A. Montoya-Estrada, G. Ceballos, N. Nájera, *Inorganics* **2023**, *11*, 165.
[130] M. Psurski, A. Łupicka-Słowik, A. Adamczyk-Woźniak, J. Wietrzyk, A. Sporzyński, *Investigational New Drugs* **2019**, *37*, 35-46.
[131] Y. Itoh, M. Suzuki, T. Matsui, Y. Ota, Z. Hui, K. Tsubaki, T. Suzuki, *Chemical and Pharmaceutical Bulletin* **2016**, *64*, 1124-1128.
[132] H. Wen, N. Xue, F. Wu, Y. He, G. Zhang, Z. Hu, H. Cui, *Molecules* **2018**, *23*.
[133] K. T. Howitz, *Drug Discovery Today: Technologies* **2015**, *18*, 38-48.
[134] Reaction Biology Corporation, Malvern (USA), Drug Discovery contract research organization services, (https://www.reactionbiology.com/services/target-specific-assays/epigenetic-assays/hdac-assays; accessed 11.10.2024).
[135] R. A. Friesner, J. L. Banks, R. B. Murphy, T. A. Halgren, J. J. Klicic, D. T. Mainz, M. P. Repasky, E. H. Knoll, M. Shelley, J. K. Perry, D. E. Shaw, P. Francis, P. S. Shenkin, *Journal of Medicinal Chemistry* **2004**, *47*, 1739-1749.
[136] H. M. Berman, J. Westbrook, Z. Feng, G. Gilliland, T. N. Bhat, H. Weissig, I. N. Shindyalov, P. E. Bourne, *Nucleic Acids Research* **2000**, *28*, 235-242.
[137] J. C. Shelley, A. Cholleti, L. L. Frye, J. R. Greenwood, M. R. Timlin, M. Uchimaya, *J Comput Aided Mol Des* **2007**, *21*, 681-691.